https://doi.org/10.35662/unine-thesis-2980

On the chemical and molecular ecology of deceptively pollinated *Arum maculatum* (Araceae)

Mark Andre Szenteczki

Doctoral Program in Organismal Biology
Faculty of Science, Institute of Biology
University of Neuchâtel

Accepted by the thesis committee:

Prof. Sergio Rasmann (University of Neuchâtel), directeur
Prof. Nadir Alvarez (University of Geneva & Lausanne Natural Sciences Museum), co-directeur
Dr. Marc Gibernau (University of Corsica Pasquale Paoli), rapporteur
Prof. Anahí Espíndola (University of Maryland), rapporteur
Prof. Daniel Croll (University of Neuchâtel), rapporteur

Submitted in partial fulfillment
of the requirements for the degree
of Doctor of Philosophy in Biology
at the University of Neuchâtel

23 September 2022

UNIVERSITÉ DE
NEUCHÂTEL

Faculté des Sciences
Secrétariat-décanat de Faculté
Rue Emile-Argand 11
2000 Neuchâtel – Suisse
Tél : + 41 (0)32 718 21 00
E-mail : secretariat.sciences@unine.ch

IMPRIMATUR POUR THESE DE DOCTORAT

La Faculté des sciences de l'Université de Neuchâtel
autorise l'impression de la présente thèse soutenue par

Monsieur Mark SZENTECZKI

Titre:

"On the chemical and molecular ecology of deceptively pollinated *Arum maculatum* (Araceae)"

sur le rapport des membres du jury composé comme suit:

- Prof. Sergio Rasmann, directeur de thèse, Université de Neuchâtel, Suisse
- Prof. Nadir Alvarez, co-directeur de thèse, Université de Genève, Musée cantonal des sciences naturelles, Lausanne, Suisse
- Prof. Daniel Croll, Université de Neuchâtel, Suisse
- Dr Marc Gibernau, CNRS, Ajaccio, France
- Ass. Prof. Anahi Espindola, University of Maryland, College Park, USA

Neuchâtel, le 29 septembre 2022 Le Doyen, Prof. R. Bshary

SUMMARY

Pollination is foundational to the diversity of all terrestrial ecosystems, and there is substantial evidence that pollinators are the main driver of angiosperm (flowering plant) speciation rates. Speciation can often be linked to natural selection on reproductive traits: floral color, shape, size, and scent all may represent key adaptations to local pollinator guilds. However, pollinator communities are rarely consistent through space or time, which can lead to tangled patterns of adaptation versus maladaptation, and evolution or coevolution. Consequently, understanding how highly-dimensional traits with multiple functions – such as floral scent – diversify across wide geographic ranges remains a major challenge. Specialized obligate pollination systems, where plants attract a limited number of pollinator species using volatile organic compound (VOC) emissions putatively under strong selection (*i.e.* with few trade-offs present), are a useful model to address this problem. Here, we used *Arum maculatum* (Araceae) as the model for our work. *Arum maculatum* has long fascinated botanists due to its deceptive pollination via brood-site mimicry: pollinators are attracted by a dung-like scent and are temporarily trapped during the pollination process, without any reward. Previous research has demonstrated that the two main pollinators of *A. maculatum*, the dipteran (Psychodidae) moth flies *Psychoda phalaenoides* and *P. grisescens*, were respectively trapped in two main geographic zones in Europe, which mirror the two population genetic clusters present in *A. maculatum*. In Chapter 2, we investigated whether this pattern was a result of local adaptations in floral scent. Using a combination of Europe-wide surveys of floral VOC variation and pollinator attraction patterns and a transplant experiment, we found that most *A. maculatum* populations have highly variable VOC emissions, and consequently are capable of attracting both *P. phalaenoides* and *P. grisescens*. Temporally replicated pollinator data revealed that inter-annual and decadal changes in pollinator species composition are present, and may explain why considerable VOC variation is maintained within populations. In Chapter 3, we further aimed to investigate the genetic bases of intraspecific variation in floral scent using whole transcriptome sequencing of two VOC-emitting floral tissues in *A. maculatum* (*i.e.* the appendix and male florets). These data identified candidate transcripts for several unusual *A. maculatum* VOCs, and provided insights into the tissue-specific nature of their production. Co-inertia analyses between transcript expression patterns and pollinator attraction rates further identified a correlation between male floret terpene synthases and species-specific pollinator attraction. Finally, in Chapter 4, we expanded our VOC and genetic sampling to include species from across the genus *Arum*. Here, we aimed to characterize the impacts of pollinator-mediated selection versus phylogenetic constraints on floral scent variation, at microevolutionary (*i.e.* within *A.*

maculatum) and macroevolutionary (*i.e.* genus-wide) scales. Using high throughput genotyping-by-sequencing methods, we identified thousands of putatively neutral loci; these data were used to confirm that VOCs are evolutionarily labile both within *A. maculatum* and across the genus. This adaptability may be key to deceiving a wide and variable range of dipteran species. Even though we identified VOCs associated with species-specific pollinator attraction, and the genes underlying them, natural selection has not fixed these genes within populations yet. Temporally variable pollinators appear to be an important factor in this pattern, potentially favoring diverse floral scent bouquets to ensure that a wider range of *Psychoda* species can be deceived. High floral scent diversity is also apparent at the genus level, although the extent of intraspecific variation in other species of *Arum* needs to be studied further. Taken together, the results of this thesis highlight how and why trait variation may persist within populations, even when species interactions are specific and obligate.

KEYWORDS

Arum maculatum, evolutionary ecology, floral scent, indole, next-generation sequencing, phylogenomics, pollination, Psychodidae, spatial variation, temporal variation, terpene synthases, volatile organic compounds (VOCs)

RÉSUMÉ

La pollinisation est à la base de la diversité de tous les écosystèmes terrestres, et il existe de nombreuses évidences démontrant que les pollinisateurs sont l’un des principaux mécanismes de spéciation des angiospermes (plantes à fleurs). La spéciation peut souvent être liée à la sélection naturelle des caractères reproductifs : la couleur, la forme, la taille et l'odeur des fleurs ont toutes été considérées comme des adaptations essentielles aux pollinisateurs locaux. Cependant, les communautés de pollinisateurs sont rarement homogènes dans l'espace et dans le temps, ce qui peut produire des scénarios complexes d'adaptation ou de maladaptation, d'évolution unilatérale ou de coévolution. Par conséquent, comprendre comment des caractéristiques complexes à multiples fonctions - telles que l'odeur florale - se diversifient sur de vastes distances géographiques est difficile. Les interactions de pollinisation obligatoire spécialisée, au sein desquelles une plante attire un nombre limité d'espèces de pollinisateurs, impliquent généralement l'émissions de composés organiques volatils (COVs) sous forte sélection naturelle. Ces systèmes constituent un modèle utile pour étudier la problématique du maintien d’une interaction spécialisée. Ici, nous avons étudié *Arum maculatum* (Araceae) comme modèle de notre recherche. *Arum maculatum* fascine les botanistes depuis longtemps en raison de sa pollinisation par duperie qui mime des sites de ponte : les pollinisateurs sont attirés par une odeur semblable à celle d'une bouse ou de la matière en décomposition et sont temporairement piégés pendant le processus de pollinisation, sans aucune récompense. Des recherches antérieures ont démontré que les deux principaux pollinisateurs de *A. maculatum*, les moucherons diptères (Psychodidae) *Psychoda phalaenoides* et *P. grisescens*, sont majoritairement piégées dans deux régions géographiques d’Europe, ce qui reflète largement les deux clusters génétiques trouvés chez *A. maculatum.* Dans chapitre 2, nous avons cherché à savoir si ce fonctionnement était le résultat d'adaptations locales de l'odeur des fleurs. En utilisant une analyse comparative à l'échelle européenne, de la variation des COV floraux ainsi qu'une expérience de transplantation, nous avons découvert que la plupart des populations d'*A. maculatum* présentent des émissions de COVs très variables. Ils sont donc généralement capables d'attirer à la fois *P. phalaenoides* et *P. grisescens*. Des données sur les pollinisateurs, avec réplication temporelle, ont révélé que des changements interannuels et décennaux dans la composition des espèces de pollinisateurs sont présents, et peuvent expliquer pourquoi une variation considérable des COV est maintenue au sein des populations. Dans le chapitre 3, nous avons cherché à étudier les bases génétiques de cette variation intraspécifique de l'odeur florale en utilisant le séquençage du transcriptome entier de deux tissus floraux émettant des COV de *A. maculatum* : l'appendice et les étamines. Ces données nous ont permis d'identifier des transcriptions candidates pour plusieurs COVs inhabituels d'*A. maculatum*, et ont fourni des informations sur la spécificité du tissu floral de leur production. Les analyses de co-inertie entre les modèles d'expression des transcriptions et les taux d'attraction des pollinisateurs ont également identifié une corrélation entre les émissions de sesquiterpènes par les étamines situées dans la chambre florale à la base de l'inflorescence et l'attraction des pollinisateurs spécifique à l'espèce. Finalement, dans le chapitre 4, nous avons étendu notre échantillonnage des COVs et de génétique pour inclure d'autres espèces d'*Arum*. Ici, nous avons cherché à caractériser les impacts de la sélection exercée par les pollinisateurs par rapport aux contraintes phylogénétiques sur la variation de l'odeur florale, à des échelles microévolutives (*c.-à-d.* au sein d'*A. maculatum*) et macroévolutives (*c.-à-d.* à l'échelle du genre). En utilisant des méthodes de génotypage par séquençage à haut débit, nous avons identifié des milliers de loci putativement neutres ; ces données ont été utilisées pour confirmer que les COVs sont labiles du point de vue de l'évolution à la fois au sein d'*A. maculatum* et à l'échelle du genre. Cette adaptabilité chimique peut être la clé pour tromper une gamme large et variable d'espèces de diptères. Même si nous avons identifié les COVs associés à l'attraction des pollinisateurs spécifiques à l'espèce, ainsi que les gènes qui les supportent, la sélection naturelle n'a pas encore fixé ces gènes au sein des populations. Les communautés variables de pollinisateurs dans le temps semblent être un facteur important dans ce fonctionnement, favorisant potentiellement des bouquets d'odeurs floraux diversifiés afin de s'assurer qu'un plus grand nombre d'espèces *Psychoda* puisse être trompé. Une haute diversité d'odeurs florales est également apparente au niveau du genre, bien que la variation intraspécifique chez d'autres espèces d'Arum doive encore être étudiée. Pris ensemble, les résultats de cette thèse soulignent comment et pourquoi la variation de traits floraux peut persister au sein des populations, même lorsque les interactions de pollinisation sont spécifiques et obligatoires.

MOTS-CLÉS

Arum maculatum, composés organiques volatils (COVs), écologie évolutive, indole, odeur florale, phylogénomique, pollinisation, Psychodidae, séquençage de nouvelle génération, synthases de terpènes, variation spatiale, variation temporelle

TABLE OF CONTENTS

ACKNOWLEDGEMENTS

To begin, I am grateful for the support of my co-supervisors, Sergio Rasmann and Nadir Alvarez. Sergio, thank you for welcoming me into your lab, and for guiding our research as it evolved over the years. I am grateful to have been given the opportunity to explore and expand the scope of our project, and this thesis is a product of that exploration. Nadir, thank you for your support and encouragement, which extends all the way back to 2014. Since we first met when I was an undergraduate intern, I have grown considerably as a researcher and this would not have been possible without you.

During this PhD, I was also awarded an SNSF Doc.Mobility grant (P1NEP3_191659) to pursue a research project in Ajaccio at the University of Corsica, which I am very grateful for. During this time, I had the pleasure of working under the supervision of Dr. Marc Gibernau. Thank you, Marc, for being a thoughtful and helpful guide throughout this project. This work would not have been possible without your expertise on the genus *Arum*.

I would also like to thank my committee members, Prof. Anahí Espíndola and Prof. Daniel Croll. Anahí, thank you for being an enthusiastic supporter throughout this project; your advice helped set the direction of this entire thesis, which stands on the shoulders of your extensive work on *A. maculatum* a decade ago. Daniel, I am grateful to be able to have been able share my research with you, and for your valuable feedback as well.

Last, and certainly not least, this thesis would not have been possible without Adrienne Godschalx. Adrienne, thank you for being a friend, research partner, and source of advice and encouragement throughout my PhD. Without your expertise on the GC-MS analyses and work on identifying pollinators with Marc, and your tireless efforts in the field, I never would have reached this point.

All doctoral theses should push the limits of our scientific knowledge in some small way. The field work associated with the present work also pushed the limits of what “unlimited mileage” means to rental car companies in multiple countries throughout Europe. The massive sampling effort and transplant experiment this thesis is based on would not have been possible without the dedicated assistance of several volunteers. I would like to thank Alberto Garcia Jimenez for joining me on a long trip circling most of France in 2017, during a very busy first field season. I am also grateful for Monica Fleisher’s assistance with our field sampling in the Balkans in 2019. I would also like to than Andrea Galmán, who agreed to join us during two years of field work throughout the Balkans – with special thanks for your help in rescuing Rosa, a stray puppy from the forests of Croatia who has been my faithful companion ever since.

I received valuable support and guidance during the processing of our VOC and molecular samples as well. I would especially like to thank Gregory Roeder for all his help with the analytical chemistry associated with this thesis, and Julia Bilat, for her advice and support during our ddRAD-seq library preparation.

I would also like to thank Blaise Mulhauser, Laurent Oppliger, and the rest of the team at the Jardin Botanique de Neuchâtel, for providing space and care required to maintain our transplant population of *A. maculatum*, and for allowing me to sample extensively on their grounds during my PhD. Chapter 4 also required the collaboration several botanical gardens. I am grateful for the support of Jonathan Kendon, Geoffrey Kite, and Kit Strange at the Royal Botanic Gardens, Kew, and David Scherberich at the Jardin Botanique de Lyon for allowing me to collect tissue and VOC samples from their living collections of *Arum*.

I would also like to acknowledge my early mentors, Prof. Stephen C. Lougheed and Dr. Nick Cairns, who inspired my passion for field research, ecology, and evolution at the beginning of my research journey.

I am also grateful for my many friends and colleagues in Neuchâtel and in the functional ecology lab. Special thanks to Leslie Ader and Marton Kalotay, for their support throughout my thesis, and for taking Rosa and I in without hesitation when we found ourselves temporarily stranded without a home as COVID lockdowns began in March 2020. Finally, I would like to thank my brother, Vincent, and my parents for their love and support. This thesis is dedicated to my parents, Andras and Hajnalka.

CHAPTER 1 - General Introduction

Species diversity and species interactions

Angiosperms (flowering plants) and insects are highly diverse clades of organisms; together, they represent over two thirds of all living species on Earth (Mora et al. 2011, Anderson et al. 2016, Stork 2018). Understanding this diversity requires an understanding of plant-insect interactions, which are ubiquitous in nature. Antagonistic interactions such as herbivory (Fraenkel 1959, Ehrlich and Raven 1964) and mutualistic interactions such as pollination (Grant and Grant 1965, Stebbins 1970) are both widely recognized as major drivers of trait specialization and adaptive radiations in plants and insects (Ramos and Schiestl 2019). As interacting species exert reciprocal selective pressures on one another, coevolution may occur.

The geographic mosaic of coevolution, first described by Ehrlich and Raven (1964) and further developed by Thompson (1994, 2005) extended coevolutionary theory to incorporate interactions across a range of ecological conditions and spatial scales, where genetic and ecological processes continuously reshape interactions among species. Ollerton and colleagues (2007) added that temporal variation in species interactions and environmental conditions, and the phylogenetic histories of all species involved must also be considered, and that these data should ultimately be connected to genetic variations. Consequently, while interest in how traits diversify through space and time dates back to the origins of evolutionary biology (Darwin 1859, 1862), gaining a complete understanding of the subject remains a challenge to this day.

Today, we are better equipped to understand how species interactions influence evolution than Darwin, when he concluded *Origin* with a description of natural selection acting on “tangled bank” of species interacting with one another. In *Genetics and the Origin of Species*, Dobzhansky (1937) made important contributions to the modern synthesis (Huxley 1942) by bringing together genetics and evolution, and demonstrating that microevolution (*i.e.* changes in allele frequencies within populations) can lead to macroevolution (*i.e.* higher-order evolutionary change, among species or other taxonomic groups). Since then, studies have continued to demonstrate that ecological and evolutionary changes are tightly linked (Schoener 2011), and that contemporary evolution (*i.e.* at the scale of thousands of years, or less) and ecological processes influence one another through eco-evolutionary dynamics (Pelletier et al. 2009, Hendry 2016). Within this framework, we are now able to link communities of interacting plants and insects, variations in their distributions, and patterns in abiotic conditions, in order to define pollination syndromes (Fenster et al. 2004) and plant defense syndromes (Agrawal and Fishbein 2006).

Local adaptation

Local adaptation is a key mechanism to understand the link between micro- and macroevolution (Williams 1966). When varying biotic or abiotic conditions lead to natural selection acting differently on phenotypes among populations, this can lead to individuals with higher fitness in their local environment than in other environments. Reciprocal transplant experiments are commonly used to identify patterns of local adaptation among populations (Kawecki and Ebert 2004), and common garden experiments can further disentangle phenotypic plasticity from local adaptation. As natural selection acts on phenotypes over time, changes in allele frequencies should arise; with high-throughput genome sequencing methods, it is now possible to identify the genetic bases of local adaptations (Savolainen et al. 2013, Hoban et al. 2016). The evolutionary and population genetics of plants are both influenced by local adaptation (Leimu and Fischer 2008), but the relative contributions of plant traits, habitat characteristics, and biotic interactions on floral traits remains less well known, particularly in natural populations of non-model organisms (Hunter 2002).

Highly specialized interactions (*i.e.* where one or both species interact in an obligate manner with each other) are useful natural models for studying how local adaptation and microevolution may ultimately lead to the trait and species diversity we observe today. Both plant defense (Agrawal 2011) and pollination (Thompson et al. 2013, 2017, Friberg et al. 2019) can be suitable systems for studying how biotic interactions drive local adaptation, ecological and genetic differentiation, and ultimately speciation. In the present work, our focus will be pollinator-mediated selection in a specific and obligate pollination system. Although herbivory and pollination are both important drivers of flowering plant diversity, recent phylogenetic evidence suggests that pollination played a larger role in the diversification of flowering plant lineages (Van der Niet and Johnson 2012, Hernández-Hernández and Wiens 2020).

Pollination

Pollination is the mechanism by which plants reproduce, wherein pollen grains are transferred to stigmas, germinate, and their contents are moved down the style to the ovules. Pollen transfer may occur between different individuals (*i.e.* outcrossing, or allogamy), or it may occur across the floral organs of the same flower (*i.e.* self-pollination, or autogamy); outcrossing is the predominant reproductive strategy for an estimated 85-90% of flowering plants (Takebayashi and Morrell 2001, Wright et al. 2013). Many flowering plants depend on vectors such as wind, water, or animals to transport their pollen. Insects are particularly important pollinators: the vast majority of flowering plants – over 90% of species (Kearns et al. 1998, Ollerton et al. 2011) – utilize insect pollination services. Selection from insect pollinators is often cited when discussing the comparatively rapid increases in species richness (*i.e.* relative species diversity within clades) and phenotypic (*i.e.* trait) diversity of flowering plants (Regal 1977, Faegri and Van Der Pijl 1979, Armbruster and Muchhala 2009, Crepet and Niklas 2009, Van der Niet and Johnson 2012). However, understanding the impact of specialized pollination phenotypes on speciation rates requires knowledge of the sources of selective pressure (*e.g.* pollinator species and environmental conditions), as well as potential trade-offs influencing specialized phenotypes (reviewed in Armbruster 2014).

Insects typically visit a flower in search of a resource that benefits their own survival (*e.g.* pollen, nectar, stigmatic fluid, or floral tissue), and/or reproduction (*e.g.* egg laying or mating sites). Floral traits are therefore subject to selection pressures driven by pollinator preferences, and may adapt to ensure that efficient pollen transfer takes place. Floral signals can be used to mediate pollinator attraction through novel, coevolved interactions (Cook and Rasplus 2003, Pellmyr 2003, Thompson et al. 2017), and/or through exploiting pre-existing pollinator biases or behaviors (Schiestl and Dötterl 2012). These floral signals include rewards such as nectar (Parachnowitsch et al. 2019) or pollen (Dobson and Bergström 2000), visual characteristics such as shape, size, and color (Goyret et al. 2007, Willmer 2011, Schiestl and Johnson 2013, du Plessis et al. 2018), or olfactory cues in the form of volatile organic compound (VOC) emissions (Whitehead and Peakall 2009). Since visual and olfactory cues may be uncoupled from rewards, pollinating insects may develop innate or learned preferences, which lead to selection pressure on their preferred floral traits (Knauer and Schiestl 2015). Multiple traits may also be under selection simultaneously, particularly in generalist pollination systems (Ollerton et al. 2007), and pollinators often respond to the multimodal expression of several traits (reviewed in Junker and Parachnowitsch 2015). While generalist pollination networks are a large and comparatively understudied aspect of floral evolution (Ollerton et al. 2007), we have opted to study a specialized pollination system which is mediated by a single trait: floral scent. This provided us with a more tractable system for linking pollinator mediated selection to floral trait evolution.

Floral scent

Plants emit VOCs from their flowers, leaves, fruits, and roots to mediate their interactions with microbes, animals, and other plants. Over 1700 VOCs have been identified in the relatively small subset of all flowering plants which have been studied to date (Knudsen and Gershenzon 2020). Floral scents, which are usually a bouquet of multiple VOCs, play a central role in pollinator attraction and will be the main focus of the present work (Pellmyr and Thien 1986, Knudsen and Tollsten 1993, Whitehead and Peakall 2009, Junker and

Parachnowitsch 2015). However, it should be noted that volatile emissions can also directly defend against predators and pathogens (*e.g.* herbivory-induced VOCs), or indirectly through the attraction of natural enemies of antagonists (Pichersky and Gershenzon 2002, Holopainen 2004, Irwin et al. 2004).

Most floral VOCs can be grouped into a few compound classes; some of the most abundant classes will be listed here in decreasing order of diversity. Volatile terpenoids, which include mono- (10 carbon) and sesquiterpenes (15 carbon), are produced by terpene synthases from products of the methylerythritol 4-phosphate (MEP) pathway in plastids and the mevalonate (MVA) pathway in the cytosol. Mono- and sesquiterpenes are mainly produced from MEP and MVA precursors, respectively (Hemmerlin et al. 2012). Aliphatic compounds, which consist of one to 25-carbon chains, are mainly synthesized from fatty acids and include green leaf volatiles (Pare and Tumlinson 1999). Benzenoids and phenylpropanoids are produced via the shikimate or phenylpropanoid pathways, using the amino acids phenylalanine and tyrosine or shikimate pathway intermediates (Vogt 2010). Finally, nitrogen- and sulfur-containing compounds are less common but potent VOCs, which are derived from amino acid metabolism (*e.g.* indole biosynthesis from tryptophan; Gierl and Frey 2001). Since the biosynthetic pathways to produce all of these compound classes are widely distributed among flowering plants, volatile emissions are correspondingly diverse among flowering plant families (Knudsen and Gershenzon 2020).

As mentioned above, the most common function of floral VOCs is pollinator attraction. However, VOC emissions may vary for several other reasons. For example, trade-offs between plant defense and pollination (Armbruster et al. 1997, Irwin et al. 2004, Schiestl et al. 2011) or floral color and scent (Diaz and Kite 2006, Delle-Vedove et al. 2011) may constrain VOC evolution. Phylogenetic constraints may also influence the diversity of floral VOCs within a population or clade (Levin et al. 2003, Knudsen et al. 2006), though it should be noted that floral scent appears to be an evolutionarily labile (*i.e.* highly adaptive) trait (Barkman 2001, Prieto-Benítez et al. 2016b). Abiotic factors such as temperature and moisture also influence the composition and proportional emissions of VOCs (Majetic et al. 2009, Campbell et al. 2019). VOCs may also vary temporally via circadian rhythms (Fenske and Imaizumi 2016, Prieto-Benítez et al. 2016a, Chuang et al. 2017) or due to external cues such as light (Friberg et al. 2014). Consequently, few studies have attempted to investigate how a highly dimensional trait such as floral scent diversifies across wide geographic ranges (*e.g.* Friberg et al. 2019). We have chosen to use a deceptive pollination system as our model, to address this interesting question while reducing the impact of the aforementioned external influences on floral scent.

Deceptive pollination

Thus far, I have only written of floral scent as an honest signal for pollinator attraction. However, approximately 3.7% of all angiosperms are pollinated by deception (Renner 2006); these species trick insects into providing pollination services by signaling the presence of a reward, without actually providing it (Sprengel 1793, Dafni 1984, Schiestl and Johnson 2013). Deceptive pollination has long fascinated evolutionary biologists, including Darwin’s (1862) observations of orchids, and they continue to provide interesting opportunities to study the evolutionary ecology of floral traits. Deceptive pollination is most common in Orchidaceae, with at least 6500 species pollinated via deception (Ackerman 1986, Jersáková et al. 2006). However, at least 1000 other species, spanning most major groups of flowering plants, are thought to be deceptively pollinated as well (reviewed in Renner 2006).

While floral morphology appears to be important to some sexually deceptive orchids (Gaskett 2011, de Jager and Peakall 2016), floral scents appear to be the most pervasive means of deception. Insects are known to be deceived by floral VOC emissions which mimic compounds present in their food, mating partners, and oviposition sites (reviewed in Jersáková et al. 2006; Renner 2006; Johnson and Schiestl 2016). In the chapters that follow, my main focus will be olfactory mimicry of oviposition substrates (*i.e.* brood site mimicry). Several substrates, including dung (Kite et al. 1998, Sayers et al. 2020), carrion (Stensmyr et al. 2002, van der Niet et al. 2011), fermenting fruit (Goodrich et al. 2006, Stökl et al. 2010), and fungi (Vogel and Martens 2000, Policha et al. 2016) are known to be mimicked by flowers.

Interestingly, dung and carrion scents have been hypothesized to serve as a deterrent to mammal herbivores (Lev-Yadun et al. 2009). If dung-mimicking flowers also offer no rewards to their pollinators, and exhibit specificity in their pollinator attraction patterns, then these may represent an ideal model for studying pollinator-mediated selection on floral scent (*i.e.* in the absence of trade-offs or competing selection pressures, where floral reproductive success is largely dependent on scent alone). The Araceae family contains many such species, and is the most well-studied plant group in terms of brood site mimicry (Urru et al. 2011, Johnson and Schiestl 2016). Consequently, we have selected *Arum maculatum* (Araceae) as our model for studying the evolutionary mechanisms underlying divergence in floral scents, and the genetic basis of dung-mimicking VOCs.

Arum maculatum

Arum maculatum is a common woodland plant with a Europe-wide distribution range (Boyce 1993), which has fascinated botanists due to its unusual pollination strategy (Dormer 1960, Prime 1960, Lack and Diaz 1991, Diaz and Kite 2002). Its morphology is typical of the

Areae tribe (Bröderbauer et al. 2013); the male and female florets are arranged along a central axis called the spadix, which is surrounded by a modified bract called the spathe (Figure 1.1). A chamber is formed by the base of the spathe which encloses the fertile flowers, and is separated from the upper open spathe by a constriction and hair-like staminodes growing near the opening of the constriction. The appendix serves as an osmophore and is thermogenic during anthesis, heating over 15°C above ambient temperatures (Gibernau et al. 2004, Marotz-Clausen et al. 2018).

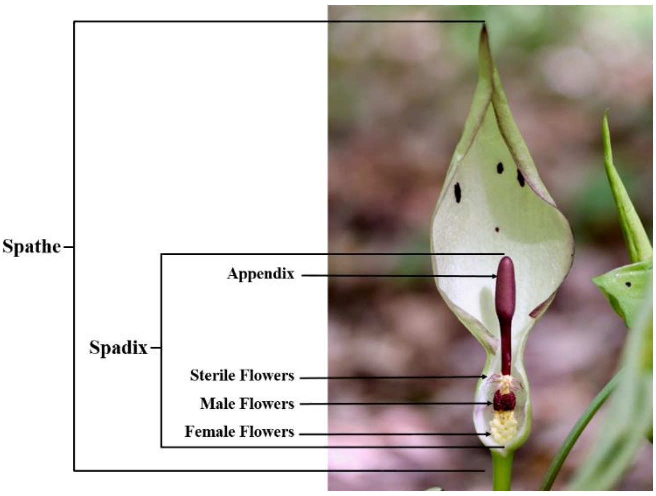

Figure 1.1. *Arum maculatum* inflorescence, highlighting key morphological features such as the spathe and spadix, and the organization of the reproductive organs. The lower spathe chamber, where attracted pollinators are temporarily held, has been dissected to reveal the male and female florets.
Photo credit: Adrienne Godschalx

It should also be noted that *A. maculatum* are tetraploid (Turco et al. 2014); although this can present challenges for genetic analyses, polyploidy via whole genome duplications (*i.e.* autopolyploidy) or hybridization events (*i.e.* allopolyploidy) can lead to increased fitness and capacity to colonize wide geographic ranges (Force et al. 1999, Bowers et al. 2003). Polyploidy may have played a role in *A. maculatum* being the most widely distributed *Arum* species in Europe as well.

The *A. maculatum* pollination cycle (reviewed in Lack and Diaz 1991, Gibernau et al. 2004) takes place over two days: on the first day, the male florets are thermogenic as the spathe unfurls in the afternoon. During the evening of the first day, pollinators are attracted by the VOC emissions of the appendix, land on the spathe, and those which are sufficiently small slip on the downward-pointing papillate cells and pass through the constriction into the lower spathe chamber. There, they crawl over the stigma of receptive female florets, depositing any pollen they may have carried from another inflorescence. Pollinators are held overnight; the following afternoon, the male florets are briefly thermogenic, and pollinators are covered in pollen before escaping the chamber as oil secretions from the papillate cells end. This protogynous reproductive strategy ensures that no selfing occurs; consequently, there should be strong selection pressure to attract efficient pollinators.

Small Psychodidae (Diptera) moth-flies are the primary pollinators of *A. maculatum*. Psychodidae are known to be efficient carriers of *Arum* pollen (Diaz and Kite 2002, Albre et al. 2003); a single individual can carry enough pollen grains to produce a large fruit set (Lack and Diaz 1991). *Psychoda phalaenoides* and *Psychoda* (*Psycha*) *grisescens* are the most frequently attracted pollinators, and together represent 87% of all insects found within floral chambers (Espíndola et al. 2011). *Psychoda setigera*, *P. albipennis* and *P. trinodulosa* are also observed within inflorescences, albeit much more infrequently, together representing 0.46% of trapped insects in Espíndola et al. (2011). The remaining pollinators include dipterans such as Chironomidae (*Smittia pratorum*), Ceratopogonidae and Sphaeroceridae (Roháček et al. 1990, Diaz and Kite 2002, Espíndola et al. 2011, Chartier et al. 2013).

As mentioned above, *A. maculatum* utilizes putative dung-mimicking floral VOCs to attract their pollinators (Figure 1.2). *Arum maculatum* inflorescences emit complex VOC blends, which are known to vary within and among populations in England (Kite 1995, Kite et al. 1998, Diaz and Kite 2002), France (Chartier et al. 2011, 2013, 2016), and across Austria, Germany, Switzerland, and northern Italy (Gfrerer et al. 2021). The *A. maculatum* floral scent bouquet is complex, and ranges from 30-60 compounds in most studies (Diaz and Kite 2002, Chartier et al. 2013, Marotz-Clausen et al. 2018) to 283 compounds in Gfrerer et al. (2021).

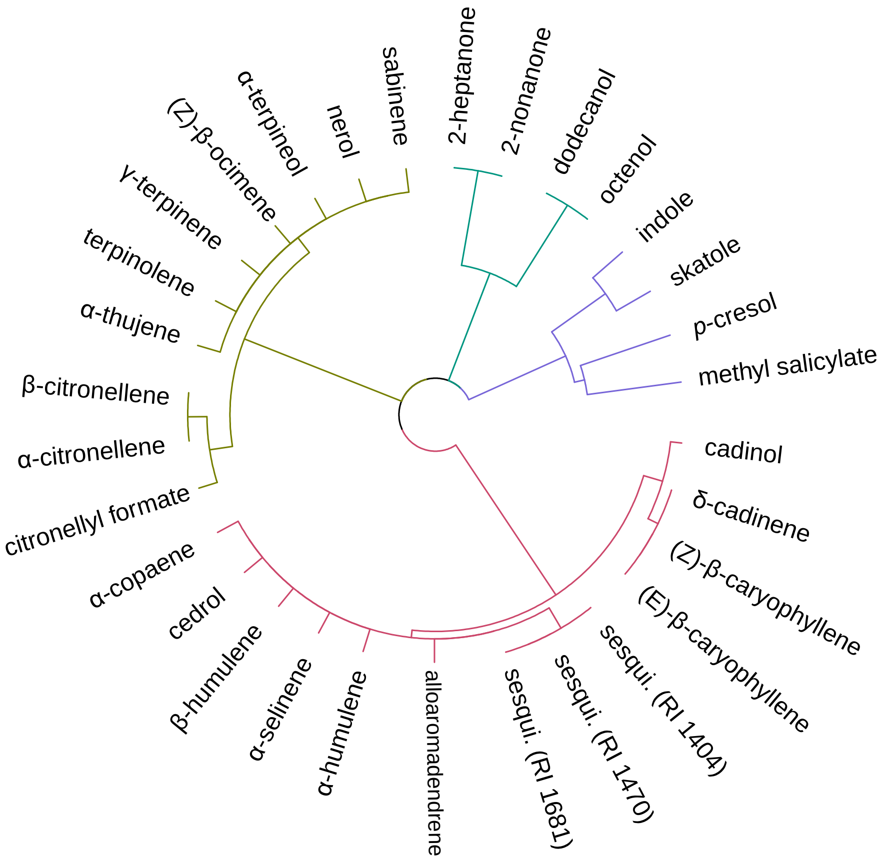

Figure 1.2. *Arum maculatum* floral VOCs identified as part of the present work, visualized based on biosynthetic similarity (*i.e.* shared enzymes and pathways). VOCs are produced by four main pathways: monoterpene (yellow) and sesquiterpene (red) synthesis, shikimate products (purple) and fatty-acid metabolism (blue).

The VOCs which we and other researchers have frequently identified include dung-mimicking compounds such as indole, *p*-cresol, and 2-heptanone (Kite et al. 1998). Sesquiterpenes also can represent a large proportion of *A. maculatum* VOC emissions, the ratio of indole to sesquiterpene in scent blends is one of the major sources of within-population variation (Chartier et al. 2013). Interestingly, these differences mirror variations in the composition of different animal feces: herbivore feces are often dominated by *p*-cresol and terpenoids, while omnivore and carnivore feces contain higher relative quantities of indole (Johnson and Jürgens 2010, Midgley et al. 2015). Indole, p-cresol, and sesquiterpenes have also recently been shown to elicit antennal responses in *P. phalaenoides* (Gfrerer et al. 2022), confirming that pollinators are able to recognize these key compounds.

A central aim of the present work was to establish whether *A. maculatum* floral VOCs co-vary with, or are influenced by pollinator communities (Figure 1.3). Notably, Espíndola and Alvarez (2011) and Espíndola et al. (2011) found that Europe-wide pollinator attraction patterns and neutral genetic variation appear to be largely concordant with one another. Specifically, the two main genetic clusters, roughly corresponding to northern/western Europe and southern/eastern Europe (ref. Fig. 1 in Espíndola and Alvarez 2011), were found to attract primarily *Psychoda phalaenoides* and *Psychoda* (*Psycha*) *grisescens*, respectively (ref. Fig. 2 in Espíndola et al. 2011). In order to address this question, we re-visited populations sampled in the aforementioned studies (Table 1.1), from northern France to southern Italy and the Balkans, to collect floral scent and pollinator data.

Figure 1.3. Photos of our study system, *Arum maculatum*. Left: Thermogenic *A. maculatum* appendix, visible through FLIR thermographic imaging. Center: *In situ* headspace VOC collection from *A. maculatum* inflorescence during our transplant experiments (Ch. 2) Right: *A. maculatum* male floret tissue, preserved in RNAlater for transcriptome sequencing (Ch. 3).

Table 1.1. *Arum maculatum* populations studied as part of this thesis. Inflorescences from each population were sampled during at least two years between 2017 and 2019. We surveyed VOCs and pollinator attraction *in situ* and following transplants (Ch. 2), sequenced whole transcriptomes from appendix and/or male floret tissue (Ch. 3), and used ddRAD-seq to study the phylogenomics of *A. maculatum* (Ch. 4), using samples collected from populations as indicated below.

Population	Country	Short Name	LAT	LONG	Ch. 2	Ch. 3	Ch.4
Forêt du Gâvre	France	GAV	47.55066	-1.86466	🟩	🟩	🟩
Conteville	France	CON	50.73731	1.73872	🟩	🟩	🟩
Chaumont	France	CHA	48.11508	5.09475	🟩	🟩	🟩
Neuchâtel	Switzerland	NEU	47.00043	6.93790	🟩	🟩	🟩
Cortaillod	Switzerland	COR	46.93205	6.83290	🟩		
Montese	Italy	MON	44.25523	10.98371	🟩	🟩	🟩
Morro Reatino	Italy	MOR	42.53585	12.85742			🟩
Jenne	Italy	JEN	41.8814	13.18219			🟩
Rifreddo	Italy	RIF	40.57235	15.82473		🟩	🟩
Visuć	Croatia	VIS	44.53128	15.76134	🟩	🟩	🟩
Gostilje	Serbia	GOS	43.65561	19.83549	🟩	🟩	🟩
Sokobanja	Serbia	SOK	43.60373	21.88755	🟩	🟩	🟩
Chiflik	Bulgaria	CHI	42.8130	24.52836	🟩	🟩	

By visiting the aforementioned populations at least twice over a span of three years, we were able to collect data on both inter-annual variation in floral scent and pollinator attraction, as well as decade-level changes when comparing against Espíndola and Alvarez (2011). Temporal replication is a crucial element for disentangling trait variation driven by natural selection from plasticity due to annual environmental variations, but with a few exceptions (Schemske and Horvitz 1989, Fishbein and Venable 1996), it is usually neglected. Building on the work of Chartier et al. (2013) in France, we also performed a range-wide transplant experiment with inflorescences from all populations. In order to identify potential locally adapted floral scents, inflorescences were transplanted to two sites with opposing pollinator communities (*i.e.* dominated by *P. phalaenoides* or *P. grisescens*). Finally, we collected genetic materials for high-throughput screening of putatively adaptive (RNA) and neutral (DNA) markers throughout these experiments, with the aim of identifying candidate genes and biosynthetic mechanisms underlying specific VOCs, as well as how floral scent diversification have been constrained by phylogenetic or phylogeographic histories. This work, and the hypotheses we aimed to test, will be detailed in greater length in the following section.

Thesis Overview

Throughout the present work, I aimed to further our understanding of the evolutionary ecology of *Arum maculatum* pollination through a combination of techniques in chemical and molecular ecology. Chemical ecology research aims to identify and understand the molecules which mediate biological processes and species interactions, from the scale of individual organisms through to ecosystems (Harborne 2001). In the case of plant-pollinator interactions, this often involves the study of semiochemicals (*i.e.* communication molecules which influence the behaviour and/or physiology of organisms), which are emitted from floral tissues as VOCs (Knudsen and Gershenzon 2020). Molecular ecology research can be highly complementary to this work, for example through the studies on the genes and pathways underlying the biosynthesis of specific compounds of interest (Bailey et al. 2009), and how they vary and may have evolved across spatial and temporal scales (Friberg et al. 2019).

As previously mentioned, understanding how trait diversity is shaped by natural selection and maintained within and among populations requires the use of diverse methods. In order to understand geographic mosaics of coevolution, one should ideally sample diversity in phenotypes, species interactions, and ecological conditions across the geographic range of species of interest (Thompson 2005). Measurements should also be temporally replicated to account for annual variations in abiotic conditions and/or biotic interactions (e.g. Fishbein and Venable 1996). The fitness of observed variations could further be tested using common garden and reciprocal transplant experiments (Kawecki and Ebert 2004). It should also be noted that observations of natural selection are not necessarily observations of evolution. The latter requires evidence of a genetic change (*e.g.* a change in the frequency of a gene within a population), and not all studies have been able to demonstrate this (Reznick and Ghalambor 2001). Phylogenetic data from entire clades of organisms could further be used to identify adaptive radiations, or conversely, constraints which may limit the trajectories of trait evolution (Felsenstein 1985). Over the chapters that follow, we tried to address each of these points as we studied the specific and obligate lure-and-trap pollination system of *A. maculatum*.

To summarize, I aimed to address the following questions in this thesis:

[Chapter 2] Does *Arum maculatum* floral scent (*i.e.* VOCs) vary to maximize pollinator attraction within their local population? In other words, are *A. maculatum* locally adapted to their pollinator communities, or is phenotypic variation instead maintained within populations?

[Chapter 3] What genes are responsible for producing common *Arum maculatum* VOCs? Does differential expression of these genes influence the sex and/or species composition of attracted pollinators?

[Chapter 4] Is VOC variation among populations of *A. maculatum* correlated with or constrained by its phylogeographic history? Expanding across the entire genus *Arum*, is there evidence of pollinators exerting selective pressures on VOC variation?

Before concluding that any observed variations are a result of natural selection, the fitness of phenotypes should be characterized and compared between different environments. In **Chapter 2**, we paired field surveys of *A. maculatum* VOC variation with a large transplant experiment. We transplanted inflorescences from ten populations spanning the species distribution range of *A. maculatum* (Table 1.1) to two different sites, each dominated by one of the main pollinator species (*i.e. Psychoda phalaenoides* or *P. grisescens*). Simultaneously, we characterized inter- annual and decadal variation in pollinator attraction within all of the studied populations, and the transplant sites. We found little evidence for local adaptation to a specific pollinator (except in Forêt du Gâvre, France, which exclusively traps *P. grisescens*); this result may be connected to the high variation in pollinator communities we observed over relatively short timescales. It appears that maintaining diverse floral scents within populations is advantageous in the case of *A. maculatum*, if inflorescences must deceive different pollinator species from year to year.

Phenotypic selection should ultimately lead to changes in allele frequencies or gene expression. In **Chapter 3**, we aimed to link total mRNA expression from two floral tissues (*i.e.* appendix and male florets) with VOC variation and pollinator attraction in ten populations of *A. maculatum* (Table 1.1). Here, we were able to i) localize the sites of synthesis for individual volatile compounds, ii) identify candidate biosynthetic pathways underlying individual *A. maculatum* VOCs, and iii) identify transcript expression correlated with sex- and species-specific pollinator attraction patterns. Through this work, we found that expression of candidate transcripts underlying putative dung-mimicking VOCs did not correlate with pollinator attraction rates. Instead, male floret terpene synthase expression in the basal spathe chamber was the only significant predictor of pollinator species trapped within inflorescences. These results validate some of the correlations between terpene emissions and pollinator attraction identified in Chapter 2. They also emphasize that the different floral scent profiles between the appendix (*i.e.* overall headspace VOCs) and male florets merits further investigation.

Comparative phylogeography and phylogenies are useful methodologies for identifying pollinator mediated selection on floral traits (Smith 2010). In **Chapter 4**, we paired molecular and VOC data to investigate micro- and macroevolutionary divergence in floral scent among twelve populations *of A. maculatum* (Table 1.1), and across the whole genus *Arum*. We were able to analyze the VOC bouquets and molecular phylogenetics for nine *Arum* species (plus *Dracunculus vulgaris* as an outgroup), and pair these data with a large SNP dataset (*i.e.* containing thousands of loci) generated through double digest restriction site-associated DNA sequencing (ddRAD-seq). The high resolution offered by our ddRAD-seq dataset allowed us to further refine the population genetic structure of *Arum maculatum*, which consists of two main genetic clusters, one of which may be split into two sub-clusters, which reflect the species' phylogeographic history. Furthermore, we observed relatively little evidence of phylogenetic constraints on VOCs production both within *A. maculatum*, and across the *Arum* phylogeny. This result likely reflects a greater influence of pollinator-driven phenotypic selection on the deceptive pollination strategy utilized by most *Arum* species.

Finally, in **Chapter 5**, I briefly review the current state of the art in our understanding in the pollination of *A. maculatum*. I will synthesize the results of our research efforts as well as other recent publications (Gfrerer et al. 2021, 2022, Laina et al. 2022); together these results have provided us with a deeper understanding of the evolutionary ecology of deceptive pollination in *A. maculatum* through space and time, and from gene expression through to pollinator attraction. With the availability of trait (*e.g.* VOC) data collected over a wide geographic range, with temporal replicates and genomic data now available, *A. maculatum* should continue to serve as a fascinating model for studying plant-pollinator interactions in the future. Although its pollination strategy is highly specialized, many of our findings may be further generalized beyond brood site mimicking species. Given the incredible diversity in floral scents we have uncovered in a highly specific, obligate deceptive pollination system, it is likely that a great deal still remains to be discovered in the broader field of chemical and molecular ecology of plant-pollinator interactions.

REFERENCES

Ackerman, J. D. 1986. Mechanisms and evolution of food-deceptive pollination systems in orchids. Lindleyana 1:108–113.

Agrawal, A. A. 2011. Current trends in the evolutionary ecology of plant defence. Functional Ecology 25:420–432.

Agrawal, A. A., and M. Fishbein. 2006. Plant Defense Syndromes. Ecology 87:S132–S149.

Albre, J., A. Quilichini, and M. Gibernau. 2003. Pollination ecology of *Arum italicum* (Araceae). Botanical Journal of the Linnean Society 141:205–214.

Anderson, S., S. Bachman, and A. Barker. 2016. State of the world's plants – 2016. Royal Botanic Gardens Kew, Kew, UK.

Armbruster, W. S. 2014. Floral specialization and angiosperm diversity: phenotypic divergence, fitness trade-offs and realized pollination accuracy. AoB PLANTS 6:plu003.

Armbruster, W. S., J. J. Howard, T. P. Clausen, E. M. Debevec, J. C. Loquvam, M. Matsuki, B. Cerendolo, and F. Andel. 1997. Do Biochemical Exaptations Link Evolution of Plant Defense and Pollination Systems? Historical Hypotheses and Experimental Tests with *Dalechampia* Vines. The American Naturalist 149:461–484.

Armbruster, W. S., and N. Muchhala. 2009. Associations between floral specialization and species diversity: cause, effect, or correlation? Evolutionary Ecology 23:159–179.

Bailey, J. K., J. A. Schweitzer, F. Ubeda, J. Koricheva, C. J. LeRoy, M. D. Madritch, B. J. Rehill, R. K. Bangert, D. G. Fischer, G. J. Allan, and T. G. Whitham. 2009. From genes to ecosystems: a synthesis of the effects of plant genetic factors across levels of organization. Philosophical transactions of the Royal Society of London. Series B, Biological sciences 364:1607–1616.

Barkman, T. J. 2001. Character coding of secondary chemical variation for use in phylogenetic analyses. Biochemical Systematics and Ecology 29:1–20.

Bowers, J. E., B. A. Chapman, J. Rong, and A. H. Paterson. 2003. Unravelling angiosperm genome evolution by phylogenetic analysis of chromosomal duplication events. Nature 422:433–438.

Boyce, P. 1993. The genus *Arum*. Royal Botanic Gardens Kew.

Bröderbauer, D., A. Weber, and A. Diaz. 2013. The design of trapping devices in pollination traps of the genus *Arum* (Araceae) is related to insect type. Botanical journal of the Linnean Society. Linnean Society of London 172:385–397.

Campbell, D. R., P. Sosenski, and R. A. Raguso. 2019. Phenotypic plasticity of floral volatiles in response to increasing drought stress. Annals of Botany 123:601–610.

Chartier, M., S. Liagre, H. Weiss-Schneeweiss, B. Kolano, J.-M. Bessière, J. Schönenberger, and M. Gibernau. 2016. Floral traits and pollination ecology of European *Arum* hybrids. Oecologia 180:439–451.

Chartier, M., L. Pélozuelo, B. Buatois, J.-M. Bessière, and M. Gibernau. 2013. Geographical variations of odour and pollinators, and test for local adaptation by reciprocal transplant of two European *Arum* species. Functional Ecology 27:1367–1381.

Chartier, M., L. Pélozuelo, and M. Gibernau. 2011. Do floral odor profiles geographically vary with the degree of specificity for pollinators? Investigation in two sapromyophilous *Arum* species (Araceae). Annales de la Société entomologique de France 47:71–77.

Chuang, Y.-C., M.-C. Lee, Y.-L. Chang, W.-H. Chen, and H.-H. Chen. 2017. Diurnal regulation of the floral scent emission by light and circadian rhythm in the *Phalaenopsis* orchids. Botanical studies 58:1–9.

Cook, J. M., and J.-Y. Rasplus. 2003. Mutualists with attitude: coevolving fig wasps and figs. Trends in Ecology & Evolution 18:241–248.

Crepet, W. L., and K. J. Niklas. 2009. Darwin's second "abominable mystery": Why are there so many angiosperm species? American journal of botany 96:366–381.

Dafni, A. 1984. Mimicry and Deception in Pollination. Annual Review of Ecology and Systematics 15:259–278.

Darwin, C. 1859. On the origin of species. Routledge, London.

Darwin, C. 1862. On the various contrivances by which British and foreign orchids are fertilised by insects, and on the good effects of intercrossing. First edition. John Murray, London.

Delle-Vedove, R., N. Juillet, J.-M. Bessière, C. Grison, N. Barthes, T. Pailler, L. Dormont, and B. Schatz. 2011. Colour-scent associations in a tropical orchid: three colours but two odours. Phytochemistry 72:735–742.

Diaz, A., and G. Kite. 2002. A comparison of the pollination ecology of *Arum maculatum* and *A. italicum* in England. Watsonia 24:171–182.

Diaz, A., and G. C. Kite. 2006. Why be a rewarding trap? The evolution of floral rewards in *Arum* (Araceae), a genus characterized by saprophilous pollination systems. Biological Journal of the Linnean Society 88:257–268.

Dobson, H. E. M., and G. Bergström. 2000. The ecology and evolution of pollen odors. Plant Systematics and Evolution 222:63–87.

Dobzhansky, T. 1937. Genetics and the Origin of Species. Columbia University Press.

Dormer, K. J. 1960. The truth about pollination in *Arum*. The New Phytologist 59:298–301.

Ehrlich, P. R., and P. H. Raven. 1964. Butterflies and plants: a study in coevolution. Evolution 18(4) 586-608.

Espíndola, A., and N. Alvarez. 2011. Comparative Phylogeography in a Specific and Obligate Pollination Antagonism. PLOS ONE 6:e28662.

Espíndola, A., L. Pellissier, and N. Alvarez. 2011. Variation in the proportion of flower visitors of *Arum maculatum* along its distributional range in relation with community-based climatic niche analyses. Oikos 120:728–734.

Faegri, K., and L. Van Der Pijl. 1979. Chapter 14 - Pollination Ecology and Speciation. Pages 151–155 *in* K. Faegri and L. Van Der Pijl, editors. Principles of Pollination Ecology. Pergamon, Amsterdam.

Felsenstein, J. 1985. Phylogenies and the comparative method. The American Naturalist 125:1–15.

Fenske, M. P., and T. Imaizumi. 2016. Circadian rhythms in floral scent emission. Frontiers in plant science 7:462.

Fenster, C. B., W. S. Armbruster, P. Wilson, M. R. Dudash, and J. D. Thomson. 2004. Pollination syndromes and floral specialization. Annual Review of Ecology, Evolution, and Systematics 35:375–403.

Fishbein, M., and D. L. Venable. 1996. Diversity and Temporal Change in the Effective Pollinators of Asclepias Tuberosa. Ecology 77:1061–1073.

Force, A., M. Lynch, F. B. Pickett, A. Amores, Y. L. Yan, and J. Postlethwait. 1999. Preservation of duplicate genes by complementary, degenerative mutations. Genetics 151:1531–1545.

Fraenkel, G. S. 1959. The Raison d’Etre of Secondary Plant Substances: These odd chemicals arose as a means of protecting plants from insects and now guide insects to food. Science 129:1466–1470.

Friberg, M., C. Schwind, P. R. Guimarães, R. A. Raguso, and J. N. Thompson. 2019. Extreme diversification of floral volatiles within and among species of Lithophragma (Saxifragaceae). Proceedings of the National Academy of Sciences 116:4406–4415.

Friberg, M., C. Schwind, L. C. Roark, R. A. Raguso, and J. N. Thompson. 2014. Floral Scent Contributes to Interaction Specificity in Coevolving Plants and Their Insect Pollinators. Journal of Chemical Ecology 40:955–965.

Gaskett, A. C. 2011. Orchid pollination by sexual deception: pollinator perspectives. Biological Reviews 86:33–75.

Gfrerer, E., D. Laina, M. Gibernau, R. Fuchs, M. Happ, T. Tolasch, W. Trutschnig, A. C. Hörger, H. P. Comes, and S. Dötterl. 2021. Floral Scents of a Deceptive Plant Are Hyperdiverse and Under Population-Specific Phenotypic Selection. Frontiers in Plant Science 12:719092.

Gfrerer, E., D. Laina, R. Wagner, M. Gibernau, A. C. Hörger, H. P. Comes, and S. Dötterl. 2022. Antennae of psychodid and sphaerocerid flies respond to a high variety of floral scent compounds of deceptive Arum maculatum L. Scientific Reports 12:5086.

Gibernau, M., D. Macquart, and G. Przetak. 2004. Pollination in the genus *Arum* – a review. Aroideana 27:148–166.

Gierl, A., and M. Frey. 2001. Evolution of benzoxazinone biosynthesis and indole production in maize. Planta 213:493–498.

Goodrich, K. R., M. L. Zjhra, C. A. Ley, and R. A. Raguso. 2006. When Flowers Smell Fermented: The Chemistry and Ontogeny of Yeasty Floral Scent in Pawpaw (Asimina triloba: Annonaceae). International Journal of Plant Sciences 167:33–46.

Goyret, J., P. M. Markwell, and R. A. Raguso. 2007. The effect of decoupling olfactory and visual stimuli on the foraging behavior of *Manduca sexta*. Journal of Experimental Biology 210:1398–1405.

Grant, V., and K. A. Grant. 1965. Flower pollination in the Phlox family. Columbia University Press, New York.

Harborne, J. B. 2001. Twenty-five years of chemical ecology. Natural product reports 18:361–379.

Hemmerlin, A., J. L. Harwood, and T. J. Bach. 2012. A raison d’être for two distinct pathways in the early steps of plant isoprenoid biosynthesis? Progress in lipid research 51:95–148.

Hendry, A. P. 2016. Eco-evolutionary Dynamics. Princeton University Press.

Hernández-Hernández, T., and J. J. Wiens. 2020. Why Are There So Many Flowering Plants? A Multiscale Analysis of Plant Diversification. The American Naturalist 195:948–963.

Hoban, S., J. L. Kelley, K. E. Lotterhos, M. F. Antolin, G. Bradburd, D. B. Lowry, M. L. Poss, L. K. Reed, A. Storfer, and M. C. Whitlock. 2016. Finding the genomic basis of local adaptation: pitfalls, practical solutions, and future directions. The American Naturalist 188:379–397.

Holopainen, J. K. 2004. Multiple functions of inducible plant volatiles. Trends in Plant Science 9:529–533.

Hunter, M. D. 2002. A breath of fresh air: beyond laboratory studies of plant volatile–natural enemy interactions. Agricultural and Forest Entomology 4:81–86.

Huxley, J. 1942. Evolution: The modern synthesis. Allen & Unwin.

Irwin, R. E., L. S. Adler, and A. K. Brody. 2004. The dual role of floral traits: Pollinator attraction and plant defense. Ecology 85:1503–1511.

de Jager, M. L., and R. Peakall. 2016. Does morphology matter? An explicit assessment of floral morphology in sexual deception. Functional Ecology 30:537–546.

Jersáková, J., S. D. Johnson, and P. Kindlmann. 2006. Mechanisms and evolution of deceptive pollination in orchids. Biological Reviews 81:219–235.

Johnson, S. D., and A. Jürgens. 2010. Convergent evolution of carrion and faecal scent mimicry in fly-pollinated angiosperm flowers and a stinkhorn fungus. South African Journal of Botany 76:796–807.

Johnson, S. D., and F. P. Schiestl. 2016. Floral mimicry. Oxford University Press.

Junker, R. R., and A. L. Parachnowitsch. 2015. Working towards a holistic view on flower traits - how floral scents mediate plant-animal interactions in concert with other floral characters. Journal of the Indian Institute of Science 95:43–67.

Kawecki, T. J., and D. Ebert. 2004. Conceptual issues in local adaptation. Ecology letters 7:1225–1241.

Kearns, C. A., D. W. Inouye, and N. M. Waser. 1998. Endangered Mutualisms: The Conservation of Plant-Pollinator Interactions. Annual Review of Ecology and Systematics 29:83–112.

Kite, G. C. 1995. The floral odour of *Arum maculatum*. Biochemical Systematics and Ecology 23:343–354.

Kite, G. C., W. L. A. Hetterscheid, M. J. Lewis, P. C. Boyce, J. Ollerton, E. Cocklin, and A. Diaz. 1998. Inflorescence odours and pollinators of *Arum* and *Amorphophallus* (Araceae). Pages 295–315 *in* S. J. Owens and P. J. Rudall, editors. Reproductive Biology. Royal Botanic Gardens Kew, London, UK.

Knauer, A. C., and F. P. Schiestl. 2015. Bees use honest floral signals as indicators of reward when visiting flowers. Ecology Letters 18:135–143.

Knudsen, J. T., R. Eriksson, J. Gershenzon, and B. Ståhl. 2006. Diversity and distribution of floral scent. The Botanical Review 72:1.

Knudsen, J. T., and J. Gershenzon. 2020. The Chemical Diversity of Floral Scent. Pages 57–78 *in* E. Pichersky and N. Dudareva, editors. Biology of Plant Volatiles. CRC Press.

Knudsen, J. T., and L. Tollsten. 1993. Trends in floral scent chemistry in pollination syndromes: floral scent composition in moth-pollinated taxa. Botanical Journal of the Linnean Society 113:263–284.

Lack, A. J., and A. Diaz. 1991. The pollination of *Arum maculatum* L. - a historical review and new observations. Watsonia 18:333–342.

Laina, D., E. Gfrerer, V. Scheurecker, R. Fuchs, M. Schleifer, C. Zittra, R. Wagner, M. Gibernau, H. P. Comes, A. C. Hörger, and S. Dötterl. 2022. Local Insect Availability Partly Explains Geographical Differences in Floral Visitor Assemblages of *Arum maculatum* L. (Araceae).

Leimu, R., and M. Fischer. 2008. A Meta-Analysis of Local Adaptation in Plants. PLOS ONE 3:e4010.

Lev-Yadun, S., G. Ne'eman, and U. Shanas. 2009. A sheep in wolf's clothing: Do carrion and dung odours of flowers not only attract pollinators but also deter herbivores? BioEssays 31:84–88.

Levin, R. A., L. A. McDade, and R. A. Raguso. 2003. The Systematic Utility of Floral and Vegetative Fragrance in Two Genera of Nyctaginaceae. Systematic Biology 52:334–351.

Majetic, C. J., R. A. Raguso, and T.-L. Ashman. 2009. Sources of floral scent variation: can environment define floral scent phenotype? Plant signaling & behavior 4:129–131.

Marotz-Clausen, G., S. Jürschik, R. Fuchs, I. Schäffler, P. Sulzer, M. Gibernau, and S. Dötterl. 2018. Incomplete synchrony of inflorescence scent and temperature patterns in *Arum maculatum* L. (Araceae). Phytochemistry 154:77–84.

Midgley, J. J., J. D. M. White, S. D. Johnson, and G. N. Bronner. 2015. Faecal mimicry by seeds ensures dispersal by dung beetles. Nature Plants 1:15141.

Mora, C., D. P. Tittensor, S. Adl, A. G. B. Simpson, and B. Worm. 2011. How many species are there on Earth and in the ocean? PLoS biology 9:e1001127.

van der Niet, T., D. M. Hansen, and S. D. Johnson. 2011. Carrion mimicry in a South African orchid: flowers attract a narrow subset of the fly assemblage on animal carcasses. Annals of botany 107:981–992.

Van der Niet, T., and S. D. Johnson. 2012. Phylogenetic evidence for pollinator-driven diversification of angiosperms. Trends in Ecology & Evolution 27:353–361.

Ollerton, J., A. Killick, E. Lamborn, S. Watts, and M. Whiston. 2007. Multiple meanings and modes: on the many ways to be a generalist flower. Taxon 56:717–728.

Ollerton, J., R. Winfree, and S. Tarrant. 2011. How many flowering plants are pollinated by animals? Oikos 120:321–326.

Parachnowitsch, A. L., J. S. Manson, and N. Sletvold. 2019. Evolutionary ecology of nectar. Annals of Botany 123:247–261.

Pare, P. W., and J. H. Tumlinson. 1999. Plant volatiles as a defense against insect herbivores. Plant physiology 121:325–332.

Pelletier, F., D. Garant, and A. P. Hendry. 2009. Eco-evolutionary dynamics. Philosophical Transactions of the Royal Society B 364: 1483–1489.

Pellmyr, O. 2003. Yuccas, Yucca Moths, and Coevolution: A Review. Annals of the Missouri Botanical Garden 90:35–55.

Pellmyr, O., and L. B. Thien. 1986. Insect Reproduction and Floral Fragrances : Keys to the Evolution of the Angiosperms? Taxon 35:76–85.

Pichersky, E., and J. Gershenzon. 2002. The formation and function of plant volatiles: Perfumes for pollinator attraction and defense. Current Opinion in Plant Biology 5:237–243.

du Plessis, M., S. D. Johnson, S. W. Nicolson, P. V Bruyns, and A. Shuttleworth. 2018. Pollination of the “carrion flowers” of an African stapeliad (*Ceropegia mixta*: Apocynaceae): the importance of visual and scent traits for the attraction of flies. Plant Systematics and Evolution 304:357–372.

Policha, T., A. Davis, M. Barnadas, B. T. M. Dentinger, R. A. Raguso, and B. A. Roy. 2016. Disentangling visual and olfactory signals in mushroom-mimicking *Dracula* orchids using realistic three-dimensional printed flowers. New Phytologist 210:1058–1071.

Prieto-Benítez, S., S. Dötterl, and L. Giménez-Benavides. 2016a. Circadian rhythm of a *Silene* species favours nocturnal pollination and constrains diurnal visitation. Annals of botany 118:907–918.

Prieto-Benítez, S., A. M. Millanes, S. Dötterl, and L. Giménez-Benavides. 2016b. Comparative analyses of flower scent in Sileneae reveal a contrasting phylogenetic signal between night and day emissions. Ecology and Evolution 6:7869–7881.

Prime, C. T. 1960. Lords and ladies. Collins.

Ramos, S. E., and F. P. Schiestl. 2019. Rapid plant evolution driven by the interaction of pollination and herbivory. Science 364:193–196.

Regal, P. J. 1977. Ecology and Evolution of Flowering Plant Dominance: Interplay of seed and pollen dispersal systems may explain angiosperm versus gymnosperm dominance. Science 196:622–629.

Renner, S. S. 2006. Rewardless flowers in the angiosperms and the role of insect cognition in their evolution. Pages 123–144 *in* N. M. Waser and J. Ollerton, editors. Plant-pollinator interactions: from specialization to generalization. University of Chicago Press, Chicago.

Reznick, D. N., and C. K. Ghalambor. 2001. The population ecology of contemporary adaptations: what empirical studies reveal about the conditions that promote adaptive evolution. Genetica 112–113:183–198.

Roháček, J., I. Beck-Haug, and K. Dobat. 1990. Sphaeroceridae associated with flowering *Arum maculatum* (Araceae) in the vicinity of Tübingen, SW-Germany. Senckenbergiana biologica 71:259–268.

Savolainen, O., M. Lascoux, and J. Merilä. 2013. Ecological genomics of local adaptation. Nature Reviews Genetics 14:807–820.

Sayers, T. D. J., M. J. Steinbauer, K. Farnier, and R. E. Miller. 2020. Dung mimicry in *Typhonium* (Araceae): explaining floral trait and pollinator divergence in a widespread species complex and a rare sister species. Botanical Journal of the Linnean Society 193:375–401.

Schemske, D. W., and C. C. Horvitz. 1989. Temporal Variation in Selection on a Floral Character. Evolution 43:461–465.

Schiestl, F. P., and S. Dötterl. 2012. The evolution of floral scent and olfactory preferences in pollinators: coevolution or pre-existing bias? Evolution; international journal of organic evolution 66:2042–2055.

Schiestl, F. P., F. K. Huber, and J. M. Gomez. 2011. Phenotypic selection on floral scent: trade-off between attraction and deterrence? Evolutionary Ecology 25:237–248.

Schiestl, F. P., and S. D. Johnson. 2013. Pollinator-mediated evolution of floral signals. Trends in Ecology and Evolution 28:307–315.

Schoener, T. W. 2011. The Newest Synthesis : Understanding Ecological Dynamics. Science 331:426–429.

Smith, S. D. W. 2010. Using phylogenetics to detect pollinator-mediated floral evolution. New Phytologist 188:354–363.

Sprengel, C. K. 1793. Das entdeckte Geheimnis der Natur im Bau und in der Befruchtung der Blumen. Wilhelm Engelmann.

Stebbins, G. L. 1970. Adaptive radiation of reproductive characteristics in angiosperms, I: pollination mechanisms. Annual Review of Ecology and Systematics:307–326.

Stensmyr, M. C., I. Urru, I. Collu, M. Celander, B. S. Hansson, and A.-M. Angioy. 2002. Rotting smell of dead-horse arum florets. Nature 420:625–626.

Stökl, J., A. Strutz, A. Dafni, A. Svatos, J. Doubsky, M. Knaden, S. Sachse, B. S. Hansson, and M. C. Stensmyr. 2010. A Deceptive Pollination System Targeting Drosophilids through Olfactory Mimicry of Yeast. Current Biology 20:1846–1852.

Stork, N. E. 2018. How many species of insects and other terrestrial arthropods are there on Earth. Annual review of entomology 63:31–45.

Takebayashi, N., and P. L. Morrell. 2001. Is self-fertilization an evolutionary dead end? Revisiting an old hypothesis with genetic theories and a macroevolutionary approach. American Journal of Botany 88:1143–1150.

Thompson, J. N. 1994. The coevolutionary process. University of Chicago press.

Thompson, J. N. 2005. The geographic mosaic of coevolution. University of Chicago Press.

Thompson, J. N., C. Schwind, and M. Friberg. 2017. Diversification of Trait Combinations in Coevolving Plant and Insect Lineages. The American Naturalist 190:171–184.

Thompson, J. N., C. Schwind, P. R. Guimarães, and M. Friberg. 2013. Diversification through multitrait evolution in a coevolving interaction. Proceedings of the National Academy of Sciences 110:11487–11492.

Turco, A., P. Medagli, A. Albano, and S. D'Emerico. 2014. Karyomorphometry on three polyploid species of *Arum* L. (Araceae, Aroideae). Comparative cytogenetics 8:71–80.

Urru, I., M. C. Stensmyr, and B. S. Hansson. 2011. Pollination by brood-site deception. Phytochemistry 72:1655–1666.

Vogel, S., and J. Martens. 2000. A survey of the function of the lethal kettle traps of *Arisaema* (Araceae), with records of pollinating fungus gnats from Nepal. Botanical Journal of the Linnean Society 133:61–100.

Vogt, T. 2010. Phenylpropanoid Biosynthesis. Molecular Plant 3:2–20.

Whitehead, M. R., and R. Peakall. 2009. Integrating floral scent, pollination ecology and population genetics. Functional Ecology 23:863–874.

Williams, G. C. 1966. Adaptation and natural selection Princeton University Press.

Willmer, P. 2011. Pollination and floral ecology. Princeton University Press.

Wright, S. I., S. Kalisz, and T. Slotte. 2013. Evolutionary consequences of self-fertilization in plants. Proceedings of the Royal Society B: Biological Sciences 280:20130133.

CHAPTER 2 - Spatial and temporal heterogeneity in pollinator communities maintains within-species floral odour variation

This manuscript is published in Oikos, 2021, Volume 130: pp. 1487-1499 (DOI: https://doi.org/10.1111/oik.08445)

Mark A. Szenteczki[1+*], Adrienne L. Godschalx[1+], Andrea Galmán[2], Anahí Espíndola[3], Marc Gibernau[4^], Nadir Alvarez[5,6^], Sergio Rasmann[1^]

[1] Université de Neuchâtel, Institut de Biologie, Rue Emile-Argand 11, 2000 Neuchâtel, Switzerland

[2] Misión Biológica de Galicia (MBG-CSIC), Pontevedra, Galicia, Spain

[3] Department of Entomology, University of Maryland, Plant Sciences Building 3138, 4291 Fieldhouse Dr., College Park, Maryland, USA

[4] CNRS – University of Corsica, Laboratory Sciences for the Environment (SPE - UMR 6134), Natural Resources Project, Vignola – Route des Sanguinaires, 20000 Ajaccio, France

[5] Geneva Natural History Museum, Route de Malagnou 1, 1208 Genève, Switzerland

[6] Department of Genetics and Evolution, University of Geneva, Quai Ernest-Ansermet 30, 1211 Geneva, Switzerland

[*] Corresponding author: M.A. Szenteczki, Tel. + 41 32 718 23 16

[+] Authors participated equally and are considered joint first authors

[^] Authors participated equally and are considered joint senior authors

ABSTRACT

Flowering plants emit complex bouquets of volatile organic compounds (VOCs) to mediate interactions with their pollinators. These bouquets are undoubtedly influenced by pollinator-mediated selection, particularly in deceptively-pollinated species that rely on chemical mimicry. However, many uncertainties remain regarding how spatially and temporally heterogeneous pollinators affect the diversity and distribution of floral odour variation. Here, we characterized and compared the floral odours of ten populations of deceptively-pollinated *Arum maculatum* (Araceae), and inter-annual and decadal variation in pollinator attraction within these populations. Additionally, we transplanted individuals from all sampled populations to two common garden sites dominated by different pollinator species (*Psychoda phalaenoides* or *Psycha grisescens*), and compared pollinator attraction rates to investigate whether populations maintained odour blends adapted to a specific pollinator. We identified high within- and among-population variation in a common blend of VOCs found across the range of *A. maculatum*. We also observed shifts in pollinator community composition within several populations over 1-2 years, as well as over the past decade. Common garden experiments further revealed that transplanted inflorescences generally attracted the dominant local pollinator species in both transplant sites. However, one population (Forêt du Gâvre, France) appears to exclusively attract *P. grisescens*, even when transplanted to a *P. phalaenoides*-dominated site. Together, our results suggest that maintaining diverse floral odour bouquets within populations may be advantageous when pollinator communities vary over short timescales. We propose that temporally-replicated ecological data are one potential key to understanding variation in complex traits such as floral odour, and in some cases may reveal resiliency to shifting pollinator communities.

KEYWORDS

balancing selection, evolutionary ecology, floral volatiles, plant-pollinator interactions, reciprocal transplant, temporal variation

INTRODUCTION

Widely distributed species are subject to an array of eco-evolutionary settings across their range, due to variation in abiotic conditions and biotic interactions through space and time. These mosaics of selection are known to influence the traits that underpin diverse plant–herbivore and plant–pollinator interactions, affecting the evolutionary trajectories of all species involved (Levin 2000, Hendry 2017). Plant–pollinator interactions appear to be a particularly important mechanism underlying the comparatively rapid rate of speciation in flowering plants (van der Niet and Johnson 2012, Hernández-Hernández and Wiens 2020); this macroevolutionary pattern is the result of microevolutionary processes acting on floral traits at the intraspecific level (Herrera et al. 2006). Understanding the evolutionary and functional ecology of complex floral traits therefore requires data on how plant–pollinator interactions vary through both space and time (Waser and Ollerton 2006). However, characterizing complex trait variation and biotic interactions across wide geographic ranges (Friberg et al. 2019) and through time (Fishbein and Venable 1996) requires substantial effort. As a result, few studies have simultaneously investigated the impact of spatial and temporal variation in pollinators on intraspecific floral trait variation.

As the dominant pollinators across all terrestrial ecosystems, insects exert key selective pressures on many floral traits. They may be attracted or repelled by odour (Whitehead and Peakall 2009), colour (Goyret et al. 2007, du Plessis et al. 2018), morphology (Ibanez et al. 2010, Murúa and Espíndola 2015), nectar (Parachnowitsch et al. 2019), pollen (Dobson and Bergström 2000) or the multimodal expression of several of these traits (reviewed in Junker and Parachnowitsch 2015). Here, we focus on floral odour bouquets, which are often complex blends of many volatile organic compounds (VOCs) that mediate diverse interactions between plants, insects and microbes (Holopainen 2004, Raguso 2008).

Recent studies on plant–pollinator interactions have identified many cases of pollinator-driven evolution of floral odour (Chess et al. 2008, Klahre et al. 2011, Breitkopf et al. 2013, Peter and Johnson 2014, Gross et al. 2016). However, a review by Delle-Vedove et al. (2017) found that floral odour variation often cannot be explained by pollinator-mediated selection alone. Several factors may explain this discrepancy, including tradeoffs between pollinator attraction and chemical defence against herbivory (Schiestl et al. 2014), the nature of the interaction (i.e. deceptive pollination; Renner 2006), biochemical and energetic limitations (Delle-Vedove et al. 2011), phylogenetic constraints in the biosynthetic pathways for VOC production (Raguso et al. 2006), gene flow (Svensson et al. 2005) or genetic drift (Suinyuy et al. 2012). Another factor that may maintain floral odour variation within populations is temporal heterogeneity in pollinator community composition, as a result of pollinator declines (Yuan et al. 2009, Thomann et al. 2013, IPBES 2016, Zattara and Aizen 2021) or shifts in pollinator phenology (Burkle and Runyon 2019). However, the impact of temporally heterogeneous pollinators on floral odour is not yet clearly understood, because most of the aforementioned studies relied on VOC and pollinator data collected at a single timepoint. Here, we aim to address this gap in our knowledge, by examining how spatio–temporal variation in pollination interactions influences floral odour variation in *Arum maculatum* (Araceae).

Arum maculatum inflorescences (Fig. 1) are pollinated deceptively, by emitting complex VOC blends which are known to vary within and among populations in England (Kite 1995, Kite et al. 1998, Diaz and Kite 2002), France (Chartier et al. 2011, 2013) and across the Alps (Gfrerer et al. 2021). The floral odour of *A. maculatum* is similar to dung or decomposing organic matter (Lack and Diaz 1991), mimicking the natural brood sites of their main pollinators, the moth flies *Psychoda phalaenoides* and *Psycha grisescens* (Diptera: Psychodidae). Since pollinators are temporarily trapped in a specialized floral chamber (Bröderbauer et al. 2013) until the day after anthesis (Gibernau et al. 2004), it is possible to collect accurate quantitative data on pollinators attracted by individual inflorescences. Furthermore, pollinators appear to be attracted by VOCs alone (Dormer 1960, Urru et al. 2011), meaning that an inflorescence's reproductive success should be closely tied to its unique floral odour. Since *A. maculatum* floral odour is known to vary, and VOCs such as indole, 2-heptanone and *p*-cresol are attractive to *Psychoda* species (Kite et al. 1998), we chose to focus on floral odour in this study. Specifically, we investigated whether VOC variation is maintained within populations due to temporally variable pollinator communities, or across the species distribution due to spatial divergence in pollinator communities.

Floral odour variation may be maintained within populations through balancing selection (Delph and Kelly 2013) and/or phenotypic plasticity (Callaway et al. 2003, Majetic et al. 2009, Campbell et al. 2019). In the case of *A. maculatum*, balancing selection may occur if relative abundances of *P. phalaenoides* and *P. grisescens* vary temporally within populations (Schemske and Horvitz 1989), or if pollinator learning or avoidance to escape deception (Ayasse et al. 2000, Baguette et al. 2020) leads to frequency-dependent selection. In either case, we would expect to observe high floral odour variation within populations of *A. maculatum* across Europe. Phenotypic plasticity under variable abiotic and biotic conditions may also promote the maintenance of trait variation (Gulisija et al. 2016). If we observe shifts in VOC emissions when *A. maculatum* inflorescences are transplanted to non-native conditions, we may conclude that plasticity also contributes to the maintenance of floral odour variation.

Alternatively, if pollinators only vary spatially, they may exert divergent selective pressures on floral VOCs, leading to locally-adapted bouquets in populations with different pollinators (Leimu and Fischer 2008, Gervasi and Schiestl 2017, Suinyuy and Johnson 2018, Sayers et al. 2020). Previous research has shown that *P. phalaenoides* and *P. grisescens* are respectively trapped by inflorescences in the northern/central and southern/eastern portions of *A. maculatum*'s distribution (Espíndola et al. 2010) – except in the Atlantic fringe of France, where inflorescences trap *P. grisescens*. Furthermore, the population genetic structure of *A. maculatum* roughly aligns with this pattern (Espíndola and Alvarez 2011). Under spatially varying selection, we may predict that distinct *A. maculatum* floral VOCs or phenological adaptations will be maintained in these two pollinator backgrounds. If these variations are local adaptations, we would expect to observe decreased pollinator attraction efficiency when inflorescences are transplanted to non-native pollinator backgrounds.

In this study, we investigated whether variation in *A. maculatum* floral odour was consistent with the patterns predicted under either of the two scenarios described above. To this aim, we surveyed variation in floral odour and pollinator attraction across Europe, and transplanted individuals from all sampled populations to two common garden sites dominated by either *P. phalaenoides* or *P. grisescens*. By selecting populations where pollinator communities were first surveyed a decade ago (Espíndola et al. 2010), we were further able to assess temporal heterogeneity in pollinators at both the inter-annual (i.e. our surveys between 2017 and 2019), and decadal scales, with the aim of understanding how temporally heterogeneous pollinators affect intraspecific floral odour variation. Our specific objectives were to 1) characterize and compare floral odour variation within and among populations of *A. maculatum*, 2) determine whether the pollinators trapped by *A. maculatum* vary spatially and/or temporally and 3) use these results to infer potential drivers of floral VOC variation, namely pollinator-driven balancing selection and local adaptation.

MATERIAL AND METHODS

Natural history and pollination ecology of Arum maculatum

Arum maculatum is a common European flowering plant, which is usually found in shaded areas of deciduous woodlands, particularly beech woods (Bown 2000). Its pollination cycle takes place over two days (reviewed in Gibernau et al. 2004). On the evening of the first day, the appendix is thermogenic and emits a dung-like odour to attract dipteran pollinators; heat alone is not sufficient to attract pollinators (Prime 1960), but likely aids in the dispersal of VOCs such as indole, *p*-cresol and 2-heptanone, which are attractive to *Psychoda* species when used in scented traps (Kite et al. 1998). Notably, the widely distributed *Psychoda phalaenoides* and *Psycha grisescens* are both trapped by *A. maculatum* across most of Europe, together representing 87.49% of all insects found within floral chambers (Espíndola et al. 2010). *Psychoda setigera*, *P. albipennis* and *P. trinodulosa* are also infrequently observed within inflorescences, together representing 0.46% of trapped insects in Espíndola et al. (2010). Other infrequently attracted dipterans include Chironomidae (*Smittia pratorum*), Ceratopogonidae and Sphaeroceridae (Brachycera) (Rohacek et al. 1990, Diaz and Kite 2002, Espíndola et al. 2010).

Psychodidae are also known to be efficient carriers of *Arum* pollen (Diaz and Kite 2002, Albre et al. 2003); one individual can carry 50–150 grains of pollen, and a significant fruit set can develop from a single trapped pollinator (Lack and Diaz 1991). Based on their similar behaviours and morphologies, the above-mentioned *Psychoda* species are all presumably efficient pollinators of *A. maculatum*. However, antennal sensilla are known to vary among Psychodidae (Faucheux and Gibernau 2011), and species may therefore vary in their responses to VOCs. Although *A. maculatum* do not provide any nutritive rewards, this should not be detrimental to trapped *P. phalaenoides* and *P. grisescens*, as they do not feed during their short adult lifespan (P. Withers, cited in Lack and Diaz 1991). The conservation status of *P. phalaenoides* and *P. grisescens* has not been assessed; however, *Psychoda* populations are known to be large and dense (up to thousands of individuals per m^2; Arshad and Moh Leng 1991) due to their reliance on modern agriculture and human activities (e.g. manure and decomposing organic matter) for reproduction (Satchell 1947, Vaillant 1971). Peak *P. phalaenoides* abundances also appear to correspond with the peak flowering period of *A. maculatum* (Ollerton and Diaz 1999).

Field sampling sites

We sampled ten populations of *A. maculatum* (Fig. 1, Supporting information), including three in France (Forêt du Gâvre, Conteville and Chaumont), two in Switzerland (Neuchâtel and Cortaillod), one in Italy (Montese), one in Croatia (Visuć), two in Serbia (Gostilje and Sokobanja) and one in Bulgaria (Chiflik). This sampling covers the majority of the *A. maculatum* species distribution range (Supporting information). During the typical flowering period of *A. maculatum* (April–May), we conducted field sampling each year between 2017 and 2019, visiting each site in at least two years during this timeframe.

Common garden experiment sites

We selected the Swiss population of Neuchâtel and the French population Forêt du Gâvre (on the Atlantic fringe) as our common garden sites, since they were respectively dominated by *Psychoda phalaenoides* and *Psycha grisescens*. We conducted common garden experiments in Neuchâtel in 2018 and 2019, and in Forêt du Gâvre in 2019. These two sites experienced a relatively similar climate; over the course of our sampling in 2019, the mean temperature and humidity in Neuchâtel at the time of sampling were 15.8°C and 61% respectively, and in Forêt du Gâvre, the mean temperature and humidity were 17.2°C and 50% respectively. Five to ten *A. maculatum* individuals with unopened inflorescences were potted in soil from their native habitat, and then transplanted from all ten populations listed above to the two common garden sites. Inflorescences from Neuchâtel and Forêt du Gâvre were also reciprocally transplanted as part of this experiment. The total numbers of inflorescences sampled in situ and in both common garden sites are given in Supporting information.

Floral odour and pollinator sampling methods

During both the field surveys and common garden experiments, we collected dynamic headspace VOCs using identical methods, and analysed them using gas chromatography coupled to mass spectrometry (GC–MS; full details in the Supporting information). Briefly, we collected VOCs from *A. maculatum* inflorescences undergoing anthesis in the early evening on polydimethylsiloxane (PDMS) coated Twister stir bars (Gerstel: Mülheim an der Ruhr, Germany), at an air flow rate of 200 ml min^{-1} for 30 min. Twisters were kept on ice in sealed glass containers until GC–MS analyses, where volatiles were thermally desorbed and separated on a HP-5MS column. During the morning following VOC sampling, we collected all insects trapped within inflorescences and preserved them in 70% ethanol until identification (full identification methods detailed in Supporting information).

Characterizing and comparing floral odour variation across the range of A. maculatum

We compared total VOC emissions within and among populations of field-sampled inflorescences (i.e. VOCs sampled in their native habitats) using Bray–Curtis distance matrices, and visualized inter-individual variation using nonmetric multidimensional scaling (NMDS). Then, to test for a significant effect of population (fixed effect factor) on the entire VOC matrix, we performed pairwise permutational multivariate analysis of variance (PERMANOVA, Bray–Curtis distance, n = 999 permutations) with Bonferroni correction using the *adonis* function in the R ver. 3.6.1 package *vegan* (Oksanen et al. 2019).

Characterizing temporal variation in pollinator community composition

We investigated inter-annual variation in pollinator community composition during our study (i.e. 2017–2019) by calculating Bray–Curtis distance matrices, comparing the mean quantities of pollinators trapped per inflorescence for all populations with in situ pollinator data collected in two or more years. We then visualized the result using nonmetric multidimensional scaling (NMDS) ordinations. Next, we repeated this process to investigate shifts in the dominant pollinators trapped by *A. maculatum* over the past decade. Using Bray–Curtis distance matrices and NMDS ordinations, we compared the mean quantities of 1) Psychodidae species only, and 2) all insect families trapped per inflorescence in our study, with those collected approximately a decade ago (2006–2008; Espíndola et al. 2010).

Identifying VOCs associated with species-specific pollinator attraction

Since we collected paired VOCs and pollinator data for each sampled inflorescence, we were able to correlate these two matrices and identify candidate compounds associated with the attraction of either *P. phalaenoides* or *P. grisescens*. To this aim, we used the Random forest implementation in the R package *randomForest* (Liaw and Wiener 2002), with permutation importance enabled (*ntree* = 500, *mtry* = 8; optimized using the *tuneRF* function). We then calculated conditional feature contributions and identified combinations of compounds which had the greatest influence on the predictive strength of the classifier, using the Python package *TreeInterpreter* (Saabas 2019). As a measure of plasticity in these candidate compounds when flowering in different habitats (i.e. transplant effects), we calculated and plotted population standard scores of these compounds for both in situ and common garden samples. We then used Mann–Whitney U-tests to test whether populations with sufficient sample sizes ($n \geq 8$) emitted different quantities of candidate compounds when transplanted to common garden sites.

Testing for local adaptation to pollinators using common garden experiments

We began by visualizing geographic patterns in mean pollinator attraction for each population in situ, and following transplants to both common garden sites. Then, following the 'local versus foreign' definition of local adaptation (Kawecki and Ebert 2004), we tested the hypotheses that: in the Neuchâtel common garden, transplanted *A. maculatum* inflorescences which attract *P. phalaenoides* in their native population should catch 1) more *P. phalaenoides* and/or 2) more pollinators in total than inflorescences which attract *P. grisescens* in their native population. We expected to observe the inverse result in the Forêt du Gâvre common garden (i.e. transplanted inflorescences that attract *P. grisescens* in their native population should perform better on average in Forêt du Gâvre). These expectations were tested using a two-way ANOVA on $\log + 1$ transformed pollinator counts, including 'native pollinator' (i.e. *P. phalaenoides*- or *P. grisescens*-dominated origin) and 'common garden location' (i.e. whether the common garden site was dominated by *P. phalaenoides* or *P. grisescens*) and their interaction as fixed factors. Here, a significant interaction would indicate local adaptation, which could be confirmed using contrasts comparing trait values between native and transplant sites. Finally, we analysed 'deme × habitat' interactions (Kawecki and Ebert 2004) for mean attraction rates of *P. phalaenoides*, *P. grisescens* and all insects. Here, deme and habitat respectively referred to an *A. maculatum* population and its local pollinator community conditions. In this analysis, data were subset based on each inflorescence's native pollinator and common garden location, as described above.

<u>RESULTS</u>

Floral odour is highly variable within and among A. maculatum populations

After filtering out compounds present in blank samples, we retained 18 *A. maculatum* floral VOCs present in relative abundances above 1% (Table 1). All of the major compounds we identified (e.g. indole, *p*-cresol, 2-heptanone, β-citronellene and three unnamed sesquiterpenes) had been previously reported in studies of *A. maculatum* floral odour (Diaz and Kite 2002, Chartier et al. 2013, Marotz-Clausen et al. 2018). We observed substantial variation in floral odour both within (Fig. 1) and among populations (Fig. 2).

Pollinator communities are variable at both annual and decadal scales

Our sampling allowed us to compare inter-annual (i.e. 2017/2018 versus 2019) variation in Psychodidae trapped by *A. maculatum* in six populations. The dominant Psychodidae species trapped by inflorescences appear to have shifted in three of these populations (Conteville, FR, Neuchâtel, CH and Visuć, HRV) over this time period (Fig. 3).

We also observed temporal shifts in the average abundances of trapped Psychodidae in several populations over the past decade (i.e. compared to Espíndola et al. 2010). The relative compositions of the complete pollinator communities trapped by A. maculatum appears to have shifted in five out of six populations where comparisons could be made; only Forêt du Gâvre remained consistent over the past decade (Supporting information). We also observed apparent shifts in the dominant Psychodidae pollinator trapped within inflorescences in four out of six populations over the past decade, in Chaumont FR, Conteville FR, Gostilje SRB and Visuć, HRV (Table 2, Supporting information).

Low population-level VOC divergence coincides with temporally variable pollinators

PERMANOVA pairwise contrasts did not identify any pairs of populations with significant divergence in their proportional emissions of VOCs sampled in their native habitats, after correction for multiple testing. This lack of population-level differentiation in VOC blends is evident when visualizing Bray–Curtis similarities between field-sampled individuals (Fig. 2), and appears to coincide with the temporal heterogeneity in pollinator communities identified in the previous section (Fig. 3, Supporting information).

Arum maculatum populations typically are not locally adapted to specific pollinators

Through Random Forest analyses (Supporting information), we identified one compound positively associated with *P. phalaenoides* attraction (β-humulene), and three compounds positively associated with *P. grisescens* attraction (unnamed sesquiterpenes RI 1470 and 1681, and α-selinene). After evaluating combined feature contributions within the Random forest classifier, we found that its predictive strength was most strongly influenced by unnamed sesquiterpene (RI 1681) alone. Other strong combinations included unnamed sesquiterpene RI 1681 paired with unnamed sesquiterpene RI 1470 or α-selinene, as well as β-humulene alone, mirroring our initial results (full *Treeinterpreter* results in the Supporting information).

The four candidate compounds we identified (β-humulene, unnamed sesquiterpenes RI 1470 and 1681, and α-selinene) were widely observed and not restricted to a specific region or pollinator background. Average emissions of these compounds remained relatively consistent between in situ collections and samples transplanted to Neuchâtel, though some appeared to increase after inflorescences were transplanted to Forêt du Gâvre (Supporting information). We only observed a significant transplant effect in one compound (an increase in unnamed sesquiterpene RI 1470) within one population, Neuchâtel (Mann–Whitney tests; full result in the Supporting information).

In both common garden sites, we observed that transplanted inflorescences typically attracted the dominant local pollinator species as efficiently as native inflorescences (Fig. 1). While common garden location had a significant effect on the quantity of *P. phalaenoides* and *P. grisescens* caught by *A. maculatum* (i.e. the two transplant sites were dominated by different Psychodidae species), no native pollinator × common garden location interaction effect was observed (2-way ANOVA, Pr(>F) > 0.05; full results in the Supporting information). Together, these results suggest that *A. maculatum* populations are generally not locally adapted to a single pollinator species (Fig. 4), with notable exceptions in Forêt du Gâvre and the two Serbian populations Gostilje and Sokobanja, which will be discussed below.

While we do not find general indications of populations being locally adapted to specific pollinators, not all inflorescences were equally attractive to all pollinator species. One population (Forêt du Gâvre) continued to exclusively attract their native pollinator *P. grisescens* when transplanted to the Neuchâtel common garden (Fig. 1). Remarkably, this exclusive attraction of *P. grisescens* was maintained even though *P. phalaenoides* was also present (and trapped by inflorescences from other populations) at the time when inflorescences from Forêt du Gâvre opened (Supporting information). Additionally, transplanted inflorescences occasionally attracted the ‘non-dominant' Psychodidae species in both common garden sites, and a third *Psychoda* species (*Psychoda trinodulosa*) was also identified within inflorescences in Croatia and Serbia during our field surveys. *Psychoda trinodulosa* was also observed in the Neuchâtel common garden, but not in Forêt du Gâvre; inflorescences from both Serbian populations (Gostilje and Sokobanja) continued to occasionally attract *P. trinodulosa* when transplanted to the Neuchâtel common garden (Fig. 1).

DISCUSSION

In this study, we identified substantial within-and among-population variation in *A. maculatum* floral odour (Fig. 1, 2) and shifts in pollinator community composition in several populations at both the inter-annual (Fig. 3) and decadal scales (Supporting information). Although some *A. maculatum* populations continued to attract their native pollinators in transplant sites (e.g. Forêt du Gâvre and Serbian populations), most populations did not exclusively attract *P. phalaenoides* or *P. grisescens* when transplanted to ‘foreign' pollinator backgrounds (Fig. 4). Since this result does not appear to be due to transplant effects/phenotypic plasticity (Supporting information), this leaves temporally heterogeneous pollinator communities as a potential mechanism underlying the maintenance of high within-population variation in floral odour.

The influence of temporally variable pollinators on A. maculatum floral odour

Overall, it appears that local pollinator availability at the time of anthesis plays a key role in the quantity and composition of pollinators trapped within *A. maculatum* inflorescences. Previous studies on *A. maculatum* pollination in England (Diaz and Kite 2002) and France (Chartier et al. 2013) arrived at a similar conclusion. The difference in sex ratios, particularly that no male *P. phalaenoides* or *P. trinodulosa* are attracted, may be due to differences in copulation timing among *Psychoda* species (i.e. immediately after adult emergence), and parthenogenetic reproduction (F. Vaillant, cited in Albre et al. 2003), or brood-site specific VOCs which are only attractive to females of these two species. While we were unable to reliably collect data on background pollinator communities as part of our sampling design, Diaz and Kite (2002) found that Psychodidae species caught on sticky traps mirrored those found within *A. maculatum* and *A. italicum* inflorescences. Therefore, our data should still allow us to infer whether the patterns in pollinator attraction we observed within each population were a consequence of balancing selection or local adaptation.

Balancing selection may maintain variation within populations through several selective regimes, including relaxed selection, negative frequency-dependent selection due to pollinator learning, or environmental heterogeneity (Delph and Kelly 2013). While relaxed selection on floral odour has been observed in some angiosperms (Salzmann et al. 2007), this is unlikely to be the case for deceptively pollinated *A. maculatum*, given that pollinator attraction is driven by VOC emissions alone (Dormer 1960, Lack and Diaz 1991). Pollinator learning has been shown to maintain polymorphism in floral colour (Gigord et al. 2001) and odour (Ayasse et al. 2000), but this is also less likely to occur in the case of *A. maculatum*. Psychodidae likely experience weak and inconsistent selective pressures caused by deception, due to their large population sizes and short generation times (Prime 1960, Lachmann et al. 2000), and potentially sex-specific attraction in some cases. Araceae also exploit pre-existing VOC detection abilities in their pollinators (Schiestl and Dötterl 2012), which likely contributes to their persistent inability to distinguish deceptive inflorescences (Renner 2006). This leaves temporal heterogeneity in pollinator communities as the mechanism most likely contributing to the maintenance of diverse floral odour bouquets in *A. maculatum*.

In this study, we demonstrated that pollinator communities can vary within populations over relatively short time periods (i.e. over the years- to decade-scale) across most of the range of *A. maculatum*. Temporally heterogeneous pollinators have long been known to influence floral traits (Schemske and Horvitz 1989), but to our knowledge, have not been investigated as a mechanism underlying floral odour variation. Further research on temporal variation in pollinators may provide clarity in other cases where floral trait variation in deceptively pollinated species cannot be explained by pollinator learning (Pellegrino et al. 2005, Jersáková et al. 2006). Temporally variable pollinators may have also contributed to the finding that, contrary to expectations, deceptively pollinated species generally do not maintain more variable floral odours than rewarding species (Ackerman et al. 2011, Delle-Vedove et al. 2017).

Currently, it is not known whether the phenologies of *P. phalaenoides* and *P. grisescens* are influenced by environmental variation; our data indicate that at least in Forêt du Gâvre, *P. grisescens* emerges slightly earlier than *P. phalaenoides* (Supporting information). A recent environmental DNA survey of cow dung (Sigsgaard et al. 2021) also identified *P. phalaenoides, P. trinodulosa* and *P. grisescens* all within a single site in Mols Bjerge, Denmark. At the time the sample was taken (June 2019; i.e. later than our field surveys), *P. phalaenoides* overwhelmingly predominated over all other insects in terms of read counts (i.e. abundance). Taken together, these results corroborate two key points: all of the major Psychodidae pollinators of *A. maculatum* are present across the range of *A. maculatum* (Ježek et al. 2018), and their relative abundances may vary temporally over the course of the flowering period.

If environmental variation influences pollinator phenology, then plasticity in floral odour based on the same environmental cues might enhance pollinator attraction. With one exception in a single population (i.e. unnamed sesquiterpene RI 1470 emitted by inflorescences from Neuchâtel), we did not observe significant shifts in the four candidate compounds linked to species-specific pollinator attraction following transplants to common gardens (i.e. phenotypic plasticity). However, as we transplanted mature inflorescences, some environmental effects may have already been in place prior to transplanting (Wund 2012). Growing *A. maculatum* for several generations in common garden sites would give a more accurate result and eliminate maternal effects, but this was not feasible within the scope of our study, as *A. maculatum* requires at least two years (and sometimes longer) from germination to flowering (Bown 2000). Given the central role of VOCs in *A. maculatum* pollination (Kite 1995, Kite et al. 1998), it is unlikely that the high variation in floral odour we observed is the result of plasticity alone. Further research tracking the VOC emissions of the same individual over multiple flowering events would provide greater resolution into environmental influences on floral odour variation.

Since *A. maculatum* are rhizomatous, variation may also persist within populations for longer periods of time compared to annual plants. Gene flow between populations may also contribute to the maintenance of floral odour variation within populations. Pollen dispersal by Psychodidae is likely limited due to their poor flying abilities and short adult lifespans (Lack and Diaz 1991), but seed dispersal by frugivorous birds (Snow and Snow 1988) could lead to gene flow among nearby populations. While there appears to be a strong barrier to gene flow between populations from north/central Europe, and from Italy and the Balkans (Espíndola and Alvarez 2011), our data suggest that floral odour variation is widely maintained across this barrier. This pattern suggests that – at least regionally – balancing selection is at work, possibly in association with phenotypic plasticity and/or local adaptation in populations with consistent pollinator communities.

The influence of spatially variable pollinators on A. maculatum floral odour

The results from our Europe-wide transplant and common garden experiment do not support the hypothesis that all *A. maculatum* populations are (locally) adapted to attract exclusively *P. phalaenoides* or *P. grisescens*. This contrasts with the patterns found in other wide-ranging deceptively pollinated species such as the sexually deceptive orchids *Ophrys sphegodes* (Breitkopf et al. 2013) and *Ophrys insectifera* (Triponez et al. 2013), but aligns with the results of a previous reciprocal transplant experiment between two *A. maculatum* populations in France (Chartier et al. 2013). However, we found that the Forêt du Gâvre population in coastal NW France appears to have lost the ability to attract *P. phalaenoides*, possibly due to local adaptation and/or genetic drift; the latter process is known to occur at the limits of species ranges (Geber 2011, Gould et al. 2013). Interestingly, Forêt du Gâvre is also the only population in this study with little recorded inter-annual and decade-scale variation in pollinator communities. It is therefore possible that the pollinator attraction patterns we observed are a result of selective pressures imposed by the likely stable population of *P. grisescens* in this site. Further transplants of Forêt du Gâvre inflorescences to additional populations are needed to test this hypothesis.

Our results also do not exclude the possibility that individual VOCs are differentially attractive to certain Psychodidae species. First, we identified four sesquiterpenes that were able to predict the attraction of *P. phalaenoides* (β-humulene) and *P. grisescens* (unidentified sesquiterpenes RI 1470 and 1681, and α-selinene) through Random Forest analyses. Additionally, both Serbian populations in this study (Gostilje and Sokobanja) attracted a third Psychodidae species (*P. trinodulosa*) in situ and following transplants to the Neuchâtel common garden, suggesting that there may also be VOCs related to species-specific attraction of *P. trinodulosa*. These patterns suggest that specific compounds emitted by inflorescences from Serbia may also be differentially attractive to *P. trinodulosa*. However, this species was too infrequently observed in our study to make any firm conclusions; further studies of these populations are needed to address this question.

In this study, the VOCs typically associated with Psychodidae brood sites (e.g. indole, *p*-cresol and 2-heptanone) were not correlated with species-specific pollinator attraction. A recent study by Gfrerer et al. (2021) also found that variation in the aforementioned foetid-smelling VOCs were not among those which significantly influenced fruit sets in *A. maculatum*. Given that blends of indole, *p*-cresol and 2-heptanone are known to be attractive to *Psychoda* species (Kite et al. 1998), these compounds appear to be generally attractive to all species. However, blends of VOCs (e.g. with specific sesquiterpenes) or the ratios at which they are emitted may be differentially attractive. Behavioural assays, where different pollinator species are presented with several *A. maculatum* inflorescences or individual VOCs, would be useful in identifying which compounds or blends elicit general or species-specific responses. Similarly, gas chromatography–electroantennography (GC–EAD; Cork et al. 1990) could be used to identify all VOCs which elicit a physiological response in different pollinator species. The *A. maculatum* populations with unique patterns in pollinator attraction identified in this study may be useful targets for future research testing whether selection is acting on specific compounds (Stensmyr et al. 2002, Urru et al. 2010), or on ‘super-attractive mixtures' (e.g. in *A. palaestinum*; Stökl et al. 2010).

Conclusion

To date, almost all studies on floral odour and pollinator variation have been carried out at a single timepoint – possibly contributing to the numerous cases where floral odour diversity appears to exceed pollinator diversity (Delle-Vedove et al. 2017). As evidenced by the extensive literature on local adaptation in plants (Leimu and Fischer 2008), spatially varying selection is an undoubtedly important driver of floral odour divergence, and appears to have influenced a few *A. maculatum* populations (e.g. Forêt du Gâvre) as well. However, the variable floral odour bouquets emitted by *A. maculatum* may also represent an important adaptation to temporally heterogeneous pollinator communities, if the pollinator shifts we observed have been occurring over longer periods of time. In closing, we advocate for increased attention on the temporal dimension of pollinator-mediated selection. By simultaneously studying spatial and temporal variation in selection, we may further our understanding of how and why flowering plants maintain high diversity in key functional traits such as floral odour.

ACKNOWLEDGEMENTS

We thank Gregory Roeder for his assistance with the processing of our VOC samples, Jérôme Albre for his assistance in Psychodidae identification, and Alberto Garcia Jimenez and Monica Fleisher for their dedicated assistance during our field sampling. We also thank Laurent Oppliger and colleagues at the Jardin Botanique de Neuchâtel for their support in hosting and maintaining our experimental populations of Arum inflorescences. We are grateful to Dr. Ignasi Bartomeus for his constructive comments on this manuscript. The project was funded by the Swiss National Science Foundation through grant 31003A_163334 awarded to NA and SR.

DATA ACCESSIBILITY

Data available from the Dryad Digital Repository:
http://dx.doi.org/10.5061/dryad.v15dv41w7 (Szenteczki et al. 2021).

AUTHOR CONTRIBUTIONS

Mark Szenteczki and Adrienne Godschalx participated equally and are considered joint first authors. Marc Gibernau, Nadir Alvarez and Sergio Rasmann participated equally and are considered joint senior authors. Mark Szenteczki: Conceptualization (equal); Formal analysis (lead); Investigation (equal); Methodology (equal); Writing – original draft (lead); Writing – review and editing (lead). Adrienne Godschalx: Conceptualization (equal); Formal analysis (equal); Investigation (equal); Methodology (equal); Writing – original draft (lead); Writing – review and editing (equal). Andrea Galmán: Methodology (equal); Writing – review and editing (equal). Anahí Espíndola: Investigation (supporting); Resources (supporting); Writing – review and editing (equal). Marc Gibernau: Conceptualization (equal); Funding acquisition (supporting); Investigation (equal); Methodology (equal); Resources (supporting); Supervision (equal); Writing – review and editing (equal). Nadir Alvarez: Conceptualization (equal); Formal analysis (supporting); Funding acquisition (lead); Investigation (equal); Methodology (equal); Supervision (equal); Writing – original draft (equal); Writing – review and editing (equal). Sergio Rasmann: Conceptualization (equal); Formal analysis (supporting); Funding acquisition (lead); Investigation (equal); Methodology (equal); Supervision (equal); Writing – original draft (equal); Writing – review and editing (equal).

REFERENCES

Ackerman, J.D., Cuevas, A.A. & Hof, D. (2011) Are deception-pollinated species more variable than those offering a reward? *Plant Systematics and Evolution*, **293**, 91–99.

Albre, J., Quilichini, A. & Gibernau, M. (2003) Pollination ecology of *Arum italicum* (Araceae). *Botanical Journal of the Linnean Society*, **141**, 205–214.

Arshad, A., & Moh Leng, K.Y. (1991) Preliminary population assessment of *Psychoda alternata* (Diptera: Psychodidae) in soil irrigated with wastewater for turf cultivation. *The Florida Entomologist*, **74**, 591–596.

Ayasse, M., Schiestl, F.P., Paulus, H.F., Löfstedt, C., Hansson, B., Ibarra, F. & Francke, W. (2000) Evolution Of Reproductive Strategies In The Sexually Deceptive Orchid *Ophrys Sphegodes*: How Does Flower-Specific Variation Of Odor Signals Influence Reproductive Success? *Evolution*, **54**, 1995–2006.

Baguette, M., Bertrand, J., Stevens, V. M., & Schatz, B. (2020) Why are there so many bee-orchid species? Adaptive radiation by intraspecific competition for mnemonic pollinators. *Biological Reviews*, **95**, 1630–1663.

Breitkopf, H., Schlüter, P.M., Xu, S., Schiestl, F.P., Cozzolino, S. & Scopece, G. (2013) Pollinator shifts between *Ophrys sphegodes* populations: might adaptation to different pollinators drive population divergence? *Journal of Evolutionary Biology*, **26**, 2197–2208.

Bröderbauer, D., Weber, A. & Diaz, A. (2013) The design of trapping devices in pollination traps of the genus *Arum* (Araceae) is related to insect type. *Botanical Journal of the Linnean Society*, **172**, 385–397.

Bown, D. (2000) *Aroids: Plants of the Arum family*. Timber Press.

Burkle, L.A., & Runyon, J.B. (2019) Floral volatiles structure plant–pollinator interactions in a diverse community across the growing season. *Functional Ecology* **33**: 2116–2129.

Callaway, R.M., Pennings, S.C. & Richards, C.L. (2003) Phenotypic Plasticity and Interactions Among Plants. *Ecology*, **84**(5), 1115–1128.

Campbell, D.R., Sosenski, P.A. & Raguso, R. (2019) Phenotypic plasticity of floral volatiles in response to increasing drought stress. *Annals of Botany*, **123**, 601–610.

Chartier, M., Pélozuelo, L. & Gibernau, M. (2011) Do floral odor profiles geographically vary with the degree of specificity for pollinators? Investigation in two sapromyophilous *Arum* species (Araceae). *Annales de la Société entomologique de France*, **47**, 71–77.

Chartier, M., Pélozuelo, L., Buatois, B., Bessière, J.-M. & Gibernau, M. (2013) Geographical variations of odour and pollinators, and test for local adaptation by reciprocal transplant of two European *Arum* species. *Functional Ecology*, **27**, 1367–1381.

Chess, S.K.R., Raguso, R.A. & Lebuhn, G. (2008) Geographic divergence in floral morphology and scent in *Linanthus dichotomus* (Polemoniaceae). *American Journal of Botany*, **95**, 1652–1659.

Cork, A., Beevor, P.S., Gough, A.J.E. & Hall, D.R. (1990) Gas Chromatography Linked to Electroantennography: A Versatile Technique for Identifying Insect Semiochemicals. *Chromatography and isolation of insect hormones and pheromones* (eds A.R. McMaffercy & I.D. Vilson), pp. 271–279. Plenum Press.

Delle-Vedove, R., Juillet, N., Bessière, J.-M., Grison, C., Barthes, N., Pailler, T., Dormont, L. & Schatz, B. (2011) Colour-scent associations in a tropical orchid: Three colours but two odours. *Phytochemistry*, **72**, 735–742.

Delle-Vedove, R., Schatz, B. & Dufay, M. (2017) Understanding intraspecific variation of floral scent in light of evolutionary ecology. *Annals of Botany*, **120**, 1–20.

Delph, L.F. & Kelly, J.K. (2013) On the importance of balancing selection in plants. *New Phytologist*, **201**, 45–56.

Diaz, A. & Kite, G.C. (2002) A comparison of pollination ecology of *Arum maculatum* and *A. italicum* in England. *Watsonia*, **24**, 171–181.

Dobson, H.E.M. & Bergström, G.E.M. (2000) The ecology and evolution of pollen odors. *Plant Systematics and Evolution*, **222**, 63–87.

Dormer, K.J. (1960) The Truth About Pollination In *Arum*. *New Phytologist*, **59**, 298–301.

du Plessis, M., Johnson, S.D., Nicolson, S.W., Bruyns, P.V. & Shuttleworth, A. (2018) Pollination of the “carrion flowers” of an African stapeliad (*Ceropegia mixta*: Apocynaceae): the importance of visual and scent traits for the attraction of flies. *Plant Systematics and Evolution*, **304**, 357–372.

Espíndola, A., Pellissier, L. & Alvarez, N. (2010) Variation in the proportion of flower visitors of Arum maculatum along its distributional range in relation with community-based climatic niche analyses. *Oikos*, **120**, 728–734.

Espíndola, A. & Alvarez, N. (2011) Comparative Phylogeography in a Specific and Obligate Pollination Antagonism. *PLoS ONE*, **6**, e28662.

Faucheux, M.J. & Gibernau, M. (2011) Antennal sensilla in five Psychodini moth flies (Diptera: Psychodidae: Psychodinae) pollinators of *Arum* spp. (Araceae). *Annales de la Société entomologique de France*, **47**, 89–100.

Fishbein, M. & Venable, D.L. (1996) Diversity and Temporal Change in the Effective Pollinators of *Asclepias Tuberosa*. *Ecology*, **77**, 1061–1073.

Friberg, M., Schwind, C., Guimarães, P.R., Raguso, R.A. & Thompson, J.N. (2019) Extreme diversification of floral volatiles within and among species of Lithophragma (Saxifragaceae). *Proceedings of the National Academy of Sciences*, **116**, 4406–4415.

Geber, M.A. (2011) Ecological and Evolutionary Limits to Species Geographic Ranges. *The American Naturalist*, **178**, S1–S5.

Gervasi, D.D.L. & Schiestl, F.P. (2017) Real-time divergent evolution in plants driven by pollinators. *Nature Communications*, **8**, 14691.

Gfrerer, E., Laina, D., Gibernau, M., Fuchs, R., Happ, M., Tolasch, T., Trutschnig, W., Hörger, A.C., Comes, H.P., & Dötterl, S. (2021) Floral scents of a deceptive plant are hyperdiverse and under population-specific phenotypic selection. *BioRxiv*, 441155 [Preprint] https://doi.org/10.1101/2021.04.28.441155

Gibernau, M., Macquart, D. & Przetak, G. (2004) Pollination in the Genus *Arum* - a Review. *Aroideana*, **27**, 148–166.

Gigord, L.D.B., Macnair, M.R. & Smithson, A. (2001) Negative frequency-dependent selection maintains a dramatic flower color polymorphism in the rewardless orchid *Dactylorhiza sambucina* (L.) Soo. *Proceedings of the National Academy of Sciences*, **98**, 6253–6255.

Gould, B., Moeller, D.A., Eckhart, V.M., Tiffin, P., Fabio, E. & Geber, M.A. (2013) Local adaptation and range boundary formation in response to complex environmental gradients across the geographical range of *Clarkia xantiana* ssp. *xantiana*. *Journal of Ecology*, **102**, 95–107.

Goyret, J., Markwell, P.M. & Raguso, R.A. (2007) The effect of decoupling olfactory and visual stimuli on the foraging behavior of *Manduca sexta*. *Journal of Experimental Biology*, **210**, 1398–1405.

Gross, K., Sun, M. & Schiestl, F.P. (2016) Why Do Floral Perfumes Become Different? Region-Specific Selection on Floral Scent in a Terrestrial Orchid. *Plos One*, **11**.

Gulisija, D., Kim, Y. & Plotkin, J.B. (2016) Phenotypic Plasticity Promotes Balanced Polymorphism in Periodic Environments by a Genomic Storage Effect. *Genetics*, **202**, 1437–1448.

Hendry, A.P. (2017) *Eco-evolutionary dynamics*. Princeton Univ. Press, Princeton.

Hernández-Hernández, T. & Wiens, J.J. (2020) Why are there so many flowering plants? A multi-scale analysis of plant diversification. *The American Naturalist*.

Herrera, C.M., Castellanos, M.C. & Medrano, M. (2006) Geographical context of floral evolution: towards an improved research programme in floral diversification. *Ecology and evolution of flowers* (eds L.D. Harder & S.C.H. Barrett), pp. 278–294. Oxford Univ. Press.

Holopainen, J. (2004) Multiple functions of inducible plant volatiles. *Trends in Plant Science*, **9**, 529–533.

Ibanez, S., Dötterl, S., Anstett, M.-C., Baudino, S., Caissard, J.-C., Gallet, C. & Després, L. (2010) The role of volatile organic compounds, morphology and pigments of globeflowers in the attraction of their specific pollinating flies. *New Phytologist*, **188**, 451–463.

IPBES (2016). *The assessment report of the Intergovernmental Science-Policy Platform on Biodiversity and Ecosystem Services on pollinators, pollination and food production.* (eds S.G. Potts, V.L. Imperatriz-Fonseca, & H.T. Ngo). Secretariat of the Intergovernmental Science-Policy Platform on Biodiversity and Ecosystem Services, Bonn, Germany.

Jersáková, J., Kindlmann, P. & Renner, S.S. (2006) Is the colour dimorphism in *Dactylorhiza sambucina* maintained by differential seed viability instead of frequency-dependent selection? *Folia Geobotanica*, **41**, 61–76.

Ježek, J., Oboňa, J., Přikryl, I., & Mikátová, B. (2018) Moth flies (Diptera: Psychodidae) of the western Hercynian mountains, Sokolov open-cast coal mines and dumps (Czech Republic). *Acta Musei Silesiae, Scientiae Naturales* **67**, 193–292.

Junker, R.R. & Parachnowitsch, A.L. (2015) Working Towards a Holistic View on Flower Traits— How Floral Scents Mediate Plant–Animal Interactions in Concert with Other Floral Characters. *Journal of the Indian Institute of Science*, **95**, 43–67.

Kawecki, T.J. & Ebert, D. (2004) Conceptual issues in local adaptation. *Ecology Letters*, **7**, 1225–1241.

Kite, G.C., Hetterscheid, W.L.A., Lewis, M.J., Boyce, P.C., Ollerton, J., Cocklin, E., Diaz, A. & Simmonds, M.S.J. (1998) Inflorescence odours and pollinators of *Arum* and *Amorphophallus* (Araceae). *Reproductive Biology* (eds S.J. Rudall & P.J. Owens), pp. 295–315. Royal Botanic Garden, Kew.

Kite, G.C. (1995) The floral odour of *Arum maculatum*. *Biochemical Systematics and Ecology*, **23**, 343–354.

Klahre, U., Gurba, A., Hermann, K., Saxenhofer, M., Bossolini, E., Guerin, P.M. & Kuhlemeier, C. (2011) Pollinator Choice in Petunia Depends on Two Major Genetic Loci for Floral Scent Production. *Current Biology*, **21**, 730–739.

Lachmann, A.D., Baier, C., & Mierke, M. (2000) Life cycle of *Psychoda cinerea*, *P. parthenogenetica* and *P. trinodulosa* (Diptera, Psychodidae). 2. Adults. *Studia dipterologica*, **7**, 533–542.

Lack, A.J. & Diaz, A.J. (1991) The pollination of *Arum maculatum* L. – a historical review and new observations. *Watsonia*, **18**, 333–342.

Leimu, R. & Fischer, M. (2008) A Meta-Analysis of Local Adaptation in Plants. *PLoS ONE*, **3**, e4010.

Levin, D.A. (2000) *The Origin, Expansion and Demise of Plant Species*. Oxford Univ. Press.

Liaw, A. & Wiener, M. (2002) Classification and Regression by randomForest. *R News*, **2**, 18–22.

Majetic, C.J., Raguso, R.A. & Ashman, T.-L. (2009) Sources of floral scent variation: can environment define floral scent phenotype? *Plant Signaling & Behavior*, **4**, 129–131.

Marotz-Clausen, G., Jürschik, S., Fuchs, R., Schäffler, I., Sulzer, P., Gibernau, M. & Dötterl, S. (2018) Incomplete synchrony of inflorescence scent and temperature patterns in *Arum maculatum* L. (Araceae). *Phytochemistry*, **154**, 77–84.

Murúa, M., & Espíndola, A. (2015) Pollination syndromes in a specialized plant-pollinator interaction: does floral morphology predict pollinators in *Calceolaria*? *Plant Biology* **17** (2): 551–557.

Ollerton, J., & Diaz, A. (1999). Evidence for stabilising selection acting on flowering time in *Arum maculatum* (Araceae): The influence of phylogeny on adaptation. *Oecologia*, **119**, 340–348.

Oksanen, J., Blanchet, F.G., Friendly, M., Kindt, R., Legendre, P., McGlinn, D., Minchin, P.R., O'Hara, R.B., Simpson, G.L., Solymos, P., Stevens, M.H.H., Szoecs, E. & Wagner, H. (2019) vegan: Community Ecology Package. R package version 2.5-6 https://CRAN.R-project.org/package=vegan

Parachnowitsch, A.L., Manson, J.S. & Sletvold, N. (2019) Evolutionary ecology of nectar. *Annals of Botany*, **123**, 247–261.

Pellegrino, G., Caimi, D., Noce, M.E. & Musacchio, A. (2005) Effects of local density and flower colour polymorphism on pollination and reproduction in the rewardless orchid *Dactylorhiza sambucina* (L.). *Plant Systematics and Evolution*, **251**, 119–129.

Peter, C.I. & Johnson, S.D. (2014) A pollinator shift explains floral divergence in an orchid species complex in South Africa. *Annals of Botany*, **113**, 277–288.

Prime, C.T. (1960) *Lords & ladies: New Naturalist monograph no.17.* Collins.

R Core Team (2019) R: A language and environment for statistical computing. R Foundation for Statistical Computing, Vienna, Austria. https://www.R-project.org/

Raguso, R.A., Schlumpberger, B.O., Kaczorowski, R.L. & Holtsford, T.P. (2006) Phylogenetic fragrance patterns in *Nicotiana* sections Alatae and Suaveolentes. *Phytochemistry*, **67**, 1931–1942.

Raguso, R.A. (2008) Wake Up and Smell the Roses: The Ecology and Evolution of Floral Scent. *Annual Review of Ecology, Evolution, and Systematics*, **39**, 549–569.

Renner, S.S. (2006) Rewardless flowers in the angiosperms and the role of insect cognition in their evolution. *Plant–pollinator interactions: from specialization to generalization* (eds N.M. Waser & J. Ollerton), pp. 123–144. Univ. of Chicago Press.

Rohacek, J., Beck-Haug, I. & Dobat, K. (1990) Sphaerocidae associated with flowering *Arum maculatum* (Araceae) in the vicinity of Tübingen, SW Germany. *Senckenbergiana biologica*, **71**, 259–268.

Saabas, A. (2019) Treeinterpreter library. https://github.com/andosa/treeinterpreter

Salzmann, C.C., Nardella, A.M., Cozzolino, S. & Schiestl, F.P. (2007) Variability in Floral Scent in Rewarding and Deceptive Orchids: The Signature of Pollinator-imposed Selection? *Annals of Botany*, **100**, 757–765.

Satchell, G.H. (1947) The ecology of the British species of *Psychoda* (Diptera, Psychodidae). *Annals of Applied Biology*, **34**, 611-621.

Sayers, T.D.J., Steinbauer, M.J., Farnier, K. & Miller, R.E. (2020) Dung mimicry in *Typhonium* (Araceae): explaining floral trait and pollinator divergence in a widespread species complex and a rare sister species. *Botanical Journal of the Linnean Society*, **193**, 375–401.

Schemske, D.W. & Horvitz, C.C. (1989) Temporal Variation in Selection on a Floral Character. *Evolution*, **43**, 461.

Schiestl, F. P., & Dötterl, S. (2012). The Evolution of Floral Scent And Olfactory Preferences In Pollinators: Coevolution Or Pre-Existing Bias? *Evolution*, **66**(7), 2042–2055.

Schiestl, F.P., Kirk, H., Bigler, L., Cozzolino, S. & Desurmont, G.A. (2014) Herbivory and floral signaling: phenotypic plasticity and tradeoffs between reproduction and indirect defense. *New Phytologist*, **203**, 257–266.

Sigsgaard, E.E., Olsen, K., Hansen, M.D.D., Hansen, O.L.P., Høye, T.T., Svenning, J.C. & Thomsen, P.F. (2020) Environmental DNA metabarcoding of cow dung reveals taxonomic and functional diversity of invertebrate assemblages. *Molecular Ecology*.

Snow, B. & Snow, D. (1988) Birds and berries. Calton Poyser, Staffordshire.

Stökl, J., Strutz, A., Dafni, A., Svatos, A., Doubsky, J., Knaden, M., Sachse, S., Hansson, B.S. & Stensmyr, M.C. (2010) A Deceptive Pollination System Targeting Drosophilids through Olfactory Mimicry of Yeast. *Current Biology*, **20**, 1846–1852.

Stensmyr, M.C., Urru, I., Collu, I., Celander, M., Hansson, B. S., & Angioy, A.M. (2002). Rotting smell of dead-horse arum florets. *Nature*, **420**(6916), 625–626.

Suinyuy, T.N., Donaldson, J.S. & Johnson, S.D. (2012) Geographical variation in cone volatile composition among populations of the African cycad *Encephalartos villosus*. *Biological Journal of the Linnean Society*, **106**, 514–527.

Suinyuy, T.N. & Johnson, S.D. (2018) Geographic variation in cone volatiles and pollinators in the thermogenic African cycad *Encephalartos ghellinckii* Lem. *Plant Biology*, **20**, 579–590.

Svensson, G.P., Hickman, M.O., Bartram, S., Boland, W., Pellmyr, O. & Raguso, R.A. (2005) Chemistry and geographic variation of floral scent in *Yucca filamentosa* (Agavaceae). *American Journal of Botany*, **92**, 1624–1631.

Thomann, M., Imbert, E., Devaux, C. & Cheptou, P.O. (2013) Flowering plants under global pollinator decline. *Trends in Plant Science*, **18**, 353–359.

Triponez, Y., Arrigo, N., Pellissier, L., Schatz, B. & Alvarez, N. (2013) Morphological, ecological and genetic aspects associated with endemism in the Fly Orchid group. *Molecular Ecology*, **22**, 1431–1446.

Urru, I., Stökl, J., Linz, J., Krügel, T., Stensmyr, M. C., & Hansson, B.S. (2010). Pollination strategies in Cretan Arum lilies. *Biological Journal of the Linnean Society*, **101**(4), 991–1001.

Urru, I., Stensmyr, M.C. & Hansson, B.S. (2011) Pollination by brood-site deception. *Phytochemistry*, **72**, 1655–1666.

Vaillant, F. (1971) 9d. Psychodidae-Psychodinae. *Die Fliegen der Palaearktischen Region* (ed. E. Lindner). E. Schweizerbart‘sche Verlagsbuchhandlung.

van der Niet, T. & Johnson, S.D. (2012) Phylogenetic evidence for pollinator-driven diversification of angiosperms. *Trends in Ecology & Evolution*, **27**, 353–361.

Waser, N.M. & Ollerton, J. (2006) *Plant-Pollinator Interactions: from Specialization to Generalization*. Univ. of Chicago Press.

Wund, M.A. (2012) Assessing the Impacts of Phenotypic Plasticity on Evolution. *Integrative and Comparative Biology*, **52**(1), 5–15.

Whitehead, M.R. & Peakall, R. (2009) Integrating floral scent, pollination ecology and population genetics. *Functional Ecology*, **23**, 863–874.

Yuan, J.S., Himanen, S.J., Holopainen, J.K., Chen, F. & Stewart, C.N. (2009) Smelling global climate change: mitigation of function for plant volatile organic compounds. *Trends in Ecology & Evolution*, **24**, 323–331.

Zattara, E.E. & Aizen, M.A. (2021) Worldwide occurrence records suggest a global decline in bee species.

FIGURES

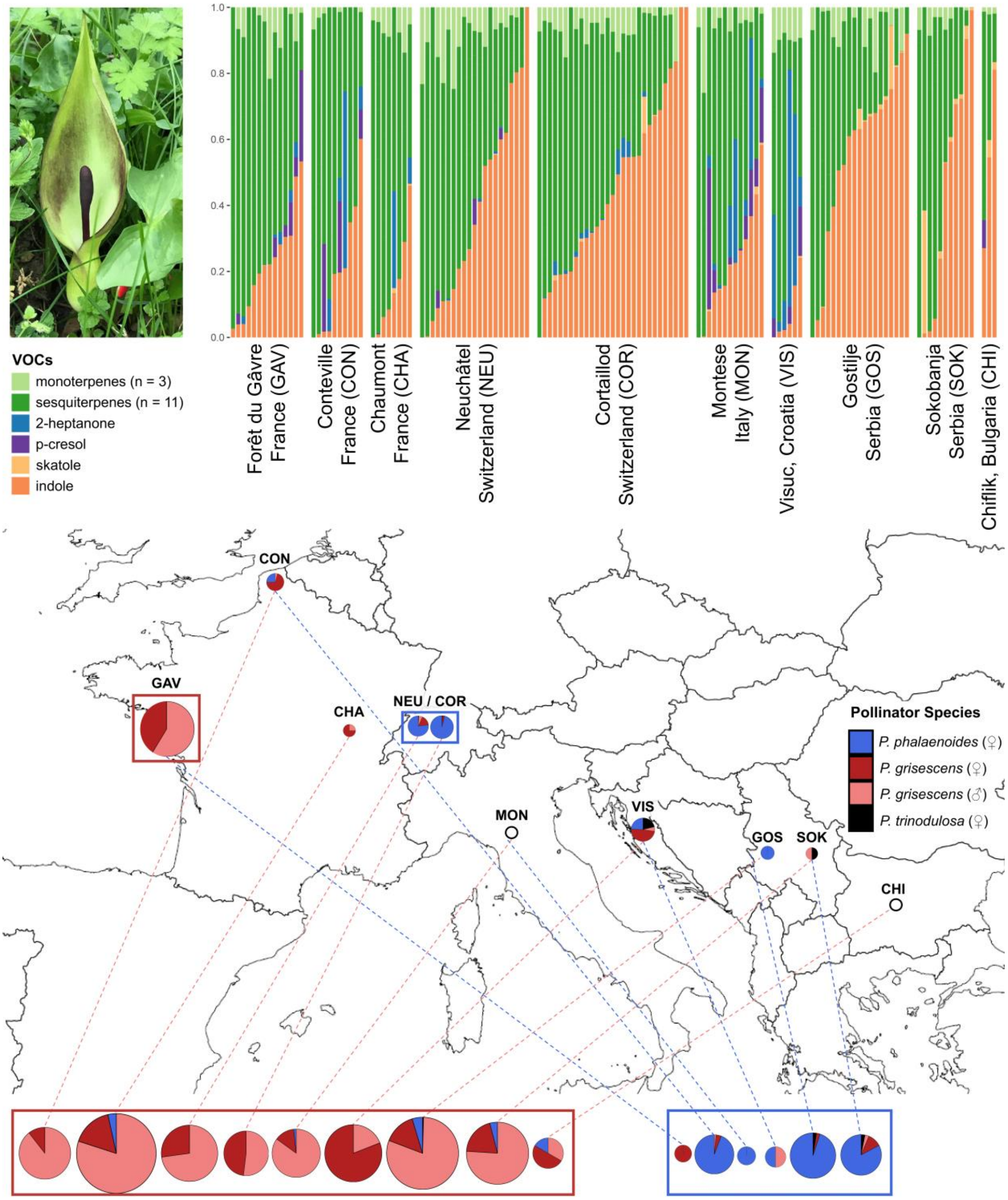

Figure 1. Europe-wide variation in floral volatile organic compounds (VOCs) and pollinator attraction of *Arum maculatum*. Stacked barplots present the relative quantities of VOCs in two terpene classes (mono- and sesquiterpenes) and four dung-mimicking VOCs emitted by individual inflorescences. Pie charts indicate the composition of Psychodidae trapped by *A. maculatum* inflorescences during field surveys (on map), and following transplants to two common garden sites (below map), scaled to represent mean quantities of Psychodidae per plant. Dotted lines link each field result with corresponding transplant results. Note: empty chart = no Psychodidae attracted during our surveys.

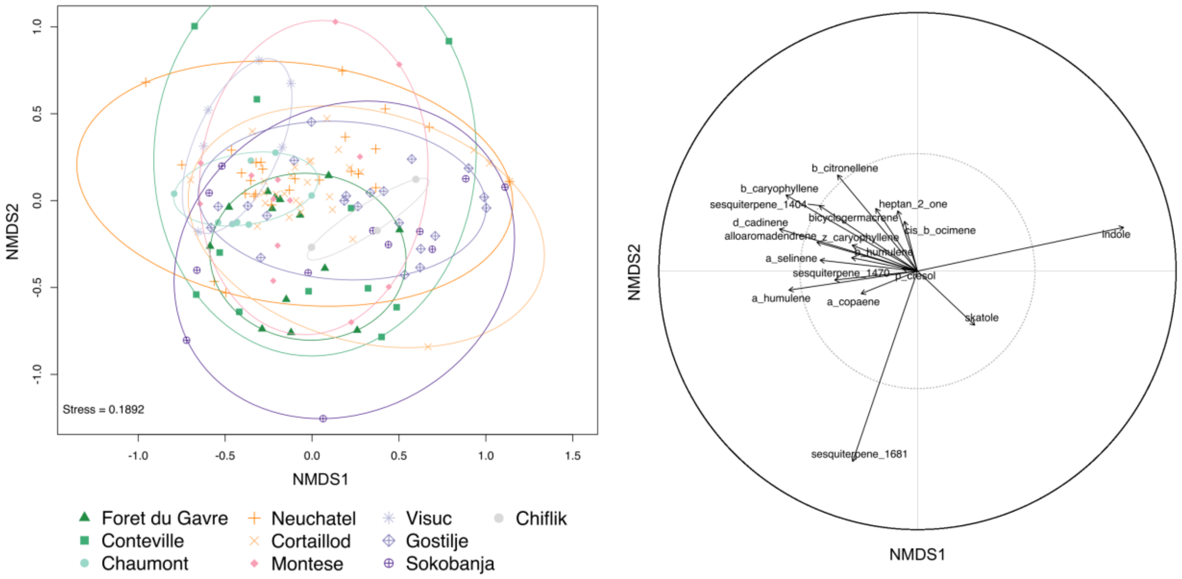

Figure 2. (A) Multivariate representation of *Arum maculatum* floral volatile organic compound (VOC) emissions, using nonmetric multidimensional scaling (NMDS) of Bray–Curtis distances between individuals. Points and ellipses are coloured according to individuals' population of origin. (B) Circle plot visualizing the correlations between all VOCs and the NMDS axes.

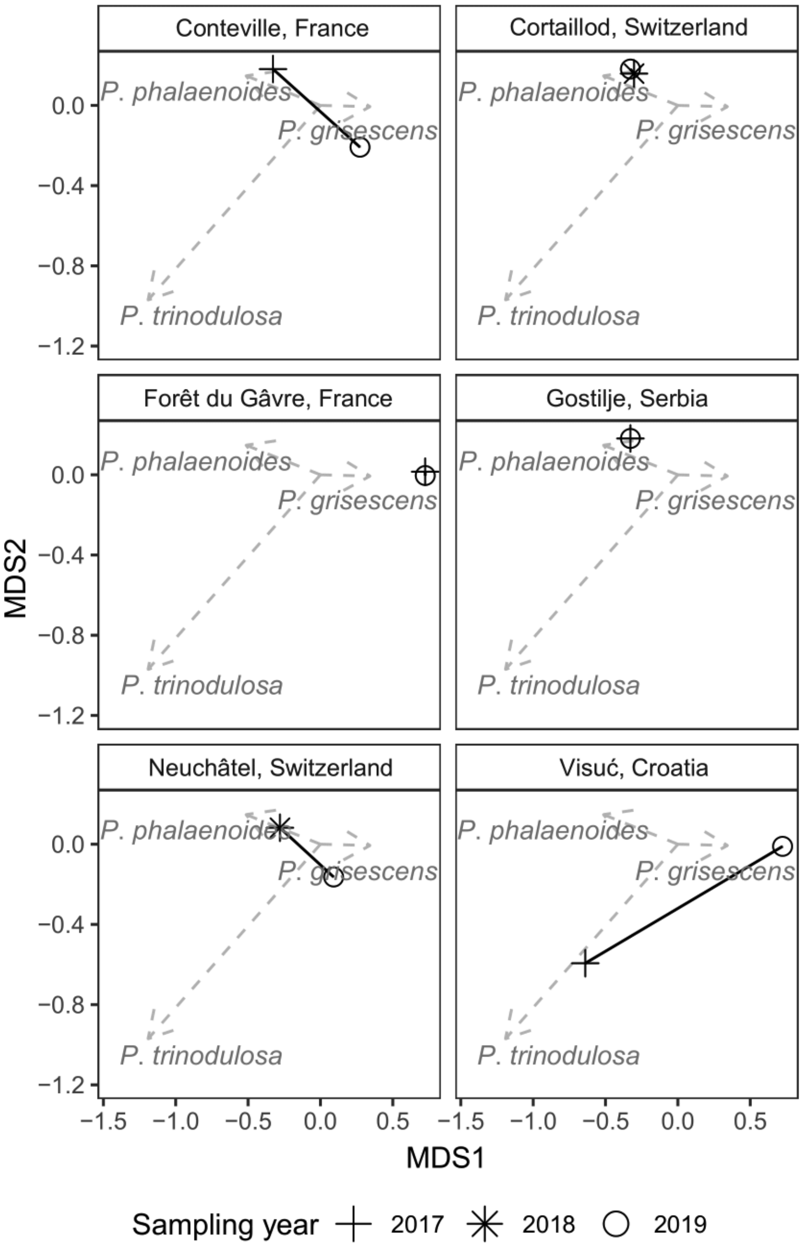

Figure 3. Interannual changes (2017/2018 versus 2019) in the average composition of Psychodidae pollinators trapped by six *Arum maculatum* populations. [NMDS; Bray–Curtis distance; overall stress = 0.005].

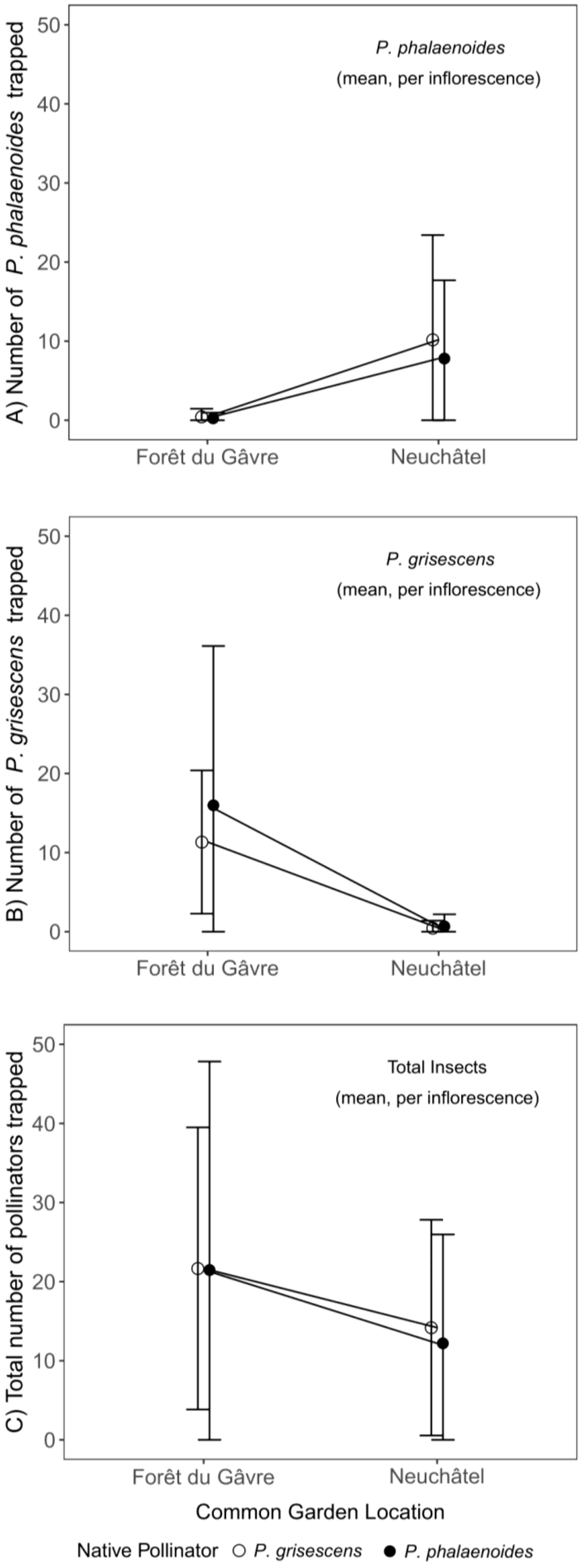

Figure 4. Pollinator attraction in the reciprocal transplant experiment. Plots show the mean (± SE) numbers of (A) *Psychoda phalaenoides*, (B) *Psycha grisescens* and (C) all insects trapped by inflorescences, transplanted from either *P. phalaenoides*-dominated populations (filled circles) or *P. grisescens*-dominated populations (hollow circles). No deme × habitat interactions (indicative of local adaptation) were identified.

TABLES

Table 1. Average proportional emissions (M) of volatile organic compounds (+/- SD) emitted by populations of *Arum maculatum*. Compounds representing more than 5% of the average total blend are highlighted in bold.

		Forêt du Gâvre, France (n = 14)			**Conteville, France** (n = 10)			**Chaumont, France** (n = 8)			**Neuchâtel, Switzerland** (n = 21)			**Cortaillod, Switzerland** (n = 29)		
VOC	**RI**	M	SD	Freq	M	SD	Freq	M	SD	Freq	M	SD	Freq	M	SD	Freq
2-heptanone	891	1.09	1.69	50.0	**7.74**	**16.54**	**40.0**	4.68	10.37	25.0	0.14	0.29	28.6	1.12	2.01	41.4
β-citronellene	943	3.58	6.02	64.3	0.02	0.07	10.0	2.25	2.28	75.0	**6.32**	**7.17**	**81.0**	3.39	3.74	82.8
cis β-ocimene	1037	0.10	0.37	7.1	0.00	0.00	0.0	0.02	0.05	12.5	0.32	0.75	33.3	0.51	1.02	27.6
p-cresol	1076	4.04	7.54	42.9	**5.71**	**10.15**	**30.0**	0.04	0.12	12.5	0.79	2.11	14.3	0.00	0.00	0.0
indole	1289	**22.50**	**15.45**	**100**	**19.92**	**20.11**	**90.0**	**15.23**	**15.61**	**87.5**	**39.02**	**30.26**	**95.2**	**46.26**	**26.81**	**96.6**
skatole	1383	1.89	2.84	50.0	1.44	2.13	50.0	4.21	2.28	87.5	1.59	1.84	57.1	1.62	1.41	69.0
α-copaene	1374	0.02	0.04	28.6	0.01	0.02	20.0	0.25	0.53	25.0	0.02	0.07	14.3	0.48	2.06	20.7
Z-caryophyllene	1405	**9.26**	**11.07**	**71.4**	1.87	4.44	30.0	2.11	2.00	62.5	**8.39**	**7.52**	**85.7**	3.94	4.74	75.9
β-caryophyllene	1416	1.48	2.14	50.0	**7.87**	**9.84**	**70.0**	1.92	2.30	62.5	1.37	1.93	47.6	2.82	5.68	72.4
α-humulene	1452	**5.15**	**4.43**	**71.4**	**17.55**	**22.93**	**70.0**	**11.32**	**2.66**	**100**	**5.82**	**5.44**	**76.2**	3.87	3.10	72.4
alloaromadendrene	1459	4.66	3.81	85.7	3.96	4.53	60.0	**7.02**	**4.26**	**87.5**	**5.62**	**4.41**	**85.7**	**8.09**	**9.94**	**82.8**
β-humulene	1473	**5.46**	**7.02**	**64.3**	1.24	1.95	40.0	**10.13**	**5.87**	**87.5**	4.97	6.45	85.7	2.72	1.91	82.8
α-selinene	1491	2.06	3.68	35.7	0.35	1.12	10.0	3.97	4.52	62.5	1.66	3.43	28.6	0.43	1.18	17.2
bicyclogermacrene	1493	0.58	1.02	42.9	0.87	2.75	10.0	1.18	1.70	50.0	2.64	4.07	57.1	**6.46**	**9.51**	**75.9**
d-cadinene	1520	0.48	1.09	35.7	1.63	4.66	20.0	**9.59**	**12.96**	**100**	3.75	6.47	57.1	1.55	2.14	58.6
Unnamed sesqui.	1404	0.63	1.21	42.9	0.04	0.14	10.0	0.20	0.37	37.5	4.94	10.48	57.1	2.49	6.65	37.9
Unnamed sesqui.	1470	4.62	6.00	71.4	2.17	3.98	30.0	**11.17**	**5.59**	**100**	3.48	3.27	76.2	3.96	2.82	79.3
Unnamed sesqui.	1681^	**32.39**	**20.75**	**100**	**27.61**	**17.68**	**80.0**	**14.71**	**8.88**	**100**	**9.15**	**14.36**	**81.0**	**10.29**	**10.45**	**75.9**

		Montese, Italy (n = 13)			**Visuć, Croatia** (n = 6)			**Gostilje, Serbia** (n = 19)			**Sokobanja, Serbia** (n = 11)			**Chiflik, Bulgaria** (n = 3)		
VOC	**RI**	M	SD	Freq	M	SD	Freq	M	SD	Freq	M	SD	Freq	M	SD	Freq
2-heptanone	891	**8.28**	**14.17**	**61.5**	**29.36**	**27.79**	**100**	0.00	0.00	0.0	0.00	0.00	0.0	0.00	0.00	0.0
β-citronellene	943	3.26	5.49	69.2	**8.77**	**2.18**	**100**	0.65	2.12	21.1	0.05	0.15	9.1	0.00	0.00	0.0
cis β-ocimene	1037	0.21	0.40	30.8	0.32	0.79	16.7	0.01	0.04	5.3	0.00	0.00	0.0	0.00	0.00	0.0
p-cresol	1076	**7.58**	**11.99**	**61.5**	4.34	5.81	66.7	0.00	0.00	0.0	0.00	0.00	0.0	2.85	4.94	33.3
indole	1289	**22.38**	**16.81**	**92.3**	**7.99**	**9.73**	**83.3**	**55.41**	**26.79**	**100**	**43.41**	**37.98**	**90.9**	**54.24**	**27.05**	**100**
skatole	1383	1.46	1.49	61.5	1.07	1.10	66.7	4.34	5.80	73.7	2.92	3.19	63.6	1.84	0.45	100
α-copaene	1374	0.32	0.64	46.2	0.10	0.20	50.0	1.61	4.51	68.4	4.46	10.94	72.7	2.52	2.65	66.7
Z-caryophyllene	1405	**12.78**	**14.31**	**69.2**	**22.25**	**20.66**	**83.3**	4.65	6.29	63.2	**9.88**	**19.53**	**45.5**	**6.90**	**3.86**	**100**
β-caryophyllene	1416	0.88	1.20	38.5	1.96	2.50	50.0	0.54	2.06	15.8	0.73	2.34	18.2	0.00	0.00	0.0
α-humulene	1452	6.25	8.75	76.9	**6.11**	**5.24**	**100**	**6.91**	**10.62**	**57.9**	1.81	3.34	27.3	0.70	1.21	33.3
alloaromadendrene	1459	2.89	2.70	69.2	2.04	1.65	83.3	1.86	3.22	36.8	4.71	5.97	54.5	0.73	1.26	33.3
β-humulene	1473	**8.07**	**13.22**	**100**	0.75	1.09	50.0	1.54	2.77	42.1	2.64	4.09	36.4	0.67	1.16	33.3
α-selinene	1491	0.88	1.55	30.8	0.00	0.00	0.0	1.38	3.12	31.6	0.47	1.11	18.2	0.00	0.00	0.0
bicyclogermacrene	1493	0.43	0.69	38.5	0.00	0.00	0.0	1.02	1.60	47.4	0.97	2.18	27.3	**6.95**	**12.04**	**33.3**
d-cadinene	1520	1.36	2.55	46.2	0.62	0.96	33.3	2.36	8.28	21.1	0.28	0.76	18.2	0.00	0.00	0.0
Unnamed sesqui.	1404	0.47	0.87	30.8	0.00	0.00	0.0	0.99	2.61	42.1	0.74	1.43	27.3	0.00	0.00	0.0
Unnamed sesqui.	1470	3.35	3.61	69.2	4.06	2.17	100	2.99	5.27	52.6	4.97	7.83	36.4	4.00	1.71	100
Unnamed sesqui.	1681^	**19.15**	**18.28**	**84.6**	**10.23**	**12.36**	**100**	**13.73**	**13.14**	**84.2**	**21.96**	**20.18**	**81.8**	**18.60**	**15.25**	**100**

RI = Kovats retention index (^ = RI 1716 in Diaz & Kite 2002).
Freq = proportion of chromatograms (%) in which the compound was identified in a given population.

Table 2. Mean *in-situ* abundances of *Psychoda phalaenoides* and *Psycha grisescens* individuals trapped per *Arum maculatum* inflorescence between 2006-2008 (data from Espíndola et al. 2010), and in our field surveys between 2017-2019. The number of individual inflorescences sampled *in situ* are indicated in parentheses. NAs indicate that no inflorescences were open yet at the time populations were visited.

Poll. Species / Year **Population**	***P. phalaenoides* (2008)**	***P. grisescens* (2008)**	***P. phalaenoides* (2019)**	***P. grisescens* (2019)**
Fôret du Gavre (France)	0 (5)	6.4 (5)	0 (16)	25.7 (16)
Conteville (France)	47.6 (8)	2.3 (8)	0.4 (14)	1.3 (14)
Chaumont (France)	1.6 (6)	0.5 (6)	0 (7)	0.6 (7)
Lausanne/Neuchâtel (Switzerland)	3.0 (2)	0 (2)	2.0 (44)	0.6 (44)
Montese (Italy)	0 (5)	2 (5)	NA	NA
Visuć (Croatia)	0.1 (7)	0.6 (7)	1.3 (6)	3.0 (6)
Gostilje (Serbia)	0 (5)	2.4 (5)	0.4 (18)	0 (18)
Sokobanja (Serbia)	0 (5)	0.2 (5)	0 (21)	0.1 (21)
Chiflik (Bulgaria)	0.4 (7)	4.3 (7)	NA	NA

APPENDIX S1 – SUPPLEMENTARY FIGURES & TABLES

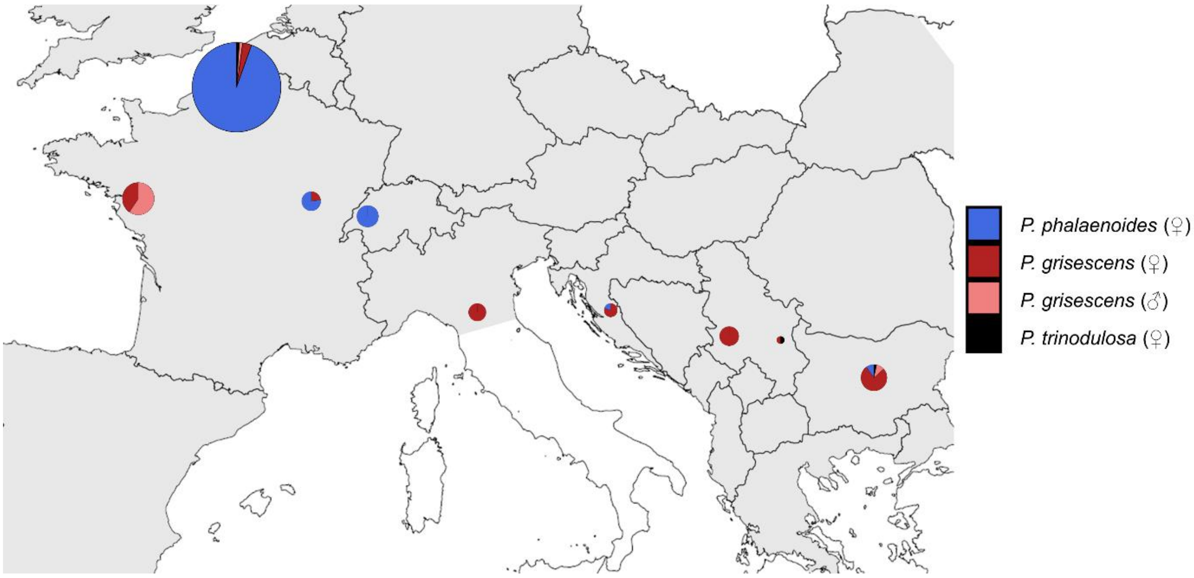

Figure S1. The species distribution of *Arum maculatum* (highlighted in grey), per Boyce (1993). Here, sampling sites are indicated by pie charts, which visualize data on Psychodidae trapped by inflorescences between 2007-2009 (Espíndola et al. 2010), for comparison with our results in Figure 1.

Note: Graph sizes represent the square root (plus one to visualize species differences in small pies) of the mean number of psychodids per plant in each population. Swiss pollinator data in this figure represents Lausanne, replaced by Neuchâtel and Cortaillod populations in the present study.

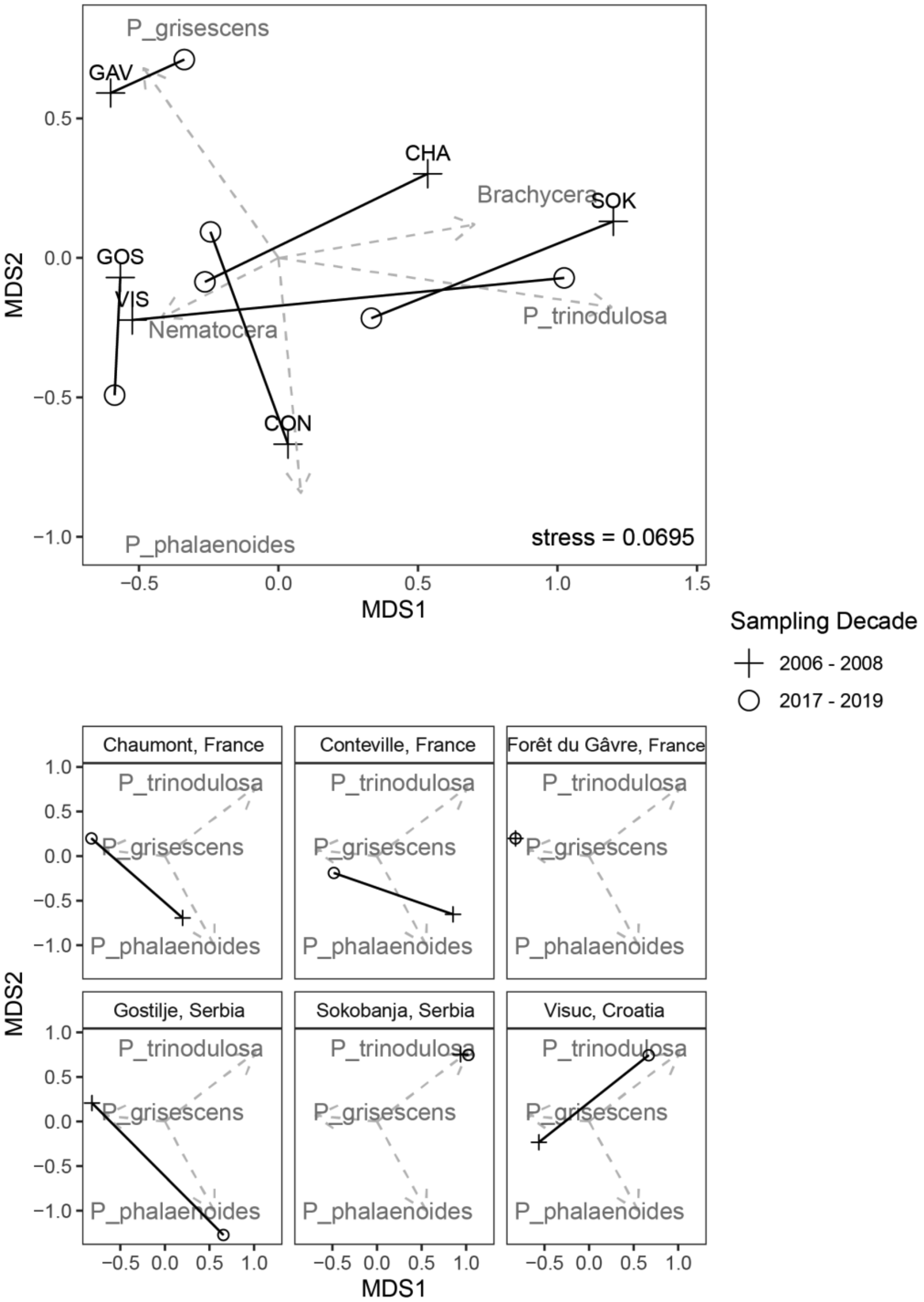

Figure S2. Shifts in the total pollinator communities (upper plot) and Psychodidae only (lower plots) trapped by *Arum maculatum* inflorescences over the past decade. The dominant Psychodid pollinator species appears to have shifted in four out of six re-sampled populations.

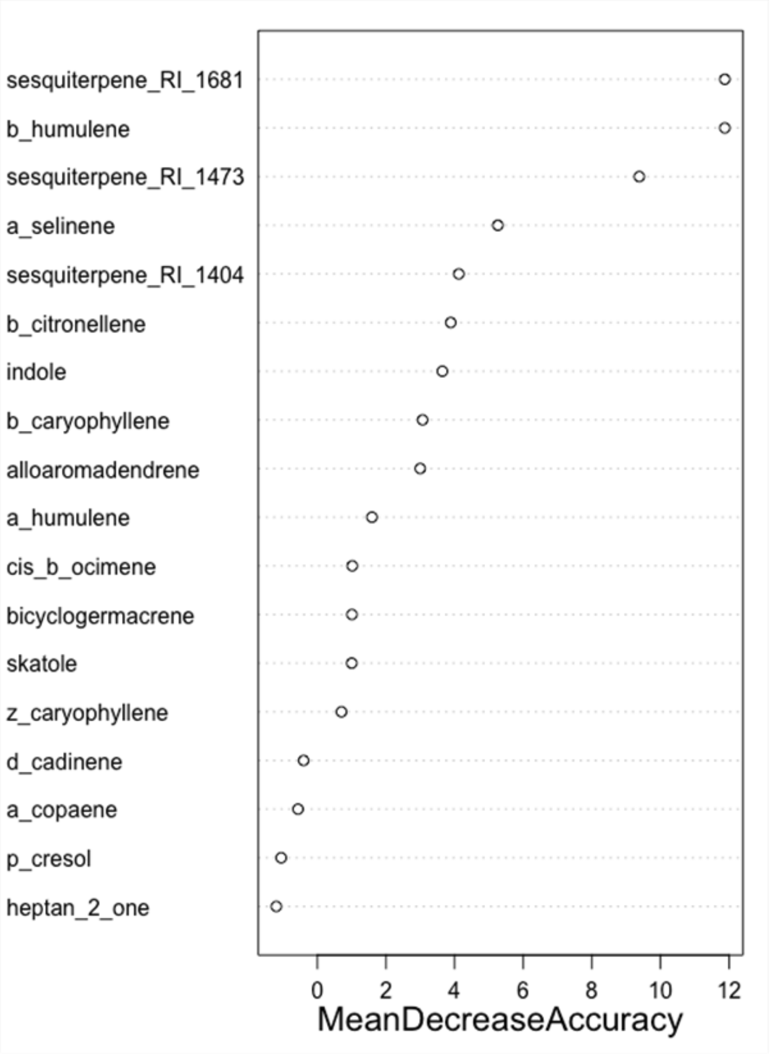

Figure S3. Variable importance plot, highlighting the *Arum maculatum* VOCs with the greatest effect on the random forest classifier accuracy. Here, VOCs with the greatest mean decrease in accuracy values are the strongest predictors of whether an inflorescence would catch predominantly *Psychoda phalaenoides* (as opposed to *Psycha grisescens*)**.**

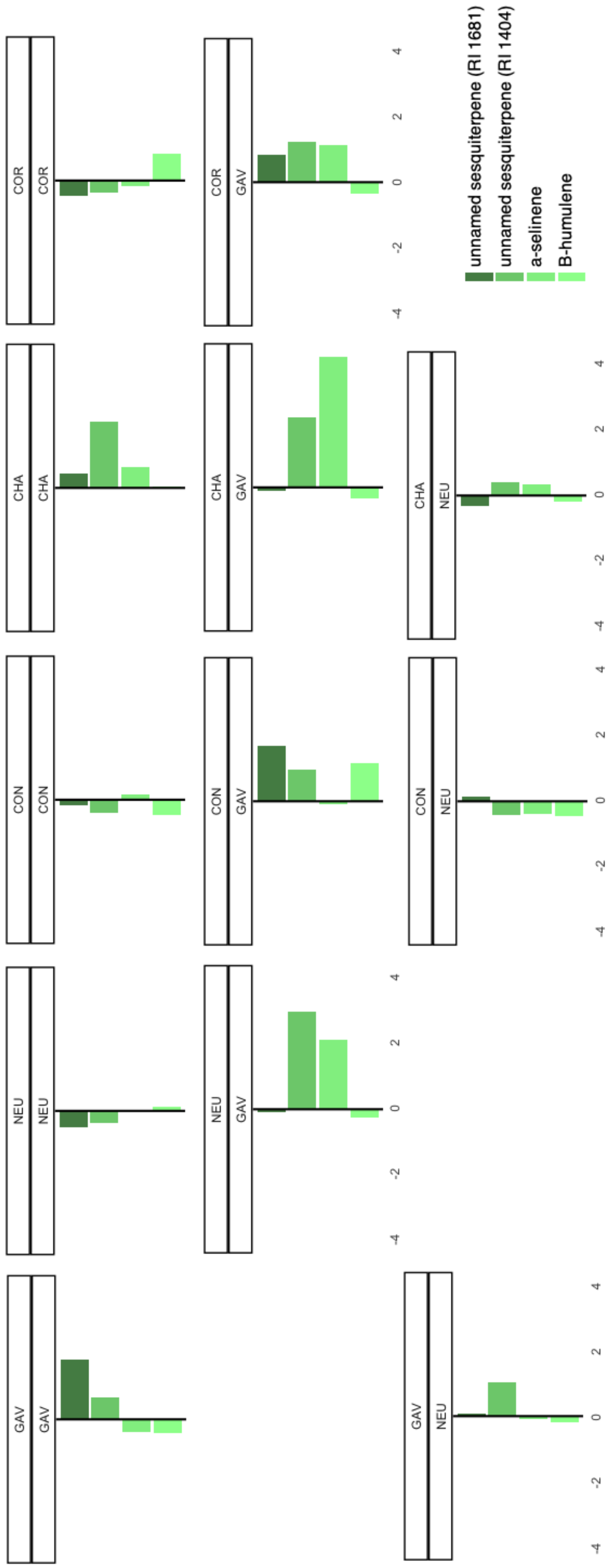

Figure S4. Shifts in the mean population standard scores (calculated as: [(raw individual VOC quantity – mean individual VOC quantity) / VOC std. dev.]) for the four *Arum maculatum* VOCs which were the strongest predictors of whether an inflorescence would trap predominantly *P. phalaenoides* or *P. grisescens*. Two Swiss populations (COR and NEU) and one Serbian population (GOS) shifted to more sesquiterpene-dominated blends following transplants to the Forêt du Gâvre common garden. By contrast, most populations remained relatively consistent in their emissions of these sesquiterpenes following transplant to the Neuchâtel common garden.

Note: Upper facet box represents population origin, lower facet box represents site of VOCs collection.

[FIGURE CONTINUED ON NEXT PAGE]

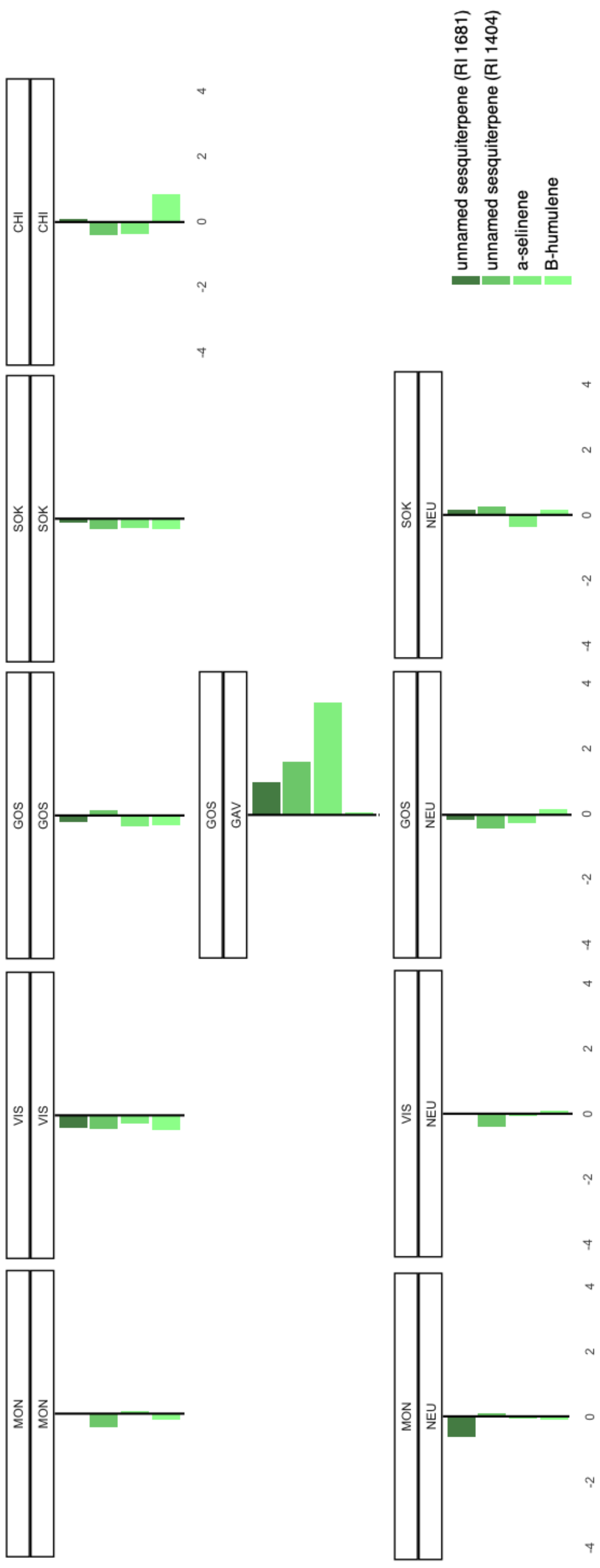

Figure S4 (cont.) – see caption on previous page

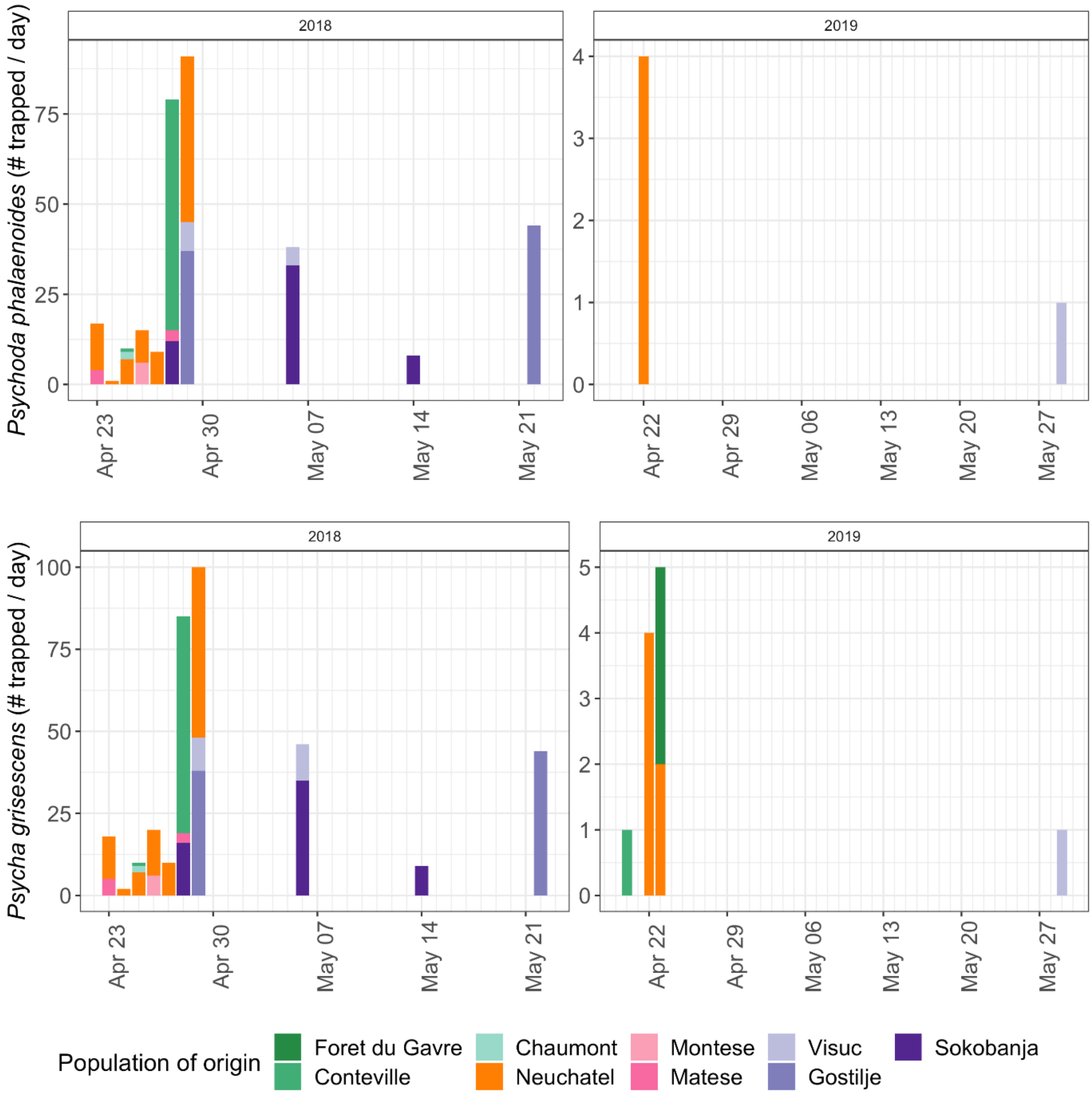

Figure S5a. Pollinators trapped by *Arum maculatum* inflorescences in the Neuchâtel common garden (*i.e. Psychoda phalaenoides*-dominated) over two years of sampling. Both *P. phalaenoides* and *P. grisescens* were present and trapped by inflorescences during most of the sampling season.

Note: Y-axis scale varies substantially between plots. Bar colours represent the populations of origin for sampled inflorescences.

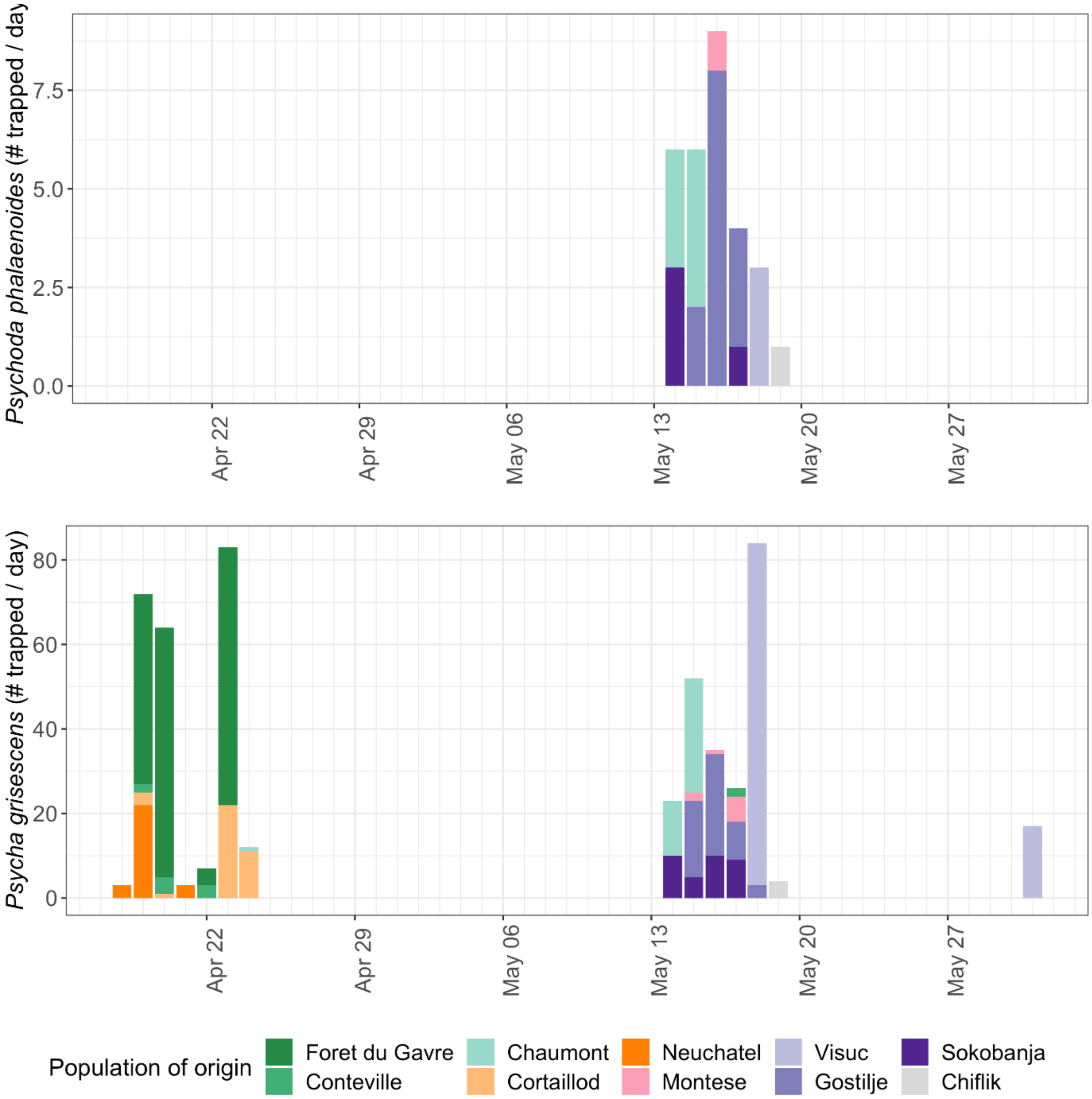

Figure S5b. Pollinators trapped by *Arum maculatum* inflorescences in the Forêt du Gâvre common garden (*i.e. Psycha grisescens*-dominated) in 2019. *P. grisescens* were trapped by inflorescences over most of the sampling season, while *P. phalaenoides* were only trapped in the latter half of the season.

Note: Y-axis scale varies substantially between plots. Bar colours represent the populations of origin for sampled inflorescences. No pollinator sampling was conducted between 25.Apr and 14.May.

Table S1. List of study sites, GPS coordinates, number of Arum *maculatum* VOC samples passing all quality filters, and number of inflorescences with insect data. VOC and insect sample sizes from 1) *in situ* field surveys and 2) transplant / common garden experiments are separately indicated below.

Population	**Country**	**Latitude**	**Longitude**	**Alt. ASL (m)**	**# sampled VOCs (in situ)**	**# sampled VOCs (NEU, transplant)**	**# sampled VOCs (GAV, transplant)**	**# sampled insects (in situ)**	**# sampled insects (NEU, transplant)**	**# sampled insects (GAV, transplant)**
Forêt du Gâvre	FR	47.55066	-1.86466	16	10	4	NA	5 (16)	3 (3)	NA
Conteville	FR	50.73731	1.73872	60	8	2	1	0 (5)	1 (4)	1 (6)
Chaumont	FR	48.11508	5.09475	296	1	6	2	1 (5)	2 (2)	1 (5)
Neuchâtel	CH	47.00043	6.93790	556	18	NA	3	8 (30)	NA	3 (5)
Cortaillod	CH	46.93205	6.83290	430	27	NA	2	9 (14)	NA	2 (6)
Montese	IT	44.25523	10.98371	707	6	6	2	0 (0)	1 (1)	2 (4)
Visuć	HRV	44.53128	15.76134	810	6	2	0	3 (4)	2 (4)	0 (2)
Gostilje	SRB	43.65561	19.83549	785	17	3	2	4 (10)	3 (4)	2 (8)
Sokobanja	SRB	43.60373	21.88755	844	10	2	0	1 (11)	2 (4)	0 (5)
Chiflik	BG	42.8130	24.52836	786	3	0	0	0 (0)	0 (0)	0 (1)

Table S2. The top ten combinations of *Arum maculatum* VOCs with the greatest contribution to the predictive strength of the random forest classifier (see Figure S3). Unnamed sesquiterpene (RI 1681) alone was the strongest predictor of the species composition of pollinators trapped by individual *A. maculatum* inflorescences.

Compound Blend	**Feature Contribution**
unnamed sesquiterpene (RI 1681)	0.1947778
unnamed sesquiterpene (RI 1470) + unnamed sesquiterpene (RI 1681)	0.0592275
α-selinene + unnamed sesquiterpene (RI 1681)	0.0502504
β-humulene	0.0436112
β-citronellene	0.0361404
α-selinene	0.0320748
β-humulene + unnamed sesquiterpene (RI 1681)	0.0180302
β-citronellene + indole	0.0138245
unnamed sesquiterpene (RI 1404) + unnamed sesquiterpene (RI 1681)	0.0119733
unnamed sesquiterpene (RI 1404)	0.0114971

Table S3. Mann Whitney U (Wilcoxon rank-sum) test results, comparing the emissions of four VOCs associated with species-specific Psychodidae attraction. To test for shifts in VOCs related to environmental variation, comparisons were made between samples collected in the Forêt du Gâvre common garden and in the Neuchâtel common garden.

Pop.	α-selinene (*p*)	Z	β-humulene (*p*)	Z	Sesquiterpene RI 1473 (*p*)	Z	Sesquiterpene RI 1681 (*p*)	Z
GAV	0.0105	2.5584	0.0213	-2.302	0.3706	-0.895	0.1111	1.8557
NEU	0.0102	2.5700	0.7428	-0.328	**0.0004 ***	**3.5475**	0.3128	1.0094
CHA	0.2857	1.4652	0.8591	-0.177	0.5942	0.5327	0.8571	0.4637
MON	1.0000	0.0000	0.8591	0.1776	1.0000	0.0000	0.1798	1.3413

* *Significant after Bonferroni correction for multiple testing*

Table S4. Two-way ANOVA results for pollinators trapped by transplanted *Arum maculatum* growing in two common garden sites, dominated by either *Psychoda phalaenoides* or *Psycha grisescens*.

ALL POLLINATORS	df	SumSq	MeanSq	F value	Pr(>F)
common garden loc.	1	2.34	2.3369	2.138	0.153
native poll.	1	0.16	0.162	0.148	0.703
common garden loc : native poll.	1	0.05	0.0538	0.049	0.826
Residuals	34	37.16	1.0928		

P. PHALAENOIDES	df	SumSq	MeanSq	F value	Pr(>F)
common garden loc. ***	1	18.38	18.379	16.2	0.000301
native poll.	1	0.15	0.152	0.134	0.716174
common garden loc. : native poll.	1	0.01	0.008	0.007	0.931867
Residuals	34	38.57	1.134		

P. GRISESCENS	df	SumSq	MeanSq	F value	Pr(>F)
common garden loc. ***	1	36.28	36.28	55.84	1.14E-08
native poll.	1	0.19	0.19	0.287	0.596
common garden loc. : native poll.	1	0.1	0.1	0.155	0.696
Residuals	34	22.09	0.65		

Factors: **Native pollinator** (whether an inflorescence traps *P. phalaenoides* or *P. grisescens* in their native population) and **Common Garden Location** (Neuchâtel, a site dominated *P. phalaenoides*, or Forêt du Gâvre, a site dominated by *P. grisescens*). F-statistics are shown above (df = 1).

*** P<0.001, ** P<0.01, * P<0.05

APPENDIX S2 – SUPPLEMENTARY METHODS

Floral odour collection and identification

Arum maculatum inflorescences open for an anthesis cycle of roughly 24h, with VOC emissions peaking in the late afternoon / early evening of the first flowering day. We therefore carried out all floral odour sampling between 18:00 at the earliest and 20:30 at the latest. We sampled dynamic headspace volatile organic compounds (VOCs) using polydimethylsiloxane (PDMS) coated Gerstel Twister® (Mülheim an der Ruhr, Germany) stir bar sorptive extraction. Inflorescences were wrapped in inert oven bags (Tangan No34 distributed by Migros, Zurich, Switzerland) cut open at least 8cm above the tip of the spathe to prevent condensation, due to the strong thermogenesis of the appendix. Twisters® were inserted in a glass tube through the oven bag at a height even with, but not contacting, the tip of the spadix. 6L of air was pumped over Twisters® at a standard rate of 200mL per minute for 30 minutes – except for five samples from Conteville, France, where sampling was carried out at the same rate over only 15 minutes. At every sampling site, at least one empty oven bag was placed approximately 5 meters away from any inflorescences, and ambient air was passed over Twisters® identically to *A. maculatum* inflorescences; these samples were used as controls to filter out ambient air VOCs. All samples were transported in glass vials on ice, and stored at -21°C until analysis.

Gas Chromatography

We applied 1µL of internal standard (5µg mg/mL naphthalene in dichloromethane) directly to each Twister® immediately before processing. Using a Multipurpose Sampler (Gerstel, Mülheim an der Ruhr, Germany), VOCs were thermally desorbed and separated on a HP-5MS column, 30 m x 0.25mm x 0.25µm at 40°C for 30 sec, increasing temperature by 5°C per min to 160°C, which was held for 0.01 min before increasing 3°C per min to reach 200°C, which was held for 4 min, finally increasing at 10°C per min. until reaching 250°C for 3 min.

Volatile Data Processing

We aligned peaks by retention time within each population. Major ions were recorded for each integrated peak using Agilent Chemstation software. Putative compound identifications were then derived from NIST 2.3 (library version 17) hits confirmed for the same peak in several spectra; all names used in the final analysis should be considered hypotheses. Compounds present in blank samples with a mean quantity anywhere near those within *A. maculatum* samples were removed prior to further analyses. Quantitative values were obtained by dividing compound peak areas by the internal standard, then multiplying by the internal standard concentration, and finally scaling based on sampling time (for the few samples run for less than 30 minutes).

Pollinator identification

On the morning after floral odour collection, all trapped pollinators were collected from within each inflorescence and preserved in 70% ethanol. All pollinators were identified to at least the suborder level. Psychodidae were further identified to species level using taxonomic information and illustrations (Ježek 1990). First, the number of antennal segments were counted. 15 segments indicated specimens were likely *P. phalaenoides* or *P. crassipennis*. 16 segments indicated either *P. grisescens* or *P. trinodulosa* - wing venation patterns were then examined for 16-segmented specimens, as *P. trinodulosa* has a characteristic disconnection in one branched vein. To confirm the final species identity (particularly when intact antennae were not available) and sex of all psychodids, the reproductive anatomy of specimens were also examined: Psychodid abdomens were separated, flattened, cleared in a diluted solution of potash, and mounted on a slide in glycerol beside their decapitated head, and wings laid out flat.

REFERENCES

Ježek, J. (1990) Redescriptions of Nine Common Palaearctic And Holarctic Species of Psychodini. *Acta Entomologica Musei Nationalis Pragae*, **43**, 33-83.

CHAPTER 3 - Transcriptomic analysis of deceptively pollinated *Arum maculatum* (Araceae) reveals association between terpene synthase expression in floral trap chamber and species-specific pollinator attraction

This manuscript is published in G3 Genes|Genomes|Genetics, 2022, Volume 12(9): jkac175 (DOI: https://doi.org/10.1093/g3journal/jkac175)

Mark A. Szenteczki[1*], Adrienne L. Godschalx[1], Jérémy Gauthier[2], Marc Gibernau[3 +], Sergio Rasmann[1 +], Nadir Alvarez[2 4 +]

[1] Université de Neuchâtel, Institut de Biologie, Rue Emile-Argand 11, 2000 Neuchâtel, Switzerland
[2] Geneva Natural History Museum, Route de Malagnou 1, 1208 Genève, Switzerland
[3] CNRS – University of Corsica, Laboratory Sciences for the Environment (SPE - UMR 6134), Natural Resources Project, Vignola – Route des Sanguinaires, 20000 Ajaccio, France
[4] Department of Genetics and Evolution, University of Geneva, Quai Ernest-Ansermet 30, 1211 Geneva, Switzerland
[*] Corresponding author: M.A. Szenteczki mark.szenteczki@unine.ch Tel. + 41 32 718 23 16
[+] Authors participated equally and are considered joint senior authors

ABSTRACT

Deceptive pollination often involves volatile organic compound emissions that mislead insects into performing nonrewarding pollination. Among deceptively pollinated plants, *Arum maculatum* is particularly well-known for its potent dung-like volatile organic compound emissions and specialized floral chamber, which traps pollinators—mainly *Psychoda phalaenoides* and *Psychoda grisescens*—overnight. However, little is known about the genes underlying the production of many *Arum maculatum* volatile organic compounds, and their influence on variation in pollinator attraction rates. Therefore, we performed de novo transcriptome sequencing of *Arum maculatum* appendix and male floret tissue collected during anthesis and postanthesis, from 10 natural populations across Europe. These RNA-seq data were paired with gas chromatography–mass spectrometry analyses of floral scent composition and pollinator data collected from the same inflorescences. Differential expression analyses revealed candidate transcripts in appendix tissue linked to malodourous volatile organic compounds including indole, *p*-cresol, and 2-heptanone. In addition, we found that terpene synthase expression in male floret tissue during anthesis significantly covaried with sex- and species-specific attraction of *Psychoda phalaenoides* and *Psychoda grisescens*. Taken together, our results provide the first insights into molecular mechanisms underlying pollinator attraction patterns in *Arum maculatum* and highlight floral chamber sesquiterpene (e.g. bicyclogermacrene) synthases as interesting candidate genes for further study.

KEYWORDS

chemical ecology; GC-MS; molecular ecology; plant-pollinator interactions; RNA-seq; sesquiterpenes

INTRODUCTION

Angiosperms have evolved to produce a wide array of specialized metabolites to mediate their interactions with other organisms and their environment, including volatile organic compounds (VOCs) emitted from flowers, leaves, fruits, and roots. While VOCs represent a relatively small proportion of all plant metabolomic diversity (Knudsen and Gershenzon 2020), they play important functional roles in defence against predators, pathogens, and abiotic stresses (Pichersky and Gershenzon 2002; Holopainen 2004; Irwin *et al.* 2004) and as cues for pollinator attraction (Pellmyr and Thien 1986; Knudsen and Tollsten 1993; Whitehead and Peakall 2009; Junker and Parachnowitsch 2015). Pollination, particularly by insects, appears to be a major driver of angiosperm diversification (Van der Niet and Johnson 2012; Schiestl and Johnson 2013; Hernández-Hernández and Wiens 2020). Recent research has hypothesized and partially demonstrated that floral trait diversity is the result of complex interactions between plant genomic diversity among populations, pollinator network composition, and environmental conditions—all of which vary through space and time (Thompson *et al.* 2013, 2017; Friberg *et al.* 2019). Large molecular and ecological datasets, with wide spatial and temporal coverage, are therefore still needed in order to further our understanding of the evolution of key traits such as floral scent.

Pollinator-mediated selection is known to influence floral morphology (Bröderbauer *et al.* 2013; Gervasi and Schiestl 2017) and colour (Schemske and Bradshaw 1999; Newman *et al.* 2012; Trunschke *et al.* 2021), and recent studies have also identified strong evidence for variation in VOC emissions driven by pollinator preferences. Notably, comparative community ecology data and gas chromatography–mass spectrometry (GC–MS) have been combined to identify convergent VOC bouquets in unrelated plant species with similar pollinators (Fenster *et al.* 2004; Schiestl and Johnson 2013; Junker and Parachnowitsch 2015), and divergent VOC bouquets in related species with different pollinators (Dobson *et al.* 1997; Urru *et al.* 2010; Byers *et al.* 2014; Friberg *et al.* 2019). Moreover, the discovery of biochemical pathways underlying floral VOCs has greatly accelerated by next-generation sequencing technologies such as mRNA sequencing (Dhandapani *et al.* 2017; Wong, Pichersky, *et al.* 2017; Xiao *et al.* 2019). Here, we aimed to combine these techniques, in order to understand how pollinator-mediated selection influences transcriptomic variation underlying floral scent divergence among populations of deceptively pollinated *Arum maculatum* L. (Araceae).

A. maculatum is a common European woodland flower with a long history of study, due to its deceptive pollination strategy which involves olfactory deception through brood-site mimicry (Schmucker 1925; Knoll 1926; Vogel 1965; Lack and Diaz 1991). Specifically, *A. maculatum* emit VOCs (e.g. 2-heptanone, indole, and *p*-cresol) during anthesis which are also present in cow manure (Kite 1995) and decomposing organic material (Gfrerer *et al.* 2021, 2022): the breeding substrates of *Psychoda phalaenoides* L. and *Psychoda* (*Psycha*) *grisescens* (Tonnoir) (Espíndola *et al.* 2011; Szenteczki *et al.* 2021). These 2 dipteran (Psychodidae) moth flies are trapped at varying frequencies across the geographic distribution of *A. maculatum* (Espíndola *et al.* 2011; Szenteczki *et al.* 2021; Gfrerer *et al.* 2021). Geographic variation in *A. maculatum* floral scent has also been observed, first in England (Kite *et al.* 1998; Diaz and Kite 2002) and France (Chartier *et al.* 2011, 2013), and recently, across most of the species distribution range (Gfrerer *et al.* 2021; Szenteczki *et al.* 2021), and may be linked to variation in pollinator attraction (Gfrerer *et al.* 2021; Szenteczki *et al.* 2021).

A. maculatum VOC emissions during anthesis are highly variable, and also include several sesquiterpenes and other aliphatic, aromatic, monoterpene, and nitrogen-containing minor compounds which may also contribute to pollinator attraction (Kite 1995; Gfrerer *et al.* 2021; Szenteczki *et al.* 2021). Intra- and interpopulation VOC variation mainly centers around variation in the proportion of indole to terpenes (Chartier *et al.* 2013; Szenteczki *et al.* 2021), which are respectively produced by aromatic amino acid (AAA; i.e. phenylalanine, tyrosine, and tryptophan) metabolism and terpene synthases (TPSs) via the mevalonate or methylerythritol 4-phosphate (MEP) pathways. Experiments in England with scented bait traps have shown that indole, 2-heptanone, and *p*-cresol are attractive to *P. phalaenoides* (Kite *et al.* 1998). Large-scale field studies have further demonstrated that sesquiterpenes may also play a role in differential attraction of *P. phalaenoides* and *P. grisescens* (Szenteczki *et al.* 2021) and influence fruit set size (Gfrerer *et al.* 2021).

Another recognizable feature of *A. maculatum* is its inflorescence morphology. Like other monoecious Araceae, *A. maculatum* produce densely clustered, unisexual male and female florets arranged along a central spike (the spadix), which is surrounded by a leaf-like bract (the spathe). The spathe surrounds the fertile flowers, creating a basal trap chamber with only a narrow opening at the top of the chamber, which is surrounded by a ring of hair-like sterile flowers. The scent of the floral chamber during anthesis appears to be dominated by 1 sesquiterpene, bicyclogermacrene (Kite *et al.* 1998), which was previously misidentified as germacrene B (Kite 1995). The purple colour of the appendix (the sterile apex of the spadix) and stamens is due to anthocyanin pigments (Williams *et al.* 1981). Purple pigmentation in the appendix of Araceae appears to be attractive to Sphaeroceridae pollinators (Roháček *et al.* 1990; Angioy *et al.* 2004), but it is not currently known whether it is also attractive to Psychodidae, the main pollinators of *A. maculatum*. Tradeoffs between pigmentation and VOCs could also exist; however these would be limited to benzenoids (e.g. *p*-cresol and skatole) and not terpenes, which form a proportionally larger part of the floral scent bouquet in *A. maculatum* (Chartier *et al.* 2016).

The *A. maculatum* reproductive cycle takes place over 2 days (reviewed in Gibernau 2004): on the evening of the first day, the appendix is thermogenic, heating up to 15°C above ambient air temperature. Pollinators are attracted by VOCs emitted by the appendix, and fall into the trap chamber, where they crawl over the male and female florets. No rewards are provided to pollinators within the chamber. A small amount of stigmatic secretions have been observed, but the low (9–12.5%) sucrose content suggests that this fluid is not nectar (Lack and Diaz 1991), and more likely is produced to collect pollen grains (Paiva *et al.* 2021). The following morning, after the female florets are no longer receptive, pollen is released onto the trapped pollinators. Finally, pollinators are able to escape later in the day, as the sterile hairs at the opening of the trap chamber begin to wither.

In the closely related *Arum italicum*, sesquiterpene biosynthesis appears to begin in the male florets several days prior to anthesis, but the full range of characteristic floral VOCs such as *p*-cresol and skatole are only detected on the day of anthesis, in appendix tissue (Leguet *et al.* 2014). To date, the biosynthetic pathways underlying the production of *p*-cresol and skatole have only been characterized in bacteria (Selmer and Andrei 2001; Liu *et al.* 2018), and it is unclear whether *A. maculatum* and other angiosperms use similar AAA fermentation pathways to produce these VOCs. Furthermore, tissue-specific RNA-seq of *Arum concinnatum* identified more diverse transcript expression in male floret tissue on the day of anthesis rather than in the appendix (Onda *et al.* 2015), even though *A. concinnatum* also emits dung-like VOCs from its appendix (Urru *et al.* 2010). Consequently, many questions remain regarding the specific biosynthetic pathways underlying *A. maculatum* VOCs, the localization of their expression, and whether mRNA expression related to VOC production varies with geographic distance or pollinator community composition.

Here, we aim to address each of the aforementioned gaps in our knowledge. Our specific objectives were to: (1) investigate variation in *A. maculatum* transcript expression between appendix and male floret tissue during anthesis, (2) use these results to identify differentially expressed transcripts putatively related to VOC biosynthesis, and (3) to characterize and compare differential expression in these transcripts across Europe, with a focus on populations with divergent pollinator attraction patterns. We predicted that during anthesis, AAA metabolism would be highly expressed in appendix tissue, while sesquiterpene synthases would be highly expressed in male floret tissue. We further expected to observe differential expression of transcripts associated with AAA metabolism and TPSs in inflorescences with dung-like (i.e. indole, 2-heptanone, and *p*-cresol) vs. sesquiterpene-dominated floral bouquets, respectively. Finally, given that the *A. maculatum* population in Forêt du Gâvre, France, appears to attract almost exclusively *P. grisescens* (Espíndola *et al.* 2011; Szenteczki *et al.* 2021), we predicted that putative locally adapted transcripts associated with particular VOCs may exist within this population. To test these predictions, we surveyed VOC variation, pollinator attraction, and mRNA expression in both appendix and male floret tissue, across most of the *A. maculatum* species distribution range.

MATERIALS AND METHODS

Sampling design

We sampled 10 natural populations of *A. maculatum* between April and May 2019 (Fig. 1): 3 in France (Forêt du Gâvre, Conteville, and Chaumont), 1 in Switzerland (Neuchâtel), 2 in Italy (Montese and Rifreddo), 1 in Croatia (Visuć), 2 in Serbia (Gostilje and Sokobanja), and 1 in Bulgaria (Chiflik). Full details on sample data and population coordinates are given in Supplementary Table 1.

Before collecting tissue samples, we noninvasively sampled the dynamic headspace VOCs emitted by each *A. maculatum* inflorescence, following the methods detailed in (Szenteczki *et al.* 2021). Briefly, this involved placing polydimethylsiloxane coated Twister stir bars (Gerstel) in glass tubes near the appendices of *A. maculatum* inflorescences on the evening of the day of anthesis (18:00–19:00), and pumping air over them for 30 min at an air flow rate of 200 ml/min. All samples were analyzed using a gas chromatography (Agilent 7890a) mass spectrometry (Agilent 5975c) system. Desorption of the VOCs was carried out in a thermal desorption unit (TDU, Gerstel) with an initial temperature of 50°C, followed by a ramp of 60°C/min until 250°C (followed by a 3.5-min hold time). Before injection, the VOCs were cryo-focused (CIS, Gerstel) at −80°C, then released with a ramp of 12°C/min until 260°C (hold time 6 min). PTV solvent vent at 14 PSI and 50 ml/min flow was used for injection into a HP5-MS column in constant flow mode (0.9 ml/min) with helium as the carrier gas. The Mass Selective Detector (MSD) transfer line was set at 280°C. Scan mode was used for the MS acquisition with a solvent delay (1 min), over a mass range of 33–300 *m*/*z*; MS source and quadrupole temperatures were set at 230 and 150°C, respectively. Electron ionization (70 eV) was used. Major ions were recorded for each integrated peak using Agilent Chemstation, and compound identifications were derived from NIST 2.3 (library v.17) and published Kovats retention indices; all names used in our analyses should therefore be considered hypotheses. Appendix temperatures were recorded at the time of VOC sampling using FLIR thermographic imaging, and ambient air temperature was recorded using a thermistor.

Immediately following VOC sampling (i.e. during anthesis), we used sterile scalpel blades to collect 1-mm thick slices of appendix and/or male floret tissue. As a control, male floret tissue samples were also collected from inflorescences the following morning, after pollinator attraction had ended. All samples were individually preserved in RNAlater (Thermo Fischer Scientific) and stored at −80°C until extraction. After collecting each during-anthesis male floret tissue sample, we closed and sealed the small window we cut in floral chamber, so that pollinator trapping was not affected. During the morning following anthesis, we collected all insects trapped within inflorescences, preserved them in 70% ethanol and identified them to at least the suborder level. Psychodidae were further identified to species level (including sex) following taxonomic descriptions and illustrations (Ježek 1990).

Preprocessing raw read data

We performed an initial quality filtering of all raw read files using fastp (Chen *et al.* 2018) to remove adapter sequences and polyA tails, trim reads with phred quality values below 30, and remove reads with >1 “N” bases. Then, we used rCorrector (Song and Florea 2015) to remove reads containing erroneous k-mers (25-mers). Finally, we discarded unfixable read pairs following quality filtering with *FilterUncorrectablePEfastq.py* (https://github.com/harvardinformatics/TranscriptomeAssemblyTools).

De novo transcriptome assembly, annotation, and expression quantification

We merged all of the quality filtered reads and assembled a single de novo reference *A. maculatum* transcriptome (i.e. from all samples, tissue types, and populations) using Trinity v2.11.0 (Grabherr *et al.* 2011) with in silico normalization, a k-mer size of 25, minimum contig size of 200 bp, and strand-specific assembly enabled. Then, we tested 2 methods to filter out redundant transcripts with poor coding potential (i.e. minor isoforms resulting from incomplete assembly, sequencing errors, and/or heterozygosity introduced by our wide geographic sampling range): (1) CD-HIT (Li and Godzik 2006; Fu *et al.* 2012) clustering at 95 % identity with a word size of 5 and (2) the *tr2aacds* v4 pipeline from EvidentialGene (Gilbert 2019), which classifies sequences into primary, alternate, and redundant sets based on coding sequence length and similarity. When using EvidentialGene, we kept only the primary transcripts, removing the alternate and redundant isoforms. We then calculated assembly scores and assessed transcriptome completeness of both filtering methods with BUSCO v5.0.0, using the Embryophyta_odb10 dataset (Seppey *et al.* 2019).

Next, we used dammit v1.2 (Scott *et al.* 2019) to annotate our deduplicated assembly. This pipeline uses Transdecoder (https://github.com/TransDecoder/TransDecoder) to identify candidate coding regions and searches the OrthoDB, Pfam-A, Rfam, and uniref90 protein databases for transcript annotations, with an E-value threshold of 1×10^{-5}. Unannotated transcripts were not removed from the final *A. maculatum* reference transcriptome. We also uploaded the EvidentialGene output to the Kyoto Encyclopedia of Genes and Genomes (KEGG) Automatic Annotation Server (Moriya *et al.* 2007) to generate KEGG Orthology (KO) annotations and pathway maps. Finally, we mapped the cleaned raw reads of each sample to our annotated reference transcriptome using Bowtie2 v2.3.5.1 (Langmead and Salzberg 2012) and quantified transcript expression using RSEM v1.3.2 (Li and Dewey 2011).

Differential expression analyses

RSEM outputs were imported into R v.4.1.0 (R Core Team 2021) using *tximport* 1.20 (Soneson *et al.* 2015). Transcripts expressed below 0.75 counts per million (CPM) in at least 7 samples (i.e. the smallest sample size for a group in our analyses) were then filtered out prior to subsequent analyses in in DESeq2 1.3.2 (Love *et al.* 2014), using the *apeglm* log2fold change shrinkage estimation algorithm (Zhu *et al.* 2019). Transcripts with False Discovery Ratio (FDR)-corrected *P*-values <0.05 and log2fold changes greater than 1.0 or less than −1.0 were considered as significantly differentially expressed among groups. We further identified significantly enriched gene sets in each tissue type using Gene Ontology (GO) term analysis with the R package *TopGO* (Alexa and Rahnenfuhrer 2010) and visualized the result using the R package *rrvgo* 1.4 (Sayols 2020), an implementation of the semantic similarity-based GO summary tool REViGO (Supek *et al.* 2011).

We performed 3 sets of differential expression analyses, each addressing one of the main aims of our study. Our first comparison was between appendix ($n = 7$) and male floret ($n = 16$) tissue collected during anthesis (i.e. at the same phenological time point). Second, we compared male floret tissue collected during anthesis ($n = 14$) against their paired control samples from the morning following anthesis ($n = 14$). Paired control samples were not collected for 2 inflorescences from Sokobanja, Serbia; these individuals were excluded from this analysis. Finally, we compared transcript expression in during-anthesis male floret tissue sampled in the Forêt du Gâvre population against all other populations, to identify transcripts putatively linked to this population's exclusive attraction of *P. grisescens*. To account for some of the effects of isolation by distance, we further split this analysis along the 2 main neutral genetic clusters (Espíndola and Alvarez 2011): specifically, we compared during-anthesis male floret tissue from Forêt du Gâvre ($n = 5$) against during-anthesis male floret tissue from (1) France, Switzerland, and Italy ($n = 7$) and (2) Serbia ($\mathrm{n} = 4$).

Identifying transcripts underlying VOC biosynthesis

Building on the results of our differential expression analyses, we characterized and compared the expression of metabolic pathways underlying key *A. maculatum* VOCs known to be involved in the attraction of Psychodidae pollinators (Kite *et al.* 1998): indole, *p*-cresol, 2-heptanone, and sesquiterpenes. First, we reconstructed entire metabolic pathways using automated annotations, GO terms, and KEGG pathway maps generated from (1) our complete reference transcriptome and (2) sets of significantly differentially expressed genes. Since the genes responsible for the production of 2-heptanone and *p*-cresol in *A. maculatum* are unclear and unknown respectively, we also used homology searches to identify additional candidate genes. Here, we performed BLASTp searches of genes known involved in the biosynthesis of the aforementioned VOCs in other plants and bacteria, against a database of all of our Transdecoder predicted peptide sequences using, with an *e*-value cutoff of 1×10^{-5}. After all candidate transcripts were identified, we visualized variation in their average expression across all tissue types and populations using the R package *pheatmap* (Kolde 2019).

Coinertia analysis—TPSs correlated with VOCs and pollinator attraction

We extracted the coding sequences and DESeq2 normalized expression of all TPSs in our transcriptome (i.e. using uniref annotations, GO/KO terms, and PFAM domains), performed a multiple sequence alignment of these sequences using Clustal Omega (Sievers *et al.* 2011), created a Maximum Likelihood phylogeny using automatic substitution model selection and default parameters in IQ-TREE (Nguyen *et al.* 2015), and visualized the result using iTOL v5 (Letunic and Bork 2021). Then, we investigated whether TPS expression was correlated with (1) total terpene emissions during anthesis or (2) the composition (i.e. sex and/or species) of trapped pollinators within inflorescences. Specifically, we performed coinertia analysis using the R packages *vegan* (Oksanen *et al.* 2020), *RVAideMemoire* (Hervé 2021), and *ade4* (Thioulouse *et al.* 2018), comparing the TPS expression matrix produced above to corresponding matrices of (1) proportional emissions of terpene VOCs and (2) proportions of Psychodidae species trapped by the same *A. maculatum* inflorescences. Prior to this analysis, the gene-level TPS expression matrix was log-transformed and scaled, while the VOC and pollinator matrices were centered log ratio transformed and scaled.

RESULTS

Assembly and annotation quality

Between 27’933’352 and 66’825’898 (median: 40’354’964) paired-end reads from individual tissue samples passed all quality filtering steps (Appendix S1, Table S1). These were subsequently assembled into 273’346 Trinity genes, comprising 593’392 transcript isoforms. Trinity quality statistics (*e.g.* N50 of 1699 bp) are given in Appendix S1, Table S2. EvidentialGene filtered out a larger number of transcripts from this raw assembly (Appendix S1, Table S3) while maintaining a higher BUSCO scores than CD-HIT clustering (*e.g.* 95.6% complete versus 92.2% complete; full result in Appendix S1, Table S4). The EvidentialGene output was therefore annotated and used for all subsequent analyses. A total of 18’411 unique annotations were generated. 17’435 annotations mapped to Eukaryota (94.7%); 12’676 of these annotations further mapped to Mesangiospermae (68.9%); a relatively small number of annotations mapped to bacterial genes (692 results; 3.8%).

A total of 49’779 transcripts remained in our expression matrix following pre-filtering in DESeq2 (*i.e.* >0.75CPM in at least seven samples). Principal components analysis of filtered transcript expression (Appendix S1, Figure S1) revealed highly divergent transcript expression among male floret and appendix tissue during anthesis along the first PCA axis. Along the second PCA axis, samples were further divided between two main geographic regions – namely, northern populations (*i.e.* France, Switzerland, and northern Italy) and Balkan populations (*i.e.* Croatia, Serbia, and Bulgaria). This regional split is consistent with the two main genetic clusters identified using neutral (AFLP) markers (Espíndola and Alvarez 2011).

Differential transcript expression between appendix and male floret tissue

Differential expression analysis comparing appendix and male floret tissue (both collected during anthesis) revealed 8683 transcripts with significantly greater expression in appendix tissue, and 6581 transcripts with significantly greater expression in male floret tissue (FDR corrected p-values <0.05; log2fold change ±1), after controlling for population effects. Furthermore, we found that VOC biosynthetic activity is significantly elevated in *A. maculatum* appendix tissue during anthesis. Many major biosynthetic pathways (e.g. tryptophan/indole synthesis, terpene synthesis, and phenylpropanoid synthesis) were significantly enriched in the appendix tissue during anthesis, whereas transcripts related to pollen production were significantly enriched in male floret tissue (Figure 2).

Differential transcript expression in male florets during- versus post-anthesis

When comparing during- and post-anthesis male floret tissue samples in a differential expression analysis that incorporated the paired nature of these samples, we identified 3847 transcripts with significantly greater expression during anthesis, and 2920 transcripts with significantly greater expression post-anthesis (FDR corrected p-values <0.05; log2fold change ±1). While tryptophan (*i.e.* indole) biosynthesis was elevated in male florets during anthesis, we did not identify increased expression of other putative VOC biosynthetic pathways (Figure 3). The full list of significantly enriched GO terms from both our first and second set of differential expression analyses are available in Appendix S2.

Differential transcript expression associated with exclusive attraction of P. grisescens

Our third and final set of differential expression analyses, comparing male floret tissue during anthesis among populations, revealed that i) 84 and 9 transcripts were respectively differentially expressed in Forêt du Gâvre versus all other French, Swiss, and northern Italian populations (FDR corrected p-value <0.05; log2fold change ±1) and ii) 327 and 175 transcripts were respectively differentially expressed in Forêt du Gâvre versus Serbian populations (FDR corrected p-value <0.05; log2fold change ±1). However, no transcripts putatively linked to VOC biosynthesis were identified among these transcripts.

Candidate genes underlying A. maculatum floral VOCs

Consistent with recent large-scale surveys of *A. maculatum* floral scent (Szenteczki *et al.* 2021; Gfrerer *et al.* 2021) we observed considerable within-population variation in VOC bouquet composition among our samples (Appendix S1, Figure S2 and Table S5). We further identified candidate genes putatively linked to the biosynthesis of several dung-mimicking *A. maculatum* VOCs. First, we identified transcripts in both appendix and male floret tissue homologous with tryptophan synthase alpha subunit (TSA), which catalyses the conversion of indole-3-glycerolphosphate to indole.

Second, we identified homologs of two proteins which catalyse the degradation of tyrosine to 4-hydroxyphenyllactate: aromatic aminotransferase (ISS1) and hydroxyphenylpyruvate reductase (HPPR). Pearson correlation tests further identified several transcripts correlated with HPPR expression in appendix tissue during anthesis (Appendix S1, Table S6); notably, this included a putative dehydratase/shikimate dehydrogenase (Pearson $r = 0.988$, $p < 0.001$). This enzyme may further catalyse the conversion of 4-hydroxyphenyllactate to *p*-coumaric acid. However, we did not identify any homologs of bacterial proteins linked to the production of 4-hydroxyphenylacetate and/or *p*-cresol (Saito *et al.* 2018), such as hydroxyphenylacetate decarboxylase (4-Hpd).

Third, while phenylalanine-derived precursor molecules for several common floral benzenoid/phenylpropanoid (FBP) compounds – particularly *p*-coumaric acid – appear to be produced by *A. maculatum*, transcripts responsible for the production of benzenoid and phenylpropanoid VOCs generally appeared to be absent or weakly expressed in *A. maculatum*. Finally, we identified putative homologs of methylketone synthases (MKS1 and MKS2), which are known to be involved in 2-heptanone biosynthesis (Ben-Israel *et al.* 2009; Khuat *et al.* 2019). Heatmaps of the expression patterns for all of the aforementioned candidate transcripts are shown in Figure 4.

We identified *A. maculatum* transcripts putatively encoding all proteins in both the mevalonate and methyl-D-erythritol 4-phosphate (MEP) pathways. During anthesis, the MEP pathway appears to be more highly expressed than the mevalonate pathway, particularly in appendix tissue (Appendix S1, Figure S3). The first enzyme of the MEP pathway, 1-deoxy-D-xylulose-5-phosphate synthase (DXS), which was highly expressed in appendix tissue, also featured the greatest isoform diversity among all terpene backbone synthesis genes. Furthermore, we identified 108 putative TPS transcripts expressed in appendix and male floret tissue during anthesis. A phylogeny of all putative *A. maculatum* terpene synthases is given in Appendix S1, Figure S4, and expression patterns of TPS transcripts which passed our initial CPM filtering threshold are visualized in Figure 5.

Some of the putative terpene synthases we identified are homologs of proteins known to produce common *A. maculatum* VOCs (e.g. humulenes and germacrenes); others, such as 2-methylisoborneol (2-MIB) synthase, catalyse the production of terpenes not previously described in *A. maculatum*. However, in the case of the latter, the transcript we identified likely encodes a novel TPS, given that we identified an uncharacterized *Colocasia esculenta* (Araceae) gene which shares 92.5% identity with our transcript, as opposed to approximately 22.8% identity with the bacterial 2-MIB synthase (Appendix S1, Figure S5). Transcripts annotated as trimethyltridecatetraene synthase (Cyt P450 92C6) may represent another such novel TPS. This gene was the only putative VOC synthase we identified that was significantly overexpressed (FDR corrected p-values <0.05; log2fold change >1) in appendix tissue samples emitting high quantities of an unnamed sesquiterpene with a non-polar Kovats Retention Index of 1681, which is known to be a strong predictor of *P. grisescens* attraction (Szenteczki *et al.* 2021).

Male floret terpene synthase transcript expression is correlated with pollinator attraction

Coinertia analyses did not identify covariation between putative TPS expression in male floret tissue, and proportional emissions of terpenes in VOC bouquets ($p = 0.964$, Monte-Carlo test, 999 replicates). However, we did identify significant concordance between putative TPS expression in male floret tissue and Psychodidae pollinator composition trapped within inflorescences ($p = 0.047$, Monte-Carlo test, 999 replicates); the first coinertia axis split TPS expression based on species (i.e. *P. grisescens* vs *P. phalaenoides*), while the second coinertia axis split TPS expression based on sex (Appendix S1, Figure S6). Consequently, while our coinertia analyses could not disentangle covariation in TPS expression and specific terpene VOC emissions, it appears that TPS expression in male florets is correlated with sex- and/or species-specific attraction of Psychodidae.

DISCUSSION

High-throughput transcriptome sequencing is rapidly advancing our understanding of the biosynthesis of floral volatile compounds. In this study, we were able to overcome some of the challenges associated with studying the genes underlying VOC biosynthesis in non-model systems (Wong *et al.* 2017b), by surveying transcript expression variation in multiple VOC-emitting floral tissues, across the Europe-wide distribution range of *A. maculatum* (Figure 1). This allowed us to identify i) elevated VOC biosynthetic activity in the appendix of *A. maculatum* during anthesis (Figure 2), ii) candidate transcripts for the production of several VOCs such as *p*-cresol, 2-heptanone, and sesquiterpenes (Figures 4 and 5), and iii) covariation between male floret terpene synthase expression and the relative proportions of *Psychoda phalaenoides* and *P. grisescens* trapped within inflorescences (Appendix S1, Figure S6).

Differential expression analyses

During anthesis, diverse VOC metabolic processes were significantly enriched in *A. maculatum* appendix tissue when compared against male floret tissue. This result is consistent with previous research, suggesting that the thermogenic appendix plays a central role in diffusing the potent VOC bouquets of Araceae (Meeuse 1975; Angioy *et al.* 2004; Barthlott *et al.* 2009). Although we expected to observe elevated TPS activity in male florets during anthesis compared to the morning following anthesis, it appears that many terpene synthases continued to be expressed at approximately equal levels in paired control samples collected the following morning; several factors may explain this pattern. First, given that sesquiterpenes are known to be synthesized and stored in *A. italicum* male floret tissue during the days leading up to anthesis (Leguet *et al.* 2014), mevalonate pathway and TPS expression may have peaked prior to our during-anthesis tissue sampling. However, Araceae are known to emit particularly concentrated VOC blends during anthesis (Skubatz *et al.* 1995, 1996), which should require continuous biosynthesis and emission (Widhalm *et al.* 2015). It is therefore likely that the large number of terpene synthases we identified in the *A. maculatum* transcriptome include those which are most relevant to pollinator attraction.

The timing of our post-anthesis tissue sampling may have also influenced the above result. Post-anthesis sampling occurred within one hour after we collected and preserved all pollinators within the floral chamber; it is therefore likely that most pollinators normally would have still been trapped at this time. Both early (Dormer 1960; Prime 1960; Lack and Diaz 1991) and more recent studies (Bröderbauer *et al.* 2013) of *A. maculatum* have highlighted morphological features related to pollinator retention, namely the sterile flowers partially blocking the exit of the trap, and downward-pointing papillate cells on the inner wall of the spathe. However, continued expression of some TPS transcripts during the morning following anthesis may also highlight sesquiterpenes putatively involved in pollinator retention within the trap chamber. Consequently, our paired 'post-anthesis' samples may not have acted as a negative control for comparison to during-anthesis samples, as we initially intended. Further research is needed to confirm whether the end of male floret VOC emissions may also serve as a cue for pollinator release, which occurs during the afternoon on the second day of the pollination cycle (Prime 1960; Lack and Diaz 1991; Chartier *et al.* 2013).

After comparing male floret transcript expression among populations during anthesis, we did not identify any putative VOC synthases which were unique to Forêt du Gâvre, France. High inter-individual variation in VOC emissions has been widely observed in *A. maculatum* (Szenteczki *et al.* 2021; Gfrerer *et al.* 2021) and this variability is also evident in our transcriptomic dataset. Although our differential expression analyses were unable to identify unique VOC synthases in the Forêt du Gâvre population, targeted investigations into candidate genes underlying key compound classes did provide further insights into species-specific pollinator attraction in *A maculatum*.

Candidate transcripts linked to A. maculatum VOCs

Most inter-individual variation in *A. maculatum* floral scent centres around variation in the ratio of aromatic amino acid-derived VOCs to sesquiterpenes (Szenteczki *et al.* 2021). Correspondingly, we identified abundant expression of transcripts putatively involved in the biosynthesis of these two compound classes. As predicted, indole synthesis via the tryptophan synthase alpha subunit (TSA) was highly expressed in appendix tissue in all studied populations. Some of the TSA transcripts we identified also appear to be homologs of BX1, which more efficiently cleaves indole-3-glycerol phosphate without any interaction with the beta subunit (Frey *et al.* 1997; Kriechbaumer *et al.* 2008). Conversely, TSB was more abundantly expressed in male floret tissue, which would limit indole emissions within the floral trap chamber.

Skatole (3-methylindole) has also been reported in *A. maculatum* VOC emissions (Szenteczki *et al.* 2021; Gfrerer *et al.* 2021), but we did not identify any homologs of indoleacetate decarboxylase in the *A. maculatum* transcriptome, which would produce this compound (Whitehead *et al.* 2008). This may be due to low emissions of skatole by inflorescences sampled in this study; ultimately, the mechanism by which *A. maculatum* produces skatole remains unclear. Prior to this study, it was also unclear whether *A. maculatum* produced *p*-cresol (4-methylphenol) via a pathway homologous to tyrosine degradation in bacteria (Selmer and Andrei 2001; Saito *et al.* 2018), or using one or more novel proteins. We were able to identify candidate transcripts (*i.e.* ISS1 and HPPR homologs) which may catalyse the conversion of tyrosine to *p*-coumaric acid, but were ultimately unable to identify transcripts which could further produce *p*-cresol from *p*-coumaric acid.

Homologs of phenylalanine ammonia-lyase (PAL) and cinnamate 4-hydroxylase (C4H), which produce *p*-coumaric acid from phenylalanine, where also abundantly expressed in the appendix during anthesis. However, downstream proteins producing common floral benzenoid/phenylpropanoid (FBP) VOCs (e.g. eugenol, isoeugenol, benzyl benzoate, benzaldehyde, and phenylacetaldehyde; Muhlemann *et al.* 2014) were largely absent or lowly expressed in both our VOC and transcriptomic datasets. Typically, *p*-coumarate-3-hydroxylase (C3H) would further modify *p*-coumaric acid into precursors for the aforementioned FBP VOCs, but this gene was expressed at relatively low levels in appendix tissue. Interestingly, experimental knock-outs of C3H in *Petunia* × *hybrida* have demonstrated that downregulation of this gene also leads to unexpected production of *p*-cresol (Kim *et al.* 2019). Given that we observed similar patterns in *A. maculatum*, it appears that flowering plants may have a novel mechanism for producing *p*-cresol involving *p*-coumaric acid, which is distinct from known bacterial proteins such as hydroxyphenylacetate decarboxylase.

While not derived from amino acids, 2-heptanone is another abundant *A. maculatum* VOC with a ‘fermented’ scent. In this study, we were able to identify several methylketone synthase homologs (MKS1 and MKS2), which produce 2-heptanone and related compounds in tomato plants (Ben-Israel *et al.* 2009; Khuat *et al.* 2019). 2-heptanone is known to be attractive to fruit flies (Prokopy *et al.* 1998) and beetles (Torto *et al.* 2007); however, it has not yet been linked with the attraction of specific pollinators of *A. maculatum* (Espíndola *et al.* 2011; Szenteczki *et al.* 2021). While this compound is infrequent in VOC bouquets, it can be a proportionally large component of VOC emissions when it is produced (Szenteczki *et al.* 2021); further research is therefore needed to determine whether this compound is also under selection (*e.g.* by Drosophilidae).

We also found that 1-deoxy-D-xylulose-5-phosphate synthase (DXS) activity was elevated in *A. maculatum* appendix tissue during anthesis. An identical expression pattern was also identified in *Arum concinnatum,* where it was hypothesized that DXS is the rate-limiting step in monoterpene synthesis (Onda *et al.* 2015). If DXS is also a rate-limiting enzyme in *A. maculatum*, then this may explain the proportionally smaller quantities of monoterpenes in its floral blend, in comparison to other VOC chemical families.

Finally, we identified many putative terpene synthases in the *A. maculatum* transcriptome, the majority of which appear to produce sesquiterpene VOCs. These include cytochrome P450 enzymes (P450s), which can further modify volatile terpenes through oxidation, methylation, or acylation (Hamberger and Bak 2013). P450s were the first proteins identified in *Arum* appendices (Yáhiel *et al.* 1974), and our transcriptomic data further confirm that a diverse suite of P450s are expressed in *A. maculatum* appendix and male floret tissue during anthesis. Notably, we found that a trimethyltridecatetraene synthase (Cyt P450 92C6) homolog appears to be correlated with the production of at least one unnamed *A. maculatum* sesquiterpene (Kovats RI 1681). This unnamed sesquiterpene was the single strongest predictor of *P. grisescens* attraction in a large-scale survey of *A. maculatum* pollinators (Szenteczki *et al.* 2021). Until now, it has not been possible to experimentally test whether this compound alone is attractive to Psychodidae. However, the candidate gene we identified could be useful in future research aiming to produce this compound through heterologous expression in yeasts (Dhandapani *et al.* 2017; Kutyna and Borneman 2018).

Our results also confirm that bicyclogermacrene synthase (Crocoll *et al.* 2010) is consistently and almost exclusively expressed in male floret tissue during anthesis, in accordance with the dominance of this sesquiterpene in *A. maculatum* floral chamber scent (Kite *et al.* 1998). Interestingly, previous studies have demonstrated that 9-methyl germacrene B is a sex pheromone produced by male *Lutzomyia longipalpis* (Psychodidae) to attract females (Hamilton *et al.* 1996; Gordon C. Hamilton *et al.* 1999). Consequently, *A. maculatum* may emit bicyclogermacrene, or a closely related sesquiterpene compound as a as part of their deceptive pollination strategy (*i.e.* as a pheromone mimic). Such terpene emissions in the floral chamber could stimulate the movement of trapped Psychodidae over the male and female florets, aiding in pollination and pollen dispersal; however, further experiments are needed to test these hypotheses. A recent gas chromatography–electroantennography (GC–EAD; Schiestl and

Marion-Poll 2002) study demonstrated that *P. phalaenoides* antennae responded most strongly to *p*-cresol, germacrene D, and several other unnamed mono- and sesquiterpenes (Gfrerer *et al.* 2022); these findings are consistent with our transcriptomic results. However, *P. grisescens* antennal responses were not tested as part of this study. Consequently, the results of our coinertia analyses could be used to formulate hypotheses for future GC-EAD research.

Male floret-specific terpene synthases and their influence on pollinator attraction

There is growing evidence to suggest that tissue-specific transcript expression of VOC synthases is a common characteristic of deceptive pollination systems (Wong *et al.* 2017a, and references therein), and our results confirm similar patterns in *A. maculatum*. Specifically, our coinertia analyses identified significant covariation between male floret terpene synthase expression, and the communities of Psychodidae pollinators trapped by inflorescences. While the floral scent of *A. maculatum* is often described as dung-like due to abundant emissions of amino acid-derived VOCs, our results suggest that terpene VOCs may be subject to pollinator-mediated selection as well. Recent large-scale ecological studies also support this hypothesis, with sesquiterpene compounds, rather than so-called “dung-mimicking” compounds, being a better predictor of variation in pollinator attraction patterns (Szenteczki *et al.* 2021) and fruit set size (Gfrerer *et al.* 2021) in *A. maculatum*.

Some of the main compounds related to sex- and species-specific attraction in our coinertia analysis included humulene (covarying with female *P. phalaenoides*), and the aforementioned trimethyltridecatetraene synthase homolog, which may produce an unnamed sesquiterpene with a Kovats Retention Index of 1681 (covarying with *P. grisescens*). Notably, these same compounds were highlighted as key predictors of pollinator species trapped by *A. maculatum* inflorescences in a random forest analysis with a larger sample size (Szenteczki *et al.* 2021). Further research is therefore needed in order to assess the importance of male floret VOCs for pollinator attraction in *A. maculatum*, and to confirm the true identities of the compounds produced by the candidate terpene synthases we identified.

Conclusion

Our data provide a deeper understanding of the relationships between transcript expression, floral scent, and pollinator attraction in *A. maculatum*, and may lead to the identification of new VOC biosynthetic genes in the future. It appears that *A. maculatum* inflorescences employ a combination of highly diverse appendix VOCs including 2-heptanone, indole, and *p*-cresol to attract a broad range of coprophilous dipterans to their inflorescences, and specialized sesquiterpene emissions to further lure specific Psychodidae into the floral trap chamber. Male floret-specific VOCs, particularly bicyclogermacrene, may also play a role in retaining pollinators until the pollination cycle is complete. While Kite and colleagues (Kite 1995; Kite *et al.* 1998) separately characterized *A. maculatum* appendix and trap chamber VOC emissions, all subsequent studies analysed total headspace profiles (*i.e.* a blend of appendix and trap chamber VOCs). Our results highlight a need for further focused study of VOCs within the trap chamber, given that specific sesquiterpenes appear to be an important aspect of this highly specialized lure-and-trap pollination system.

ACKNOWLEDGEMENTS

We thank Monica Fleisher, Andrea Galmán, and Alberto Garcia Jimenez for their dedicated assistance during our field sampling, and Laurent Oppliger and colleagues for allowing us to sample VOCs and tissue from the native population of *A. maculatum* at the Jardin Botanique de Neuchâtel. We also thank Dessislava Savova Bianchi for her support during RNA extractions, Johann Weber for his advice on our RNA-seq library preparation, and Eran Pichersky for his advice on the biosynthesis of some floral VOCs.

FUNDING STATEMENT

This project was funded by the Swiss National Science Foundation through grant P1NEP3_191659 awarded to MAS and grant 31003A_163334 awarded to NA and SR**.**

DATA ACCESSIBILITY

Appendices S1 and S2 contains supporting figures and tables referenced in the main text. Raw Illumina RNA-seq reads have been deposited in the NCBI SRA database under the BioProject Accession PRJNA856436 (https://www.ncbi.nlm.nih.gov/bioproject/PRJNA856436). Additional data, including the files and R code needed to reproduce all analyses and figures have been archived in the Zenodo repository 6806366 (https://doi.org/10.5281/zenodo.6806365).

AUTHOR CONTRIBUTIONS

MAS, ALG, MG, SR, and NA designed the experiments. MAS and ALG conducted the field sampling. MAS prepared tissue samples for RNA-Seq library preparation, and ALG and MG analyzed the headspace VOC samples and identified pollinators. MAS and JG designed and performed the bioinformatic analyses, and MG contributed to the interpretation of the results. MAS wrote the manuscript. All coauthors contributed to the revision of the manuscript, and have approved it for publication.

REFERENCES

Alexa, A., and J. Rahnenfuhrer, 2010 topGO: enrichment analysis for gene ontology. R package version 2.0.

Angioy, A. M., M. C. Stensmyr, I. Urru, M. Puliafito, I. Collu *et al.*, 2004 Function of the heater: the dead horse arum revisited. Proceedings. Biol. Sci. 271 Suppl: S13-5.

Barthlott, W., J. Szarzynski, P. Vlek, W. Lobin, and N. Korotkova, 2009 A torch in the rain forest: thermogenesis of the Titan arum (*Amorphophallus titanum*). Plant Biol. (Stuttg). 11: 499–505.

Ben-Israel, I., G. Yu, M. B. Austin, N. Bhuiyan, M. Auldridge *et al.*, 2009 Multiple biochemical and morphological factors underlie the production of methylketones in tomato trichomes. Plant Physiol. 151: 1952–1964.

Bröderbauer, D., A. Weber, and A. Diaz, 2013 The design of trapping devices in pollination traps of the genus *Arum* (Araceae) is related to insect type. Bot. J. Linn. Soc. 172: 385–397.

Byers, K. J. R. P., H. D. Bradshaw, and J. A. Riffell, 2014 Three floral volatiles contribute to differential pollinator attraction in monkeyflowers (*Mimulus*). J. Exp. Biol. 217: 614–623.

Chartier, M., S. Liagre, H. Weiss-Schneeweiss, B. Kolano, J.-M. Bessière *et al.*, 2016 Floral traits and pollination ecology of European *Arum* hybrids. Oecologia 180: 439–451.

Chartier, M., L. Pélozuelo, B. Buatois, J.-M. Bessière, and M. Gibernau, 2013 Geographical variations of odour and pollinators, and test for local adaptation by reciprocal transplant of two European *Arum* species.Funct. Ecol. 27: 1367–1381.

Chartier, M., L. Pélozuelo, and M. Gibernau, 2011 Do floral odor profiles geographically vary with the degree of specificity for pollinators? Investigation in two sapromyophilous *Arum* species (Araceae). Ann. la Société Entomol. Fr. 47: 71–77.

Chen, S., Y. Zhou, Y. Chen, and J. Gu, 2018 fastp: an ultra-fast all-in-one FASTQ preprocessor. Bioinformatics 34: i884–i890.

Crocoll, C., J. Asbach, J. Novak, J. Gershenzon, and J. Degenhardt, 2010 Terpene synthases of oregano (*Origanum vulgare* L.) and their roles in the pathway and regulation of terpene biosynthesis. Plant Mol. Biol. 73: 587–603.

Dhandapani, S., J. Jin, V. Sridhar, R. Sarojam, N.-H. Chua *et al.*, 2017 Integrated metabolome and transcriptome analysis of *Magnolia champaca* identifies biosynthetic pathways for floral volatile organic compounds. BMC Genomics 18: 463.

Diaz, A., and G. Kite, 2002 A comparison of the pollination ecology of *Arum maculatum* and *A. italicum* in England. Watsonia 24: 171–182.

Dobson, H. E. M., J. Arroyo, G. Bergström, and I. Groth, 1997 Interspecific variation in floral fragrances within the genus *Narcissus* (Amaryllidaceae). Biochem. Syst. Ecol. 25: 685–706.

Dormer, K. J., 1960 The truth about pollination in *Arum*. New Phytol. 59: 298–301.

Espíndola, A., and N. Alvarez, 2011 Comparative Phylogeography in a Specific and Obligate Pollination Antagonism. PLoS One 6: e28662.

Espíndola, A., L. Pellissier, and N. Alvarez, 2011 Variation in the proportion of flower visitors of *Arum maculatum* along its distributional range in relation with community-based climatic niche analyses. Oikos 120: 728–734.

Fenster, C. B., W. S. Armbruster, P. Wilson, M. R. Dudash, and J. D. Thomson, 2004 Pollination syndromes and floral specialization. Annu. Rev. Ecol. Evol. Syst. 35: 375–403.

Frey, M., P. Chomet, E. Glawischnig, C. Stettner, S. Grün *et al.*, 1997 Analysis of a chemical plant defense mechanism in grasses. Science 277: 696–699.

Friberg, M., C. Schwind, P. R. Guimarães, R. A. Raguso, and J. N. Thompson, 2019 Extreme diversification of floral volatiles within and among species of *Lithophragma* (Saxifragaceae). Proc. Natl. Acad. Sci. 116: 4406–4415.

Fu, L., B. Niu, Z. Zhu, S. Wu, and W. Li, 2012 CD-HIT: accelerated for clustering the next-generation sequencing data. Bioinformatics 28: 3150–3152.

Gervasi, D. D. L., and F. P. Schiestl, 2017 Real-time divergent evolution in plants driven by pollinators. Nat. Commun. 8: 14691.

Gfrerer, E., D. Laina, M. Gibernau, R. Fuchs, M. Happ *et al.*, 2021 Floral Scents of a Deceptive Plant Are Hyperdiverse and Under Population-Specific Phenotypic Selection. Front. Plant Sci. 12: 719092.

Gfrerer, E., D. Laina, R. Wagner, M. Gibernau, A. C. Hörger *et al.*, 2022 Antennae of psychodid and sphaerocerid flies respond to a high variety of floral scent compounds of deceptive *Arum maculatum* L. Sci. Rep. 12: 1–11.

Gibernau, M., 2004 Pollination in the genus *Arum* – a review. Aroideana 27: 148–166.

Gilbert, D. G., 2019 Longest protein, longest transcript or most expression, for accurate gene reconstruction of transcriptomes? bioRxiv 829184.

Gordon C. Hamilton, J., H. C. Ibbotson, A. M. Hooper, and J. A. Pickett, 1999 9-Methylgermacrene-B is confirmed as the sex pheromone of the sandfly *Lutzomyia longipalpis* from Lapinha, Brazil, and the absolute stereochemistry defined as S. Chem. Commun. 2335–2336.

Grabherr, M. G., B. J. Haas, M. Yassour, J. Z. Levin, D. A. Thompson *et al.*, 2011 Full-length transcriptome assembly from RNA-Seq data without a reference genome. Nat. Biotechnol. 29: 644–652.

Hamberger, B., and S. Bak, 2013 Plant P450s as versatile drivers for evolution of species-specific chemical diversity. Philos. Trans. R. Soc. London. Ser. B, Biol. Sci. 368: 20120426.

Hamilton, J. G., G. W. Dawson, and J. A. Pickett, 1996 9-Methylgermacrene-B; proposed structure for novel homosesquiterpene from the sex pheromone glands of *Lutzomyia longipalpis* (Diptera: Psychodidae) from Lapinha, Brazil. J. Chem. Ecol. 22: 1477–1491.

Hernández-Hernández, T., and J. J. Wiens, 2020 Why Are There So Many Flowering Plants? A Multiscale Analysis of Plant Diversification. Am. Nat. 195: 948–963.

Hervé, M., 2021 RVAideMemoire: Diverse basic statistical and graphical functions. R package version 0.9-81.

Holopainen, J. K., 2004 Multiple functions of inducible plant volatiles. Trends Plant Sci. 9: 529–533.

Irwin, R. E., L. S. Adler, and A. K. Brody, 2004 The dual role of floral traits: Pollinator attraction and plant defense. Ecology 85: 1503–1511.

Ježek, J., 1990 Redescriptions of nine common palaearctic and holarctic species of Psychodini end. (Diptera: Psychodidae). Acta Entomol. Musei Natl. Pragae 43: 33–83.

Junker, R. R., and A. L. Parachnowitsch, 2015 Working towards a holistic view on flower traits - how floral scents mediate plant-animal interactions in concert with other floral characters. J. Indian Inst. Sci. 95: 43–67.

Khuat, V. L. U., V. T. T. Bui, H. T. D. Tran, N. X. Truong, T. C. Nguyen *et al.*, 2019 Characterization of Solanum melongena Thioesterases Related to Tomato Methylketone Synthase 2. Genes 10: 549.

Kim, J. Y., R. T. Swanson, M. I. Alvarez, T. S. Johnson, K. H. Cho *et al.*, 2019 Down regulation of p-coumarate 3-hydroxylase in petunia uniquely alters the profile of emitted floral volatiles. Sci. Rep. 9: 8852.

Kite, G. C., 1995 The floral odour of *Arum maculatum*. Biochem. Syst. Ecol. 23: 343–354.

Kite, G. C., W. L. A. Hetterscheid, M. J. Lewis, P. C. Boyce, J. Ollerton *et al.*, 1998 Inflorescence odours and pollinators of *Arum* and *Amorphophallus* (Araceae), pp. 295–315 in *Reproductive Biology,* edited by S. J. Owens and P. J. Rudall. Royal Botanic Gardens Kew, London, UK.

Knoll, F., 1926 Insekten und Blumen, die *Arum* - Blütenstände und ihre Besucher. Anhandlungen der Zool. und Bot. Gesellschaft Wien 12: 379–481.

Knudsen, J. T., and J. Gershenzon, 2020 The Chemical Diversity of Floral Scent, pp. 57–78 in *Biology of Plant Volatiles*, edited by E. Pichersky and N. Dudareva. CRC Press.

Knudsen, J. T., and L. Tollsten, 1993 Trends in floral scent chemistry in pollination syndromes: floral scent composition in moth-pollinated taxa. Bot. J. Linn. Soc. 113: 263–284.

Kolde, R., 2019 pheatmap: Pretty Heatmaps. R package version 1.0.12.

Kriechbaumer, V., L. Weigang, A. Fiesselmann, T. Letzel, M. Frey *et al.*, 2008 Characterisation of the tryptophan synthase alpha subunit in maize. BMC Plant Biol. 8: 44.

Kutyna, D. R., and A. R. Borneman, 2018 Heterologous Production of Flavour and Aroma Compounds in Saccharomyces cerevisiae. Genes 9: 326.

Lack, A. J., and A. Diaz, 1991 The pollination of *Arum maculatum* L. - a historical review and new observations. Watsonia 18: 333–342.

Langmead, B., and S. L. Salzberg, 2012 Fast gapped-read alignment with Bowtie 2. Nat. Methods 9: 357–359.

Leguet, A., M. Gibernau, L. Shintu, S. Caldarelli, S. Moja *et al.*, 2014 Evidence for early intracellular accumulation of volatile compounds during spadix development in *Arum italicum* L. and preliminary data on some tropical Aroids. Naturwissenschaften 101: 623–635.

Letunic, I., and P. Bork, 2021 Interactive Tree Of Life (iTOL) v5: an online tool for phylogenetic tree display and annotation. Nucleic Acids Res. 49: W293–W296.

Li, B., and C. N. Dewey, 2011 RSEM: accurate transcript quantification from RNA-Seq data with or without a reference genome. BMC Bioinformatics 12: 323.

Li, W., and A. Godzik, 2006 Cd-hit: a fast program for clustering and comparing large sets of protein or nucleotide sequences. Bioinformatics 22: 1658–1659.

Liu, D., Y. Wei, X. Liu, Y. Zhou, L. Jiang *et al.*, 2018 Indoleacetate decarboxylase is a glycyl radical enzyme catalysing the formation of malodorant skatole. Nat. Commun. 9: 4224.

Love, M. I., W. Huber, and S. Anders, 2014 Moderated estimation of fold change and dispersion for RNA-seq data with DESeq2. Genome Biol. 15: 550.

Meeuse, B. J. D., 1975 Thermogenic Respiration in Aroids. Annu. Rev. Plant Physiol. 26: 117–126.

Moriya, Y., M. Itoh, S. Okuda, A. C. Yoshizawa, and M. Kanehisa, 2007 KAAS: An automatic genome annotation and pathway reconstruction server. Nucleic Acids Res. 35: 182–185.

Muhlemann, J. K., A. Klempien, and N. Dudareva, 2014 Floral volatiles: from biosynthesis to function. Plant. Cell Environ. 37: 1936–1949.

Newman, E., B. Anderson, and S. D. Johnson, 2012 Flower colour adaptation in a mimetic orchid. Proceedings. Biol. Sci. 279: 2309–2313.

Nguyen, L.-T., H. A. Schmidt, A. von Haeseler, and B. Q. Minh, 2015 IQ-TREE: A Fast and Effective Stochastic Algorithm for Estimating Maximum-Likelihood Phylogenies. Mol. Biol. Evol. 32: 268–274.

Van der Niet, T., and S. D. Johnson, 2012 Phylogenetic evidence for pollinator-driven diversification of angiosperms. Trends Ecol. Evol. 27: 353–361.

Oksanen, J., F. G. Blanchet, M. Friendly, R. Kindt, P. Legendre *et al.*, 2020 vegan: Community Ecology Package. R package version 2.5-7.

Onda, Y., K. Mochida, T. Yoshida, T. Sakurai, R. S. Seymour *et al.*, 2015 Transcriptome analysis of thermogenic *Arum concinnatum* reveals the molecular components of floral scent production. Sci. Rep. 5: 8753.

Paiva, É. A. S., I. Ballego-Campos, and M. Gibernau, 2021 True nectar or stigmatic secretion? Structural evidence elucidates an old controversy regarding nectaries in *Anthurium*. Am. J. Bot. 108: 37–50.

Pellmyr, O., and L. B. Thien, 1986 Insect Reproduction and Floral Fragrances : Keys to the Evolution of the Angiosperms? Taxon 35: 76–85.

Pichersky, E., and J. Gershenzon, 2002 The formation and function of plant volatiles: Perfumes for pollinator attraction and defense. Curr. Opin. Plant Biol. 5: 237–243.

Prime, C. T., 1960 *Lords and ladies*. Collins, London.

Prokopy, R. J., X. Hu, E. B. Jang, R. I. Vargas, and J. D. Warthen, 1998 Attraction of mature *Ceratitis capitata* females to 2-heptanone, a component of coffee fruit odor. J. Chem. Ecol. 24: 1293–1304.

R Core Team, 2021 R: A Language and Environment for Statistical Computing.

Roháček, J., I. Beck-Haug, and K. Dobat, 1990 Sphaeroceridae associated with flowering *Arum maculatum* (Araceae) in the vicinity of Tübingen, SW-Germany. Senckenb. Biol. 71: 259–268.

Saito, Y., T. Sato, K. Nomoto, and H. Tsuji, 2018 Identification of phenol- and p-cresol-producing intestinal bacteria by using media supplemented with tyrosine and its metabolites. FEMS Microbiol. Ecol. 94:.

Sayols, S., 2020 rrvgo: a Bioconductor package to reduce and visualize Gene Ontology terms. R package version 1.4.

Schemske, D. W., and H. D. Bradshaw, 1999 Pollinator preference and the evolution of floral traits in monkeyflowers (*Mimulus*). Proc. Natl. Acad. Sci. 96: 11910 LP – 11915.

Schiestl, F. P., and S. D. Johnson, 2013 Pollinator-mediated evolution of floral signals. Trends Ecol. Evol. 28: 307–315.

Schiestl, F. P., and F. Marion-Poll, 2002 Detection of physiologically active flower volatiles using gas chromatography coupled with electroantennography, pp. 173–198 in *Analysis of taste and aroma*, Springer.

Schmucker, T., 1925 Beiträge zur Biologie und Physiologie von *Arum maculatum*. Flora oder Allg. Bot. Zeitung 460–475.

Scott, C., T. Pierce, L. K. Johnson, C. T. Brown, C. Reid *et al.*, 2019 dib-lab/dammit: dammit v1.2.

Selmer, T., and P. I. Andrei, 2001 p-Hydroxyphenylacetate decarboxylase from *Clostridium difficile*. A novel glycyl radical enzyme catalysing the formation of *p*-cresol. Eur. J. Biochem. 268: 1363–1372.

Seppey, M., M. Manni, and E. M. Zdobnov, 2019 BUSCO: Assessing Genome Assembly and Annotation Completeness BT - Gene Prediction: Methods and Protocols, pp. 227–245 in edited by M. Kollmar. Springer New York, New York, NY.

Sievers, F., A. Wilm, D. Dineen, T. J. Gibson, K. Karplus *et al.*, 2011 Fast, scalable generation of high-quality protein multiple sequence alignments using Clustal Omega. Mol. Syst. Biol. 7: 539.

Skubatz, H., D. D. Kunkel, W. N. Howald, R. Trenkle, and B. Mookherjee, 1996 The *Sauromatum guttatum* appendix as an osmophore: Excretory pathways, composition of volatiles and attractiveness to insects. New Phytol. 134: 631–640.

Skubatz, H., D. D. Kunkel, J. M. Patt, W. N. Howald, T. G. Hartman *et al.*, 1995 Pathway of terpene excretion by the appendix of *Sauromatum guttatum*. Proc. Natl. Acad. Sci. U. S. A. 92: 10084–10088.

Soneson, C., M. I. Love, and M. D. Robinson, 2015 Differential analyses for RNA-seq: transcript-level estimates improve gene-level inferences. F1000Research 4: 1521.

Song, L., and L. Florea, 2015 Rcorrector: efficient and accurate error correction for Illumina RNA-seq reads. Gigascience 4: 48.

Supek, F., M. Bošnjak, N. Škunca, and T. Šmuc, 2011 REVIGO summarizes and visualizes long lists of gene ontology terms. PLoS One 6: e21800.

Szenteczki, M. A., A. L. Godschalx, A. Galmán, A. Espíndola, M. Gibernau *et al.*, 2021 Spatial and temporal heterogeneity in pollinator communities maintains within-species floral odour variation. Oikos 130: 1487–1499.

Thioulouse, J., S. Dray, A.-B. Dufour, A. Siberchicot, T. Jombart *et al.*, 2018 *Multivariate Analysis of Ecological Data with ade4*. Springer, New York, NY.

Thompson, J. N., C. Schwind, and M. Friberg, 2017 Diversification of Trait Combinations in Coevolving Plant and Insect Lineages. Am. Nat. 190: 171–184.

Thompson, J. N., C. Schwind, P. R. Guimarães, and M. Friberg, 2013 Diversification through multitrait evolution in a coevolving interaction. Proc. Natl. Acad. Sci. 110: 11487–11492.

Torto, B., D. G. Boucias, R. T. Arbogast, J. H. Tumlinson, and P. E. A. Teal, 2007 Multitrophic interaction facilitates parasite–host relationship between an invasive beetle and the honey bee. Proc. Natl. Acad. Sci. 104: 8374 LP – 8378.

Trunschke, J., K. Lunau, G. H. Pyke, Z.-X. Ren, and H. Wang, 2021 Flower Color Evolution and the Evidence of Pollinator-Mediated Selection. Front. Plant Sci. 12: 1096.

Urru, I., J. Stökl, J. Linz, T. Krügel, M. C. Stensmyr *et al.*, 2010 Pollination strategies in Cretan Arum lilies. Biol. J. Linn. Soc. 101: 991–1001.

Vogel, S., 1965 Kesselfallen–Blumen. Umschau 65: 12–17.

Whitehead, T. R., P. N. P., D. H. L., and C. M. A., 2008 Catabolic Pathway for the Production of Skatole and Indoleacetic Acid by the Acetogen *Clostridium drakei*, *Clostridium scatologenes*, and Swine Manure. Appl. Environ. Microbiol. 74: 1950–1953.

Whitehead, M. R., and R. Peakall, 2009 Integrating floral scent, pollination ecology and population genetics. Funct. Ecol. 23: 863–874.

Widhalm, J. R., R. Jaini, J. A. Morgan, and N. Dudareva, 2015 Rethinking how volatiles are released from plant cells. Trends Plant Sci. 20: 545–550.

Williams, C. A., J. B. Harborne, and S. J. Mayo, 1981 Anthocyanin pigments and leaf flavonoids in the family araceae. Phytochemistry 20: 217–234.

Wong, D. C. J., R. Amarasinghe, C. Rodriguez-Delgado, R. Eyles, E. Pichersky *et al.*, 2017a Tissue-Specific Floral Transcriptome Analysis of the Sexually Deceptive Orchid *Chiloglottis trapeziformis* Provides Insights into the Biosynthesis and Regulation of Its Unique UV-B Dependent Floral Volatile, Chiloglottone 1. Front. Plant Sci. 8: 1260.

Wong, D. C. J., E. Pichersky, and R. Peakall, 2017b The biosynthesis of unusual floral volatiles and blends involved in orchid pollination by deception: Current progress and future prospects. Front. Plant Sci. 8: 1955.

Xiao, H., Y. Zhang, and M. Wang, 2019 Discovery and Engineering of Cytochrome P450s for Terpenoid Biosynthesis. Trends Biotechnol. 37: 618–631.

Yáhiel, V., M. G. Cotte-Martinon, and G. Ducet, 1974 Un cytochrome de type P450 dans le spadice d'arum. Phytochemistry 13: 1649–1651.

Zhu, A., J. G. Ibrahim, and M. I. Love, 2019 Heavy-Tailed prior distributions for sequence count data: Removing the noise and preserving large differences. Bioinformatics 35: 2084–2092.

<u>FIGURES</u>

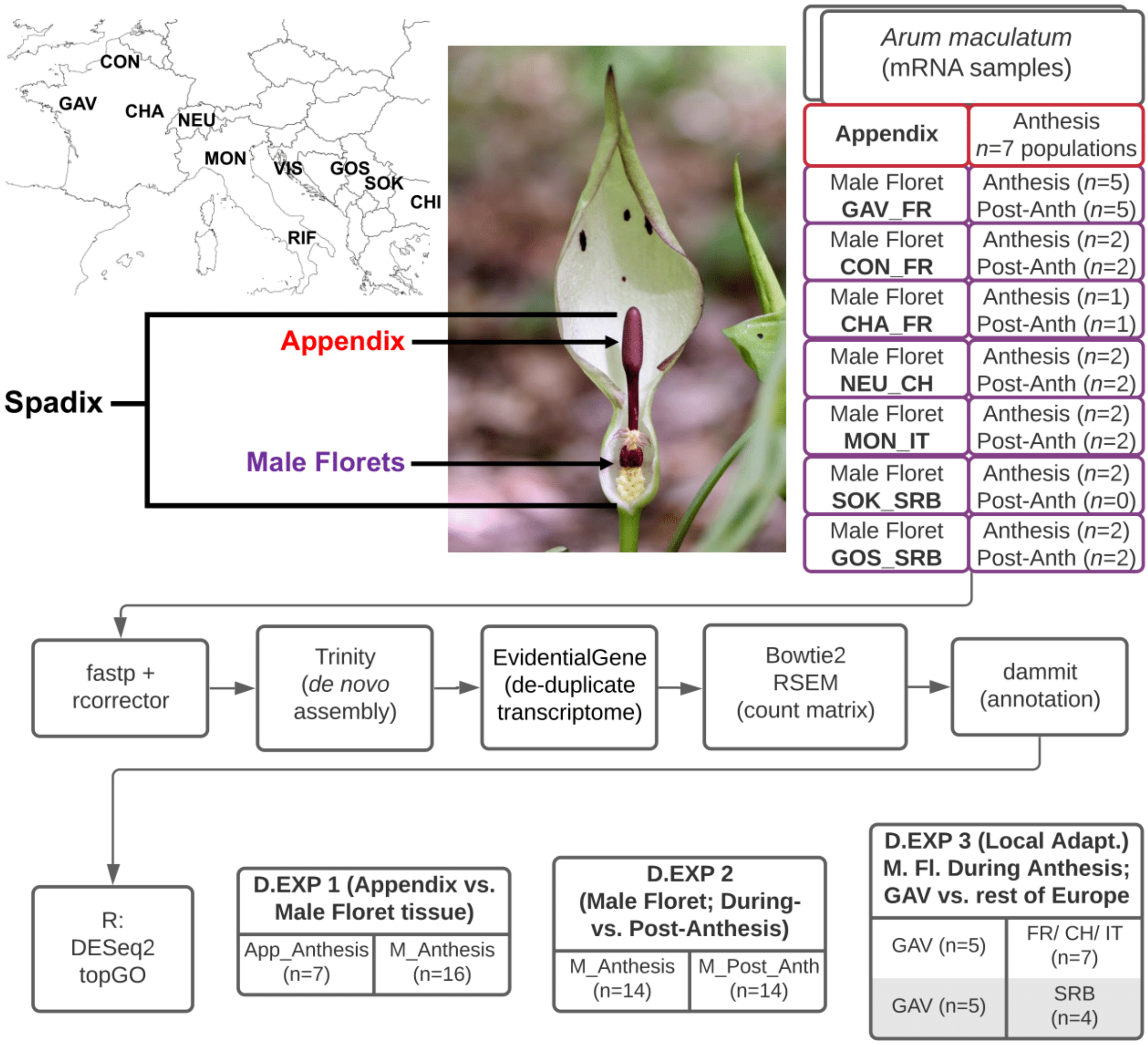

Arum maculatum (mRNA samples)	
Appendix	Anthesis *n*=7 populations
Male Floret **GAV_FR**	Anthesis (*n*=5) Post-Anth (*n*=5)
Male Floret **CON_FR**	Anthesis (*n*=2) Post-Anth (*n*=2)
Male Floret **CHA_FR**	Anthesis (*n*=1) Post-Anth (*n*=1)
Male Floret **NEU_CH**	Anthesis (*n*=2) Post-Anth (*n*=2)
Male Floret **MON_IT**	Anthesis (*n*=2) Post-Anth (*n*=2)
Male Floret **SOK_SRB**	Anthesis (*n*=2) Post-Anth (*n*=0)
Male Floret **GOS_SRB**	Anthesis (*n*=2) Post-Anth (*n*=2)

Figure 1. Overview of the sampling design, bioinformatic pipeline, and differential expression analyses in this study. Inset photo: *A. maculatum inflorescence*, with the lower spathe chamber dissected to reveal the male and female florets. Inset map: population codes, placed over their approximate locations.

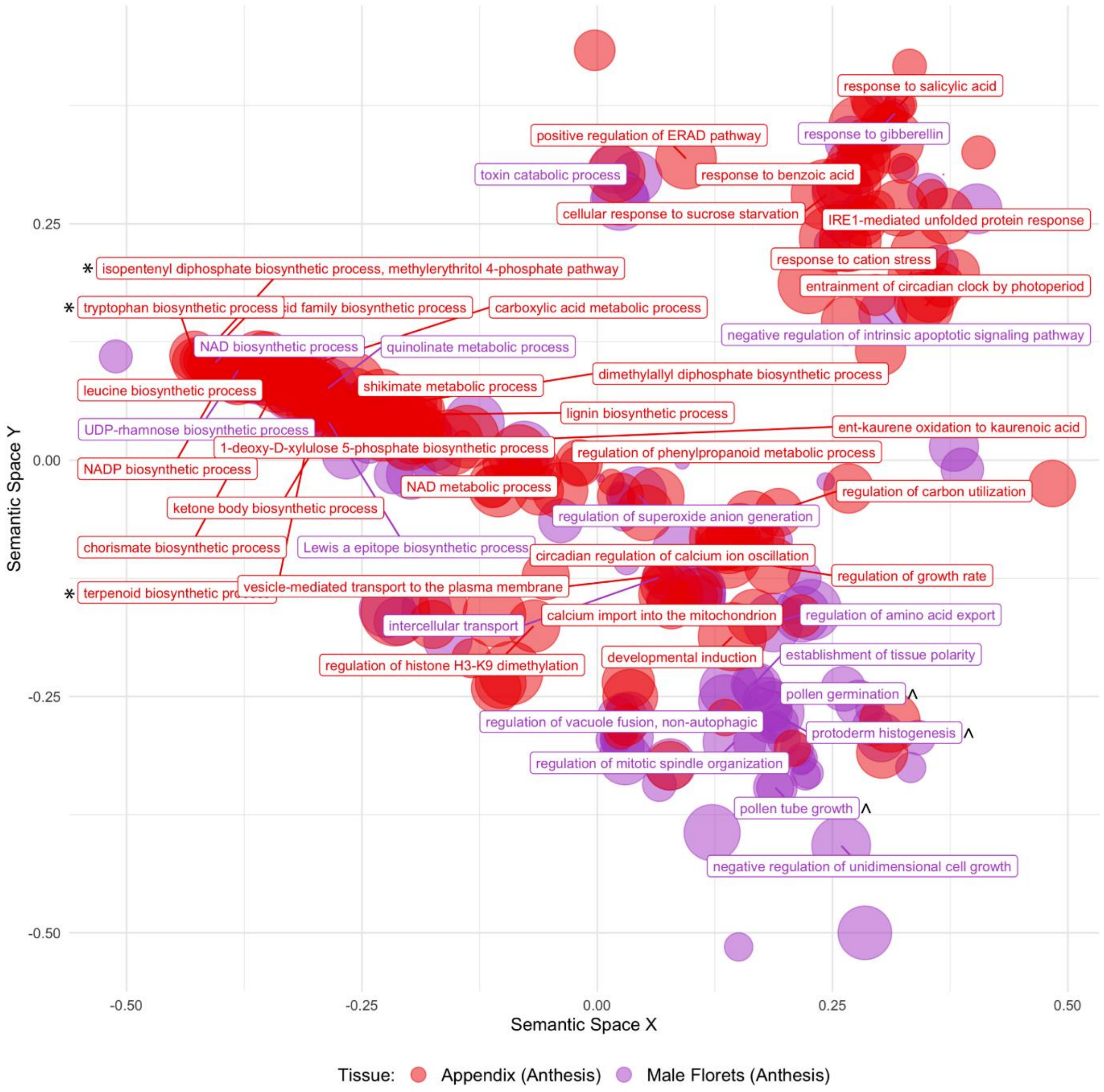

Figure 2. Significantly enriched GO terms when comparing *A. maculatum* appendix (n = 7) and male floret (n = 16) transcript expression during anthesis. Nonredundant GO terms are visualized in semantic similarity space (allowed similarity = 0.8); the full list of GO terms represented above is available in Supplementary Appendix 2.

[*] indicates parent groups linked to the biosynthesis of volatile compounds and [^] indicates parent groups linked to pollen production

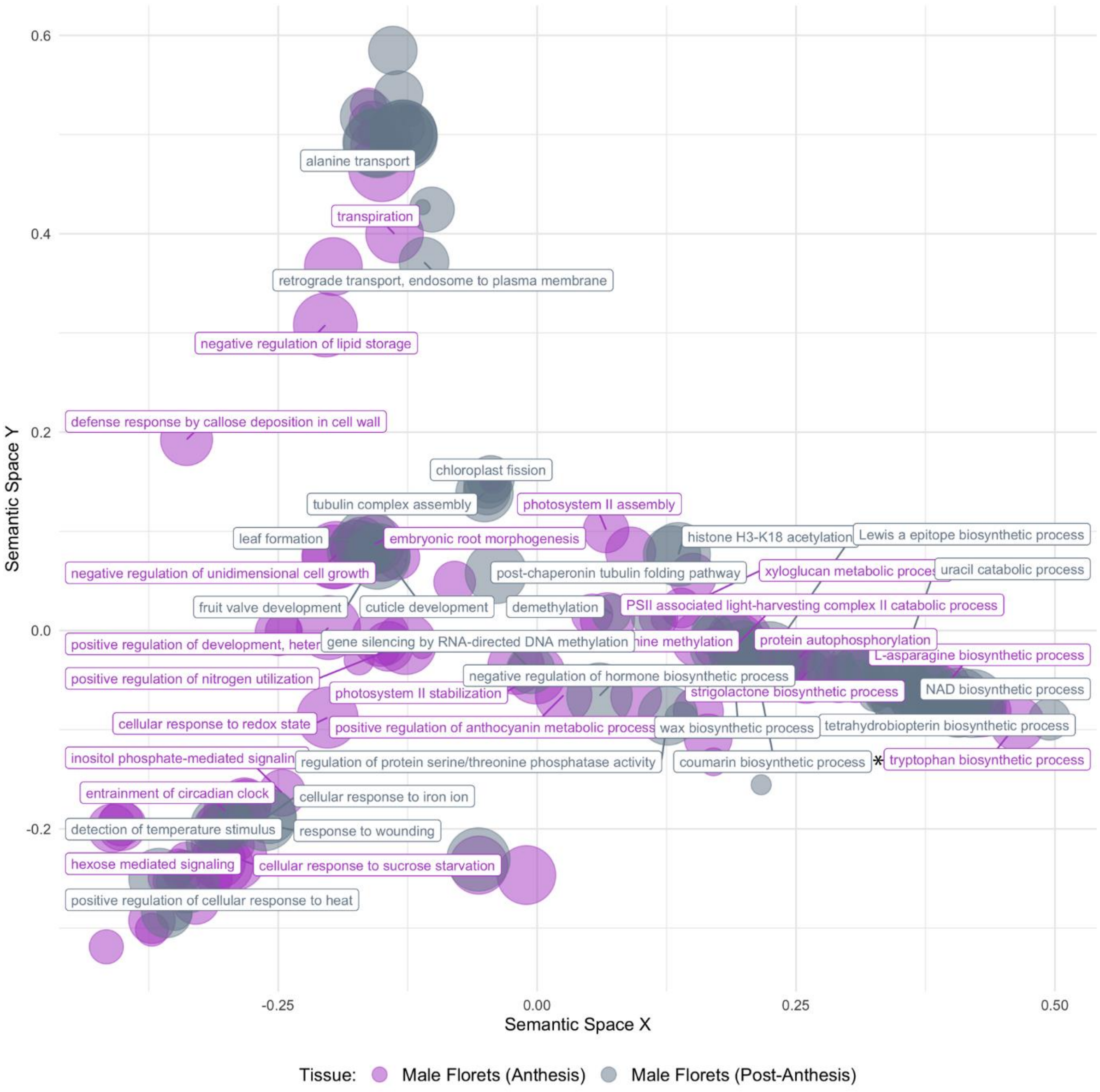

Figure 3. Significantly enriched GO terms when comparing *A. maculatum* transcript expression in male floret tissue during anthesis (n = 14), vs. approximately 18 h after anthesis (n = 14). Nonredundant GO terms are visualized in semantic similarity space (allowed similarity = 0.8); the full list of GO terms represented above is available in Supplementary Appendix 2.

[*] indicates parent groups linked to the biosynthesis of volatile compounds

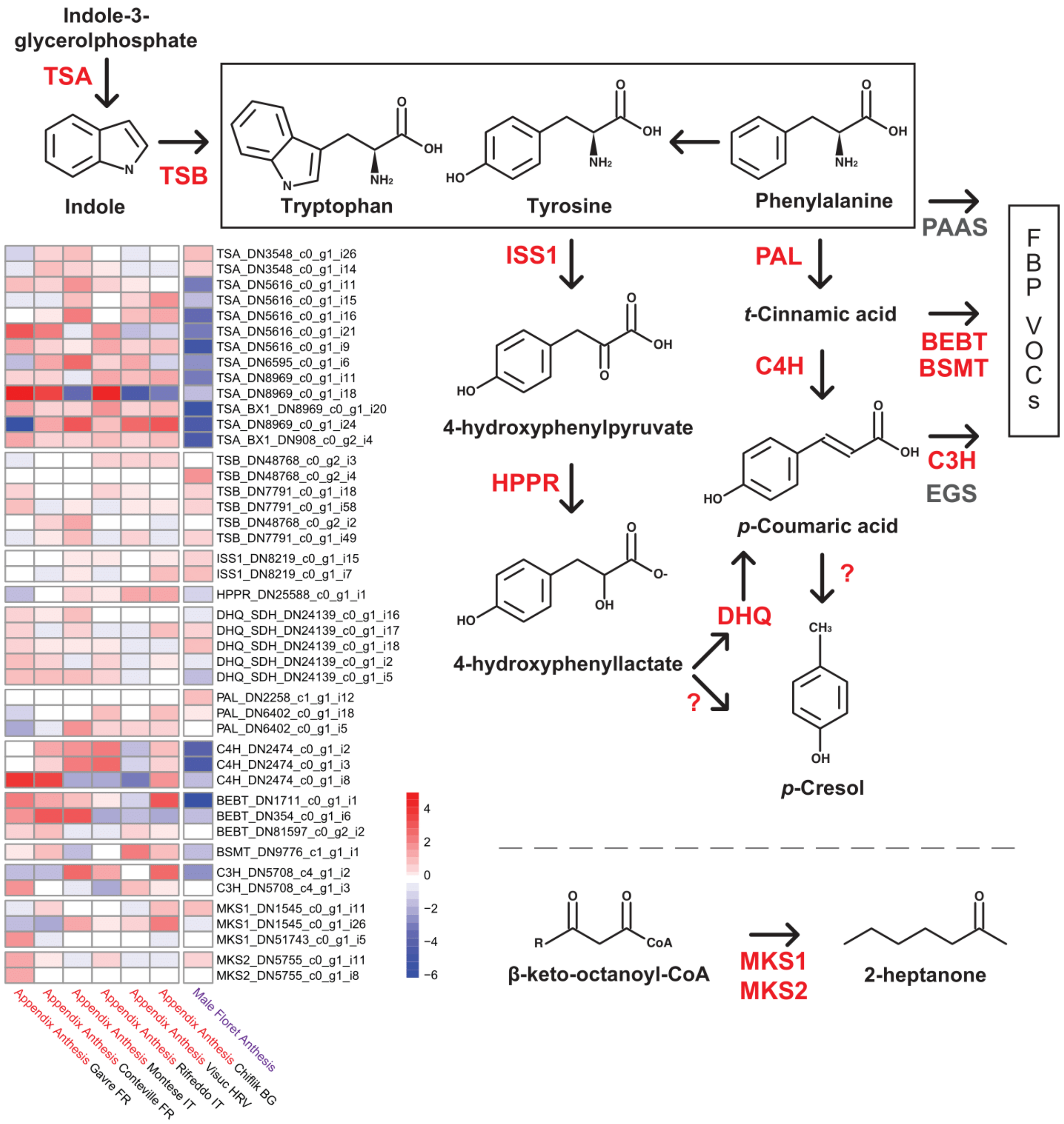

Figure 4. A simplified overview of key proteins involved in producing aromatic amino acid-derived *A. maculatum* VOCs, and a heatmap of their vst-transformed expression during anthesis. Color scale represents whether expression in a given group (i.e. tissue type and population) is above or below the transcript's mean expression across all samples. Genes in gray are absent from the A. maculatum transcriptome. Gene names: BEBT = benzyl alcohol O-benzoyltransferase; BSMT, benzoic acid/salicylic acid carboxyl methyltransferase; DHQ, 3-dehydroquinate dehydratase/shikimate dehydrogenase; EGS, eugenol synthase; MKS, methylketone synthase; PAAS, phenylacetaldehyde synthase; TSA/B, tryptophan synthase alpha/beta subunit; ?, unknown gene(s).

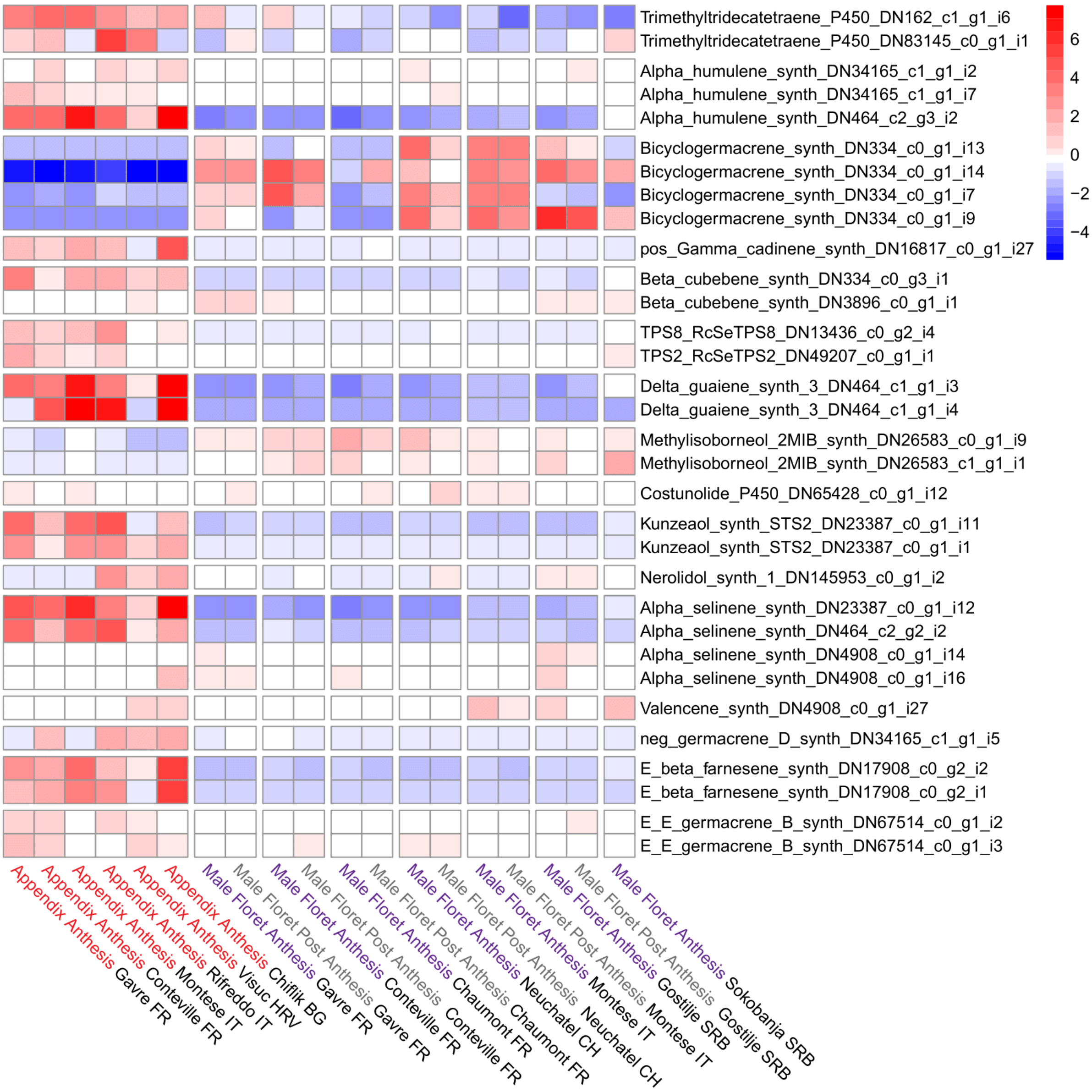

Figure 5. Heatmap of vst-transformed expression of putative terpene synthases in *A. maculatum*. Colour scale represents whether expression in a given group (i.e. tissue type, stage of anthesis, and population) is above or below the transcript's mean expression across all samples.

APPENDIX S1

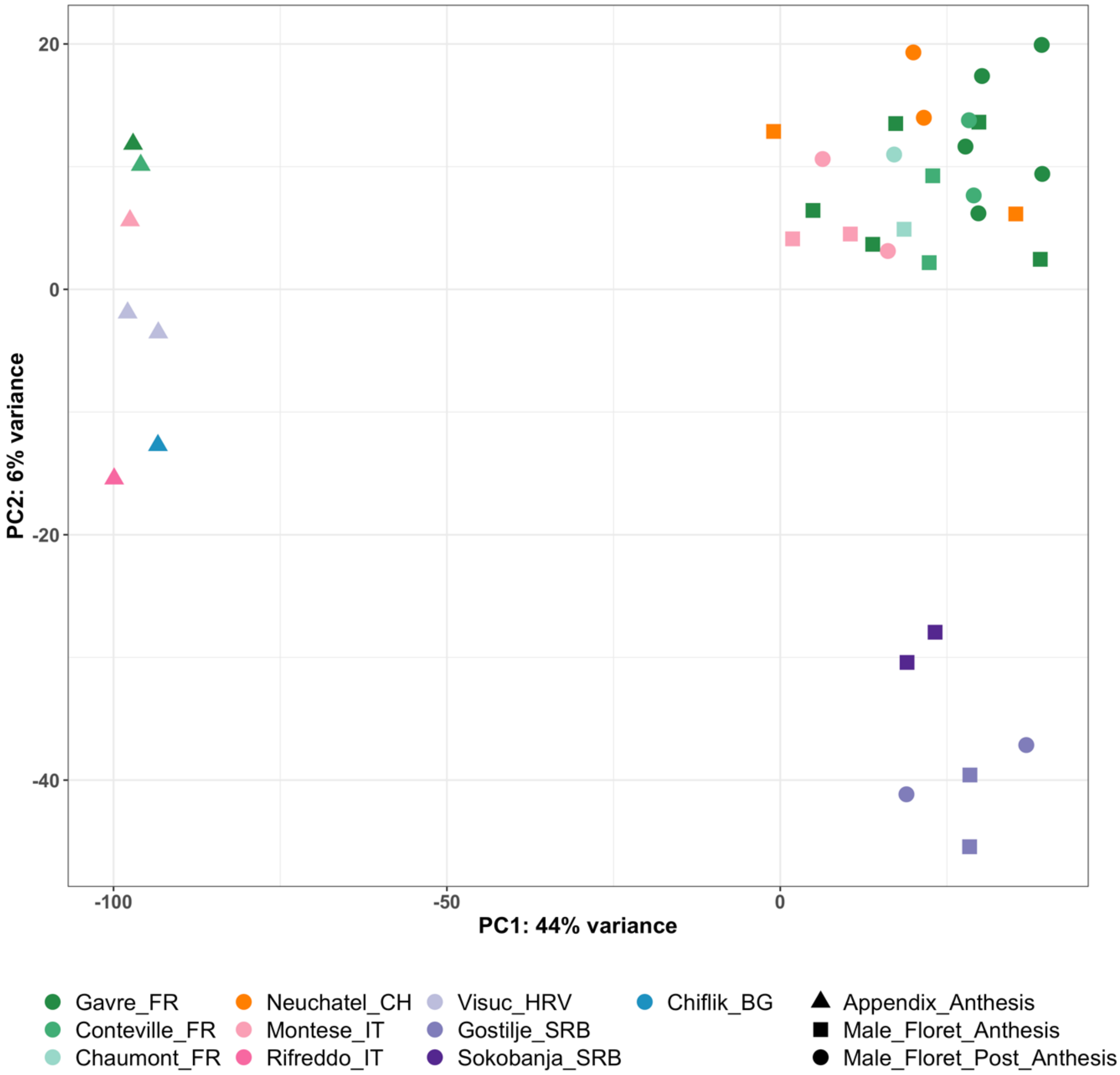

Figure S1. Principal components analysis visualizing *Arum maculatum* transcript expression among all populations (denoted by color) and tissue types/sampling times (denoted by shape) in this study. This analysis included all 49’779 transcripts remaining following filtering in DESeq2 (*i.e.* >0.75CPM in at least seven samples).

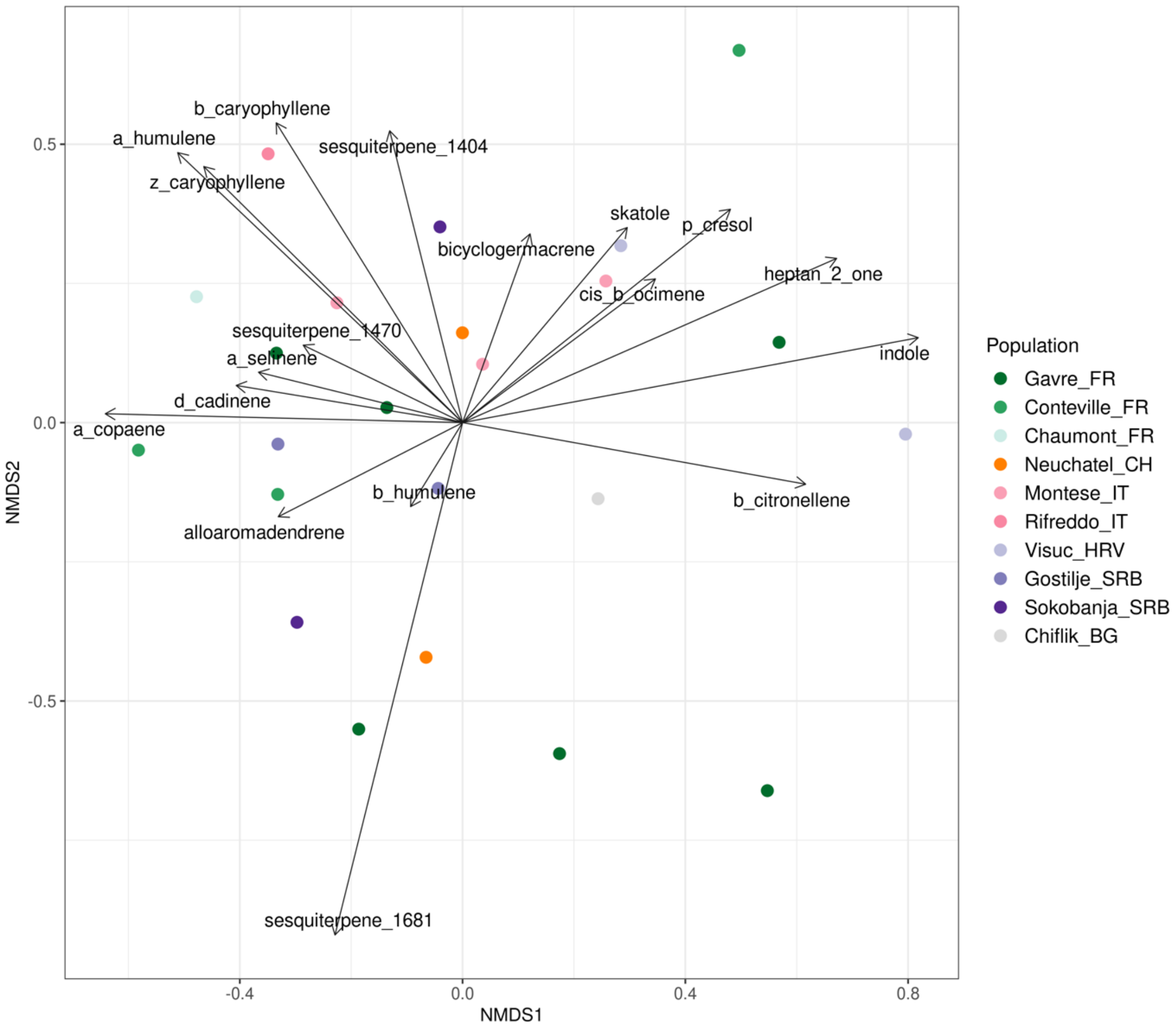

Figure S2. Nonmetric multidimensional scaling (NMDS; Bray–Curtis dissimilarity, stress = 0.0582) plot of floral scent differentiation among individual *Arum maculatum* inflorescences sequenced as part of this study. Analyses were performed on a matrix of the proportional abundances of all 18 volatile organic compounds identified in *A. maculatum* bouquets (see Table S5, below).

Figure S3. Heatmaps visualizing expression of the methyl-D-erythritol 4-phosphate (MEP; above) and mevalonate pathway (following page) for terpenoid precursor biosynthesis in *Arum maculatum*. Color scale represents the *vst*-transformed mean expression of transcripts across tissue types, populations, and stages of anthesis.

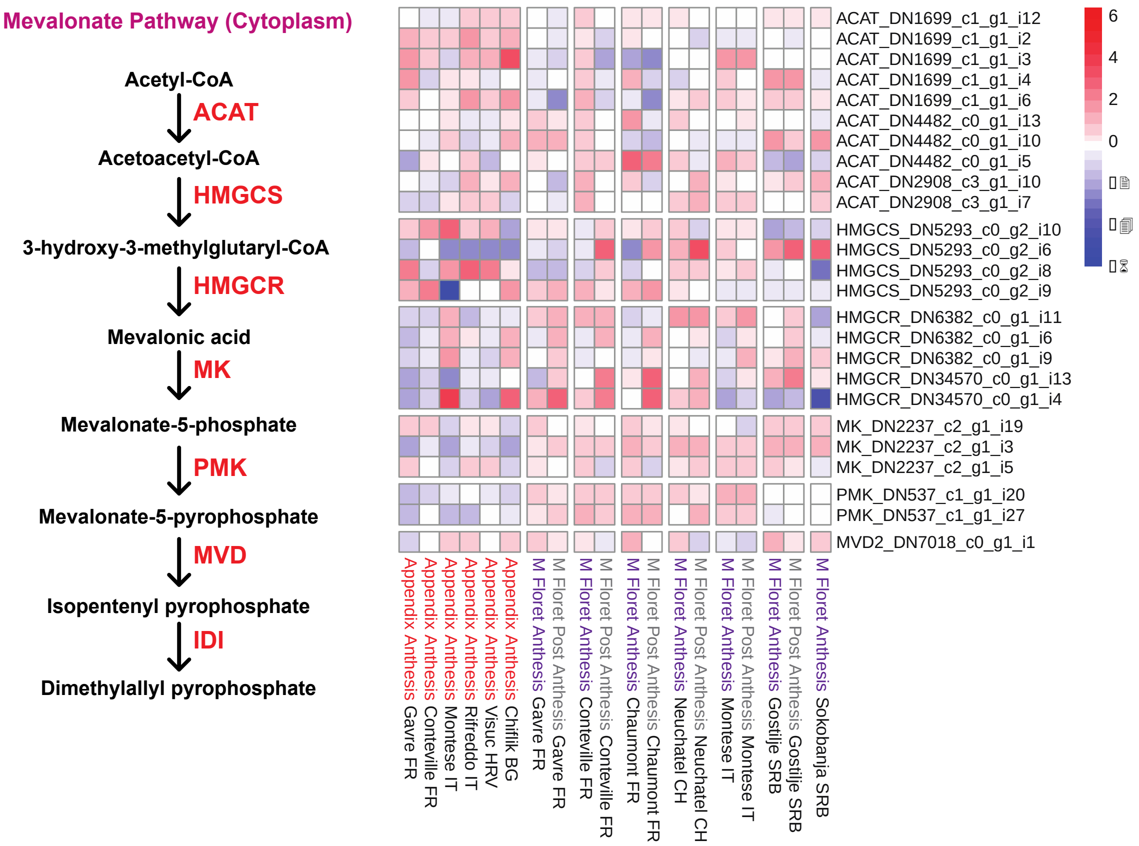

Figure S3 (cont.)

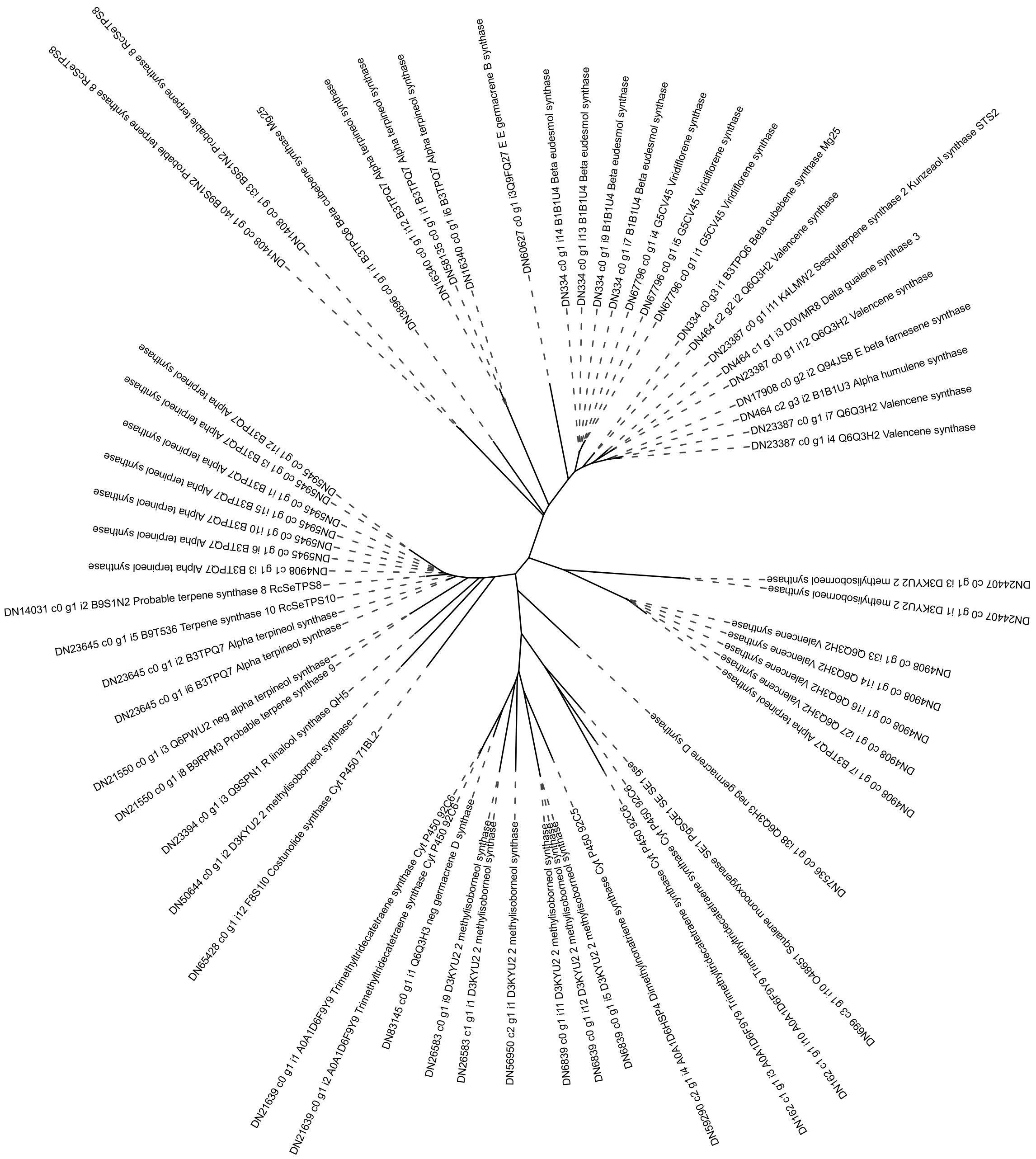

Figure S4. Unrooted phylogeny of all putative *Arum maculatum* terpene synthase isoforms expressed in appendix and male floret tissue during anthesis.

Note: Gene names were derived from automated annotation alone, and should therefore be considered hypotheses

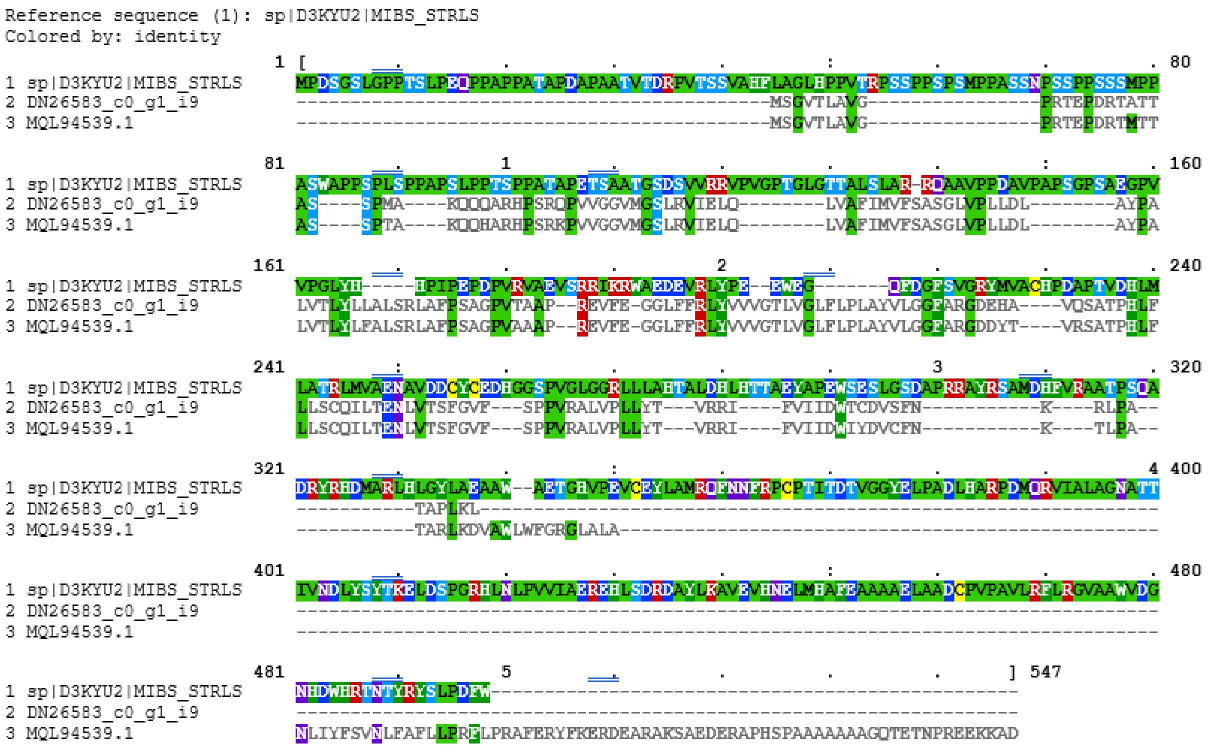

```
Reference sequence (1): sp|D3KYU2|MIBS_STRLS
Colored by: identity

                        1 [        .         .         .         .         :         .         .         . 80
1 sp|D3KYU2|MIBS_STRLS    MPDSGSLGPPTSLPEQPPAPPATAPDAPAATVTDRPVTSSVAHFLAGLHPPVTRPSSPPSPSMPPASSNPSSPPSSSMPP
2 DN26583_c0_g1_i9        --------------------------------------------MSGVTLAVG----------------PRTEPDRTATT
3 MQL94539.1              --------------------------------------------MSGVTLAVG----------------PRTEPDRTMTT

                       81          .         1         .         .         .         .         :         . 160
1 sp|D3KYU2|MIBS_STRLS    ASWAPPSPLSPPAPSLPPTSPPATAPETSAATGSDSVVRRVPVGPTGLGTTALSLAR-RQAAVPPDAVPAPSGPSAEGPV
2 DN26583_c0_g1_i9        AS----SPMA----KQQQARHPSRQPVVGGVMGSLRVIELQ--------LVAFIMVFSASGLVPLLDL--------AYPA
3 MQL94539.1              AS----SPTA----KQQHARHPSRKPVVGGVMGSLRVIELQ--------LVAFIMVFSASGLVPLLDL--------AYPA

                      161          .         .         .         2         .         .         .         . 240
1 sp|D3KYU2|MIBS_STRLS    VPGLYH-----HPIPEPDPVRVAEVSRRIKRWAEDEVRLYPE--EWEG-------QFDGFSVGRYMVACHPDAPTVDHLM
2 DN26583_c0_g1_i9        LVTLYLLALSRLAFPSAGPVTAAP--REVFE-GGLFFRLYVVVGTLVGLFLPLAYVLGGFARGDEHA----VQSATPHLF
3 MQL94539.1              LVTLYLFALSRLAFPSAGPVAAAP--REVFE-GGLFFRLYVVVGTLVGLFLPLAYVLGGFARGDDYT----VRSATPHLF

                      241          :         .         .         .         .         3         .         . 320
1 sp|D3KYU2|MIBS_STRLS    LATRLMVAENAVDDCYCEDHGGSPVGLGGRLLLAHTALDHLHTTAEYAPEWSESLGSDAPRRAYRSAMDHFVRAATPSQA
2 DN26583_c0_g1_i9        LLSCQILTENLVTSFGVF---SPPVRALVPLLYT---VRRI----FVIIDWTCDVSFN-----------K----RLPA--
3 MQL94539.1              LLSCQILTENLVTSFGVF---SPPVRALVPLLYT---VRRI----FVIIDWIYDVCFN-----------K----TLPA--

                      321          .         .         :         .         .         .         .         4 400
1 sp|D3KYU2|MIBS_STRLS    DRYRHDMARLHLGYLAEAAW--AETGHVPEVCEYLAMRQFNNFRPCPTITDTVGGYELPADLHARPDMQRVIALAGNATT
2 DN26583_c0_g1_i9        -----------TAPLKL---------------------------------------------------------------
3 MQL94539.1              -----------TARLKDVAWLWFGRGLALA--------------------------------------------------

                      401          .         .         .         .         :         .         .         . 480
1 sp|D3KYU2|MIBS_STRLS    IVNDLYSYTKELDSPGRHLNLPVVIAEREHLSDRDAYLKAVEVHNELMHAFEAAAAELAADCPVPAVLRFLRGVAAWVDG
2 DN26583_c0_g1_i9        --------------------------------------------------------------------------------
3 MQL94539.1              --------------------------------------------------------------------------------

                      481          .         5         .         .         .         .      ] 547
1 sp|D3KYU2|MIBS_STRLS    NHDWHRTNTYRYSLPDFW-------------------------------------------------
2 DN26583_c0_g1_i9        -------------------------------------------------------------------
3 MQL94539.1              NLIYFSVNLFAFLLPRFLPRAFERYFKERDEARAKSAEDERAPHSPAAAAAAAGQTETNPREEKKAD
```

Figure S5. Multiple sequence alignment of 1) *Streptomyces lasaliensis* 2-methylisoborneol synthase, 2) the TransDecoder predicted peptide sequence of an *Arum maculatum* (Araceae) transcript in our dataset, and 3) an unknown gene identified in the *Colocasia esculenta* (Araceae) genome. While the latter two proteins share 92.5% identity, both share approximately 23% identity with the bacterial 2-methylisoborneol synthase gene.

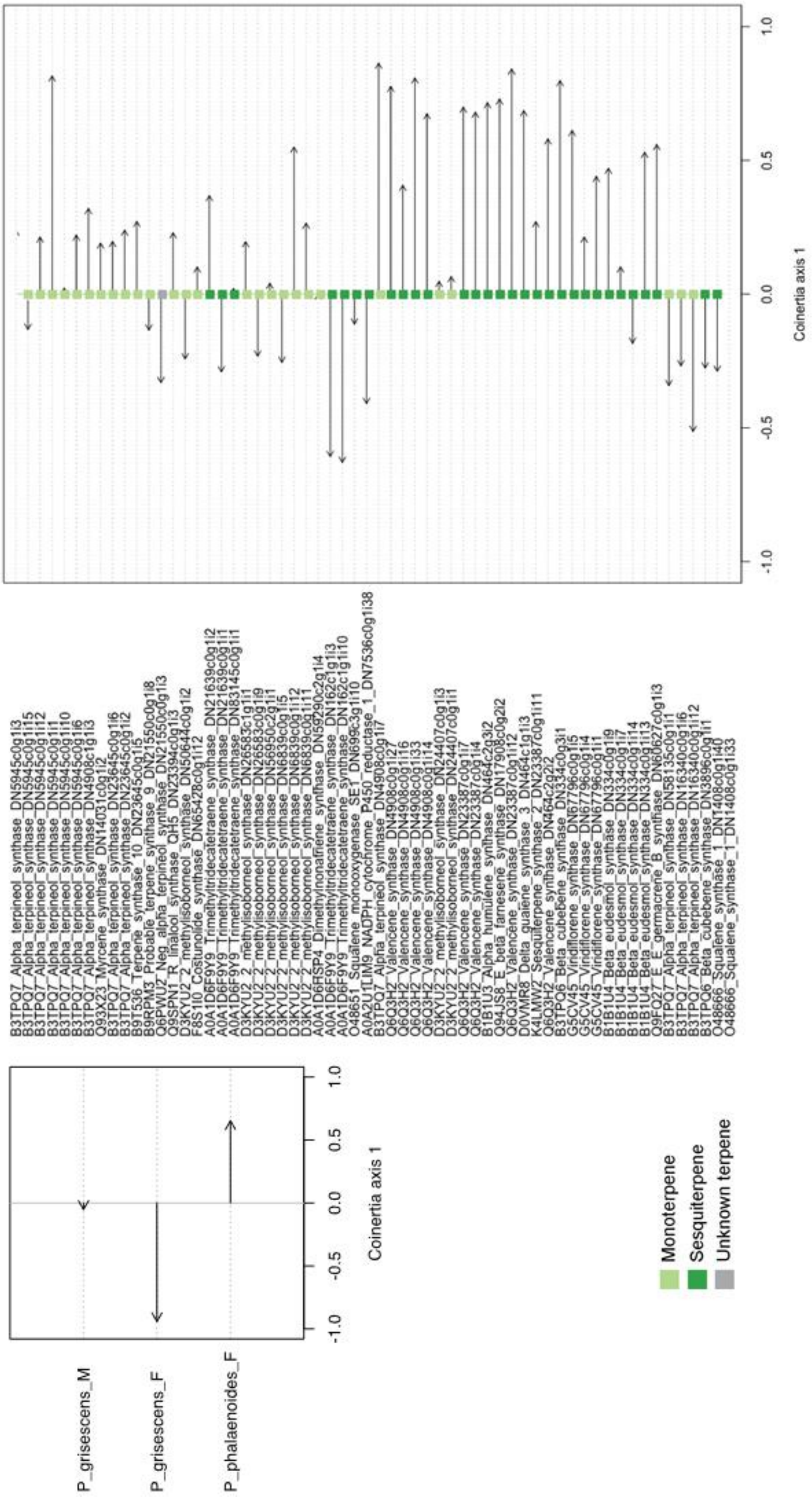

Figure S6. Covariation in sex- and species-specific Psychodidae pollinator attraction rates (left plots), and terpene synthase expression in *Arum maculatum* male floret tissue during anthesis (right plots) along the first coinertia axis.

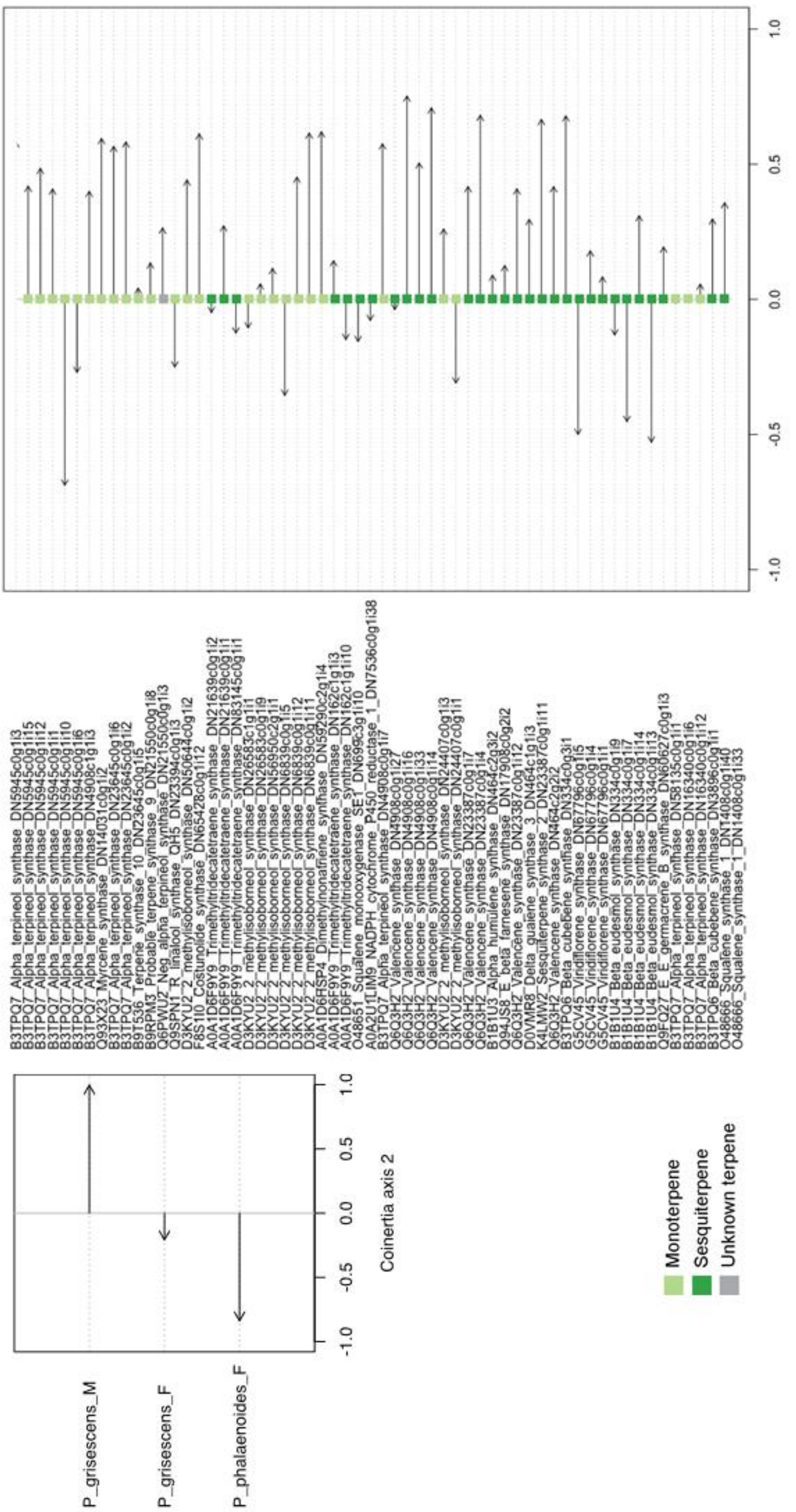

Figure S6 (cont.) Covariation in sex- and species-specific Psychodidae pollinator attraction rates (left plots), and terpene synthase expression in *Arum maculatum* male floret tissue during anthesis (right plots) along the second coinertia axis.

Table S1. Summary of *Arum maculatum* samples collected in this study, and the number of initial (raw) and post-filtering (clean) 150bp paired-end RNA-seq reads generated for each sample.

Sample ID	**Tissue Type**	**Collection Time**	**# reads (raw)**	**# reads (clean)**	**Population**	**Lat.**	**Long.**
GAV_010	Appendix	During-Anthesis	72'325'850	66'717'458	Forêt du Gâvre, France	47.55066	-1.86466
CON_016	Appendix	During-Anthesis	70'056'626	64'913'424	Conteville, France	50.73731	1.73872
MON_001	Appendix	During-Anthesis	62'848'894	57'520'886	Montese, Italy	44.25523	10.98371
RIF_006	Appendix	During-Anthesis	59'312'732	54'350'550	Rifreddo, Italy	40.57235	15.82473
VIS_001	Appendix	During-Anthesis	65'991'730	60'876'804	Visuc, Croatia	44.53128	15.76134
VIS_003	Appendix	During-Anthesis	72'409'196	66'825'898	Visuc, Croatia	44.53128	15.76134
CHI_003	Appendix	During-Anthesis	63'427'166	58'606'672	Chiflik, Bulgaria	42.8130	24.52836
GAV_004SA	Male Floret	During-Anthesis	36'812'088	27'933'352	Forêt du Gâvre, France	47.55066	-1.86466
GAV_004CO	Male Floret	Post-Anthesis	35'212'458	29'293'214	Forêt du Gâvre, France	47.55066	-1.86466
GAV_005SA	Male Floret	During-Anthesis	39'396'020	32'399'440	Forêt du Gâvre, France	47.55066	-1.86466
GAV_005CO	Male Floret	Post-Anthesis	40'842'454	33'212'278	Forêt du Gâvre, France	47.55066	-1.86466
GAV_007SA	Male Floret	During-Anthesis	39'637'246	32'386'282	Forêt du Gâvre, France	47.55066	-1.86466
GAV_007CO	Male Floret	Post-Anthesis	40'504'024	32'982'626	Forêt du Gâvre, France	47.55066	-1.86466
GAV_008SA	Male Floret	During-Anthesis	40'045'110	32'600'164	Forêt du Gâvre, France	47.55066	-1.86466
GAV_008CO	Male Floret	Post-Anthesis	42'181'532	33'104'832	Forêt du Gâvre, France	47.55066	-1.86466
GAV_111SA	Male Floret	During-Anthesis	45'280'290	39'923'042	Forêt du Gâvre, France	47.55066	-1.86466
GAV_111CO	Male Floret	Post-Anthesis	46'879'738	41'891'194	Forêt du Gâvre, France	47.55066	-1.86466
CHA_001SA	Male Floret	During-Anthesis	46'799'844	42'716'744	Chaumont, France	48.11508	5.09475
CHA_001CO	Male Floret	Post-Anthesis	49'827'838	46'503'400	Chaumont, France	48.11508	5.09475
CON_003SA	Male Floret	During-Anthesis	39'875'808	39'875'808	Conteville, France	50.73731	1.73872
CON_003CO	Male Floret	Post-Anthesis	37'195'130	29'515'252	Conteville, France	50.73731	1.73872
CON_005SA	Male Floret	During-Anthesis	47'294'348	41'537'476	Conteville, France	50.73731	1.73872
CON_005CO	Male Floret	Post-Anthesis	49'998'560	44'422'700	Conteville, France	50.73731	1.73872
NEU_002SA	Male Floret	During-Anthesis	37'467'370	29'802'078	Neuchâtel, Switzerland	47.00043	6.9379
NEU_002CO	Male Floret	Post-Anthesis	42'504'012	34'460'112	Neuchâtel, Switzerland	47.00043	6.9379
NEU_008SA	Male Floret	During-Anthesis	49'278'902	43'503'888	Neuchâtel, Switzerland	47.00043	6.9379
NEU_008CO	Male Floret	Post-Anthesis	45'181'684	39'358'012	Neuchâtel, Switzerland	47.00043	6.9379
MON_002SA	Male Floret	During-Anthesis	44'700'402	39'507'032	Montese, Italy	44.25523	10.98371
MON_002CO	Male Floret	Post-Anthesis	52'575'366	46'259'886	Montese, Italy	44.25523	10.98371
MON_005SA	Male Floret	During-Anthesis	45'849'700	40'354'964	Montese, Italy	44.25523	10.98371
MON_005CO	Male Floret	Post-Anthesis	50'195'542	43'370'534	Montese, Italy	44.25523	10.98371
GOS_001SA	Male Floret	During-Anthesis	47'615'578	42'110'792	Gostilje, Serbia	43.65561	19.83549
GOS_001CO	Male Floret	Post-Anthesis	47'897'388	41'765'298	Gostilje, Serbia	43.65561	19.83549
GOS_008SA	Male Floret	During-Anthesis	42'165'118	34'880'800	Gostilje, Serbia	43.65561	19.83549
GOS_008CO	Male Floret	Post-Anthesis	41'497'178	33'537'420	Gostilje, Serbia	43.65561	19.83549
SOK_104SA	Male Floret	During-Anthesis	48'025'822	41'973'970	Sokobanja, Serbia	43.60373	21.88755
SOK_005SA	Male Floret	During-Anthesis	36'079'684	29'352'734	Sokobanja, Serbia	43.60373	21.88755

Table S2. Basic assembly quality metrics for our complete *Arum maculatum* transcriptome (all contigs). The single Trinity assembly was constructed from all of the appendix and male floret samples listed in Table S1.

Method	**N50 (bp)**	**GC (%)**	**Median length (bp)**	**Average length (bp)**	**Assembled bases**
Trinity	1699	45.1	503	949	563’420’622

Table S3. Results from two de-duplication techniques, used to reduce the quantity of redundant isoforms in the raw assembly output by Trinity.

Method	**# of transcripts (raw trinity assembly)**	**# of transcripts (post-filtering output)**	**N50 (bp)**	**GC (%)**	**Average length (bp)**
EvidentialGene	593’392	195’892	1195	44.5	1140
CD-HIT (95% ID)	593’392	240’758	7908	47.1	925

Table S4. BUSCO v5.0.0 completeness of the raw Trinity assembly, and two de-duplicated assemblies. EvidentialGene removed a larger quantity of sequences while also better preserving transcriptome completeness, and was therefore used for all subsequent analyses in DESeq2.

Method	**Complete [C]**	**Single-Copy [S]**	**Duplicated [D]**	**Fragmented [F]**	**Missing [M]**
Trinity (raw)	95.9%	6.6%	89.3%	2.0%	2.1%
EvidentialGene	95.6%	19.5%	76.1%	2.2%	2.2%
CD-HIT	92.2%	48.3%	43.9%	5.2%	2.6%

Table S5. Average proportional emissions of volatile organic compounds (VOCs) emitted by individual *Arum maculatum* in this study. Additional sample metadata are given in Table S1.

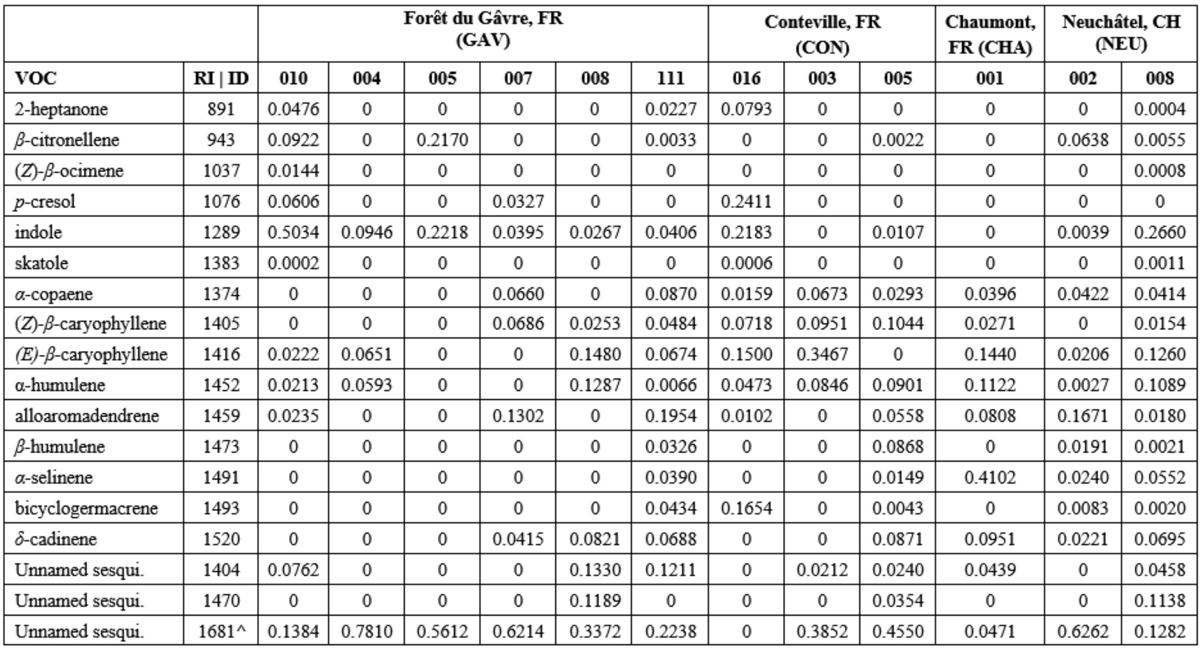

		Forêt du Gâvre, FR (GAV)						Conteville, FR (CON)			Chaumont, FR (CHA)	Neuchâtel, CH (NEU)	
VOC	**RI | ID**	**010**	**004**	**005**	**007**	**008**	**111**	**016**	**003**	**005**	**001**	**002**	**008**
2-heptanone	891	0.0476	0	0	0	0	0.0227	0.0793	0	0	0	0	0.0004
β-citronellene	943	0.0922	0	0.2170	0	0	0.0033	0	0	0.0022	0	0.0638	0.0055
(*Z*)-*β*-ocimene	1037	0.0144	0	0	0	0	0	0	0	0	0	0	0.0008
p-cresol	1076	0.0606	0	0	0.0327	0	0	0.2411	0	0	0	0	0
indole	1289	0.5034	0.0946	0.2218	0.0395	0.0267	0.0406	0.2183	0	0.0107	0	0.0039	0.2660
skatole	1383	0.0002	0	0	0	0	0	0.0006	0	0	0	0	0.0011
α-copaene	1374	0	0	0	0.0660	0	0.0870	0.0159	0.0673	0.0293	0.0396	0.0422	0.0414
(*Z*)-*β*-caryophyllene	1405	0	0	0	0.0686	0.0253	0.0484	0.0718	0.0951	0.1044	0.0271	0	0.0154
(E)-*β*-caryophyllene	1416	0.0222	0.0651	0	0	0.1480	0.0674	0.1500	0.3467	0	0.1440	0.0206	0.1260
α-humulene	1452	0.0213	0.0593	0	0	0.1287	0.0066	0.0473	0.0846	0.0901	0.1122	0.0027	0.1089
alloaromadendrene	1459	0.0235	0	0	0.1302	0	0.1954	0.0102	0	0.0558	0.0808	0.1671	0.0180
β-humulene	1473	0	0	0	0	0	0.0326	0	0	0.0868	0	0.0191	0.0021
α-selinene	1491	0	0	0	0	0	0.0390	0	0	0.0149	0.4102	0.0240	0.0552
bicyclogermacrene	1493	0	0	0	0	0	0.0434	0.1654	0	0.0043	0	0.0083	0.0020
δ-cadinene	1520	0	0	0	0.0415	0.0821	0.0688	0	0	0.0871	0.0951	0.0221	0.0695
Unnamed sesqui.	1404	0.0762	0	0	0	0.1330	0.1211	0	0.0212	0.0240	0.0439	0	0.0458
Unnamed sesqui.	1470	0	0	0	0	0.1189	0	0	0	0.0354	0	0	0.1138
Unnamed sesqui.	1681^	0.1384	0.7810	0.5612	0.6214	0.3372	0.2238	0	0.3852	0.4550	0.0471	0.6262	0.1282

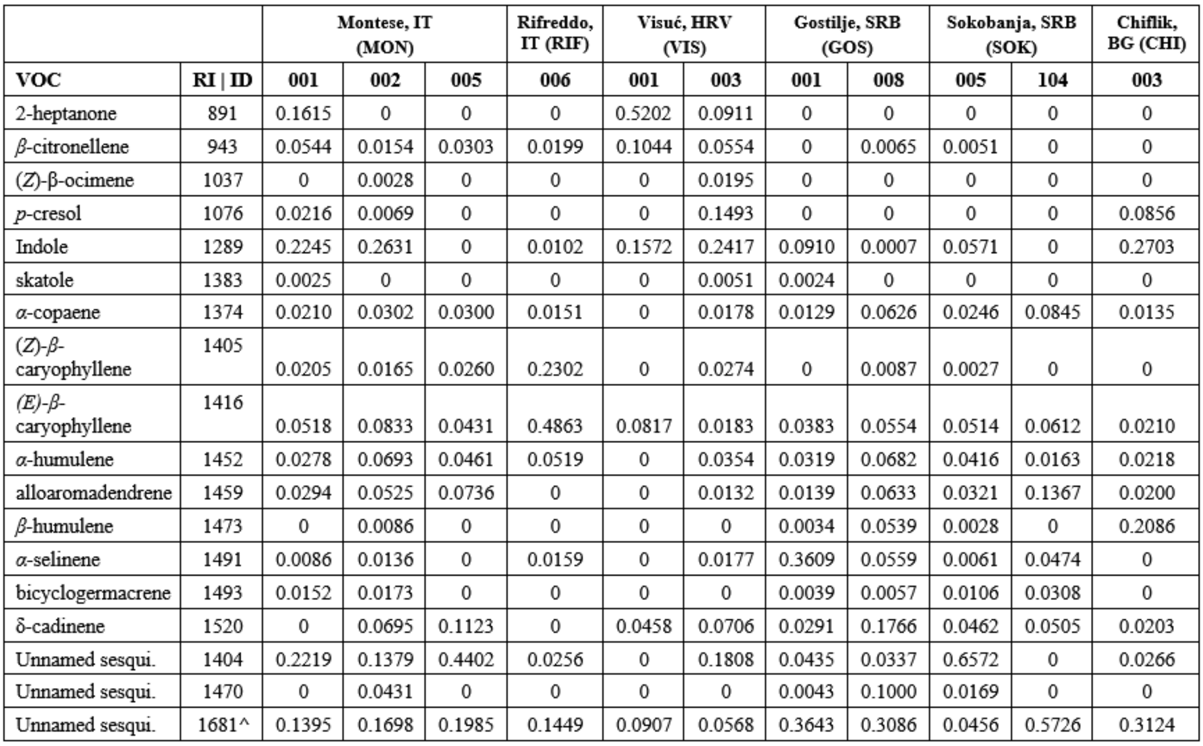

		Montese, IT (MON)			Rifreddo, IT (RIF)	Visuć, HRV (VIS)		Gostilje, SRB (GOS)		Sokobanja, SRB (SOK)		Chiflik, BG (CHI)
VOC	**RI | ID**	**001**	**002**	**005**	**006**	**001**	**003**	**001**	**008**	**005**	**104**	**003**
2-heptanone	891	0.1615	0	0	0	0.5202	0.0911	0	0	0	0	0
β-citronellene	943	0.0544	0.0154	0.0303	0.0199	0.1044	0.0554	0	0.0065	0.0051	0	0
(*Z*)-β-ocimene	1037	0	0.0028	0	0	0	0.0195	0	0	0	0	0
p-cresol	1076	0.0216	0.0069	0	0	0	0.1493	0	0	0	0	0.0856
Indole	1289	0.2245	0.2631	0	0.0102	0.1572	0.2417	0.0910	0.0007	0.0571	0	0.2703
skatole	1383	0.0025	0	0	0	0	0.0051	0.0024	0	0	0	0
α-copaene	1374	0.0210	0.0302	0.0300	0.0151	0	0.0178	0.0129	0.0626	0.0246	0.0845	0.0135
(*Z*)-*β*-caryophyllene	1405	0.0205	0.0165	0.0260	0.2302	0	0.0274	0	0.0087	0.0027	0	0
(E)-*β*-caryophyllene	1416	0.0518	0.0833	0.0431	0.4863	0.0817	0.0183	0.0383	0.0554	0.0514	0.0612	0.0210
α-humulene	1452	0.0278	0.0693	0.0461	0.0519	0	0.0354	0.0319	0.0682	0.0416	0.0163	0.0218
alloaromadendrene	1459	0.0294	0.0525	0.0736	0	0	0.0132	0.0139	0.0633	0.0321	0.1367	0.0200
β-humulene	1473	0	0.0086	0	0	0	0	0.0034	0.0539	0.0028	0	0.2086
α-selinene	1491	0.0086	0.0136	0	0.0159	0	0.0177	0.3609	0.0559	0.0061	0.0474	0
bicyclogermacrene	1493	0.0152	0.0173	0	0	0	0	0.0039	0.0057	0.0106	0.0308	0
δ-cadinene	1520	0	0.0695	0.1123	0	0.0458	0.0706	0.0291	0.1766	0.0462	0.0505	0.0203
Unnamed sesqui.	1404	0.2219	0.1379	0.4402	0.0256	0	0.1808	0.0435	0.0337	0.6572	0	0.0266
Unnamed sesqui.	1470	0	0.0431	0	0	0	0	0.0043	0.1000	0.0169	0	0
Unnamed sesqui.	1681^	0.1395	0.1698	0.1985	0.1449	0.0907	0.0568	0.3643	0.3086	0.0456	0.5726	0.3124

RI = Kovats retention index, non-polar, HP-5MS (^ = RI 1716 in Diaz & Kite 2002)

Table S6. Transcripts highly correlated with Hydroxyphenylpyruvate reductase (HPPR) expression in *A. maculatum* appendix tissue during anthesis (Pearson correlation test, $p < 0.0001$).

Trinity ID	***PCC***	***p* value**	**annotation**
DN4259_c0_g1_i27	0.998	0.000000171	P41893 Low molecular weight phosphotyrosine protein phosphatase
DN10943_c0_g2_i9	0.992	0.000010198	Q10359 Alpha-1,2-galactosyltransferase gmh3
DN11383_c0_g1_i18	0.989	0.000023743	Q9FVZ7 Membrane steroid-binding protein 1
DN17083_c0_g1_i4	0.988	0.000027273	[unannotated transcript]
DN24139_c0_g1_i18	0.988	0.000029805	Q9SQT8 Bifunctional 3-dehydroquinate dehydratase/shikimate dehydrogenase
DN3154_c0_g1_i24	-0.985	0.000055587	Q8VZG7 Ribonuclease TUDOR 1 (AtTudor1)
DN4046_c2_g1_i6	-0.984	0.000062665	Q2KIC0 Nuclear speckle splicing regulatory protein 1
DN7988_c5_g1_i11	-0.983	0.000074481	Q24206 Broad-complex core protein isoform 6
DN9669_c0_g1_i5	0.982	0.000074962	Q9SI61 Amidophosphoribosyltransferase 1
DN2090_c20_g1_i2	-0.982	0.000083468	Q9LDD1 Probable BOI-related E3 ubiquitin-protein ligase 3

PCC = Pearson correlation coefficient

APPENDIX S2

Supplementary Table S7a. Significantly enriched GO terms when comparing transcript expression between A. maculatum appendix and male floret tissue during anthesis (FDR-corrected P < 0.05; log2fold change +/- 1). Both the original annotation (Term) and topGO condensed term used in Figure 2 (parent_Term) are given below.

input_GO	Term	parent_GO	parent_Term	Condition
GO:0052865	1-deoxy-D-xylulose 5-phosphate biosynthetic process	GO:0052865	1-deoxy-D-xylulose 5-phosphate biosynthetic process	Appendix
GO:0009073	aromatic amino acid family biosynthetic process	GO:0009073	aromatic amino acid family biosynthetic process	Appendix
GO:0007039	protein catabolic process in the vacuole	GO:0009083	branched-chain amino acid catabolic process	Appendix
GO:0036444	calcium import into the mitochondrion	GO:0036444	calcium import into the mitochondrion	Appendix
GO:0043266	regulation of potassium ion transport	GO:0036444	calcium import into the mitochondrion	Appendix
GO:0019752	carboxylic acid metabolic process	GO:0019752	carboxylic acid metabolic process	Appendix
GO:0007205	protein kinase C-activating G protein-coupled receptor signaling pathway	GO:0043617	cellular response to sucrose starvation	Appendix
GO:0043617	cellular response to sucrose starvation	GO:0043617	cellular response to sucrose starvation	Appendix
GO:0009423	chorismate biosynthetic process	GO:0009423	chorismate biosynthetic process	Appendix
GO:0009690	cytokinin metabolic process	GO:0010617	circadian regulation of calcium ion oscillation	Appendix
GO:0009851	auxin biosynthetic process	GO:0010617	circadian regulation of calcium ion oscillation	Appendix
GO:0010600	regulation of auxin biosynthetic process	GO:0010617	circadian regulation of calcium ion oscillation	Appendix
GO:0010617	circadian regulation of calcium ion oscillation	GO:0010617	circadian regulation of calcium ion oscillation	Appendix
GO:0042593	glucose homeostasis	GO:0010617	circadian regulation of calcium ion oscillation	Appendix
GO:0051560	mitochondrial calcium ion homeostasis	GO:0010617	circadian regulation of calcium ion oscillation	Appendix
GO:0051562	negative regulation of mitochondrial calcium ion concentration	GO:0010617	circadian regulation of calcium ion oscillation	Appendix
GO:0090156	cellular sphingolipid homeostasis	GO:0010617	circadian regulation of calcium ion oscillation	Appendix
GO:0090354	regulation of auxin metabolic process	GO:0010617	circadian regulation of calcium ion oscillation	Appendix
GO:0097035	regulation of membrane lipid distribution	GO:0010617	circadian regulation of calcium ion oscillation	Appendix
GO:0031128	developmental induction	GO:0031128	developmental induction	Appendix
GO:0016311	dephosphorylation	GO:0050992	dimethylallyl diphosphate biosynthetic process	Appendix
GO:0046777	protein autophosphorylation	GO:0050992	dimethylallyl diphosphate biosynthetic process	Appendix
GO:0050992	dimethylallyl diphosphate biosynthetic process	GO:0050992	dimethylallyl diphosphate biosynthetic process	Appendix
GO:0008299	isoprenoid biosynthetic process	GO:0010241	ent-kaurene oxidation to kaurenoic acid	Appendix
GO:0009688	abscisic acid biosynthetic process	GO:0010241	ent-kaurene oxidation to kaurenoic acid	Appendix
GO:0010241	ent-kaurene oxidation to kaurenoic acid	GO:0010241	ent-kaurene oxidation to kaurenoic acid	Appendix
GO:0019605	butyrate metabolic process	GO:0010241	ent-kaurene oxidation to kaurenoic acid	Appendix
GO:0034434	sterol esterification	GO:0010241	ent-kaurene oxidation to kaurenoic acid	Appendix
GO:0046345	abscisic acid catabolic process	GO:0010241	ent-kaurene oxidation to kaurenoic acid	Appendix
GO:0046464	acylglycerol catabolic process	GO:0010241	ent-kaurene oxidation to kaurenoic acid	Appendix
GO:0051791	medium-chain fatty acid metabolic process	GO:0010241	ent-kaurene oxidation to kaurenoic acid	Appendix
GO:0009649	entrainment of circadian clock	GO:0043153	entrainment of circadian clock by photoperiod	Appendix

GO:0032922	circadian regulation of gene expression	GO:0043153	entrainment of circadian clock by photoperiod	Appendix
GO:0042753	positive regulation of circadian rhythm	GO:0043153	entrainment of circadian clock by photoperiod	Appendix
GO:0043153	entrainment of circadian clock by photoperiod	GO:0043153	entrainment of circadian clock by photoperiod	Appendix
GO:0006986	response to unfolded protein	GO:0036498	IRE1-mediated unfolded protein response	Appendix
GO:0009723	response to ethylene	GO:0036498	IRE1-mediated unfolded protein response	Appendix
GO:0009734	auxin-activated signaling pathway	GO:0036498	IRE1-mediated unfolded protein response	Appendix
GO:0009753	response to jasmonic acid	GO:0036498	IRE1-mediated unfolded protein response	Appendix
GO:0034620	cellular response to unfolded protein	GO:0036498	IRE1-mediated unfolded protein response	Appendix
GO:0036498	IRE1-mediated unfolded protein response	GO:0036498	IRE1-mediated unfolded protein response	Appendix
GO:0071456	cellular response to hypoxia	GO:0036498	IRE1-mediated unfolded protein response	Appendix
GO:0080037	negative regulation of cytokinin-activated signaling pathway	GO:0036498	IRE1-mediated unfolded protein response	Appendix
GO:0006081	cellular aldehyde metabolic process	GO:0019288	isopentenyl diphosphate biosynthetic process, methylerythritol 4-phosphate pathway	Appendix
GO:0019288	isopentenyl diphosphate biosynthetic process, methylerythritol 4-phosphate pathway	GO:0019288	isopentenyl diphosphate biosynthetic process, methylerythritol 4-phosphate pathway	Appendix
GO:0006112	energy reserve metabolic process	GO:0046951	ketone body biosynthetic process	Appendix
GO:0010230	alternative respiration	GO:0046951	ketone body biosynthetic process	Appendix
GO:0046951	ketone body biosynthetic process	GO:0046951	ketone body biosynthetic process	Appendix
GO:0009098	leucine biosynthetic process	GO:0009098	leucine biosynthetic process	Appendix
GO:0009809	lignin biosynthetic process	GO:0009809	lignin biosynthetic process	Appendix
GO:0019674	NAD metabolic process	GO:0019674	NAD metabolic process	Appendix
GO:0006741	NADP biosynthetic process	GO:0006741	NADP biosynthetic process	Appendix
GO:0009787	regulation of abscisic acid-activated signaling pathway	GO:2001243	negative regulation of intrinsic apoptotic signaling pathway	Appendix
GO:0019722	calcium-mediated signaling	GO:2001243	negative regulation of intrinsic apoptotic signaling pathway	Appendix
GO:0035556	intracellular signal transduction	GO:2001243	negative regulation of intrinsic apoptotic signaling pathway	Appendix
GO:1901371	regulation of leaf morphogenesis	GO:0051511	negative regulation of unidimensional cell growth	Appendix
GO:0030433	ubiquitin-dependent ERAD pathway	GO:1904294	positive regulation of ERAD pathway	Appendix
GO:1902065	response to L-glutamate	GO:1904294	positive regulation of ERAD pathway	Appendix
GO:1904294	positive regulation of ERAD pathway	GO:1904294	positive regulation of ERAD pathway	Appendix
GO:0015976	carbon utilization	GO:0043609	regulation of carbon utilization	Appendix
GO:0043609	regulation of carbon utilization	GO:0043609	regulation of carbon utilization	Appendix
GO:0040009	regulation of growth rate	GO:0040009	regulation of growth rate	Appendix
GO:0010390	histone monoubiquitination	GO:1900109	regulation of histone H3-K9 dimethylation	Appendix
GO:1900109	regulation of histone H3-K9 dimethylation	GO:1900109	regulation of histone H3-K9 dimethylation	Appendix
GO:2000762	regulation of phenylpropanoid metabolic process	GO:2000762	regulation of phenylpropanoid metabolic process	Appendix
GO:0031001	response to brefeldin A	GO:0080021	response to benzoic acid	Appendix
GO:0043401	steroid hormone mediated signaling pathway	GO:0080021	response to benzoic acid	Appendix
GO:0080021	response to benzoic acid	GO:0080021	response to benzoic acid	Appendix
GO:1902347	response to strigolactone	GO:0080021	response to benzoic acid	Appendix
GO:0043157	response to cation stress	GO:0043157	response to cation stress	Appendix
GO:0009751	response to salicylic acid	GO:0009751	response to salicylic acid	Appendix

GO:0016127	sterol catabolic process	GO:0019632	shikimate metabolic process	Appendix
GO:0019632	shikimate metabolic process	GO:0019632	shikimate metabolic process	Appendix
GO:0016114	terpenoid biosynthetic process	GO:0016114	terpenoid biosynthetic process	Appendix
GO:0000162	tryptophan biosynthetic process	GO:0000162	tryptophan biosynthetic process	Appendix
GO:0072387	flavin adenine dinucleotide metabolic process	GO:0010253	UDP-rhamnose biosynthetic process	Appendix
GO:0098876	vesicle-mediated transport to the plasma membrane	GO:0098876	vesicle-mediated transport to the plasma membrane	Appendix
GO:0006813	potassium ion transport	GO:0036444	calcium import into the mitochondrion	Male_Floret
GO:0034757	negative regulation of iron ion transport	GO:0036444	calcium import into the mitochondrion	Male_Floret
GO:0051924	regulation of calcium ion transport	GO:0036444	calcium import into the mitochondrion	Male_Floret
GO:0055085	transmembrane transport	GO:0036444	calcium import into the mitochondrion	Male_Floret
GO:1905885	positive regulation of triglyceride transport	GO:0036444	calcium import into the mitochondrion	Male_Floret
GO:0016036	cellular response to phosphate starvation	GO:0043617	cellular response to sucrose starvation	Male_Floret
GO:0006885	regulation of pH	GO:0010617	circadian regulation of calcium ion oscillation	Male_Floret
GO:0006505	GPI anchor metabolic process	GO:0010241	ent-kaurene oxidation to kaurenoic acid	Male_Floret
GO:0046488	phosphatidylinositol metabolic process	GO:0010241	ent-kaurene oxidation to kaurenoic acid	Male_Floret
GO:0007164	establishment of tissue polarity	GO:0007164	establishment of tissue polarity	Male_Floret
GO:0010208	pollen wall assembly	GO:0007164	establishment of tissue polarity	Male_Floret
GO:1905393	plant organ formation	GO:0007164	establishment of tissue polarity	Male_Floret
GO:0010496	intercellular transport	GO:0010496	intercellular transport	Male_Floret
GO:0009735	response to cytokinin	GO:0036498	IRE1-mediated unfolded protein response	Male_Floret
GO:0009744	response to sucrose	GO:0036498	IRE1-mediated unfolded protein response	Male_Floret
GO:0010182	sugar mediated signaling pathway	GO:0036498	IRE1-mediated unfolded protein response	Male_Floret
GO:0071329	cellular response to sucrose stimulus	GO:0036498	IRE1-mediated unfolded protein response	Male_Floret
GO:0005977	glycogen metabolic process	GO:0046951	ketone body biosynthetic process	Male_Floret
GO:0005978	glycogen biosynthetic process	GO:0046951	ketone body biosynthetic process	Male_Floret
GO:0005975	carbohydrate metabolic process	GO:0010493	Lewis a epitope biosynthetic process	Male_Floret
GO:0005991	trehalose metabolic process	GO:0010493	Lewis a epitope biosynthetic process	Male_Floret
GO:0006075	(1->3)-beta-D-glucan biosynthetic process	GO:0010493	Lewis a epitope biosynthetic process	Male_Floret
GO:0006096	glycolytic process	GO:0010493	Lewis a epitope biosynthetic process	Male_Floret
GO:0010493	Lewis a epitope biosynthetic process	GO:0010493	Lewis a epitope biosynthetic process	Male_Floret
GO:0019252	starch biosynthetic process	GO:0010493	Lewis a epitope biosynthetic process	Male_Floret
GO:0030244	cellulose biosynthetic process	GO:0010493	Lewis a epitope biosynthetic process	Male_Floret
GO:0045490	pectin catabolic process	GO:0010493	Lewis a epitope biosynthetic process	Male_Floret
GO:0048358	mucilage pectin biosynthetic process	GO:0010493	Lewis a epitope biosynthetic process	Male_Floret
GO:0009435	NAD biosynthetic process	GO:0009435	NAD biosynthetic process	Male_Floret
GO:0023051	regulation of signaling	GO:2001243	negative regulation of intrinsic apoptotic signaling pathway	Male_Floret
GO:2001243	negative regulation of intrinsic apoptotic signaling pathway	GO:2001243	negative regulation of intrinsic apoptotic signaling pathway	Male_Floret
GO:0009909	regulation of flower development	GO:0051511	negative regulation of unidimensional cell growth	Male_Floret
GO:0048509	regulation of meristem development	GO:0051511	negative regulation of unidimensional cell growth	Male_Floret
GO:0048581	negative regulation of post-embryonic development	GO:0051511	negative regulation of unidimensional cell growth	Male_Floret
GO:0051511	negative regulation of unidimensional cell growth	GO:0051511	negative regulation of unidimensional cell growth	Male_Floret

GO:0009555	pollen development	GO:0009846	pollen germination	Male_Floret
GO:0009846	pollen germination	GO:0009846	pollen germination	Male_Floret
GO:0010228	vegetative to reproductive phase transition of meristem	GO:0009846	pollen germination	Male_Floret
GO:0048575	short-day photoperiodism, flowering	GO:0009846	pollen germination	Male_Floret
GO:0009860	pollen tube growth	GO:0009860	pollen tube growth	Male_Floret
GO:0060416	response to growth hormone	GO:1904294	positive regulation of ERAD pathway	Male_Floret
GO:0009793	embryo development ending in seed dormancy	GO:0010068	protoderm histogenesis	Male_Floret
GO:0010068	protoderm histogenesis	GO:0010068	protoderm histogenesis	Male_Floret
GO:0010154	fruit development	GO:0010068	protoderm histogenesis	Male_Floret
GO:0046874	quinolinate metabolic process	GO:0046874	quinolinate metabolic process	Male_Floret
GO:0080143	regulation of amino acid export	GO:0080143	regulation of amino acid export	Male_Floret
GO:0140352	export from cell	GO:0080143	regulation of amino acid export	Male_Floret
GO:0009932	cell tip growth	GO:0040009	regulation of growth rate	Male_Floret
GO:0040008	regulation of growth	GO:0040009	regulation of growth rate	Male_Floret
GO:0080092	regulation of pollen tube growth	GO:0040009	regulation of growth rate	Male_Floret
GO:0080117	secondary growth	GO:0040009	regulation of growth rate	Male_Floret
GO:0032508	DNA duplex unwinding	GO:1900109	regulation of histone H3-K9 dimethylation	Male_Floret
GO:0044772	mitotic cell cycle phase transition	GO:0060236	regulation of mitotic spindle organization	Male_Floret
GO:0055047	generative cell mitosis	GO:0060236	regulation of mitotic spindle organization	Male_Floret
GO:0060236	regulation of mitotic spindle organization	GO:0060236	regulation of mitotic spindle organization	Male_Floret
GO:0032928	regulation of superoxide anion generation	GO:0032928	regulation of superoxide anion generation	Male_Floret
GO:0032889	regulation of vacuole fusion, non-autophagic	GO:0032889	regulation of vacuole fusion, non-autophagic	Male_Floret
GO:0071383	cellular response to steroid hormone stimulus	GO:0080021	response to benzoic acid	Male_Floret
GO:0009739	response to gibberellin	GO:0009739	response to gibberellin	Male_Floret
GO:0019310	inositol catabolic process	GO:0019632	shikimate metabolic process	Male_Floret
GO:0009407	toxin catabolic process	GO:0009407	toxin catabolic process	Male_Floret
GO:0006011	UDP-glucose metabolic process	GO:0010253	UDP-rhamnose biosynthetic process	Male_Floret
GO:0010253	UDP-rhamnose biosynthetic process	GO:0010253	UDP-rhamnose biosynthetic process	Male_Floret
GO:0019305	dTDP-rhamnose biosynthetic process	GO:0010253	UDP-rhamnose biosynthetic process	Male_Floret
GO:0033358	UDP-L-arabinose biosynthetic process	GO:0010253	UDP-rhamnose biosynthetic process	Male_Floret
GO:0044208	de novo AMP biosynthetic process	GO:0010253	UDP-rhamnose biosynthetic process	Male_Floret

Supplementary Table S7b. Significantly enriched GO terms when comparing transcript expression between *A. maculatum* male floret tissue during anthesis and post-anthesis (FDR-corrected P < 0.05; log2fold change +/- 1). Both the original annotation (Term) and topGO condensed term used in Figure 3 (parent_Term) are given below.

input_GO	**Term**	**parent_GO**	**parent_Term**	**Condition**
GO:0006813	potassium ion transport	GO:0032328	alanine transport	Male_Anthesis
GO:0006817	phosphate ion transport	GO:0032328	alanine transport	Male_Anthesis
GO:0008272	sulfate transport	GO:0032328	alanine transport	Male_Anthesis
GO:0008643	carbohydrate transport	GO:0032328	alanine transport	Male_Anthesis
GO:0015798	myo-inositol transport	GO:0032328	alanine transport	Male_Anthesis
GO:0010044	response to aluminum ion	GO:0071281	cellular response to iron ion	Male_Anthesis
GO:0042542	response to hydrogen peroxide	GO:0071281	cellular response to iron ion	Male_Anthesis
GO:0071461	cellular response to redox state	GO:0071461	cellular response to redox state	Male_Anthesis
GO:0009625	response to insect	GO:0043617	cellular response to sucrose starvation	Male_Anthesis
GO:0009626	plant-type hypersensitive response	GO:0043617	cellular response to sucrose starvation	Male_Anthesis
GO:0010183	pollen tube guidance	GO:0043617	cellular response to sucrose starvation	Male_Anthesis
GO:0016036	cellular response to phosphate starvation	GO:0043617	cellular response to sucrose starvation	Male_Anthesis
GO:0042594	response to starvation	GO:0043617	cellular response to sucrose starvation	Male_Anthesis
GO:0043617	cellular response to sucrose starvation	GO:0043617	cellular response to sucrose starvation	Male_Anthesis
GO:0050832	defense response to fungus	GO:0043617	cellular response to sucrose starvation	Male_Anthesis
GO:0051365	cellular response to potassium ion starvation	GO:0043617	cellular response to sucrose starvation	Male_Anthesis
GO:0009698	phenylpropanoid metabolic process	GO:0009805	coumarin biosynthetic process	Male_Anthesis
GO:0009809	lignin biosynthetic process	GO:0009805	coumarin biosynthetic process	Male_Anthesis
GO:0052544	defense response by callose deposition in cell wall	GO:0052544	defense response by callose deposition in cell wall	Male_Anthesis
GO:0080110	sporopollenin biosynthetic process	GO:0052544	defense response by callose deposition in cell wall	Male_Anthesis
GO:0009585	red, far-red light phototransduction	GO:0016048	detection of temperature stimulus	Male_Anthesis
GO:0009720	detection of hormone stimulus	GO:0016048	detection of temperature stimulus	Male_Anthesis
GO:0010086	embryonic root morphogenesis	GO:0010086	embryonic root morphogenesis	Male_Anthesis
GO:0048527	lateral root development	GO:0010086	embryonic root morphogenesis	Male_Anthesis
GO:0007623	circadian rhythm	GO:0009649	entrainment of circadian clock	Male_Anthesis
GO:0009649	entrainment of circadian clock	GO:0009649	entrainment of circadian clock	Male_Anthesis
GO:0009835	fruit ripening	GO:1990059	fruit valve development	Male_Anthesis
GO:0009414	response to water deprivation	GO:0009757	hexose mediated signaling	Male_Anthesis
GO:0009734	auxin-activated signaling pathway	GO:0009757	hexose mediated signaling	Male_Anthesis
GO:0009741	response to brassinosteroid	GO:0009757	hexose mediated signaling	Male_Anthesis
GO:0009757	hexose mediated signaling	GO:0009757	hexose mediated signaling	Male_Anthesis
GO:0009787	regulation of abscisic acid-activated signaling pathway	GO:0009757	hexose mediated signaling	Male_Anthesis
GO:0010167	response to nitrate	GO:0009757	hexose mediated signaling	Male_Anthesis
GO:0010555	response to mannitol	GO:0009757	hexose mediated signaling	Male_Anthesis
GO:0006265	DNA topological change	GO:0043971	histone H3-K18 acetylation	Male_Anthesis
GO:0006333	chromatin assembly or disassembly	GO:0043971	histone H3-K18 acetylation	Male_Anthesis

GO:0000160	phosphorelay signal transduction system	GO:0048016	inositol phosphate-mediated signaling	Male_Anthesis
GO:0048016	inositol phosphate-mediated signaling	GO:0048016	inositol phosphate-mediated signaling	Male_Anthesis
GO:0000097	sulfur amino acid biosynthetic process	GO:0070981	L-asparagine biosynthetic process	Male_Anthesis
GO:0006542	glutamine biosynthetic process	GO:0070981	L-asparagine biosynthetic process	Male_Anthesis
GO:0006636	unsaturated fatty acid biosynthetic process	GO:0070981	L-asparagine biosynthetic process	Male_Anthesis
GO:0006799	polyphosphate biosynthetic process	GO:0070981	L-asparagine biosynthetic process	Male_Anthesis
GO:0009094	L-phenylalanine biosynthetic process	GO:0070981	L-asparagine biosynthetic process	Male_Anthesis
GO:0009694	jasmonic acid metabolic process	GO:0070981	L-asparagine biosynthetic process	Male_Anthesis
GO:0010133	proline catabolic process to glutamate	GO:0070981	L-asparagine biosynthetic process	Male_Anthesis
GO:0033611	oxalate catabolic process	GO:0070981	L-asparagine biosynthetic process	Male_Anthesis
GO:0042761	very long-chain fatty acid biosynthetic process	GO:0070981	L-asparagine biosynthetic process	Male_Anthesis
GO:0070981	L-asparagine biosynthetic process	GO:0070981	L-asparagine biosynthetic process	Male_Anthesis
GO:0009911	positive regulation of flower development	GO:0010338	leaf formation	Male_Anthesis
GO:0010072	primary shoot apical meristem specification	GO:0010338	leaf formation	Male_Anthesis
GO:0010223	secondary shoot formation	GO:0010338	leaf formation	Male_Anthesis
GO:0048481	plant ovule development	GO:0010338	leaf formation	Male_Anthesis
GO:0048831	regulation of shoot system development	GO:0010338	leaf formation	Male_Anthesis
GO:0005975	carbohydrate metabolic process	GO:0010493	Lewis a epitope biosynthetic process	Male_Anthesis
GO:0015936	coenzyme A metabolic process	GO:0009435	NAD biosynthetic process	Male_Anthesis
GO:0006873	cellular ion homeostasis	GO:0032353	negative regulation of hormone biosynthetic process	Male_Anthesis
GO:0006885	regulation of pH	GO:0032353	negative regulation of hormone biosynthetic process	Male_Anthesis
GO:0009691	cytokinin biosynthetic process	GO:0032353	negative regulation of hormone biosynthetic process	Male_Anthesis
GO:0009851	auxin biosynthetic process	GO:0032353	negative regulation of hormone biosynthetic process	Male_Anthesis
GO:0010268	brassinosteroid homeostasis	GO:0032353	negative regulation of hormone biosynthetic process	Male_Anthesis
GO:0016131	brassinosteroid metabolic process	GO:0032353	negative regulation of hormone biosynthetic process	Male_Anthesis
GO:0010888	negative regulation of lipid storage	GO:0010888	negative regulation of lipid storage	Male_Anthesis
GO:0046827	positive regulation of protein export from nucleus	GO:0010888	negative regulation of lipid storage	Male_Anthesis
GO:0040008	regulation of growth	GO:0051511	negative regulation of unidimensional cell growth	Male_Anthesis
GO:0040009	regulation of growth rate	GO:0051511	negative regulation of unidimensional cell growth	Male_Anthesis
GO:0051511	negative regulation of unidimensional cell growth	GO:0051511	negative regulation of unidimensional cell growth	Male_Anthesis
GO:0051513	regulation of monopolar cell growth	GO:0051511	negative regulation of unidimensional cell growth	Male_Anthesis
GO:0010207	photosystem II assembly	GO:0010207	photosystem II assembly	Male_Anthesis
GO:0042549	photosystem II stabilization	GO:0042549	photosystem II stabilization	Male_Anthesis
GO:0080005	photosystem stoichiometry adjustment	GO:0042549	photosystem II stabilization	Male_Anthesis
GO:0031539	positive regulation of anthocyanin metabolic process	GO:0031539	positive regulation of anthocyanin metabolic process	Male_Anthesis
GO:1903508	positive regulation of nucleic acid-templated transcription	GO:0031539	positive regulation of anthocyanin metabolic process	Male_Anthesis
GO:0006970	response to osmotic stress	GO:1900036	positive regulation of cellular response to heat	Male_Anthesis
GO:0009416	response to light stimulus	GO:1900036	positive regulation of cellular response to heat	Male_Anthesis

GO:0009637	response to blue light	GO:1900036	positive regulation of cellular response to heat	Male_Anthesis
GO:0010099	regulation of photomorphogenesis	GO:1900036	positive regulation of cellular response to heat	Male_Anthesis
GO:0010114	response to red light	GO:1900036	positive regulation of cellular response to heat	Male_Anthesis
GO:0010224	response to UV-B	GO:1900036	positive regulation of cellular response to heat	Male_Anthesis
GO:0048586	regulation of long-day photoperiodism, flowering	GO:1900036	positive regulation of cellular response to heat	Male_Anthesis
GO:1901000	regulation of response to salt stress	GO:1900036	positive regulation of cellular response to heat	Male_Anthesis
GO:0045962	positive regulation of development, heterochronic	GO:0045962	positive regulation of development, heterochronic	Male_Anthesis
GO:0045848	positive regulation of nitrogen utilization	GO:0045848	positive regulation of nitrogen utilization	Male_Anthesis
GO:0018105	peptidyl-serine phosphorylation	GO:0046777	protein autophosphorylation	Male_Anthesis
GO:0046777	protein autophosphorylation	GO:0046777	protein autophosphorylation	Male_Anthesis
GO:0010304	PSII associated light-harvesting complex II catabolic process	GO:0010304	PSII associated light-harvesting complex II catabolic process	Male_Anthesis
GO:0015996	chlorophyll catabolic process	GO:0010304	PSII associated light-harvesting complex II catabolic process	Male_Anthesis
GO:0016236	macroautophagy	GO:0010304	PSII associated light-harvesting complex II catabolic process	Male_Anthesis
GO:0042744	hydrogen peroxide catabolic process	GO:0010304	PSII associated light-harvesting complex II catabolic process	Male_Anthesis
GO:0031063	regulation of histone deacetylation	GO:0080163	regulation of protein serine/threonine phosphatase activity	Male_Anthesis
GO:1900109	regulation of histone H3-K9 dimethylation	GO:0080163	regulation of protein serine/threonine phosphatase activity	Male_Anthesis
GO:0016117	carotenoid biosynthetic process	GO:1901601	strigolactone biosynthetic process	Male_Anthesis
GO:0019433	triglyceride catabolic process	GO:1901601	strigolactone biosynthetic process	Male_Anthesis
GO:0050992	dimethylallyl diphosphate biosynthetic process	GO:1901601	strigolactone biosynthetic process	Male_Anthesis
GO:1901601	strigolactone biosynthetic process	GO:1901601	strigolactone biosynthetic process	Male_Anthesis
GO:0010148	transpiration	GO:0010148	transpiration	Male_Anthesis
GO:0055085	transmembrane transport	GO:0010148	transpiration	Male_Anthesis
GO:0002939	tRNA N1-guanine methylation	GO:0002939	tRNA N1-guanine methylation	Male_Anthesis
GO:0000162	tryptophan biosynthetic process	GO:0000162	tryptophan biosynthetic process	Male_Anthesis
GO:0006596	polyamine biosynthetic process	GO:0000162	tryptophan biosynthetic process	Male_Anthesis
GO:0009308	amine metabolic process	GO:0000162	tryptophan biosynthetic process	Male_Anthesis
GO:0030837	negative regulation of actin filament polymerization	GO:0007021	tubulin complex assembly	Male_Anthesis
GO:0010411	xyloglucan metabolic process	GO:0010411	xyloglucan metabolic process	Male_Anthesis
GO:0042546	cell wall biogenesis	GO:0010411	xyloglucan metabolic process	Male_Anthesis
GO:0003333	amino acid transmembrane transport	GO:0032328	alanine transport	Male_Post_Anthesis
GO:0008645	hexose transmembrane transport	GO:0032328	alanine transport	Male_Post_Anthesis
GO:0030150	protein import into mitochondrial matrix	GO:0032328	alanine transport	Male_Post_Anthesis
GO:0032328	alanine transport	GO:0032328	alanine transport	Male_Post_Anthesis
GO:0035344	hypoxanthine transport	GO:0032328	alanine transport	Male_Post_Anthesis
GO:0035436	triose phosphate transmembrane transport	GO:0032328	alanine transport	Male_Post_Anthesis
GO:0080168	abscisic acid transport	GO:0032328	alanine transport	Male_Post_Anthesis
GO:0098702	adenine import across plasma membrane	GO:0032328	alanine transport	Male_Post_Anthesis
GO:0098710	guanine import across plasma membrane	GO:0032328	alanine transport	Male_Post_Anthesis
GO:0098721	uracil import across plasma membrane	GO:0032328	alanine transport	Male_Post_Anthesis

GO:0071281	cellular response to iron ion	GO:0071281	cellular response to iron ion	Male_Post_Anthesis
GO:0010112	regulation of systemic acquired resistance	GO:0043617	cellular response to sucrose starvation	Male_Post_Anthesis
GO:0010020	chloroplast fission	GO:0010020	chloroplast fission	Male_Post_Anthesis
GO:0009805	coumarin biosynthetic process	GO:0009805	coumarin biosynthetic process	Male_Post_Anthesis
GO:0042335	cuticle development	GO:0042335	cuticle development	Male_Post_Anthesis
GO:0009827	plant-type cell wall modification	GO:0052544	defense response by callose deposition in cell wall	Male_Post_Anthesis
GO:0070988	demethylation	GO:0070988	demethylation	Male_Post_Anthesis
GO:0016048	detection of temperature stimulus	GO:0016048	detection of temperature stimulus	Male_Post_Anthesis
GO:0080022	primary root development	GO:0010086	embryonic root morphogenesis	Male_Post_Anthesis
GO:1990059	fruit valve development	GO:1990059	fruit valve development	Male_Post_Anthesis
GO:0080188	gene silencing by RNA-directed DNA methylation	GO:0080188	gene silencing by RNA-directed DNA methylation	Male_Post_Anthesis
GO:0009738	abscisic acid-activated signaling pathway	GO:0009757	hexose mediated signaling	Male_Post_Anthesis
GO:0043200	response to amino acid	GO:0009757	hexose mediated signaling	Male_Post_Anthesis
GO:2000022	regulation of jasmonic acid mediated signaling pathway	GO:0009757	hexose mediated signaling	Male_Post_Anthesis
GO:0016584	nucleosome positioning	GO:0043971	histone H3-K18 acetylation	Male_Post_Anthesis
GO:0043971	histone H3-K18 acetylation	GO:0043971	histone H3-K18 acetylation	Male_Post_Anthesis
GO:0043972	histone H3-K23 acetylation	GO:0043971	histone H3-K18 acetylation	Male_Post_Anthesis
GO:0001516	prostaglandin biosynthetic process	GO:0070981	L-asparagine biosynthetic process	Male_Post_Anthesis
GO:0006107	oxaloacetate metabolic process	GO:0070981	L-asparagine biosynthetic process	Male_Post_Anthesis
GO:0006108	malate metabolic process	GO:0070981	L-asparagine biosynthetic process	Male_Post_Anthesis
GO:0006526	arginine biosynthetic process	GO:0070981	L-asparagine biosynthetic process	Male_Post_Anthesis
GO:0009696	salicylic acid metabolic process	GO:0070981	L-asparagine biosynthetic process	Male_Post_Anthesis
GO:0019483	beta-alanine biosynthetic process	GO:0070981	L-asparagine biosynthetic process	Male_Post_Anthesis
GO:0019676	ammonia assimilation cycle	GO:0070981	L-asparagine biosynthetic process	Male_Post_Anthesis
GO:0033481	galacturonate biosynthetic process	GO:0070981	L-asparagine biosynthetic process	Male_Post_Anthesis
GO:0036104	Kdo2-lipid A biosynthetic process	GO:0070981	L-asparagine biosynthetic process	Male_Post_Anthesis
GO:0042126	nitrate metabolic process	GO:0070981	L-asparagine biosynthetic process	Male_Post_Anthesis
GO:0055129	L-proline biosynthetic process	GO:0070981	L-asparagine biosynthetic process	Male_Post_Anthesis
GO:0097054	L-glutamate biosynthetic process	GO:0070981	L-asparagine biosynthetic process	Male_Post_Anthesis
GO:0010338	leaf formation	GO:0010338	leaf formation	Male_Post_Anthesis
GO:0048658	anther wall tapetum development	GO:0010338	leaf formation	Male_Post_Anthesis
GO:0006004	fucose metabolic process	GO:0010493	Lewis a epitope biosynthetic process	Male_Post_Anthesis
GO:0006097	glyoxylate cycle	GO:0010493	Lewis a epitope biosynthetic process	Male_Post_Anthesis
GO:0010493	Lewis a epitope biosynthetic process	GO:0010493	Lewis a epitope biosynthetic process	Male_Post_Anthesis
GO:0006096	glycolytic process	GO:0009435	NAD biosynthetic process	Male_Post_Anthesis
GO:0009435	NAD biosynthetic process	GO:0009435	NAD biosynthetic process	Male_Post_Anthesis
GO:0051156	glucose 6-phosphate metabolic process	GO:0009435	NAD biosynthetic process	Male_Post_Anthesis
GO:0032353	negative regulation of hormone biosynthetic process	GO:0032353	negative regulation of hormone biosynthetic process	Male_Post_Anthesis
GO:0006099	tricarboxylic acid cycle	GO:0010207	photosystem II assembly	Male_Post_Anthesis
GO:0006355	regulation of transcription, DNA-templated	GO:0031539	positive regulation of anthocyanin metabolic process	Male_Post_Anthesis
GO:0010286	heat acclimation	GO:1900036	positive regulation of cellular response to heat	Male_Post_Anthesis

GO:1900036	positive regulation of cellular response to heat	GO:1900036	positive regulation of cellular response to heat	Male_Post_Anthesis
GO:0007023	post-chaperonin tubulin folding pathway	GO:0007023	post-chaperonin tubulin folding pathway	Male_Post_Anthesis
GO:0016567	protein ubiquitination	GO:0046777	protein autophosphorylation	Male_Post_Anthesis
GO:0006402	mRNA catabolic process	GO:0010304	PSII associated light-harvesting complex II catabolic process	Male_Post_Anthesis
GO:0080163	regulation of protein serine/threonine phosphatase activity	GO:0080163	regulation of protein serine/threonine phosphatase activity	Male_Post_Anthesis
GO:0009611	response to wounding	GO:0009611	response to wounding	Male_Post_Anthesis
GO:0040001	establishment of mitotic spindle localization	GO:1990126	retrograde transport, endosome to plasma membrane	Male_Post_Anthesis
GO:1990126	retrograde transport, endosome to plasma membrane	GO:1990126	retrograde transport, endosome to plasma membrane	Male_Post_Anthesis
GO:0008610	lipid biosynthetic process	GO:1901601	strigolactone biosynthetic process	Male_Post_Anthesis
GO:0008654	phospholipid biosynthetic process	GO:1901601	strigolactone biosynthetic process	Male_Post_Anthesis
GO:0019432	triglyceride biosynthetic process	GO:1901601	strigolactone biosynthetic process	Male_Post_Anthesis
GO:0006729	tetrahydrobiopterin biosynthetic process	GO:0006729	tetrahydrobiopterin biosynthetic process	Male_Post_Anthesis
GO:0006730	one-carbon metabolic process	GO:0006729	tetrahydrobiopterin biosynthetic process	Male_Post_Anthesis
GO:0051179	localization	GO:0010148	transpiration	Male_Post_Anthesis
GO:0140352	export from cell	GO:0010148	transpiration	Male_Post_Anthesis
GO:0007021	tubulin complex assembly	GO:0007021	tubulin complex assembly	Male_Post_Anthesis
GO:0006144	purine nucleobase metabolic process	GO:0006212	uracil catabolic process	Male_Post_Anthesis
GO:0006166	purine ribonucleoside salvage	GO:0006212	uracil catabolic process	Male_Post_Anthesis
GO:0006168	adenine salvage	GO:0006212	uracil catabolic process	Male_Post_Anthesis
GO:0006212	uracil catabolic process	GO:0006212	uracil catabolic process	Male_Post_Anthesis
GO:0044209	AMP salvage	GO:0006212	uracil catabolic process	Male_Post_Anthesis
GO:0010025	wax biosynthetic process	GO:0010025	wax biosynthetic process	Male_Post_Anthesis

CHAPTER 4 - The evolution of floral scent in the genus *Arum* (Araceae): insights from phylogenetic and chemical ecology data

Mark A. Szenteczki[1*], Adrienne L. Godschalx[1], Julia Bilat[2], Marc Gibernau[3], Sergio Rasmann[1+], Nadir Alvarez[2 4 +]

[1] Université de Neuchâtel, Institut de Biologie, Rue Emile-Argand 11, 2000 Neuchâtel, Switzerland
[2] Geneva Natural History Museum, Route de Malagnou 1, 1208 Genève, Switzerland
[3] CNRS – University of Corsica, Laboratory Sciences for the Environment (SPE - UMR 6134), Natural Resources Project, Vignola – Route des Sanguinaires, 20000 Ajaccio, France
[4] Department of Genetics and Evolution, University of Geneva, Quai Ernest-Ansermet 30, 1211 Geneva, Switzerland
[5] Natural Sciences Museum, Place de la Riponne 6, 1006 Lausanne, Switzerland
[*] Corresponding author: M.A. Szenteczki mark.szenteczki@unine.ch Tel. + 41 32 718 23 16
[+] Authors participated equally and are considered joint senior authors

ABSTRACT

Floral scents are shaped by the interplay between selection from mutualistic and antagonistic interactions, environmental conditions, and phylogenetic history. However, disentangling the influences of these processes on the complex blends of volatile organic compounds (VOCs) that make up floral scents remains a challenge. Species which are deceptively pollinated via olfactory mimicry – such as the majority of the genus *Arum* – therefore represent a useful model for studying floral scent evolution, given the presumably strong links between VOC emissions and pollinator attraction. However, traits may also be phylogenetically constrained (*i.e.* when specific VOCs have not yet evolved or have been lost). Here, we investigated whether floral VOCs were phylogenetically constrained at both microevolutionary (*i.e.* within *Arum maculatum*) and macroevolutionary (*i.e.* across the entire genus *Arum*) scales. To this aim, we combined gas chromatography–mass spectrometry (GC-MS) characterizations of floral scents with genotyping by sequencing (GBS) data collected from i) twelve populations of *Arum maculatum* from across Europe, and ii) nine species across the genus *Arum*. Using ploidy-aware genotype calling methods, we were able to overcome the challenges associated with mixed-ploidy and polyploid genomic datasets. We generated a total of 6271 loci (13'320 SNPs) for the genus-wide dataset, and 3748 loci (7651 SNPs) for *A. maculatum* alone. We used these data to produce a phylogeny of the genus *Arum*, which confirmed the monophyly of *A. maculatum* across Europe. Our data further refined the population genetic structure of *Arum maculatum*, which consists of two or three genetic clusters which reflect the species' phylogeographic history. Finally, we observed relatively weak phylogenetic signal in VOC variation within *A. maculatum* and across the entire genus; only indole showed some indications of phylogenetic constraints at both scales. Taken together, these results indicate that most VOC diversity is not constrained by the evolutionary history of the genus, and may be a result of pollinator-mediated selection.

KEYWORDS

Arum maculatum; ddRAD-seq; GC-MS; deceptive pollination; phylogenetic signal; phylogeography

INTRODUCTION

Pollinators have been hypothesized to be a key driver of adaptive radiations in angiosperms since Darwin (1862). Today, there is growing evidence that pollinator preferences influence both floral trait microevolution (Harder and Johnson 2009, Gervasi and Schiestl 2017) and macroevolutionary patterns among flowering plant species (Whittall and Hodges 2007, Van der Niet and Johnson 2012, Friberg et al. 2019). While antagonistic interactions such as herbivory exert selective pressures on floral traits (Strauss and Whittall 2006, Schiestl 2010, Ramos and Schiestl 2019), pollinators – the vast majority of which are insects – appear to be a key contributor to angiosperm diversity (Van der Niet and Johnson 2012, Hernández-Hernández and Wiens 2020). Some of this diversity is the result of ecological speciation (Simpson 1953, Schluter 2001, Rundle and Nosil 2005, Nosil 2012), whereby divergent selection resulting from ecological factors (*e.g.* varying pollinator preferences) leads to reproductive isolation and ultimately speciation. However, relatively few studies have successfully linked pollinator-mediated microevolution to broader macroevolutionary patterns among species (*e.g.* Ramsey et al. 2003). One proposed method for bridging this gap between micro- and macroevolution in plants involves merging high-resolution genetic, ecological, and phenotypic data within an ecological speciation framework (Van der Niet et al. 2014).

Flowering plants produce diverse olfactory and visual signals, which are often perceived by pollinators as multimodal traits (reviewed in Junker and Parachnowitsch 2015). Consequently, floral scent, colour, morphology, and/or nectar and pollen may be subject to pollinator-mediated selection (Schiestl and Johnson 2013). Floral advertisements are typically honest indicators of rewards for pollinators. However, around 3.7% of angiosperms utilize deceptive pollination strategies (Renner 2006), signalling the presence of a reward without providing one (Sprengel 1793, Dafni 1984, Schiestl and Johnson 2013). Rewards such as food, shelter, mating opportunities, and/or oviposition sites are all known to be mimicked by floral volatile organic compound (VOC) emissions (reviewed in Jersáková et al. 2006). Here, we will focus on the evolution of deceptive floral VOCs in the genus *Arum* (Araceae).

Arum inflorescences have long fascinated botanists (Theophrastus 350BC, Lamarck 1783, Schmucker 1925, Vogel 1965, Boyce 1993) due to their thermogenic activity (Onda et al. 2015, Marotz-Clausen et al. 2018) and potent VOC emissions, which can range from sweet and fruity to fermented, dung-, or urine-like scents (reviewed in Gibernau 2004). Molecular phylogenies of the genus *Arum* have been completed using plastid (Espíndola et al. 2010) and nuclear/amplified fragment length polymorphism (AFLP) data (Linz et al. 2010). However, some aspects of the phylogeny, such as the placement and monophyly of *Arum maculatum* (Espíndola et al. 2010) and the evolutionary relationships between species in the most recently diverged clade (Linz et al. 2010, Espíndola et al. 2010) have not yet been fully resolved. Modern high-throughput sequencing techniques such as double-digest restriction site associated DNA sequencing (ddRAD-seq; Peterson et al. 2012, Mastretta-Yanes et al. 2015) could therefore be useful for resolving shallow phylogenetic relationships between closely related *Arum* species.

Arum maculatum, the well-studied type species for the genus *Arum*, is a common woodland plant with a Europe-wide species distribution range. *Arum maculatum* floral scent (Kite 1995, Diaz and Kite 2002, Chartier et al. 2011, 2013, Szenteczki et al. 2021, Gfrerer et al. 2021) and pollinators (Espíndola et al. 2011, Szenteczki et al. 2021, Laina et al. 2022) have been widely studied, as well as its morphology (Bröderbauer et al. 2013), genetic diversity (Espíndola and Alvarez 2011), and hybridization with *Arum italicum* (Chartier et al. 2016). Specific VOCs (*e.g.* indole, *p*-cresol, and several sesquiterpenes) which appear to mediate interactions with its two main pollinators – *Psychoda (Psychoda) phalaenoides* and *Psychoda (Psycha) grisescens* (Diptera: Psychodidae) have also been identified, through studies on insect antennal responses to *A. maculatum* floral VOCs (Gfrerer et al. 2022), and transcript expression patterns in floral tissues (Szenteczki et al. 2022). However, phylogenetic constraints (here synonymous with phylogenetic signal or effects) could also influence floral VOC variation, both i) within *A. maculatum* and ii) across the entire genus *Arum*. Molecular genetic data are therefore still needed in order to understand the extent to which pollinator-mediated selection and/or phylogenetic constraints have influenced floral VOC variation.

If floral scent is relatively diverse and evolutionarily labile across the entire genus *Arum*, as observed in *A. maculatum* (Szenteczki et al. 2021), phylogenetic constraints on floral scent composition should be limited at both micro- and macroevolutionary scales. Such a result would be consistent with previous studies on multivariate floral scent variation (Levin et al. 2003, Prieto-Benítez et al. 2016). However, some VOCs or compound classes may be influenced by phylogenetic constraints (Prieto-Benítez et al. 2016, Milet-Pinheiro et al. 2021). Therefore, we might predict that phenotypic selection will play a larger role than phylogenetic constraints in shaping VOC variation in the genus *Arum* for two main reasons. First, Araceae are also known to attract diverse pollinators (Gibernau 2003, 2011, 2016); *Arum* spp. are known to attract beetles (Bruchidae, Scarabaeideae, and Staphylinidae) and flies (Drosophilidae, Sphaeroceridae, and Psychodidae) (Gibernau 2004). Additionally, skatole and other putatively deceptive compounds (*e.g. p*-cresol, indole, and fatty acid esters) have evolved independently up to 3-4 times in the Araceae family (Schiestl and Johnson 2013), presumably through convergence following repeated pollinator shifts.

In addition to strengthening our understanding of the impact of pollinator-mediated selection on floral scent, high resolution ddRAD-seq data would also address several longstanding questions on the population genetics of *A. maculatum*. First, how many spatial genetic clusters of *A. maculatum* exist across Europe? Second, are *A. maculatum* from western Europe (France, Switzerland, and Italy) and the Balkans (Croatia and Serbia) monophyletic, or does the previously observed lack of monophyly (Espíndola et al. 2010) represent major splits requiring taxonomic revision? We expect to observe two main genetic clusters corresponding to the aforementioned geographic regions, potentially with additional sub-structuring arising from the resolution offered by high-throughput sequencing. This result would be consistent with the patterns observed using AFLP (Espíndola and Alvarez 2011) and transcriptomic (Szenteczki et al. 2022) data. Moreover, we expect that ddRAD-seq data will better resolve the *Arum* phylogeny with fewer polyphyletic taxa, particularly for more recently diverged species such as *A. maculatum*.

To address these hypotheses, we characterized and compared microevolutionary (*i.e.* within-species) and macroevolutionary (*i.e.* genus-wide) divergence at the molecular and chemical levels in the genus *Arum*. Specifically, we generated a large SNP dataset for the genus *Arum* and 12 populations of *A. maculatum* using ddRAD-seq. We paired these data with GC-MS characterizations of floral scents for all studied species. This allowed us to address whether floral scent evolution has been influenced by phylogenetic constraints, selection from plant–pollinator interactions, or both mechanisms.

MATERIALS AND METHODS

Sampling design

We sampled fresh leaf tissue from nine *Arum* species across all sections of the genus (Appendix S1, Table S1) plus *Dracunculus vulgaris* as an outgroup. Individuals of the different species were sampled from the living collections at the Royal Botanic Gardens Kew, the Jardin Botanique de Lyon, and the Jardin Botanique de Neuchâtel. We also sampled fresh leaf tissue from twelve natural populations of *Arum maculatum*: three in France (Forêt du Gâvre, Conteville, and Chaumont), two in Switzerland (Cortaillod and Neuchâtel), four in Italy (Montese, Morro Reatino, Jenne, and Rifreddo), one in Croatia (Visuć), and two in Serbia (Gostilje and Sokobanja). In total, thirty *A. maculatum* plants were sampled; full sampling details and population coordinates are given in Appendix S1, Table S2. Leaves were placed in coffee filter paper and stored individually in silica gel at room temperature until molecular analyses.

ddRAD-seq library preparation

We extracted DNA from 10mg of dried leaf tissue using a Qiagen DNeasy Plant Mini Kit, following the manufacturer's recommended protocol, except that i) RNase treatment was omitted, and ii) 100 microlitres (µL) of elution buffer was pre-heated to 56°C and left for on the spin column for two minutes prior to elution to increase DNA yields. We followed a standard ddRAD-seq protocol (Peterson et al. 2012, Mastretta-Yanes et al. 2015); briefly, 6 µL of each sample (with concentrations ranging from 43-184 ng/µL) were restriction digested using MseI and PstI (NEB) as the frequent and rare cutters, respectively. P1 and P2 adapters were ligated using T4 DNA ligase (NEB); we used P1 adapters with six different barcode sequences, and P2 adapters with the same sequence for all samples. The ligation products were then purified using CleanNGS Solid Phase Reversible Immobilization (SPRI) beads (CleanNA) at a 1.5:1 ratio of bead solution to DNA.

Following a double indexing approach, we performed PCR amplification using Illumina primers with 8 unique barcode sequences and the following thermal cycling profile: 98º C for 30 seconds; 30 cycles of 98ºC for 10 seconds followed by 72ºC for 45 seconds; a final extension at 72ºC for 5 minutes. Each sample was amplified in three separate reactions to reduce PCR biases; these triplicate PCR products were then pooled and purified with SPRI beads at a 0.8:1 ratio. Finally, samples were quantified using a PicoGreen Fluorometer, pooled in an equimolar ratio, and size selected with PippinPrep (Sage Science) around 350-600bp. Quality controls using a Fragment Analyser (Agilent) were carried out after PCR, pooling, and size selection steps. A final purification and concentration was completed using SPRI beads at a 1:1 ratio, and samples were then sequenced at the Lausanne Genomics Technologies Facility (LGTF) using an Illumina HiSEQ2500 to obtain 150bp single-end reads.

Ploidy-aware assembly and SNP calling

Following an initial quality check with *FastQC* (Andrews 2010), we performed quality filtering and trimmed adapter sequences from the raw Illumina reads using *AdapterRemoval* v2.3.3 (Schubert et al. 2016) and demultiplexed samples using *Cutadapt* v4.1 (Martin 2011). Only reads with zero barcode mismatches and zero uncalled bases (Ns) were retained. *De novo* assembly and SNP calling was performed using *ipyrad* v0.9.84 (Eaton and Overcast 2020), with default settings and the following modifications based on preliminary analyses: a clustering threshold of 0.88, a minimum read depth of 6, a minimum of 6 samples with data to retain a locus, and a maximum of 20 shared polymorphic sites per locus. As our data contained a mix of diploid, tetraploid, and hexaploid taxa, we used a branched *ipyrad* workflow with the parameters described above in both the i) diploid and ii) polyploid branches. The maximum number of SNPs in a locus was increased from two to four in the polyploid branch. Joint estimation of heterozygosity and error rate and consensus base calling were performed separately for diploids and polyploids, and the branches were then merged for clustering, mapping, and aligning reads and the final filtering and output file export.

The *ipyrad* assembly and read depth data (in VCF format) were imported into R (R Core Team 2021) for analysis with *polyRAD* v1.6 (Clark et al. 2019), a Bayesian genotype calling pipeline which can differentiate putatively Mendelian markers from collapsed paralogous loci using the H_{ind}/H_E statistic (Clark et al. 2022). Two python scripts – *ipyrad2polyrad.py* and *polyVCFtoStructure.py* – (https://github.com/tkchafin/polyrad_scripts) were used to create a input VCF file compatible with *polyRAD*, and to convert the *polyRAD* output to a STRUCTURE input file, respectively (Chafin et al. 2021). We filtered out loci with a minor allele frequency below 5%, and loci which were not statistically consistent with diploid expectations (*i.e.* loci where $H_{ind}/H_E > 0.5$) following analysis in *polyRAD*. The resulting bi-allelic SNP matrix was exported in VCF format for further phylogenetic analysis.

Phylogenetic analysis

We converted the polyRAD output to a fasta alignment with IUPAC encoding for heterozygous sites, and used RAxML-NG v1.1.0 (Kozlov et al. 2019) to infer a maximum likelihood (ML) phylogeny for the entire genus *Arum*, including all available *A. maculatum* samples. We tested three models, using default parameters and standard/slow bootstrapping with 200 replicates to estimate support values for each analysis. We tested both the DNA model without ascertainment bias correction (*i.e.* GTR+G), and genotype model with ASC correction (*i.e.* GTGTR4+G+ASC_LEWIS) and without it (*i.e* GTGTR4+G). Finally, the best supported tree in terms of *post-hoc* bootstrap convergence and supports was visualized using iTOL v6 (Letunic and Bork 2021) and retained for subsequent analyses.

Population genetic structure in Arum maculatum

To characterize the population genetic structure within *A. maculatum*, we re-ran polyRAD with only *A. maculatum* individuals. We used identical parameters as described above (*e.g.* only retaining loci found in at least six *A. maculatum* individuals prior to analysis), except that loci which were statistically consistent with tetraploidy (i.e. $H_{ind}/H_E < 0.75$) were retained in the output, and tetraploid loci were permitted. We then used STRUCTURE v2.3.4 (Pritchard et al. 2000), as it is more robust than other model-based methods for resolving clusters in polyploid datasets (Meirmans et al. 2018, Stift et al. 2019). We performed ten replicate analyses for each K value (*i.e.* number of assumed populations) from $K = 1$ to $K = 10$, using a total MCMC length of 1’000’000 iterations with a 100’000 iteration burn-in period. We then determined the optimal K value using the Evanno (ΔK) method (Evanno et al. 2005) in Structure Harvester (Earl and vonHoldt 2012). We summarized the replicate analyses for each K using CLUMPP (Jakobsson and Rosenberg 2007) and visualized the major clusters for optimal K values at the individual and population levels.

Floral scent analysis

The dynamic headspace VOCs for 17 *A. maculatum* individuals sequenced in this study were characterized during previous research (Szenteczki et al. 2021); these data covered all populations in this study except Visuć, Croatia and Jenne, Italy. In this study, we further characterized the dynamic headspace VOCs for the seven other *Arum* species, plus *D. vulgaris* (n = 13 new samples in total). We followed identical methods to Szenteczki et al. (2021), including identical thermal desorption and processing parameters on the same GC- (Agilent 7890a) MS (Agilent 5975c) system and column (HP-5MS). However, Tenax TA® (2,6-diphenylene oxide polymer resin) was used as the adsorptive material in place of Gerstel Twister® stir bars (polydimethylsiloxane). Since the quantities of VOCs detected varied between Twister and Tenax results, we converted the absolute measurements to proportional abundances (*i.e.* relative to the sum of all compounds in a given sample) when the two datasets were combined. Following the recommendations of Hervé et al. (2018), we i) used fourth-root transformed absolute concentrations when analysing *A. maculatum* data alone, and ii) centered log ratio (clr) transformed the combined compositional dataset prior to further analysis.

3.7 – Phylogenetic PCA analyses

Phylogenetic PCA (pPCA) analysis (Revell 2009) can be used to test for phylogenetic signal, which occurs when traits of interest – here, floral VOCs – are more similar in closely related taxa than would be expected by chance. The first (*i.e.* strongest positive autocorrelation) and last (*i.e.* strongest negative autocorrelation) PC axes represent global and local phylogenetic structures, respectively (Jombart et al. 2010); global structures highlight where closely related taxa have more similar traits (*i.e.* an indication of phylogenetic signal), while local structures highlight where closely related taxa have more divergent traits compared to randomly selected taxa (*i.e.* a possible indication of recent divergent selective pressures). We performed two pPCA analyses using the *adephylo* package in R (Jombart and Dray 2010). For the first pPCA analysis, we analysed the 17 *A. maculatum* individuals with fourth-root transformed VOC concentration data. The second pPCA analysis further included the data from our genus-wide molecular and VOC sampling, increasing the sample size to 30 individuals in a *clr* transformed compositional VOC matrix. Following both pPCA analysis, we also calculated Blomberg's multivariate K (Adams 2014) as an additional measure of phylogenetic signal in the complete VOC matrix.

We also tested for phylogenetic signal at the individual compound level, in the both the *A. maculatum* and genus *Arum* datasets, using univariate analyses. Specifically, we calculated Abouheif's C_{mean} and Pagel's λ for the subset of VOCs with the greatest indications of phylogenetic signal in the two preceding analyses (*i.e.* the top and bottom 5% of loadings on pPCA PC1) using the *abouheif.moran* and *phylosig* functions in *adephylo* (Jombart and Dray 2010) and *phytools* (Revell 2009), respectively. These statistics were chosen based on their ability to detect phylogenetic signal at the sample sizes used in this study (Münkemüller et al. 2012).

RESULTS

ddRAD-seq assembly and genotyping

We obtained 229’200’000 raw reads from our Illumina sequencing runs. Following initial quality filtering steps, 186’800’000 adapter-trimmed reads remained; read counts ranged from 806’014 to 7’731’500 reads per individual (median: 1’640’455 reads). *ipyrad* recovered 52’203 loci following all filtering steps; the number of loci per individual ranged from 1176 to 29’297 (median: 11’360 loci). Individual-level read and loci count data are provided in Appendix S1, Table S1 and S2. After processing in *polyRAD*, 6271 loci (13’320 SNPs) were retained for the genus-wide dataset, and 3748 loci (7651 SNPs) were retained for the *A. maculatum*-only dataset.

Genus Arum phylogeny

Among the models tested in RAxML-NG, the genotype model produced trees with better log likelihoods than the DNA model; the genotype model without ASC correction produced the tree with the best final log likelihood and node supports (Figure 1). Our results strongly support the monophyly of *A. maculatum* (98% support), which is an improvement over previous research (Espíndola et al. 2010); we found that the species is further divided into three main sub-clades with strong (100%) support. These subclades comprise i) western European populations (Forêt du Gâvre, Conteville, Chaumont, Neuchâtel, Cortaillod) plus the northernmost Italian population (Montese), ii) central/southern Italian populations (Morro Reatino, Jenne, and Rifreddo) plus Visuć, Croatia, and iii) Serbian populations (Gostilje and Sokobanja).

Population genetic structure within Arum maculatum

The ΔK table for STRUCTURE runs from K=1 to K=10 indicated that K=2 was the most probable number of populations (ΔK = 229.96), while mean LnP(K) values plateaued around K=4 (Appendix S1, Table S3). At K=2, the first cluster included populations from France, Switzerland, and northern Italy population (Montese), while the second cluster included southern Italy, Croatia, and Serbia (Figure 2, Appendix S1, Figure S1). Although less supported by the Evanno method results, K=3 further subdivided populations in southern Italy and Croatia from Serbia, mirroring the three clades identified in our phylogeny (Figure 3a). These three clusters were also present following probabilistic PCA analysis of the posterior genotype probabilities of loci passing all filtering steps in *polyRAD* (Appendix S1, Figure S2).

Phylogenetic PCA (pPCA) analyses

Through our genus-wide sampling of *Arum* floral odours, we identified a total of 54 VOCs (visualized in Appendix S1, Figure S3) which passed all filtering criteria (*i.e.* not present at high concentrations in blank / ambient air samples, and present at relative abundances below 1% in all samples). 19 of these VOCs were present in *A. maculatum*. These VOC data were combined with our molecular phylogeny for two phylogenetic PCA analyses, at the within (*i.e. A. maculatum*) and among species (*i.e.* genus-wide) levels.

Arum maculatum

Consistent with other large-scale surveys of *A. maculatum* floral scent (Gfrerer et al. 2021), we found that volatile compounds were widely distributed and highly variable at the within-population level. Consequently, no compounds were unique to a specific subclade in our phylogeny (Figure 3b). Within *A. maculatum*, the multivariate Bloomberg′s K indicated the presence of phylogenetic signal, but the result was not significant (K = 0.9160, p = 0.167), meaning that phylogenetic signal within the species is relatively weak overall. In our pPCA analysis of *A. maculatum* VOCs (Figure 4), high global and local phylogenetic signal in southern Italian populations was driven by sesquiterpenes, namely cedrol, while indole had the strongest contribution to global phylogenetic signal in French and Swiss populations (Appendix S1, Figure S4). Univariate analyses further identified one VOC – indole – with a significant Abouheif's C_{mean} score (*P* = 0.048; Table 1). Indole was the only compound where Pagel's λ was also equal to 1.

Genus Arum

Across the entire genus *Arum*, the multivariate Bloomberg′s K score indicated weak phylogenetic signal (K = 0.2033, *p* = 0.047); in other words, closely related taxa had more divergent VOC bouquets than expected. In our pPCA analysis of genus-wide VOC variation (Figure 4), the first axis separated *A. maculatum* from the rest of the genus with comparable global phylogenetic signal in the two groups. Indole and unnamed sesquiterpene (Kovats RI 1404) were among the strongest contributors to positive scores for *A maculatum*. High local phylogenetic signal was also identified in the clade containing *A. balansanum*, *A. apulum,* and *A. cyrenaicum*, which were split based on proportionally high emissions of i) 3,7-dimethyl-1-octene and β-citronellene or benzoic acid, and ii) 2-(methylamino)-, propyl ester and 6-methyl-2-heptanone (Appendix S1, Figure S5). Through univariate analyses, we further identified one VOC in the genus-wide dataset – unnamed sesquiterpene (Kovats RI 1404) – with a significant Abouheif's C_{mean} score (*P* = 0.011; Table 2).

DISCUSSION

Using genome-wide SNPs identified through ddRAD-seq and ploidy-aware genotyping methods, we were able to investigate the extent to which *Arum* floral scent variation was constrained by phylogenetic history. Our molecular dataset provided the resolution required to i) confirm that *A. maculatum* is monophyletic, and ii) can be divided into either two or three geographically structured genetic clusters. Phylogenetic PCA analyses further demonstrated that iii) floral scent variation in the genus *Arum* is relatively unconstrained by phylogeny, with a few notable exceptions. Specifically, iv) indole appears to contribute to global phylogenetic signal both within *A. maculatum*, and among *Arum* species.

Genus Arum phylogeny

The topology of our tree derived from 13'320 ddRAD-seq SNPs is consistent with previous plastid (Espíndola et al. 2010) and AFLP (Linz et al. 2010) phylogenies of the genus *Arum*. Our phylogeny also supports the monophyly of *Arum maculatum* from northern France to Serbia (*i.e.* the majority of its distribution range except Turkey and the Caucasus, which we did not sample). The only notable difference in our phylogeny is the placement of *A. palaestinum* as a sister species to *A. creticum*, rather than being in a sister clade. Given the stark contrast in morphology and floral scents between sweet-smelling and bee-pollinated *A. creticum* (Urru et al. 2010) and fruity-fermented scented, *Drosophila*-pollinated *A. palaestinum* (Stökl et al. 2010), the placement of *A. palaestinum* in our phylogeny may be due to our low species coverage of this section of the genus. Additional ddRAD-seq data from closely related species (*e.g. A. dioscoridis*) should be able to better resolve the placement of *A. palaestinum*.

Population genetic structure within A. maculatum

In both our STRUCTURE analysis of 7651 *A. maculatum* SNPs at *K*=3 and in our phylogeny, we identified genetic clusters corresponding to i) France, Switzerland and northern Italy, ii) central / southern Italy and Croatia, and iii) Serbia. However, *K*=2 – which merged the second and third clusters described above – was better supported by our Δ*K* (Evanno) results. An identical result was obtained by Espíndola and Alvarez (2011) using AFLP data, where *K*=2 was most strongly supported, but *K*-means analysis identified sub-structuring among southern European populations east and west of the Carpathians. In the aforementioned study, however, it was not clear whether *A. maculatum* in northern / western Europe formed a single contiguous genetic cluster; our results suggest that this is in fact the case.

Although more advanced analyses for estimating demographic parameters (*e.g.* effective population size, divergence time, and migration rate) using approximate Bayesian computation (ABC; Beaumont et al. 2002, Csilléry et al. 2012) and/or ancestral state reconstruction (*e.g.* RASP; Yu et al. 2015, 2020) were beyond the scope of this study, our data still allowed us to investigate the phylogeography of *A. maculatum*. As reported by Espíndola and Alvarez (2011), we found that *A. maculatum* has a well-defined spatial genetic structure, that appears to reflect its two likely glacial refugia and subsequent re-colonization of northern Europe at the end of the last glacial retraction ca. 13ka BP (Hewitt 1999). The admixture patterns we identified in Croatia at *K*=3 also likely reflects its biogeographical history. During the last glacial maximum (LGM; ca. 24ka BP), the northern Adriatic Sea had receded and a land bridge was present (Mussi 1990, Seguinot et al. 2018); this may have facilitated migration and admixture of populations from southern Italy and east of the Carpathians in this region.

The Alps mountain range has been proposed to be a barrier leading to differentiation in floral scent and/or pollinator communities in *A. maculatum* (Gfrerer et al. 2021, Laina et al. 2022). However, our results indicate that all of the populations in the aforementioned studies – which did not sample further south than Montese, Italy – belong to the same (northern) clade and STRUCTURE genetic cluster. Consequently, the reported chemical differentiation in scent north and south of the Alps is not reflected in the species' evolutionary history. The high contemporary variation in floral scent may therefore be partially driven by phenotypic plasticity in response to environmental variation (Majetic et al. 2009), and/or continuous and varied selection pressure from pollinator communities over short timescales (Szenteczki et al. 2021).

Finally, our results also support the extension of the range of *A. maculatum* towards southern Italy. While key taxonomic literature (Boyce 1993, 2006) defined the range limit of *A. maculatum* in northern Italy, both our field surveys (Szenteczki et al. 2021) and previous research by (Espíndola et al. 2011) sampled *A. maculatum* up to ca. 570 km south of Montese (straight line distance). Our samples from Morro Reatino, Jenne, and Rifreddo appeared to be part of the larger *A. maculatum* clade in our phylogeny, and not in a sister clade with *A. concinnatum* – as we would expect if these individuals were in fact *A. italicum* according to Espíndola et al. (2010). Thus, it appears that all of these populations indeed contain *A. maculatum*. Since *A. italicum* is co-distributed with *A. maculatum* in Italy and across most of its distribution range, and the two species readily hybridize (Chartier et al. 2016), these southern Italian populations may represent interesting areas for future research into the effects of ancient (*i.e.* during the LGM) and contemporary hybridization between the two species.

Phylogenetic PCA across the genus Arum and within A. maculatum

As expected, we found relatively weak multivariate phylogenetic signal in floral scent using both concentration and proportional VOC datasets within *A. maculatum* and among nine *Arum* species, respectively. Several factors likely contributed to this result. Weak phylogenetic signal is expected for traits which are under selection and/or have undergone adaptive radiations (Felsenstein 1985), and floral scents in annual plants are known to rapidly evolve within the span of a few generations response to pollinator-mediated selection (Zu et al. 2016, Gervasi and Schiestl 2017). Repeated gains and losses of key VOCs have also been identified over the evolution of Araceae (Schiestl and Dötterl 2012). Furthermore, floral VOC blends are also known to vary both in terms of composition and proportional emissions as a result of environmental conditions (Majetic et al. 2009, Farré-Armengol et al. 2014, Glenny et al. 2018). However, we would expect that the deceptive pollination strategy of all *Arum* spp. in this study except *A. creticum* would have a greater influence on floral scent evolution than plasticity in response to environmental variation, given the importance of producing an effective mimic to attract pollinators through deception (Renner 2006).

In our pPCA analyses, some indications of phylogenetic signal were identified for *A. maculatum*; notably, *A. maculatum* was separated from all other species along the first axis of the pPCA in the genus-wide analysis. This is likely a result of the high diversity in compounds produced by *A. maculatum*, its wide geographic range compared to other species in this study, and its specialization on Psychodidae pollinators (mainly *Psychoda phalaenoides* and *P. grisescens*). However, a wider and more balanced sampling across the genus is still needed to confirm whether *A. maculatum* VOC bouquets are exceptionally diverse within the genus.

Within *A. maculatum*, indole was the only compound with global multivariate phylogenetic signal which was also significant under both univariate tests (*i.e.* Abouheif's C_{mean} and Pagel’s λ). This result suggests that indole emissions are restricted to specific clades, or subclades in the case of *A. maculatum* – likely as a result of either recent divergence events (*i.e.* due to pollinator-mediated selection) or loss/silencing of indole synthases. Indole is a ubiquitous compound in nature, which mediates inter-kingdom interactions among bacteria, plants, and insects (Lee et al. 2015, Tomberlin et al. 2017). It has also recently been shown to elicit electroantennographic responses in both Psychodidae and Sphaeroceridae flies (Gfrerer et al. 2022), validating prior studies which used traps baited with indole to attract a wide range of dung-breeding dipterans, including *Psychoda* spp. (Mulla et al. 1977, Kite et al. 1998). However, if variation in indole emissions is more influenced by phylogenetic constraints as opposed to selection (*i.e.* if it serves as a general lure, rather than a specific lure shaped by selection), then this result may further support the importance of sesquiterpenes in sex- and species-specific pollinator attraction in *A. maculatum* (Szenteczki et al. 2022).

Future directions

In this study, we were able to gain insights into the constraints on floral scent evolution in *Arum* using a combination of samples from across the genus, as well as population-level sampling of *A. maculatum* across Europe. As mentioned above, our primary limitation compared to previous phylogenetic studies of the genus *Arum* (Linz et al. 2010, Espíndola et al. 2010) was the relatively small number of species we sequenced using ddRAD-seq (*i.e.* 9 out of ca. 35 species; Peter Boyce, pers. comm.). Nonetheless, we were able to produce a phylogeny that is consistent with the aforementioned studies, and confirms the monophyly of *A. maculatum*.

One key species missing from our current dataset is *A. italicum*, which overlaps considerably with *A. maculatum* across its range (Linz et al. 2010). Since these two species are capable of hybridizing, we have carefully selected *A. maculatum* individuals to limit the possibility of sampling hybrids, following the descriptions of hybrid VOCs and morphology given in Chartier et al. (2016). Since none of our *A. maculatum* samples were placed near *A. concinnatum* – the sister species to *A. italicum* – in our phylogeny, it would appear that we did not unintentionally sequence any hybrids as part of this study. However, high-throughput sequencing data would be useful for accessing the extent of hybridization between these two species in the wild, and investigating whether hybridization may have played a role in establishing both of their wide geographic ranges (Moore et al. 2021)

Finally, while our phylogenetic PCA results yielded the expected results (*i.e.* relatively low phylogenetic signal), our dataset contained many more *A. maculatum* individuals than other species. Therefore, as more species are added, we might expect the number of *A. maculatum* VOCs displaying global phylogenetic signal to decrease. In order to partially account for this issue, we made use of multiple methods (*e.g.* multivariate Bloomberg's K, pPCA, Abouheif's C_{mean}, and Pagel's λ) to identify compounds of interest, and ensured that the methods we used were compatible with the sample sizes of our phylogenetic trees (Münkemüller et al. 2012). Pairing our results with a phylogenetically aligned component analysis (PACA; Collyer and Adams 2021) to distinguish between weak phylogenetic signal and strong phylogenetic signal may be another approach to account for our relatively unbalanced sampling. As in all pPCA analyses, we also only considered two axes of variation; this may yield an incomplete or biased sample of the true multivariate pattern (Uyeda et al. 2015). Phylogenetic comparative methods which are truly multivariate would address some of these problems (Adams and Collyer 2017), but additional research is still needed to develop these tools (Collyer et al. 2022).

Conclusion

This study demonstrates that phylogenomic and population genomic analyses of non-model flowering plants with a mix of ploidies is possible, as long as SNP identification is carried out in a ploidy-aware manner and downstream analyses are compatible with heterozygous and/or polyploid datasets. Even though relatively few species across the genus were included in the present study, we were still able to gain insights into phylogenetic constraints on scent variation, and identify VOCs such as indole which appear to differentiate *A. maculatum* subclades, as well as *A. maculatum* from other *Arum* species. Our results also highlight the exceptional diversity of floral scent in *A. maculatum*, which may have both been influenced by and contributed to its comparatively large Europe-wide geographic range. The relatively weak phylogenetic signal we identified at both the within- and among-species scale also supports the importance of pollinator-mediated selection in the genus. Taken together, these results provide useful context for understanding the evolution of *Arum* floral scent: a key trait underlying deceptive plant-pollinator interactions across the genus.

ACKNOWLEDGEMENTS

Our floral VOC sampling across the genus *Arum* was supported by Jonathan Kendon, Geoffrey Kite, and Kit Strange at the Royal Botanical Gardens, Kew, David Scherberich at the Jardin Botanique de Lyon, and Blaise Mulhauser at the Jardin Botanique de Neuchâtel; we thank them all for providing us with access to their collections and assisting with sampling. We also thank Gregory Roeder for his assistance with the processing of our VOC samples.

FUNDING STATEMENT

This research was funded by the Swiss National Science Foundation through grant P1NEP3_191659 awarded to MAS and grant 31003A_163334 awarded to NA and SR**.**

COMPETING INTERESTS

The authors declare no competing interests.

AUTHORS' CONTRIBUTIONS

M.A.S., M.G., S.R., and N.A. designed the experiments. M.A.S. and A.L.G. conducted the sampling. J.B. and M.A.S. performed the ddRAD-seq library preparation. A.L.G and M.G. analysed the floral scent collections. M.A.S. designed and performed the bioinformatic and statistical analyses. M.A.S. wrote the manuscript. All co-authors contributed to the revision of the manuscript, and have approved it for publication.

REFERENCES

Adams, D. C. 2014. A Generalized K Statistic for Estimating Phylogenetic Signal from Shape and Other High-Dimensional Multivariate Data. Systematic Biology 63:685–697.

Adams, D., and M. Collyer. 2017. Multivariate Phylogenetic Comparative Methods: Evaluations, Comparisons, and Recommendations. Systematic biology 67.

Andrews, S. 2010. FastQC: a quality control tool for high throughput sequence data.

Beaumont, M. A., W. Zhang, and D. J. Balding. 2002. Approximate Bayesian computation in population genetics. Genetics 162:2025–2035.

Boyce, P. 1993. The genus *Arum*. Royal Botanic Gardens Kew.

Boyce, P. C. 2006. *Arum* - A decade of change. Aroideana 29:132–137.

Bröderbauer, D., A. Weber, and A. Diaz. 2013. The design of trapping devices in pollination traps of the genus *Arum* (Araceae) is related to insect type. Botanical journal of the Linnean Society. Linnean Society of London 172:385–397.

Chafin, T. K., B. Regmi, M. R. Douglas, D. R. Edds, K. Wangchuk, S. Dorji, P. Norbu, S. Norbu, C. Changlu, and G. P. Khanal. 2021. Parallel introgression, not recurrent emergence, explains apparent elevational ecotypes of polyploid Himalayan snowtrout. Royal Society open science 8:210727.

Chartier, M., S. Liagre, H. Weiss-Schneeweiss, B. Kolano, J.-M. Bessière, J. Schönenberger, and M. Gibernau. 2016. Floral traits and pollination ecology of European *Arum* hybrids. Oecologia 180:439–451.

Chartier, M., L. Pélozuelo, B. Buatois, J.-M. Bessière, and M. Gibernau. 2013. Geographical variations of odour and pollinators, and test for local adaptation by reciprocal transplant of two European *Arum* species. Functional Ecology 27:1367–1381.

Chartier, M., L. Pélozuelo, and M. Gibernau. 2011. Do floral odor profiles geographically vary with the degree of specificity for pollinators? Investigation in two sapromyophilous *Arum* species (Araceae). Annales de la Société entomologique de France 47:71–77.

Clark, L. V, A. E. Lipka, and E. J. Sacks. 2019. polyRAD: Genotype Calling with Uncertainty from Sequencing Data in Polyploids and Diploids. G3 Genes|Genomes|Genetics 9:663–673.

Clark, L. V, W. Mays, A. E. Lipka, and E. J. Sacks. 2022. A population-level statistic for assessing Mendelian behavior of genotyping-by-sequencing data from highly duplicated genomes. BMC Bioinformatics 23:101.

Collyer, M. L., and D. C. Adams. 2021. Phylogenetically aligned component analysis. Methods in Ecology and Evolution 12:359–372.

Collyer, M. L., E. K. Baken, and D. C. Adams. 2022. A standardized effect size for evaluating and comparing the strength of phylogenetic signal. Methods in Ecology and Evolution 13:367–382.

Csilléry, K., O. François, and M. G. B. Blum. 2012. abc: an R package for approximate Bayesian computation (ABC). Methods in Ecology and Evolution 3:475–479.

Dafni, A. 1984. Mimicry and Deception in Pollination. Annual Review of Ecology and Systematics 15:259–278.

Darwin, C. 1862. On the various contrivances by which British and foreign orchids are fertilised by insects, and on the good effects of intercrossing. First edition. John Murray, London.

Diaz, A., and G. Kite. 2002. A comparison of the pollination ecology of *Arum maculatum* and *A. italicum* in England. Watsonia 24:171–182.

Earl, D. A., and B. M. vonHoldt. 2012. STRUCTURE HARVESTER: A website and program for visualizing STRUCTURE output and implementing the Evanno method. Conservation Genetics Resources 4:359–361.

Eaton, D. A. R., and I. Overcast. 2020. ipyrad: Interactive assembly and analysis of RADseq datasets. Bioinformatics 36:2592–2594.

Espíndola, A., and N. Alvarez. 2011. Comparative Phylogeography in a Specific and Obligate Pollination Antagonism. PLOS ONE 6:e28662.

Espíndola, A., S. Buerki, M. Bedalov, P. Küpfer, and N. Alvarez. 2010. New insights into the phylogenetics and biogeography of *Arum* (Araceae): unravelling its evolutionary history. Botanical Journal of the Linnean Society 163:14–32.

Espíndola, A., L. Pellissier, and N. Alvarez. 2011. Variation in the proportion of flower visitors of *Arum maculatum* along its distributional range in relation with community-based climatic niche analyses. Oikos 120:728–734.

Evanno, G., S. Regnaut, and J. Goudet. 2005. Detecting the number of clusters of individuals using the software structure: a simulation study. Molecular Ecology 14:2611–2620.

Farré-Armengol, G., I. Filella, J. Llusià, Ü. Niinemets, and J. Peñuelas. 2014. Changes in floral bouquets from compound-specific responses to increasing temperatures. Global Change Biology 20:3660–3669.

Felsenstein, J. 1985. Phylogenies and the comparative method. The American Naturalist 125:1–15.

Friberg, M., C. Schwind, P. R. Guimarães, R. A. Raguso, and J. N. Thompson. 2019. Extreme diversification of floral volatiles within and among species of *Lithophragma* (Saxifragaceae). Proceedings of the National Academy of Sciences 116:4406–4415.

Gervasi, D. D. L., and F. P. Schiestl. 2017. Real-time divergent evolution in plants driven by pollinators. Nature Communications 8:14691.

Gfrerer, E., D. Laina, M. Gibernau, R. Fuchs, M. Happ, T. Tolasch, W. Trutschnig, A. C. Hörger, H. P. Comes, and S. Dötterl. 2021. Floral Scents of a Deceptive Plant Are Hyperdiverse and Under Population-Specific Phenotypic Selection. Frontiers in Plant Science 12:719092.

Gfrerer, E., D. Laina, R. Wagner, M. Gibernau, A. C. Hörger, H. P. Comes, and S. Dötterl. 2022. Antennae of psychodid and sphaerocerid flies respond to a high variety of floral scent compounds of deceptive Arum maculatum L. Scientific Reports 12:5086.

Gibernau, M. 2003. Pollinators and visitors of aroid inflorescences. Aroideana 26:73–91.

Gibernau, M. 2004. Pollination in the genus Arum – a review. Aroideana 27:148–166.

Gibernau, M. 2011. Pollinators and visitors of aroid inflorescences: an addendum. Aroideana 34:70–83.

Gibernau, M. 2016. Pollinators and visitors of aroid inflorescences III-Phylogenetic & Chemical insights. Aroideana 39:4–22.

Glenny, W. R., J. B. Runyon, and L. A. Burkle. 2018. Drought and increased CO(2) alter floral visual and olfactory traits with context-dependent effects on pollinator visitation. The New phytologist 220:785–798.

Harder, L. D., and S. D. Johnson. 2009. Darwin's beautiful contrivances: evolutionary and functional evidence for floral adaptation. New Phytologist 183:530–545.

Hernández-Hernández, T., and J. J. Wiens. 2020. Why Are There So Many Flowering Plants? A Multiscale Analysis of Plant Diversification. The American Naturalist 195:948–963.

Hervé, M. R., F. Nicolè, and K.-A. Lê Cao. 2018. Multivariate Analysis of Multiple Datasets: a Practical Guide for Chemical Ecology. Journal of Chemical Ecology 44:215–234.

Hewitt, G. M. 1999. Post-glacial re-colonization of European biota. Biological Journal of the Linnean Society 68:87–112.

Jakobsson, M., and N. A. Rosenberg. 2007. CLUMPP: a cluster matching and permutation program for dealing with label switching and multimodality in analysis of population structure. Bioinformatics 23:1801–1806.

Jersáková, J., S. D. Johnson, and P. Kindlmann. 2006. Mechanisms and evolution of deceptive pollination in orchids. Biological Reviews 81:219–235.

Jombart, T., and S. Dray. 2010. Adephylo: exploratory analyses for the phylogenetic comparative method. Bioinformatics 26:1–21.

Jombart, T., S. Pavoine, S. Devillard, and D. Pontier. 2010. Putting phylogeny into the analysis of biological traits: A methodological approach. Journal of Theoretical Biology 264:693–701.

Junker, R. R., and A. L. Parachnowitsch. 2015. Working towards a holistic view on flower traits - how floral scents mediate plant-animal interactions in concert with other floral characters. Journal of the Indian Institute of Science 95:43–67.

Kite, G. C. 1995. The floral odour of *Arum maculatum*. Biochemical Systematics and Ecology 23:343–354.

Kite, G. C., W. L. A. Hetterscheid, M. J. Lewis, P. C. Boyce, J. Ollerton, E. Cocklin, and A. Diaz. 1998. Inflorescence odours and pollinators of *Arum* and *Amorphophallus* (Araceae). Pages 295–315 *in* S. J. Owens and P. J. Rudall, editors. Reproductive Biology. Royal Botanic Gardens Kew, London, UK.

Kozlov, A. M., D. Darriba, T. Flouri, B. Morel, and A. Stamatakis. 2019. RAxML-NG: a fast, scalable and user-friendly tool for maximum likelihood phylogenetic inference. Bioinformatics 35:4453–4455.

Laina, D., E. Gfrerer, V. Scheurecker, R. Fuchs, M. Schleifer, C. Zittra, R. Wagner, M. Gibernau, H. P. Comes, A. C. Hörger, and S. Dötterl. 2022. Local Insect Availability Partly Explains Geographical Differences in Floral Visitor Assemblages of *Arum maculatum* L. (Araceae).

Lamarck, M. M. 1783. Encyclopédie méthodique – Botanique. Tome 3. Panckoucke, Paris.

Lee, J.-H., T. K. Wood, and J. Lee. 2015. Roles of Indole as an Interspecies and Interkingdom Signaling Molecule. Trends in Microbiology 23:707–718.

Letunic, I., and P. Bork. 2021. Interactive Tree Of Life (iTOL) v5: an online tool for phylogenetic tree display and annotation. Nucleic Acids Research 49:W293–W296.

Levin, R. A., L. A. McDade, and R. A. Raguso. 2003. The Systematic Utility of Floral and Vegetative Fragrance in Two Genera of Nyctaginaceae. Systematic Biology 52:334–351.

Linz, J., J. Stökl, I. Urru, T. Krügel, M. C. Stensmyr, and B. S. Hansson. 2010. Molecular phylogeny of the genus *Arum* (Araceae) inferred from multi–locus sequence data and AFLPs. Taxon 59:405–415.

Majetic, C. J., R. A. Raguso, and T.-L. Ashman. 2009. Sources of floral scent variation: can environment define floral scent phenotype? Plant signaling & behavior 4:129–131.

Marotz-Clausen, G., S. Jürschik, R. Fuchs, I. Schäffler, P. Sulzer, M. Gibernau, and S. Dötterl. 2018. Incomplete synchrony of inflorescence scent and temperature patterns in *Arum maculatum* L. (Araceae). Phytochemistry 154:77–84.

Martin, M. 2011. Cutadapt removes adapter sequences from high-throughput sequencing reads. EMBnet.journal; Vol 17, No 1: Next Generation Sequencing Data Analysis.

Mastretta-Yanes, A., N. Arrigo, N. Alvarez, T. H. Jorgensen, D. Piñero, and B. C. Emerson. 2015. Restriction site-associated DNA sequencing, genotyping error estimation and de novo assembly optimization for population genetic inference. Molecular Ecology Resources 15:28–41.

Meirmans, P. G., S. Liu, and P. H. van Tienderen. 2018. The Analysis of Polyploid Genetic Data. Journal of Heredity 109:283–296.

Milet-Pinheiro, P., P. S. Santos, S. Prieto-Benítez, M. Ayasse, and S. Dötterl. 2021. Differential Evolutionary History in Visual and Olfactory Floral Cues of the Bee-Pollinated Genus *Campanula* (Campanulaceae). Plants 10(7): 1356.

Moore, A. J., J. A. Messick, and J. W. Kadereit. 2021. Range and niche expansion through multiple interspecific hybridization: a genotyping by sequencing analysis of *Cherleria* (Caryophyllaceae). BMC Ecology and Evolution 21:40.

Mulla, M. S., Y.-S. Hwang, and H. Axelrod. 1977. Attractants for Synanthropic Flies: Chemical Attractants for Domestic Flies. Journal of Economic Entomology 70:644–648.

Münkemüller, T., S. Lavergne, B. Bzeznik, S. Dray, T. Jombart, K. Schiffers, and W. Thuiller. 2012. How to measure and test phylogenetic signal. Methods in Ecology and Evolution 3:743–756.

Mussi, M. 1990. Continuity and change in Italy at the Last Glacial Maximum. Pages 126–147 *in* O. Soffer and C. Gamble, editors. The world at 18000 BP. Unwin Hyman, London.

Van der Niet, T., and S. D. Johnson. 2012. Phylogenetic evidence for pollinator-driven diversification of angiosperms. Trends in Ecology & Evolution 27:353–361.

Van der Niet, T., R. Peakall, and S. D. Johnson. 2014. Pollinator-driven ecological speciation in plants: new evidence and future perspectives. Annals of botany 113:199–211.

Nosil, P. 2012. Ecological speciation. Oxford University Press.

Onda, Y., K. Mochida, T. Yoshida, T. Sakurai, R. S. Seymour, Y. Umekawa, S. A. Pirintsos, K. Shinozaki, and K. Ito. 2015. Transcriptome analysis of thermogenic *Arum concinnatum* reveals the molecular components of floral scent production. Scientific Reports 5:8753.

Peterson, B. K., J. N. Weber, E. H. Kay, H. S. Fisher, and H. E. Hoekstra. 2012. Double Digest RADseq: An Inexpensive Method for De Novo SNP Discovery and Genotyping in Model and Non-Model Species. PLOS ONE 7:e37135.

Prieto-Benítez, S., A. M. Millanes, S. Dötterl, and L. Giménez-Benavides. 2016. Comparative analyses of flower scent in Sileneae reveal a contrasting phylogenetic signal between night and day emissions. Ecology and Evolution 6:7869–7881.

Pritchard, J. K., M. Stephens, and P. Donnelly. 2000. Inference of population structure using multilocus genotype data. Genetics 155:945–959.

R Core Team. 2021. R: A Language and Environment for Statistical Computing. Vienna, Austria.

Ramos, S. E., and F. P. Schiestl. 2019. Rapid plant evolution driven by the interaction of pollination and herbivory. Science 364:193–196.

Ramsey, J., H. D. J. Bradshaw, and D. W. Schemske. 2003. Components of reproductive isolation between the monkeyflowers *Mimulus lewisii* and *M. cardinalis* (Phrymaceae). Evolution 57:1520–1534.

Renner, S. S. 2006. Rewardless flowers in the angiosperms and the role of insect cognition in their evolution. Pages 123–144 *in* N. M. Waser and J. Ollerton, editors. Plant-pollinator interactions: from specialization to generalization. University of Chicago Press, Chicago.

Revell, L. J. 2009. Size-correction and principal components for interspecific comparative studies. Evolution 63:3258–3268.

Rundle, H. D., and P. Nosil. 2005. Ecological speciation. Ecology letters 8:336–352.

Schiestl, F. P. 2010. The evolution of floral scent and insect chemical communication. Ecology Letters 13:643–656.

Schiestl, F. P., and S. Dötterl. 2012. The evolution of floral scent and olfactory preferences in pollinators: coevolution or pre-existing bias? Evolution; international journal of organic evolution 66:2042–2055.

Schiestl, F. P., and S. D. Johnson. 2013. Pollinator-mediated evolution of floral signals. Trends in Ecology and Evolution 28:307–315.

Schluter, D. 2001. Ecology and the origin of species. Trends in ecology & evolution 16:372–380.

Schmucker, T. 1925. Beiträge zur Biologie und Physiologie von *Arum maculatum*. Flora oder Allgemeine Botanische Zeitung:460–475.

Schubert, M., S. Lindgreen, and L. Orlando. 2016. AdapterRemoval v2: rapid adapter trimming, identification, and read merging. BMC Research Notes 9:88.

Seguinot, J., S. Ivy-Ochs, G. Jouvet, M. Huss, M. Funk, and F. Preusser. 2018. Modelling last glacial cycle ice dynamics in the Alps. The Cryosphere 12:3265–3285.

Simpson, G. G. 1953. The major features of evolution. Columbia University Press, New York.

Sprengel, C. K. 1793. Das entdeckte Geheimnis der Natur im Bau und in der Befruchtung der Blumen. Wilhelm Engelmann.

Stift, M., F. Kolář, and P. G. Meirmans. 2019. Structure is more robust than other clustering methods in simulated mixed-ploidy populations. Heredity 123:429–441.

Stökl, J., A. Strutz, A. Dafni, A. Svatos, J. Doubsky, M. Knaden, S. Sachse, B. S. Hansson, and M. C. Stensmyr. 2010. A Deceptive Pollination System Targeting Drosophilids through Olfactory Mimicry of Yeast. Current Biology 20:1846–1852.

Strauss, S. Y., and J. B. Whittall. 2006. Non-pollinator agents of selection on floral traits. Page (L. D. Harder and S. C. H. Barrett, Eds.) Ecology and evolution of flowers. Oxford University Press, Oxford, UK.

Szenteczki, M. A., A. L. Godschalx, A. Galmán, A. Espíndola, M. Gibernau, N. Alvarez, and S. Rasmann. 2021. Spatial and temporal heterogeneity in pollinator communities maintains within-species floral odour variation. Oikos 130:1487–1499.

Szenteczki, M. A., A. L. Godschalx, J. Gauthier, M. Gibernau, S. Rasmann, and N. Alvarez. 2022. Transcriptomic analysis of deceptively pollinated *Arum maculatum* (Araceae) reveals association between terpene synthase expression in floral trap chamber and species-specific pollinator attraction. G3 Genes|Genomes|Genetics 12:jkac175.

Theophrastus. 350BC. The enquiry into plants (Historia Plantarum) Volume II. W. Heinemann, London, UK.

Tomberlin, J. K., T. L. Crippen, G. Wu, A. S. Griffin, T. K. Wood, and R. M. Kilner. 2017. Indole: An evolutionarily conserved influencer of behavior across kingdoms. BioEssays 39:1600203.

Urru, I., J. Stökl, J. Linz, T. Krügel, M. C. Stensmyr, and B. S. Hansson. 2010. Pollination strategies in Cretan *Arum* lilies. Biological Journal of the Linnean Society 101:991–1001.

Uyeda, J. C., D. S. Caetano, and M. W. Pennell. 2015. Comparative Analysis of Principal Components Can be Misleading. Systematic Biology 64:677–689.

Vogel, S. 1965. Kesselfallen–Blumen. Umschau 65:12–17.

Whittall, J. B., and S. A. Hodges. 2007. Pollinator shifts drive increasingly long nectar spurs in columbine flowers. Nature 447:706–709.

Yu, Y., C. Blair, and X. He. 2020. RASP 4: Ancestral State Reconstruction Tool for Multiple Genes and Characters. Molecular Biology and Evolution 37:604–606.

Yu, Y., A. J. Harris, C. Blair, and X. He. 2015. RASP (Reconstruct Ancestral State in Phylogenies): A tool for historical biogeography. Molecular Phylogenetics and Evolution 87:46–49.

Zu, P., W. U. Blanckenhorn, and F. P. Schiestl. 2016. Heritability of floral volatiles and pleiotropic responses to artificial selection in *Brassica rapa*. New Phytologist 209:1208–1219.

FIGURES

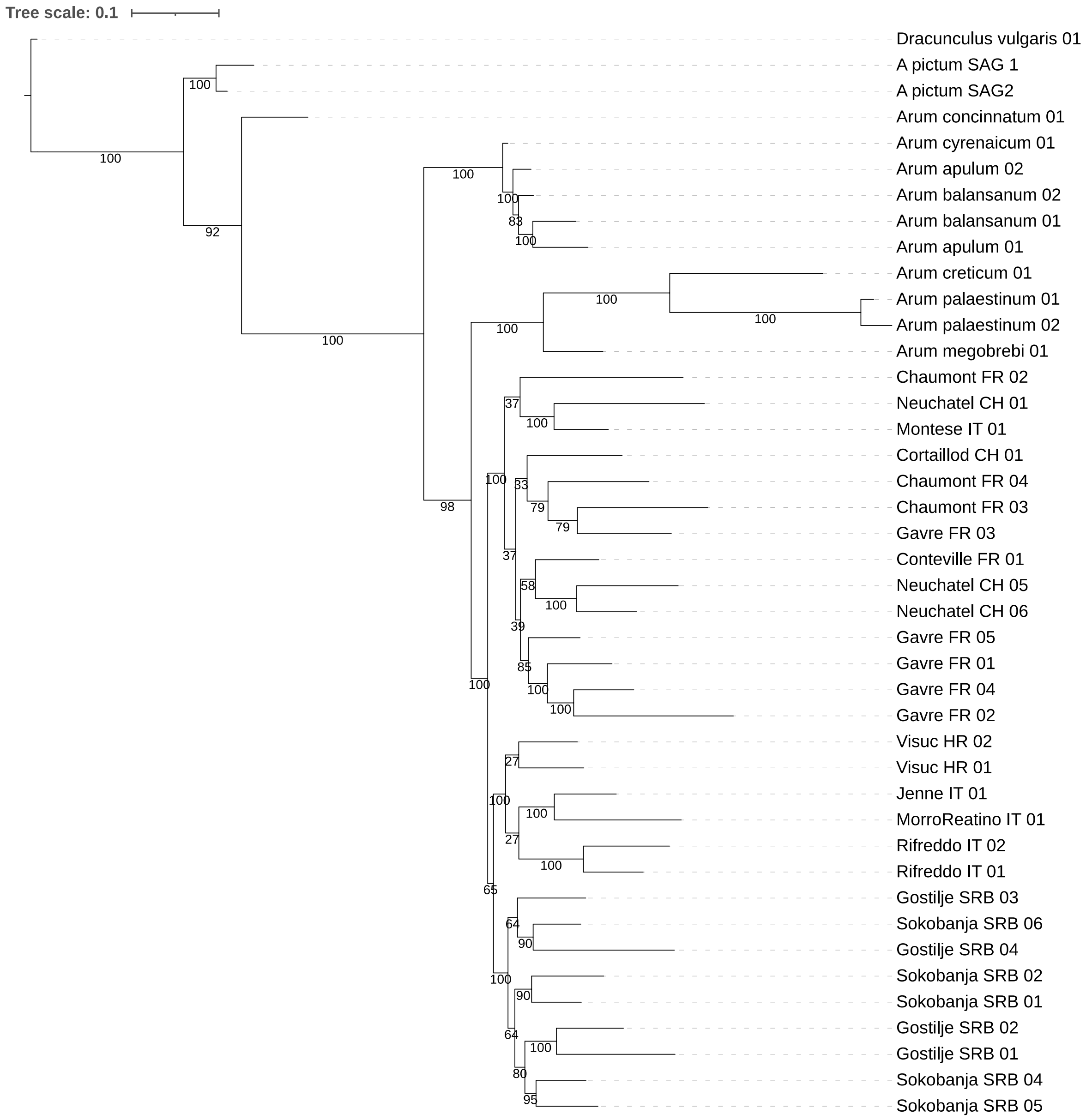

Figure 1. Phylogenetic relationships in the genus *Arum* constructed from 13’320 ddRAD-seq SNPs. Topology and branch lengths were calculated using maximum likelihood inference in RAxML-NG; node supports were calculated from 200 bootstrap trees.

Note: All taxa with no species name given are *Arum maculatum*; instead, the population where each *A. maculatum* individual was sampled is indicated above.

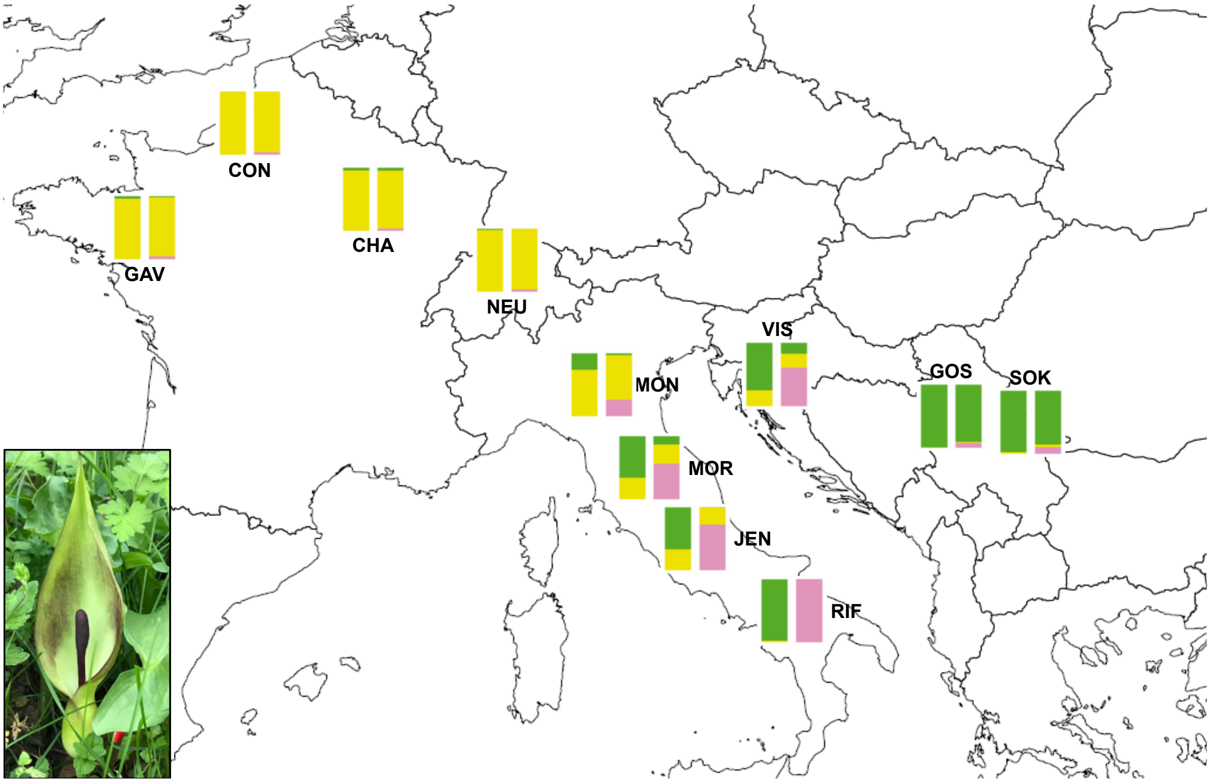

Figure 2. Barplots illustrating STRUCTURE admixture coefficients (*i.e.* the probability of belonging to one of *K* unique genetic clusters) for *Arum maculatum* populations across Europe. Left and right barplots respectively visualize *K*=2 and *K*=3 results over the approximate locations of each population. Population averages, calculated in CLUMPP across 10 replicate STRUCTURE runs per *K*, are shown above. Individual-level STRUCTURE results are shown in Figures 3 and S1. Inset photo: *A. maculatum* inflorescence.

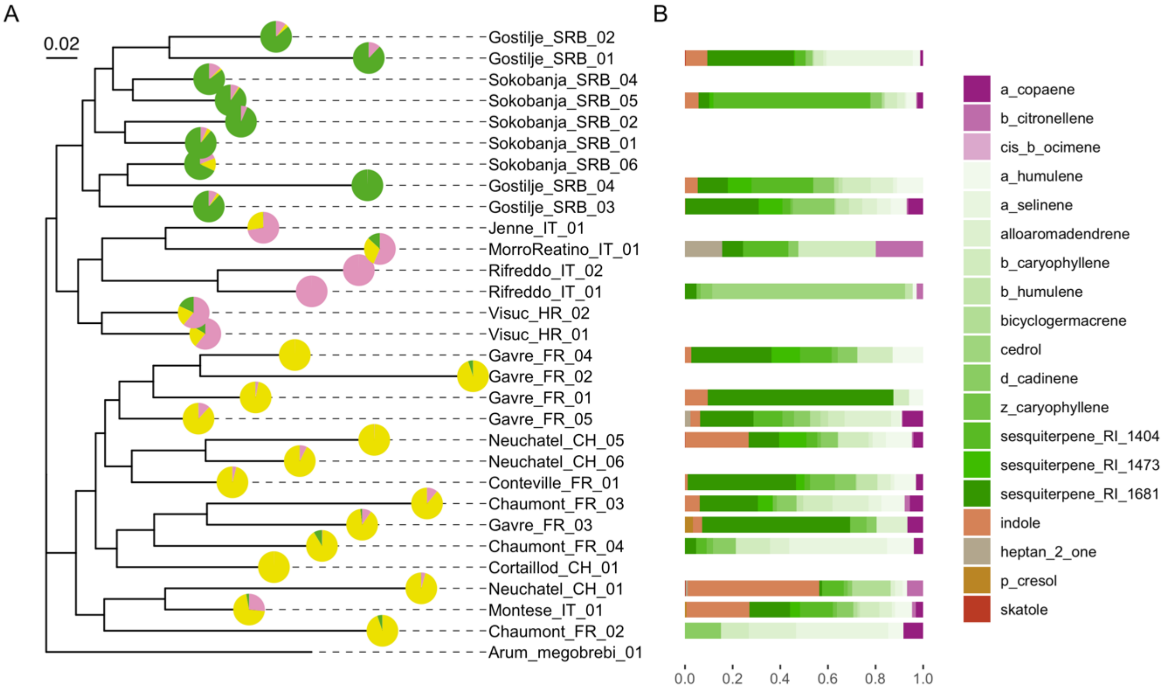

Figure 3. (A) Maximum likelihood inference tree (described in Figure 1) for *Arum maculatum*; STRUCTURE results for each individual at *K*=3, represented as pie charts, have been added to their corresponding branches. (B) Bar charts representing the relative quantities of monoterpene (purple), sesquiterpene (green) and putative dung-mimicking VOCs (earth tones) emitted by individual inflorescences.

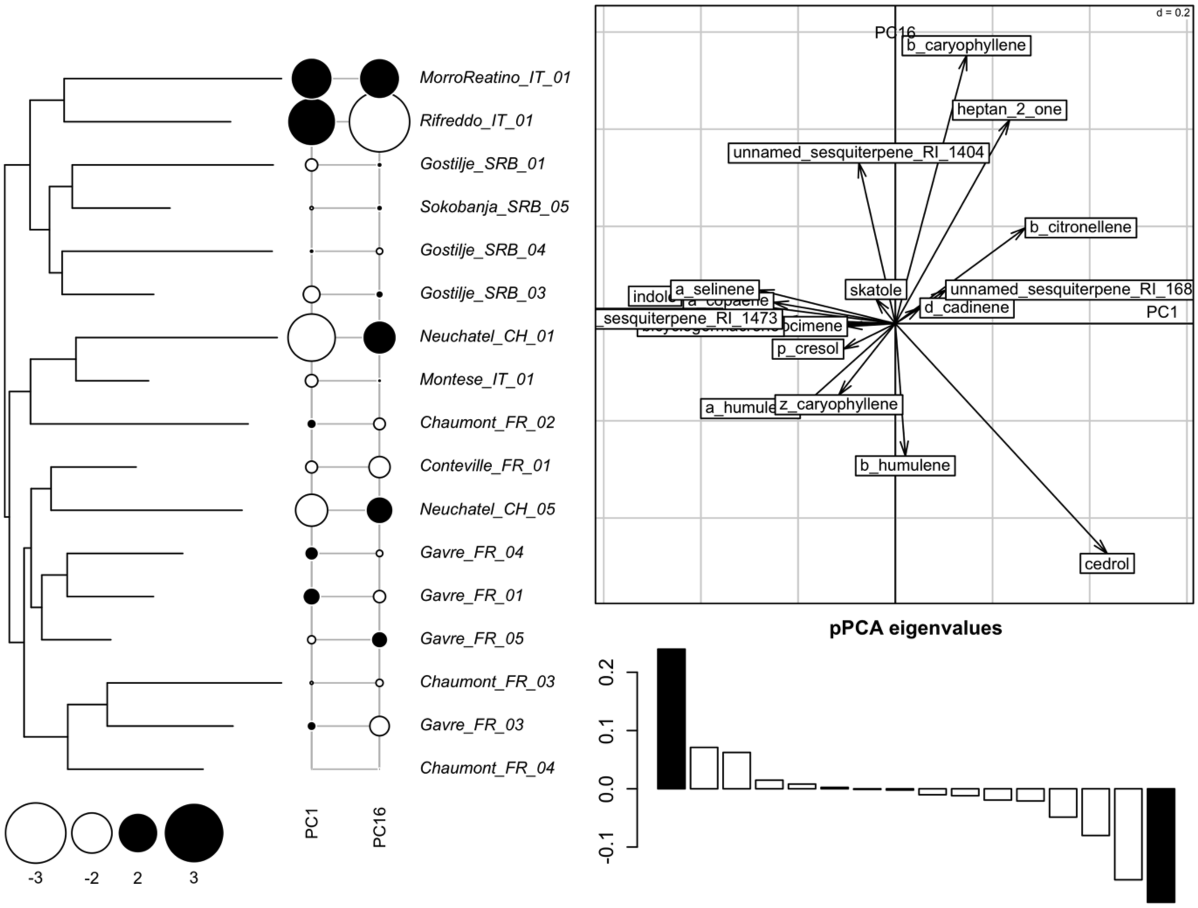

Figure 4. Phylogenetic PCA results for *Arum maculatum* alone. Left**:** maximum likelihood inference tree (described in Figure 1); patterns of global (PC1) and local (PC16) phylogenetic structuring are highlighted on the dot chart. Right: loadings for all volatile compounds on PC1 and PC16, indicating compounds which contributed the most to global and local structures, respectively.

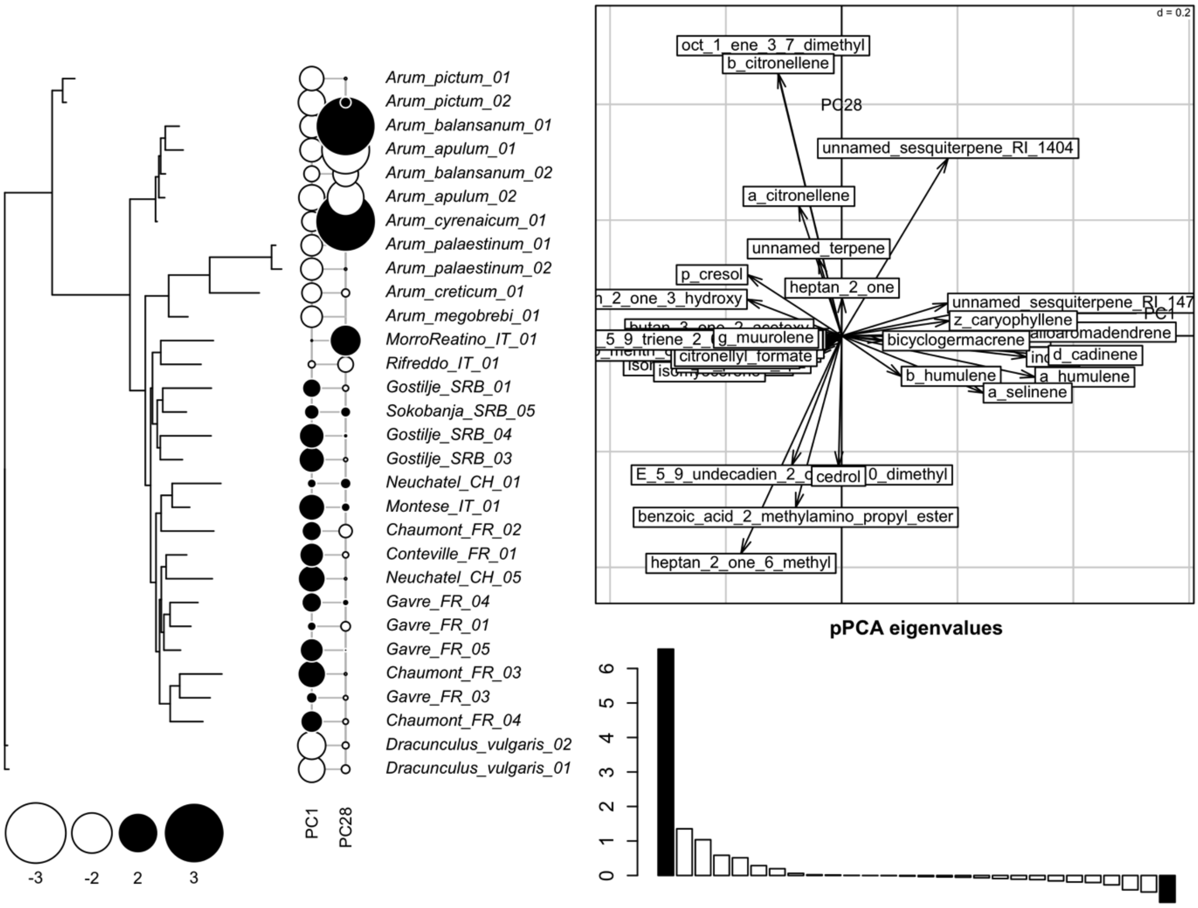

Figure 5. Phylogenetic PCA results for the genus *Arum*. Left: maximum likelihood inference tree (described in Figure 1); patterns of global (PC1) and local (PC16) phylogenetic structuring are highlighted on the dot chart. Right: loadings for all volatile compounds on PC1 and PC16, indicating compounds which contributed the most to global and local structures, respectively.

Note: All taxa with no species name given are *Arum maculatum*; instead, the population where each individual was sampled is indicated above.

<u>TABLES</u>

Table 1. *Arum maculatum* floral VOCs with the greatest indications of phylogenetic signal (*i.e.* top and bottom 5% of loadings on pPCA PC1). Following phylogenetic autocorrelation tests (Abouheif's C_{mean}), a significant correlation was only observed for indole.

Compound	**Obs**	**Std.Obs**	***p* value**
indole	0.23576602	2.2327654	0.048
cedrol	-0.06311524	-0.4084823	0.504

Table 2. Floral VOCs across the genus *Arum* with the greatest indications of phylogenetic signal (*i.e.* top and bottom 5% of loadings on pPCA PC1). Following phylogenetic autocorrelation tests (Abouheif's C_{mean}), a significant correlation was observed for unnamed sesquiterpene (Kovats RI 1404).

Compound	**Obs**	**Std.Obs**	***p* value**
3-hydroxy 2-butanone	0.19212376	2.33149433	0.057
6-methyl 2-heptanone	0.11237433	1.43310325	0.103
benzyl alcohol	-0.0346071	-0.0820108	0.291
p-cresol	-0.0475328	-0.3352295	0.464
indole	0.04957567	0.67024104	0.225
unk. sesquiterpene (RI 1404)	0.2555952	3.05230478	0.011
β-caryophyllene	0.12332618	1.38399436	0.104
α-selinene	0.06190385	0.91830806	0.131

SUPPLEMENTARY FIGURES AND TABLES

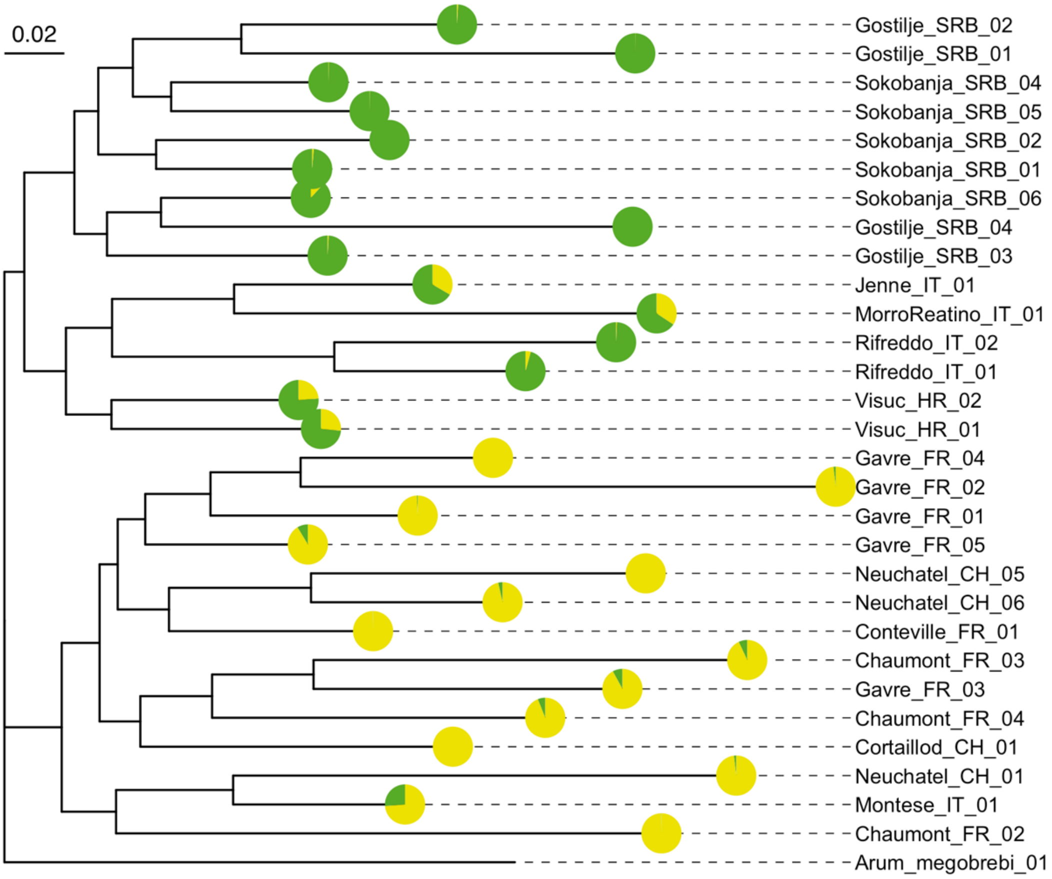

Figure S1. Maximum likelihood inference tree (described in Figure 1) for *Arum maculatum*. STRUCTURE results for each individual at K=2, represented as pie charts, have been added to their corresponding branches.

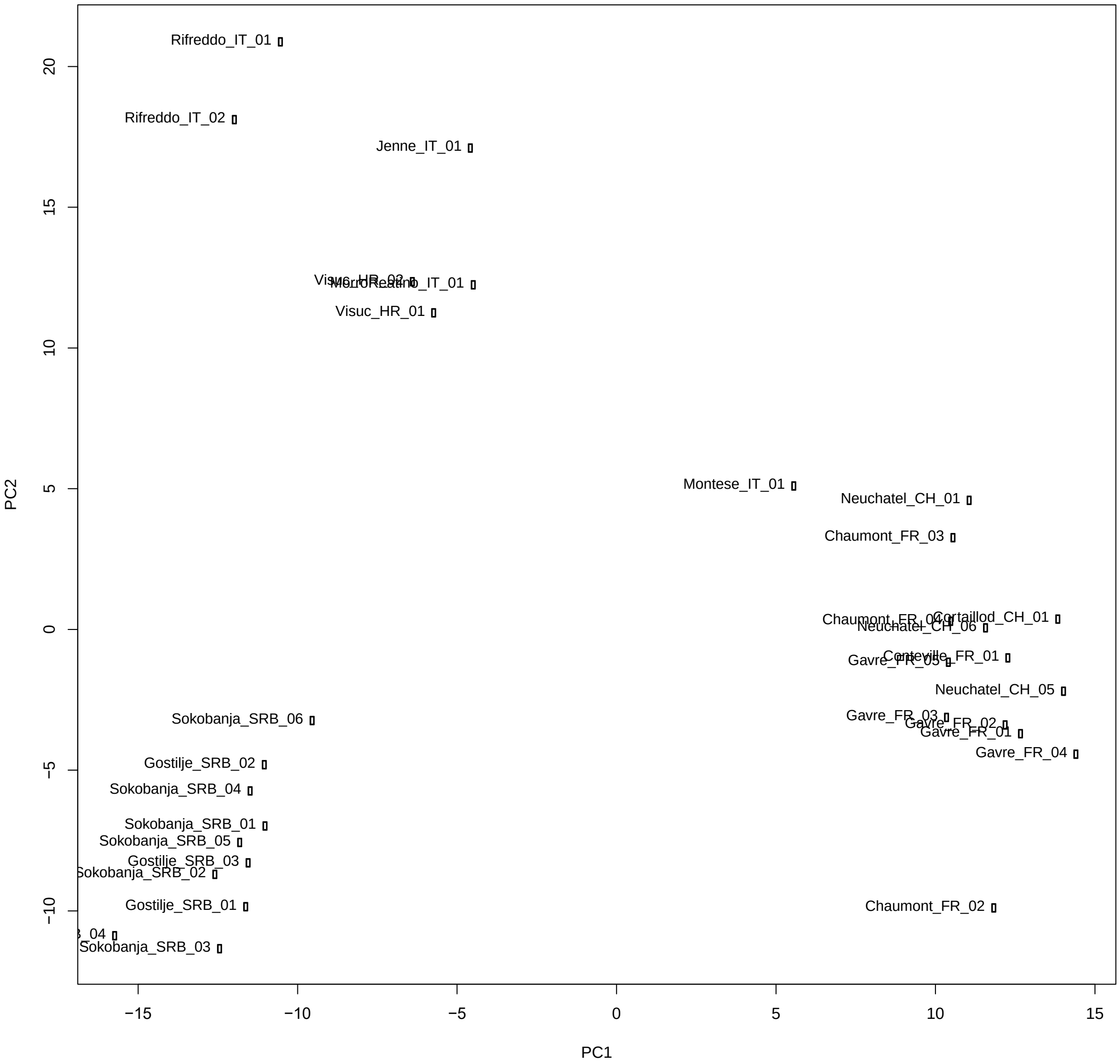

Figure S2. Probabilistic PCA result generated from all *Arum maculatum* SNPs called by polyRAD. Loci which were not statistically consistent with tetraploid expectations (*i.e.* $H_{ind}/H_E > 0.75$) and/or had a minor allele frequency below 5% were removed prior to analysis.

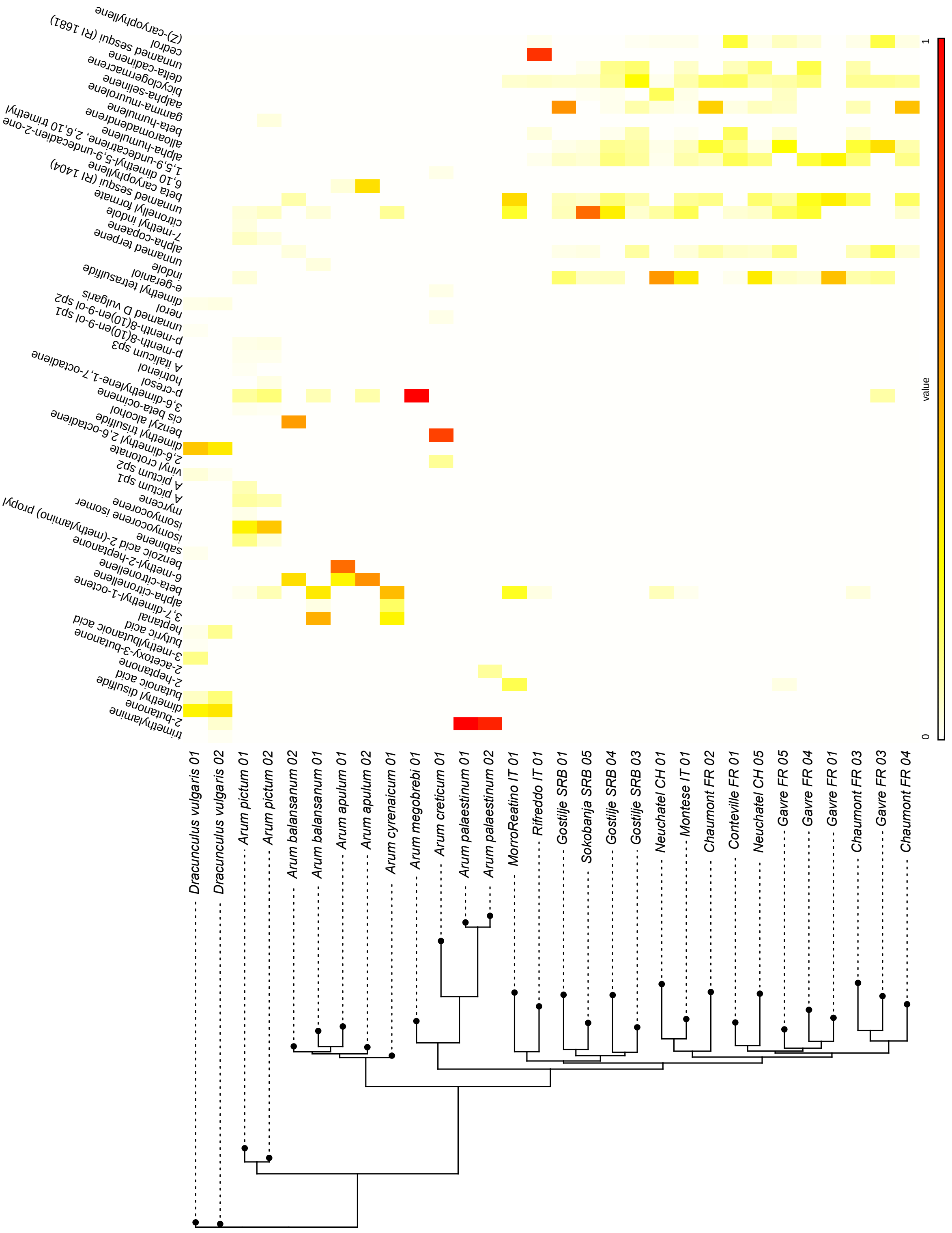

Figure S3. Heatmap visualizing proportional VOC emissions of all *Arum* spp. sampled in this study (*n* = 54 VOCs, which appear in an individual bouquet at least once above 1%). 19 compounds were identified in *A. maculatum* (i.e. leaves on the phylogeny with population names given instead of species names).

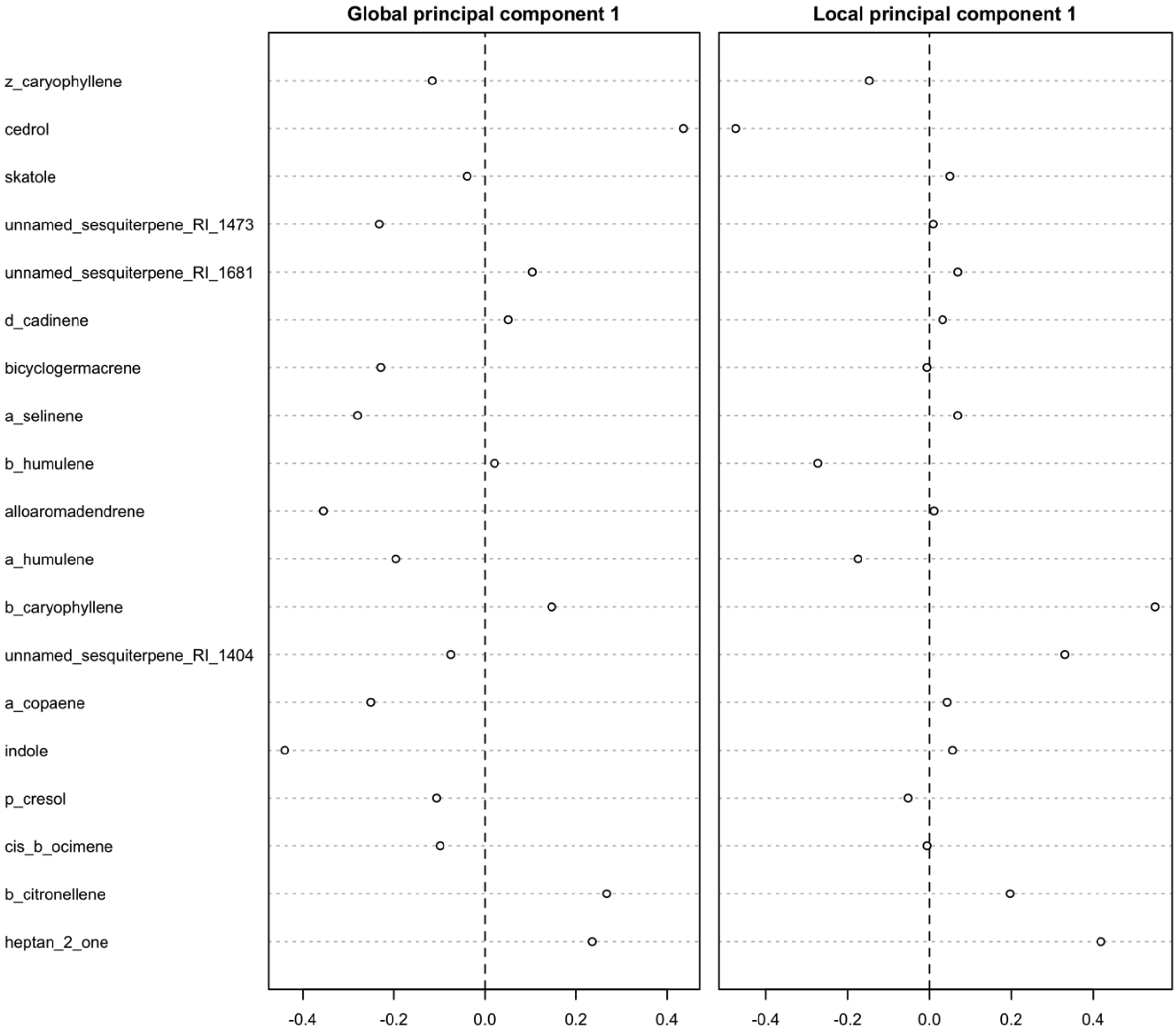

Figure S4. Phylogenetic PCA (pPCA) loadings on the first and last axes, which respectively correspond to global and local phylogenetic signal in our analysis of *Arum maculatum* floral scent (see Figure 4).

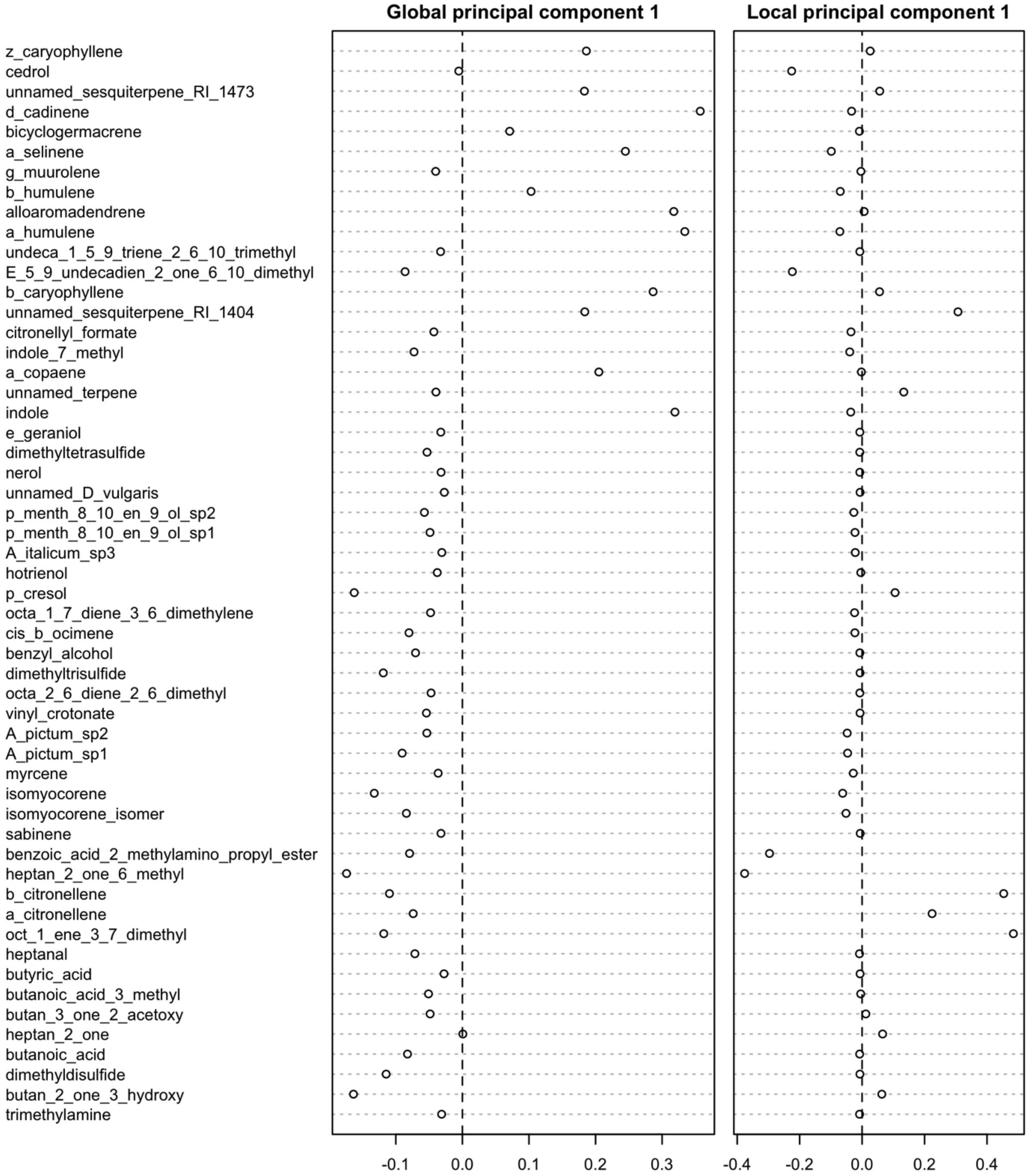

Figure S5. Phylogenetic PCA (pPCA) loadings on the first and last axes, which respectively correspond to global and local phylogenetic signal in our analysis floral scents across the genus *Arum* (see Figure 5).

Table S1. Summary of *Arum* tissue samples collected for this study, and the number of ddRAD-seq reads generated for each sample.

Sample ID	Source	# reads (clean)	est. heterozyg.	# loci ipyrad
Dracunculus_vulgaris_01	J. Bot. Neuch.	1 694 429	0.0072	4770
Dracunculus_vulgaris_02	J. Bot. Neuch.	1 640 455	0.0079	4161
A_pictum_SAG_1	Marc Gibernau	3 321 651	0.0070	6872
A_pictum_SAG_2	Marc Gibernau	2 883 578	0.0049	4060
Arum_apulum_01	RBG Kew	2 405 549	0.0101	4610
Arum_apulum_02	RBG Kew	1 514 887	0.0145	16 988
Arum_balansanum_01	RBG Kew	1 562 768	0.0082	7453
Arum_balansanum_02	RBG Kew	1 515 716	0.0141	16 321
Arum_concinnatum_01	RBG Kew	3 026 037	0.0168	25 845
Arum_creticum_01	RBG Kew	1 555 199	0.0071	9648
Arum_cyrenaicum_01	RBG Kew	1 48 1226	0.0183	19 333
Arum_megobrebi_01	J. Bot. Lyon	3 503 941	0.0129	1176
Arum_palaestinum_01	RBG Kew	1 790 180	0.0069	8817
Arum_palaestinum_02	RBG Kew	3 436 902	0.0073	16 715

CHAPTER 5 – Conclusion and perspectives

Arum maculatum pollination biology: a brief synthesis

In *Lords and Ladies*, Prime (1960) concluded that even though *A. maculatum* had long interested botanists, many aspects of its pollination biology remained unknown. Since then, additional studies have continued to advance our understanding of this fascinating deceptive pollination system. Early research focused mainly on aspects of the physical trapping mechanism (Dormer 1960, Jones 1977) and the consumption of *A. maculatum* fruits by blackbirds (Snow and Snow 1988). Then, Lack and Diaz (1991) began the modern era of *A. maculatum* research with their comprehensive study of its pollination ecology in England. Notably, their finding that even a single pollen-carrying *Psychoda phalaenoides* could produce a substantial fruit set highlighted why selection may have favored specialization on Psychodidae, rather than the more general deceptive system utilized by *A. italicum* (Diaz and Kite 2002, Chartier et al. 2011). Ollerton and Diaz (1999) also found evidence supporting stabilizing selection on flowering time. Given the short eight- and twelve-day adult lifespan of *P. phalaenoides* and *P. grisescens* respectively (Satchell 1947), a coordinated bloom would facilitate greater pollen transfer between inflorescences. In parallel with this research, the first GC-MS analyses of *A. maculatum* floral VOCs (Kite 1995) and a follow-up comparative study of several *Arum* and *Amorphophallus* species' VOCs (Kite et al. 1998) identified the chemical constituents of the "urine-" or "dung-like" scent characteristic of *A. maculatum*: indole, *p*-cresol, and 2-heptanone. Kite (1995) also identified bicyclogermacrene emissions in the basal spathe chamber and high sesquiterpene emissions from the appendices of some inflorescences.

In the years that followed, the geographic scale of studies on *A. maculatum* pollination increased. Espíndola et al. (2011) studied *A. maculatum* across nearly its entire distribution range, highlighting geographic variation in pollinators: *Psychoda phalaenoides* were predominantly trapped in northern and western Europe (*e.g.* England, France, Switzerland, Austria, and Germany), while *P. grisescens* were predominantly trapped in southern and eastern Europe (*e.g.* Italy, Croatia, Serbia, and Bulgaria). These patterns coincided with neutral genetic divergence among populations of *A. maculatum*, which could be divided into two spatial genetic clusters in northern and southern Europe (Espíndola and Alvarez 2011). Taken together, these two studies indicated that the regional genetic clusters may be adapted to their local pollinator communities. During this time, phylogenies of the genus *Arum* derived from plastid (Espíndola et al. 2010) and nuclear (Linz et al. 2010) markers were also completed.

Studies on geographic variation in VOCs continued as well. Notably, Chartier and colleagues i) compared the inflorescence odors and pollinators of *A. maculatum* and *A. italicum*

(Chartier et al. 2011), ii) performed a transplant experiment among three populations in France, which found no effect of population origin on VOCs or pollinator attraction patterns (Chartier et al. 2013), and iii) studied the VOC bouquets and morphologies of *A. maculatum* × *A. italicum* hybrids (Chartier et al. 2016). These three studies highlighted high diversity in *A. maculatum* floral scent, between populations which were relatively close to one another. They also indicated that the pollinators trapped by *A. maculatum* were at least partially driven by local insect availability. Over the last few years, several other studies on *A. maculatum* VOCs and pollination ecology have been published (Marotz-Clausen et al. 2018, Gfrerer et al. 2021, 2022, Laina et al. 2022). These studies will be discussed in parallel with our findings below.

Building on this long history of study, we were interested in characterizing *A. maculatum* floral VOC variation across Europe, and linking genotype, phenotype (*i.e.* floral scent), and selection (*i.e.* pollinator preferences) for the most complete understanding of *A. maculatum* pollination yet. We identified three main areas of research which had yet to be addressed; these became the primary aims of the preceding research chapters. First, we aimed to identify geographic variation in floral scent and pollinator attraction across most of the species distribution of *A. maculatum*, and to test whether these variations represented adaptations to local pollinator communities (Chapter 2; Szenteczki et al. 2021). Second, we aimed to identify the genetic bases (*i.e.* candidate genes) for individual *A. maculatum* VOCs, and identify links between transcript expression and pollination interactions which may have been shaped by natural selection (Chapter 3; Szenteczki et al. 2022). Third, we aimed to use the high resolution of next-generation sequencing (*i.e.* ddRAD-seq) data to investigate the extent to which phenotypic selection and/or phylogenetic constraints influenced VOC evolution within *A. maculatum*, and among nine *Arum* species (Chapter 4). From this work, a few key patterns emerged, which we will discuss below in the context of the past and present research on *A. maculatum*.

General Discussion

First and foremost, it is clear that *A. maculatum* floral scent is highly variable, both within populations and across its range. Intra-population variation in *A. maculatum* VOCs has been consistently detected, regardless of the location(s) studied or VOC sampling methods used. This diversity can be discussed in terms of the total number of VOCs – which can be measured in the hundreds if minor compounds are not excluded (Gfrerer et al. 2021) – and in terms of the proportional blends of compounds emitted, particularly the ratio of indole to sesquiterpenes (Kite 1995, Chartier et al. 2013, Szenteczki et al. 2021, Gfrerer et al. 2021). In spite of this high variation, signs of pollinator-mediated selection on some compounds are present. Notably, sesquiterpene VOC emissions appear to be correlated with *in situ* pollinator attraction (Szenteczki et al. 2021) and fruit set (Gfrerer et al. 2021). These results suggest that *P. phalaenoides* and *P. grisescens* may have different VOC preferences and detection capabilities, but natural selection has not fixed these differences in floral VOC variation within populations of *A. maculatum*. Several factors are likely responsible for this pattern, which will be discussed in the general conclusion to this chapter.

Second, temporally replicated data are important for understanding spatial patterns (or the lack thereof) between species interactions and traits. Our work is not the first to come to this conclusion (Endler 1986, Herrera 1988, Schemske and Horvitz 1989, Fishbein and Venable 1996, Thompson and Fernandez 2006, Ollerton et al. 2007), and interest in short- and long-term temporal replicates of pollination interactions remains high (CaraDonna and Waser 2020, Schwarz et al. 2020) in spite of the difficulty in collecting temporal data. Here, we identified temporal heterogeneity in *Psychoda* pollinators trapped by *A. maculatum* inflorescences over relatively short time scales (*i.e.* over 1-2 years, and approximately 10 years since Espíndola et al. 2011). If the dominant pollinator available to *A. maculatum* inflorescences varies regularly, then this may explain the lack of local adaptation to a specific *Psychoda* species observed in Chapter 2. Furthermore, since *A. maculatum* are rhizomatous perennials, shorter bursts of selection are less likely to result in rapid evolution as observed in annual plants (*e.g.* Gervasi and Schiestl 2017). However, it is interesting to note that the *A. maculatum* population in Forêt du Gâvre, France was the only population where the dominant pollinator (*P. grisescens*) was consistent over both inter-annual and decadal scales, and floral scent showed signs of local adaptation in our transplant experiment. However, further transplants of inflorescences from Forêt du Gâvre to other locations are needed. Our results appear to indicate that temporally heterogeneous pollinators are a mechanism to maintaining VOC diversity within *A. maculatum* populations.

Third, collecting total headspace VOCs may obscure adaptations to the scent of specific floral tissues. VOCs are known to vary between petals, stamens, pistils, sepals, pollen and/or nectar (reviewed in Muhlemann et al. 2014) and tissue-specific variation exists in *A. maculatum* as well. Kite (1995) separately quantified the VOC profiles of *A. maculatum* appendices and basal spathe chambers, and found that the highly diverse appendix VOC bouquet was contrasted by specific emissions of bicyclogermacrene from the male florets. However, all studies on *A. maculatum* VOCs since then – including the present work – utilized headspace sampling alone; this method samples a mix of appendix and male floret VOCs. Our transcriptomic results (Chapter 3) highlighted that at least two VOCs – bicyclogermacrene and an unknown sesquiterpene possibly related to 2-methylisoborneol – are produced exclusively by the male florets. We also found that terpene synthase expression in the male florets, but not the appendix, was linked to differential attraction of *P. phalaenoides* and *P. grisescens*. Controlled pollinator choice experiments are still needed to disentangle the effects of local pollinator communities in the studied populations (Szenteczki et al. 2021, Laina et al. 2022) on this result. However, future studies may find evidence of natural selection at a much smaller spatial scale (*i.e.* along the spadix of a single inflorescence) than we did across a wide geographic range in the present work.

Finally, *Arum* floral scent appears to be evolutionarily labile not only within *A. maculatum*, but across the entire genus. Our studies on co-variation between VOCs and phylogenetic relationships (Chapter 4) found little evidence that specific VOCs were restricted to subclades within *A. maculatum*, or individual taxa on our genus *Arum* phylogeny. Although a wider sampling of *Arum* species with next-generation sequencing and VOC data are still needed, our results are consistent with the prediction that *Arum* scent should adapt relatively quickly in response to pollinator shifts. The same pattern was also observed by Schiestl and Dötterl (2012) in their study of other Araceae pollinated by scarab beetles, where plants evolved in response to pollinator preferences, but pollinators did not experience reciprocal selection as a consequence of deception.

Future Directions

As is often the case in scientific research, the present work generated as many new questions as it addressed. Below, I will briefly discuss a few open questions related to our research.

What about the pollinators' perspective?

Previous research indicates that deceptive pollination of *A. maculatum* likely does not exert substantial selective pressure on populations of deceived Psychodidae pollinators. Although being trapped by multiple *A. maculatum* means that a nontrivial proportion of a pollinator's adult life may be spent inside inflorescences, female *Psychoda* do not lay eggs in the floral chamber (Diaz and Kite 2002). Thus, their individual reproductive success is not necessarily reduced by *A. maculatum*. The brief overlap between *A. maculatum* flowering and 1-3 generations of Psychodidae (*i.e.* out of 12-18 per year; Vaillant (1971) in Espíndola (2010)) could mean that any selection for pollinator learning is lost to genetic drift in subsequent generations. Furthermore, the microenvironment of the basal spathe chamber also appears to be adapted to Psychodidae. Although the stigmatic secretions are not consumed by Psychodidae (Lack and Diaz 1991), appropriate oxygen and humidity levels are maintained in the chamber with the aid of lacunae: intercellular spaces in the wall of the spathe chamber

(Dormer 1960, Bröderbauer et al. 2013). However, Laina et al. (2022) found that fruit set size could decrease in extreme cases (*i.e.* where hundreds of pollinators were trapped); in these situations, pollinators may die as well (Dormer 1960). This phenomenon appears to be restricted to more northern populations (*e.g.* in Germany), as we observed very few pollinator mortalities in the populations we sampled. Consequently, while pollinator preferences may exert selective pressures on *A. maculatum* floral scent, there is little evidence for reciprocal selection on pollinators.

During the present work, and indeed most studies of *A. maculatum* pollination, comparatively little attention has been paid to Psychodidae beyond taxonomic identifications of pollinators trapped within inflorescences (but see Espíndola and Alvarez 2011, where the phylogeographic histories of Psychodidae and *A. maculatum* were studied in parallel). Recent electroantennographic (GC-EAD) research by Gfrerer et al. (2022), conducted on the antennae of *P. phalaenoides* and other dipterans exposed to *A. maculatum* floral VOCs and manure, represents an important advance in this area. This study highlighted that *P. phalaenoides* respond to germacrene D and unnamed sesquiterpenes in >80% of trials, bicyclogermacrene and *p*-cresol in >50% of trials and indole in 25-50% of trials. Thus, it has been confirmed that many of the compounds identified as putatively under selection in the present work are indeed perceived by *P. phalaenoides*. Since *P. grisescens* antennae were not tested by Gfrerer et al. (2022), an important next step in this area would be to characterize their antennal responses, and compare them to *P. phalaenoides*. Further research in this area could identify variations in their respective preferences, and narrow the list of candidate VOCs putatively under selection by each species.

What role, if any, does hybridization play in Arum floral scent diversity?

Chartier et al. (2016) characterized natural hybridization events between *A. maculatum* and *A. italicum,* and the morphology and floral scents of hybrid offspring in great detail. Since *A. italicum* and *A. maculatum* are both widely distributed species which overlap over much of their ranges (Boyce 1993) and share Psychodidae as one of their main pollinators, pollen transfer between species is possible. However, hybrids of *A. maculatum* (tetraploid) and *A. italicum* (hexaploid) are pentaploid, which would lead to infertility in most cases. Nonetheless, the presence of hybrids could negatively affect the pollination of the two parent species through competition for pollinators. However, as Chartier et al. (2016) discuss, these inflorescences could also produce novel scent compounds, which could open up a new pollination niches for hybrids. Paired with chromosomal eliminations and/or polyploidization events, this could potentially lead to a viable new species. Conversely, the presence of nonviable hybrids may also create divergent selective pressures on the two parent species' floral scents to deter interbreeding. This may be why, despite Psychodidae also being an efficient pollinator for *A. italicum*, it is more generalized to other dipteran taxa (Diaz and Kite 2002, Chartier et al. 2011).

In the present work, we sought to limit the possibility of sampling *A. italicum* or hybrids in our molecular analyses, by considering only inflorescences with characteristic *A. maculatum* morphological traits (*i.e.* purple appendix, purple stamens, no white venation on leaves). However, future research could deliberately sample both species and their putative hybrids. The ploidy-aware genotype calling (Clark et al. 2019) method we used could be modified to work with mixed ploidy datasets as well. These molecular data could be used to estimate the prevalence of hybrids across the range of *A. maculatum*. Comparative transcriptomics of *A. maculatum* and *A. italicum* may also be interesting. These methods could be used to investigate whether greater divergence in VOC synthase expression is observed in sites with a mix of both species, versus in sites with one species alone.

Conclusion: Why is *Arum maculatum* scent so variable?

Darwin's realization that intraspecific trait variation can drive natural selection was, and remains, a foundational component of evolutionary theory. When trait variation has a heritable genetic basis, species interactions can establish feedback loops between ecological processes and trait evolution (Hendry 2016). Flowering plant diversification as a result of interactions with pollinators is one well-known example of this process (Hernández-Hernández and Wiens 2020). Throughout the preceding chapters, we identified considerable variation in *A. maculatum* floral scent. This variation appears to be maintained within populations in spite of i) a specialized pollination system with only two pollinators (*Psychoda phalaenoides* and *P. grisescens*) accounting for the majority of visitors, and ii) presumably strong selection pressure for efficient pollinator attraction (*e.g.* due to protogyny and no pollinator rewards).

One explanation for this pattern, which is backed by empirical research, is that higher VOC diversity is maintained in deceptive plants due to the antagonistic nature of their interactions with pollinators (Ackerman et al. 2011). Unlike rewarding plants, where balancing selection may lead to "constancy" in floral scent to provide a clear signal to pollinators, deceptively pollinated plants may benefit from inconsistent signals which prevent pollinator learning (Salzmann et al. 2007). However, *A. maculatum* is a brood site mimic, and as discussed above, likely has a neutral effect on the fitness of its pollinators. Thus, negative frequency-dependent selection due to pollinator learning is less likely to maintain floral scent variation in *A. maculatum*, compared to bee-pollinated deceptive plants. Relaxed selection may also cause variation in VOC bouquets (Salzmann et al. 2007). Based on our transcriptomic results, one could speculate that relaxed selection is occurring at the appendix, but not male floret VOCs. If, for example, there is little selection on appendix VOCs beyond acting as a general lure for dung-breeding dipterans, then this may lead to higher variation in VOC emissions. Conversely, selection could maintain *Psychoda*-attractive sesquiterpene VOCs in the basal spathe chamber to better retain pollinators during the pollination process, or to increase its efficiency (*i.e.* by stimulating movement and therefore pollen dispersal). Alternatively, temporally variable pollinators may favor the maintenance of a diverse VOC bouquet, to ensure that some pollinators are caught every year regardless of whether *P. phalaenoides* or *P. grisescens* is more abundant. It should be noted that Gfrerer et al. (2021) did not find annual variation in pollinators to the same extent in the "core" of *A. maculatum*'s distribution north and south of the Alps, but greater variability should be expected as one samples more towards the fringes of a species range, where drift and selection from novel environments are more likely as well.

In closing, we were able to further our understanding of *A. maculatum* pollination through a combination of methodologies – some widely used in the species (*e.g.* field surveys and GC-MS characterization of floral scent), and some used for the first time (*e.g.*, tissue-specific RNAseq, ddRAD-seq, and a range-wide transplant experiment). By re-visiting populations sampled by Espíndola et al. (2011), we were also able to add a temporal dimension to our study, which proved to be valuable for understanding why *A. maculatum* scent may be so variable. It is likely that additional insights can be gained from future multidisciplinary research and comparative studies among both *A. maculatum* populations, and several *Arum* species. Over decades of research, we have continued to refine our knowledge of *A. maculatum* pollination biology, and it will continue to serve as a valuable model for studying plant-pollinator interactions across wide spatial and temporal ranges in the years to come.

REFERENCES

Ackerman, J. D., A. A. Cuevas, and D. Hof. 2011. Are deception-pollinated species more variable than those offering a reward? Plant Systematics and Evolution 293: 91–99.

Boyce, P. 1993. The genus *Arum*. Royal Botanic Gardens Kew.

Bröderbauer, D., A. Weber, and A. Diaz. 2013. The design of trapping devices in pollination traps of the genus *Arum* (Araceae) is related to insect type. Botanical journal of the Linnean Society 172:385–397.

CaraDonna, P. J., and N. M. Waser. 2020. Temporal flexibility in the structure of plant–pollinator interaction networks. Oikos 129:1369–1380.

Chartier, M., S. Liagre, H. Weiss-Schneeweiss, B. Kolano, J.-M. Bessière, J. Schönenberger, and M. Gibernau. 2016. Floral traits and pollination ecology of European *Arum* hybrids. Oecologia 180:439–451.

Chartier, M., L. Pélozuelo, B. Buatois, J.-M. Bessière, and M. Gibernau. 2013. Geographical variations of odour and pollinators, and test for local adaptation by reciprocal transplant of two European *Arum* species. Functional Ecology 27:1367–1381.

Chartier, M., L. Pélozuelo, and M. Gibernau. 2011. Do floral odor profiles geographically vary with the degree of specificity for pollinators? Investigation in two sapromyophilous *Arum* species (Araceae). Annales de la Société entomologique de France 47:71–77.

Clark, L. V, A. E. Lipka, and E. J. Sacks. 2019. polyRAD: Genotype Calling with Uncertainty from Sequencing Data in Polyploids and Diploids. G3 Genes|Genomes|Genetics 9:663–673.

Diaz, A., and G. Kite. 2002. A comparison of the pollination ecology of *Arum maculatum* and *A. italicum* in England. Watsonia 24:171–182.

Dormer, K. J. 1960. The truth about pollination in *Arum*. The New Phytologist 59:298–301.

Endler, J. A. 1986. Natural selection in the wild. Princeton University Press, Princeton, NJ.

Espíndola, A. 2010. Inferring reciprocal evolutionary histories in associated species of plants and insects in two European pollination systems. Doctoral Thesis, Université de Neuchâtel.

Espíndola, A., and N. Alvarez. 2011. Comparative Phylogeography in a Specific and Obligate Pollination Antagonism. PLOS ONE 6:e28662.

Espíndola, A., S. Buerki, M. Bedalov, P. Küpfer, and N. Alvarez. 2010. New insights into the phylogenetics and biogeography of *Arum* (Araceae): unravelling its evolutionary history. Botanical Journal of the Linnean Society 163:14–32.

Espíndola, A., L. Pellissier, and N. Alvarez. 2011. Variation in the proportion of flower visitors of *Arum maculatum* along its distributional range in relation with community-based climatic niche analyses. Oikos 120:728–734.

Fishbein, M., and D. L. Venable. 1996. Diversity and Temporal Change in the Effective Pollinators of *Asclepias Tuberosa*. Ecology 77:1061–1073.

Gervasi, D. D. L., and F. P. Schiestl. 2017. Real-time divergent evolution in plants driven by pollinators. Nature Communications 8:14691.

Gfrerer, E., D. Laina, M. Gibernau, R. Fuchs, M. Happ, T. Tolasch, W. Trutschnig, A. C. Hörger, H. P. Comes, and S. Dötterl. 2021. Floral Scents of a Deceptive Plant Are Hyperdiverse and Under Population-Specific Phenotypic Selection. Frontiers in Plant Science 12:719092.

Gfrerer, E., D. Laina, R. Wagner, M. Gibernau, A. C. Hörger, H. P. Comes, and S. Dötterl. 2022. Antennae of psychodid and sphaerocerid flies respond to a high variety of floral scent compounds of deceptive *Arum maculatum* L. Scientific Reports 12:5086.

Hendry, A. P. 2016. Eco-evolutionary dynamics. Princeton university press.

Hernández-Hernández, T., and J. J. Wiens. 2020. Why Are There So Many Flowering Plants? A Multiscale Analysis of Plant Diversification. The American Naturalist 195:948–963.

Herrera, C. M. 1988. Variation in mutualisms: the spatiotemporal mosaic of a pollinator assemblage. Biological Journal of the Linnean Society 35:95–125.

Jones, D. H. T. 1977. Studying Lords and Ladies, *Arum maculatum* (L.). Journal of Biological Education 11:253–260.

Kite, G. C. 1995. The floral odour of *Arum maculatum*. Biochemical Systematics and Ecology 23:343–354.

Kite, G. C., W. L. A. Hetterscheid, M. J. Lewis, P. C. Boyce, J. Ollerton, E. Cocklin, and A. Diaz. 1998. Inflorescence odours and pollinators of *Arum* and *Amorphophallus* (Araceae). Pages 295–315 *in* S. J. Owens and P. J. Rudall, editors. Reproductive Biology. Royal Botanic Gardens Kew, London, UK.

Lack, A. J., and A. Diaz. 1991. The pollination of *Arum maculatum* L. - a historical review and new observations. Watsonia 18:333–342.

Laina, D., E. Gfrerer, V. Scheurecker, R. Fuchs, M. Schleifer, C. Zittra, R. Wagner, M. Gibernau, H. P. Comes, A. C. Hörger, and S. Dötterl. 2022. Local Insect Availability Partly Explains Geographical Differences in Floral Visitor Assemblages of *Arum maculatum* L. (Araceae). Frontiers in Plant Science 13:838391.

Linz, J., J. Stökl, I. Urru, T. Krügel, M. C. Stensmyr, and B. S. Hansson. 2010. Molecular phylogeny of the genus *Arum* (Araceae) inferred from multi–locus sequence data and AFLPs. Taxon 59:405–415.

Marotz-Clausen, G., S. Jürschik, R. Fuchs, I. Schäffler, P. Sulzer, M. Gibernau, and S. Dötterl. 2018. Incomplete synchrony of inflorescence scent and temperature patterns in *Arum maculatum* L. (Araceae). Phytochemistry 154:77–84.

Muhlemann, J. K., A. Klempien, and N. Dudareva. 2014. Floral volatiles: from biosynthesis to function. Plant, cell & environment 37:1936–1949.

Ollerton, J., and A. Diaz. 1999. Evidence for stabilising selection acting on flowering time in *Arum maculatum* (Araceae): the influence of phylogeny on adaptation. Oecologia 119:340–348.

Ollerton, J., A. Killick, E. Lamborn, S. Watts, and M. Whiston. 2007. Multiple meanings and modes: on the many ways to be a generalist flower. Taxon 56:717–728.

Prime, C. T. 1960. Lords and ladies. Collins, London.

Salzmann, C. C., A. M. Nardella, S. Cozzolino, and F. P. Schiestl. 2007. Variability in floral scent in rewarding and deceptive orchids: the signature of pollinator-imposed selection? Annals of botany 100:757–765.

Satchell, G. H. 1947. The ecology of the British species of *Psychoda* (Diptera: Psychodidae). Annals of Applied Biology 34:611–621.

Schemske, D. W., and C. C. Horvitz. 1989. Temporal Variation in Selection on a Floral Character. Evolution 43:461–465.

Schiestl, F. P., and S. Dötterl. 2012. The evolution of floral scent and olfactory preferences in pollinators: coevolution or pre-existing bias? Evolution; international journal of organic evolution 66:2042–2055.

Schwarz, B., D. P. Vázquez, P. J. CaraDonna, T. M. Knight, G. Benadi, C. F. Dormann, B. Gauzens, E. Motivans, J. Resasco, N. Blüthgen, L. A. Burkle, Q. Fang, C. N. Kaiser-Bunbury, R. Alarcón, J. A. Bain, N. P. Chacoff, S.-Q. Huang, G. LeBuhn, M. MacLeod, T. Petanidou, C. Rasmussen, M. P. Simanonok, A. H. Thompson, and J. Fründ. 2020. Temporal scale-dependence of plant–pollinator networks. Oikos 129:1289–1302.

Snow, B., and D. Snow. 1988. Birds and berries. Calton Poyser, Staffordshire.

Szenteczki, M. A., A. L. Godschalx, A. Galmán, A. Espíndola, M. Gibernau, N. Alvarez, and S. Rasmann. 2021. Spatial and temporal heterogeneity in pollinator communities maintains within-species floral odour variation. Oikos 130:1487–1499.

Szenteczki, M. A., A. L. Godschalx, J. Gauthier, M. Gibernau, S. Rasmann, and N. Alvarez. 2022. Transcriptomic analysis of deceptively pollinated *Arum maculatum* (Araceae) reveals association between terpene synthase expression in floral trap chamber and species-specific pollinator attraction. G3 Genes|Genomes|Genetics 12:jkac175.

Thompson, J. N., and C. C. Fernandez. 2006. Temporal dynamics of antagonism and mutualism in a geographically variable plant–insect interaction. Ecology 87:103–112.

Vaillant, F. 1971. Psychodidae-Psychodinae (page 358) *in* E. Lindner, editor. Die Fliegen der palaearktischen Region. E. Schweizerbartische Verlagsbuchhandlung, Stuttgart.

Mark Szenteczki

orcid.org/0000-0002-3049-8327
mark.szenteczki@unine.ch

SUMMARY

I am interested in the genetics underlying chemically-mediated interactions between plants, insects, and microbes. Currently, I study how plant-pollinator interactions shape variation in floral odour, by integrating field-collected trait measurements and massive molecular datasets.

EDUCATION

PhD - Organismal Biology **Mar. 2017 - Sept.2022**
Université de Neuchâtel (CH)

Doctoral thesis co-supervised by Nadir Alvarez & Sergio Rasmann.
Thesis title: On the chemical and molecular ecology of deceptively pollinated *Arum maculatum* (Araceae)

MSc Molecular Life Sciences - Bioinformatics **Sept. 2015 - Jan. 2017**
Université de Lausanne (CH)

Thesis supervised by Prof. Nadir Alvarez. Thesis title: Characterizing and comparing the microbiomes of Large Blue butterflies (*Maculinea alcon*) and their ant hosts

BSc.H Biology **Sept. 2010 - May 2014**
Queen's University (Kingston, ON, CAN)

Thesis supervised by Prof. Stephen C Lougheed. Thesis title: Using Approximate Bayesian Computation to understand the distribution of genetic diversity in eastern Massasauga rattlesnakes (*Sistrurus catenatus*)

EMPLOYMENT HISTORY

PhD Student - Laboratory of Functional Ecology **Mar. 2017 - Present**
Université de Neuchatel - SNSF Project Grant 163334

My current research combines GC-MS characterizations of volatile compounds emitted by *Arum maculatum* and neutral (ddRADseq) and adaptive (RNA-seq) molecular data, to test for local adaptation in floral scent

Student-Assistant (Assistant-étudiant) **Apr. 2016 - Dec. 2016**
Université de Lausanne - Prof. Nadir Alvarez

During my MSc studies, I was also employed to perform general lab duties (DNA extraction and PCR), and to develop a custom pipeline in Python & Bash for phylogenetic analyses of polyploid plants using RNAseq data

Research Associate **Sept. 2014 - Sept. 2015**
Queen's University - Lougheed Lab

I managed the operation of the molecular lab facilities, including teaching basic molecular techniques to new undergraduate students and organizing and ordering equipment and consumables

PEER-REVIEWED PUBLICATIONS

Szenteczki MA, Godschalx AL, Gauthier J, Gibernau M, Rasmann S & Alvarez N (2022) Transcriptomic analysis of deceptively pollinated *Arum maculatum* (Araceae) reveals association between terpene synthase expression in floral trap chamber and species-specific pollinator attraction. **G3 Genes|Genomes|Genetics**, 12(9), jkac175. DOI:10.1093/g3journal/jkac175

Szenteczki MA, Godschalx A, Galmán A, Espíndola A, Giberneau M, Alvarez N, & Rasmann S. (2021) Spatial and temporal heterogeneity in pollinator communities maintains within-species floral odour variation. **Oikos**, 130(9), 1487-1499. DOI:10.1111/oik.08445

Galmán A, Abdala-Roberts L, Wartalska P, Covelo F, Röder G, **Szenteczki MA**, Moreira X, & Rasmann S. (2020). Elevational gradients in constitutive and induced oak defences based on individual traits and their correlated expression patterns. **Oikos** 130(3): 396-407. DOI:10.1111/oik.07588

Hinojosa JC, Koubínová D, **Szenteczki MA**, Pitteloud C, Dincă V, Alvarez N & Vila R (2019) A mirage of cryptic species: Genomics uncover striking mitonuclear discordance in the butterfly *Thymelicus sylvestris*. **Molecular Ecology** 28(17): 3857-3868. DOI:10.1111/mec.15153

Szenteczki MA, Pitteloud C, Casacci LP, Kešnerová L, Whitaker MRL, Engel P, Vila R, & Alvarez N (2019) Bacterial communities within *Phengaris* (*Maculinea*) *alcon* caterpillars are shifted following transition from solitary living to social parasitism of *Myrmica* ant colonies. **Ecology and Evolution** 9: 4452-4464. DOI:10.1002/ece3.5010

RESEARCH PROJECTS

SNSF Doc.Mobility Fellowship 191659 (51,440 CHF) **Apr. 2020 - Jun. 2021**
Awarded for "The evolution of deceptive pollination in the genus Arum (Araceae)". Project conducted at the University of Corsica Pasquale Paoli in Ajaccio, France

MAJOR GRANTS & SCHOLARSHIPS

UNIL Master's Grant (25,600 CHF) **Sept. 2015 - Jan. 2017**
Awarded on a competitive basis to international applicants of a very high level, who distinguished themselves in their university studies

ThinkSwiss Travel Grant (1,200 CHF) **July 2014**
Awarded to highly motivated and qualified students from the US and Canada, for participation in a Swiss research stay (up to 3 months)

Chancellor's Scholarship ($36,000 CAD) **Sept. 2010 - May 2014**
Queen's University major admission award given for superior academic ability, creative and original thinking, and proven leadership qualities

SELECTED PRESENTATIONS

DPOB Seminar Series (Neuchâtel, CH) **Mar. 2021**
Oral pres.; "Why do floral odours vary? Linking VOC emissions, pollinator attraction, and transcript expression in deceptively pollinated Arum maculatum"

Ecology and Evolution of Flowers (Zürich, CH) **Nov. 2018**
Poster; "Geographic variation in transcript expression and floral volatile production in deceptively pollinated Arum maculatum"

SeeDS Symposium (Neuchâtel, CH) **Nov. 2018**
Oral pres.; "Tracking local adaptation in Arum maculatum floral scent"

Macroecology in Space and Time (Vienna, AT) **Apr. 2017**
Oral pres.; "Microbial communities in Maculinea alcon caterpillars change following trophic shift"

Dept. of Ecology & Evolution Seminar (Lausanne, CH) **Dec. 2016**
Oral pres.; "Characterizing and comparing microbiomes of Large Blue butterflies and their ant hosts"

ThinkSwiss Alumni Event (Washington DC) **Nov 2016**
Invited Speaker; I presented a talk titled "The Butterfly Effect" at the Swiss embassy, highlighting the past, present, and future of my research in Switzerland

Queen's University Biological Station (CAN) **Jun. 2014**
Invited Demonstrator; I presented a poster (Molecular Ecology of Snakes), along with several live specimens in an interactive experience for all ages & educational backgrounds

BIOL 537 Poster Day (Queen's University, CAN) **Apr. 2014**
Poster; "Understanding the demography and extensive population structuring of E. Massasauga rattlesnakes (Sistrurus catenatus) in Ontario"

TEACHING ACTIVITIES

Guest Lecturer (Université de Neuchâtel) **Mar. 2018**
Genes to Ecosystems

I lectured UNINE Master's students on leading-edge molecular techniques, and how we can use them to study plants from the level of genes up to population-level adaptations

Teaching Assistant (Queen's University) **Aug. 2015**
Aquatic Biodiversity & Environmental Assessment: Canada-China Exchange Field Course

I provided in-field support to undergraduate students from Canada and China, covering surveys of wetland diversity, wetland classification techniques, and the impacts of human development on wetlands.

Teaching Assistant (Queen's University) **May 2015**
Herpetology Field Course (BIOL 307)

I provided in-field support to undergraduate students, covering the ecology of reptiles and amphibians in Ontario, and techniques for using herpetiles as models to test hypotheses in ecology, evolution, and conservation.

Teaching Assistant (Queen's University) **Sept. 2014 - Dec. 2014**
Mendelian & Molecular Genetics (BIOL 205)

I instructed biweekly 3 hour undergraduate labs. I prepared lectures covering both theory and practical lab skills (e.g. working with *Drosophila* and *S. pombe*, and DNA extraction/Gel Electrophoresis).

ACADEMIC AWARDS

Poster Award **2014**
1st place (tied) for best poster at Queen's University undergraduate thesis symposium

Book Award **2014**
Queen's University: top mark in 'Geographic Information Systems' (GPHY 243)

Thomas Nugent Memorial Award **2012**
Queen's University: awarded in recognition of creativity, dedication, and passion

Award of Academic Excellence **2010**
Awarded by the Mayor of Clarington (ON, Canada), for academic merit & volunteer work

PERSONAL DATA

Digital competences	Bash, Python, and R for bioinformatic pipelines LaTeX and Rmarkdown for documents and reports
Nationality	Canadian & Hungarian
Residency	Switzerland: L Permit (Aug. 2015 - Present)
Languages	English (Native/Fluent) Hungarian (Fluent) French (Intermediate Spoken & Written)